UNIVERSITY OF ILLINOIS
URBANA

AERONOMY REPORT NO. 13

INSTRUMENTATION AND PRELIMINARY RESULTS FROM SHIPBOARD MEASUREMENTS OF VERTICAL INCIDENCE IONOSPHERIC ABSORPTION

by
George W. Henry, Jr.

October 1, 1966

Supported by
National Aeronautics and
Space Administration
Grant NsG-511

Aeronomy Laboratory
Department of Electrical Engineering
University of Illinois
Urbana, Illinois

CITATION POLICY

Since much of the material in this report may be published in accepted aeronomic journals, it would be appreciated if persons wishing to cite work contained herein would first contact the authors to ascertain if the relevant material is part of a paper published or in process.

AERONOMY REPORT NO. 13

INSTRUMENTATION AND PRELIMINARY RESULTS FROM SHIPBOARD MEASUREMENTS OF VERTICAL INCIDENCE IONOSPHERIC ABSORPTION

by

George W. Henry, Jr.

October 1, 1966

Supported by
National Aeronautics and
Space Administration
Grant NsG-511

Aeronomy Laboratory
Department of Electrical Engineering
University of Illinois
Urbana, Illinois

ABSTRACT

This report discusses the design of the instrumentation used to measure vertical incidence absorption and partial reflections on board the USNS Croatan aircraft carrier as a portion of the NASA research expedition in 1965 to the southern Pacific Ocean. Preliminary data reduced from film records is presented and discussed briefly. Also discussed briefly in this report is the instrumentation being used for similar measurements at Wallops Island and at the Aeronomy field station near Urbana, Illinois.

ACKNOWLEDGEMENT

Considerable assistance in the preparation of this report has been given by Dr. K. G. Balmain and Mr. T. W. Knecht of the Aeronomy Laboratory of the University of Illinois. Dr. Balmain authored the first portion of Chapter 6 dealing with model studies of the antenna system and antenna polarization alignment and directed the research in this field. Mr. Knecht authored the first portion of Chapter 5 dealing with timing and control system design and constructed a majority of the timing systems described. Mr. Knecht has also been of great service in the editing and organization of this report.

The author is deeply grateful to Professor S. A, Bowhill for his interest and guidance throughout the design, construction, and operation of the instrumentation described in this report. The author also wishes to specifically thank Professors G. A. Deschamps and J. D. Dyson of the Antenna Laboratory of the University of Illinois for their assistance with the model studies and polarization research of antennas suitable for use on board an aircraft carrier. Thanks are also due to Miss Brenda Key for her prompt and efficient typing of this report and to Mr. David Bauman for his careful and accurate preparation of the many drawings necessary to fully describe the instrumentation designed. The author would also like to thank the following personnel of the Technical Services Department of the Aeronomy Laboratory for their assistance in the design, construction, and operation of the instrumentation:

Mr. A, B. Gschwendtner
Mr. Robert W. Leach
Mr. Jerry E, Russell
Mr. Larry A. Schick

Mr. Andrew W. Seacord

Mr. Jack Strong

Mr. George A. Tagge

The research described in this report was supported by the National Aeronautics and Space Administration under contract NsG-511.

TABLE OF CONTENTS

TABLE OF CONTENTS (continued)

LIST OF ILLUSTRATIONS

LIST OF ILLUSTRATIONS (continued)

LIST OF ILLUSTRATIONS (continued)

LIST OF ILLUSTRATIONS (continued)

LIST OF ILLUSTRATIONS (continued)

1. INTRODUCTION

Measurement of height distribution of free electrons in the ionosphere has long been the object of many experiments. Swept-frequency ionosondes and rocket-borne experiments are probably the most successful, but have the disadvantages that ionosonde records are difficult to interpret for heights less than 90 km and that rocket experiments observe the ionosphere only at the isolated times of launch and do not present a continuous picture of daily ionospheric variations. The vertical incidence absorption and partial reflection experiments are land-based experiments and do provide for both continuous observation and investigation of ionospheric characteristics below 90 km.

The vertical incidence absorption experiment involves transmission of pulses of radio energy in a vertical direction and reception of ionospherically reflected pulses. The amplitudes of these received pulses are interpreted in terms of the attenuation produced by an equivalent lossy reflector placed at the apparent reflection height. The attenuation is expressed as that amount of loss contributed by the ionosphere for the double path (up-leg and down-leg) that is over and above the normal free-space path loss. The apparent or virtual height of the reflecting medium is measured as the time delay between the transmitted pulse and the received pulse in the same manner as in the swept-frequency ionosonde or as in the range indicator of a radar system.

The partial reflection experiment is much the same as the vertical incidence absorption experiment in that pulses of radio energy are transmitted vertically and the ionospheric reflections are received and

recorded. However, the partial reflection technique involves transmission of pulses of both ordinary and extraordinary polarizations in sequence. The amplitudes of the reflections received from each polarization are then compared to determine a differential absorption between the two modes, from which an electron density profile can be obtained. The partial reflection technique allows measurements of electron densities in the height range of approximately 50 to 90 km. These partially reflected echoes, weakly back-scattered from small irregularities in electron density, are 50 to 60 dB weaker in amplitude than the reflections received from the normal E layer. Therefore, considerably more system gain is required for measurement of partial reflections than is required for the vertical incidence absorption experiment.

Use of the vertical incidence absorption and partial reflection techniques yields considerable information concerning lower ionosphere behavior, particularly when used in conjunction with a swept-frequency ionosonde and/or rocket instrumentation for measurement of electron densities. For these reasons, a system capable of vertical incidence absorption and partial reflection measurements has been installed at Wallops Island, Va. This system has been used in conjunction with University of Illinois rocket experiments for measurement of D-layer differential absorption and has proven particularly valuable in sensing the occurrence of winter anomaly in absorption.

A second system similar to that used at Wallops Island was designed and constructed for use on board the USNS Croatan aircraft carrier during the NASA research expedition to the southern Pacific. Operation of the

absorption/partial reflection sounder aboard the ship allowed measurement of lower ionospheric conditions in conjunction with the rocket experiments and the swept-frequency ionosonde. Additionally, the ship provided an excellent opportunity to measure the latitudinal variation of the ionospheric absorption. Although the physical dimensions of the ship did not permit an antenna system of optimum size to be erected for partial reflection measurements, the remainder of the system was designed so that, although marginal, some partial reflection data might be recorded. The design and construction of this system for shipboard use is the primary concern of this report. Also included is a brief description of the instrumentation at Wallops Island and the instrumentation in use at the University of Illinois Aeronomy Laboratory Field Station. Preliminary results of the vertical incidence absorption measurements are included in this report.

Since instrumentation for use in the measurement of vertical incidence absorption and partial reflections is quite specialized and not available from commercial sources, the design of each component is treated in sufficient detail that a similar system could be constructed with a minimum of redesign time should such a system be required in the future. Additionally, it is intended that this report serve as a manual of operation and servicing for personnel at the University of Illinois,

2. GENERAL SYSTEM DESIGN

Radio measurement of vertical incidence ionospheric absorption and D-layer partial reflection phenomena requires the transmission of a pulsed RF signal in a vertical direction and reception of all signals resulting from either total or partial reflection of the transmitted signal by the ionosphere. This transmitted pulse should be of sufficient length that ionospheric dispersion will not appreciably affect the amplitude of the received reflection and as short as is consistent with good transmitter and receiver design techniques. The pulse should be definitely much shorter than the time delay between the transmitted pulse and the first reflected pulse to be received.

Measurement of vertical incidence absorption requires recording of the amplitude of each reflected signal received and the virtual height of the reflection layer, Recording of the reflected signal was accomplished in the shipboard experiment by displaying the receiver output on an oscilloscope and photographing the trace on 35 mm film. The horizontal sweep circuitry of the oscilloscope was triggered by the transmitter pulse; hence, the time delay between the transmitted pulse and received reflection were recorded on the film as well as the amplitude of the reflection. The virtual height can be readily calculated from this time delay since the wave propagates at the speed of light. A second data recording system, designed by Robert Appel (Appel and Bowhill, 1965), provides data records that are more easily reduced, and is presently in use for absorption recording at the University of Illinois.

Measurement of partial reflections from the lower regions of the ionosphere requires recording of the amplitude and virtual height of both the

ordinary and extraordinary magnetoionic component waves. The system transmits, in rapid succession, both modes of circular polarization and the resulting received reflections are, as in the case of absorption measurements, photographed from the oscilloscope screen. The output of the receiver is inverted for the transmission and reception of the second polarization so that both components are recorded on a single frame of film, one above the other. This method of recording allows rapid comparison of the amplitudes of received partial reflections of both modes at the same virtual height (Belrose et al., 1964).

The requirements of transmitter power, antenna gain, and receiver sensitivity for the system to accurately measure the above ionospheric phenomena were determined from the following path-loss calculation:

In free space, with no ionospheric attenuation, the ratio of received power to transmitted power can be expressed as

$$\frac{A\,A}{d\,\lambda} \qquad \text{(I.T. \& T., 1956)} \qquad (2.1)$$

where

P_r = power of received signal

P_t = power of transmitted signal

A_r = effective area of receiving antenna

A_t = effective area of transmitting antenna

λ = wavelength in meters

d = distance between antennas in meters

For observation of E-layer reflections, a median frequency of 3 MHz was chosen and the distance, d, is approximately 100 km X 2 = 200 km. Since

the physical arrangement of the ship required use of the same antenna system for receiving and transmitting, A_r and A_t are the same and will be referred to as **A**. The space available on the ship also dictated the use of a maximum of two crossed dipoles as the antenna system. Therefore, the effective area of the antenna system is:

$$A \approx 2(0.13\ \lambda^2) = 0.26\ \lambda^2 \qquad \text{(I.T. \& T., 1956)} \qquad (2.2)$$

Substituting **(2.2)** in **(2.1)** gives:

$$\frac{P_r}{P_t} = \frac{A^2}{d^2 \lambda^2} \approx \frac{(0.26\ \lambda^2)^2}{d^2 \lambda^2} = \frac{0.0675\ \lambda^2}{d^2} \qquad (2.3)$$

If the signal has a frequency of 3.0 MHz, λ = 100 m and d = **200** km approximately, then **2.3** becomes:

$$\frac{P_r}{P_t} = \frac{0.0675(100)^2}{(2 \times 10^5)^2} = 1.69 \times 10^{-8}$$

$$\text{or, } P_t/P_r = 5.92 \times 10^7 = 77.7 \text{ dB} \qquad (2.4)$$

The absorption of a **3.0** MHz signal by the ionosphere can be expected to be approximately 30 dB maximum for the double path at local noon. Therefore the ratio of **(2.4)** can be as great as:

$$P_t/P_r \approx 108 \text{ dB} \qquad (2.5)$$

Therefore, if a signal strength of 1000 watts is radiated, the signal at the input to the receiver can be expected to be **1.69** x 10^{-6} watts, **or** an input voltage of **0.92** mV rms across **50** ohms. This signal strength can easily be detected in a receiver of a very simple design. However, the magnitude of partially reflected signals from the D layer can be expected to be **50** to **60** dB weaker than the normal E-layer echoes (Belrose et al., **1964**). If a power of 100 kW is radiated, the received partial reflection signals will be between

9.2 μV and 2.9 μV across a 50 ohm input impedance. Both a very high power transmitter and a very sensitive receiver are thus required to achieve reliable recording of partial reflections. In addition to the losses listed above, it is also necessary to include system losses of between 10 and 20 dB to account for losses in the transmitting and receiving feedlines, the electronic transmit–receive switch, the transmitting and receiving phase–shift networks, and the antenna matching networks, and for losses due to the inefficiency of the actual antenna system on board the ship. The antenna inefficiencies are largely a result of the presence of the ship's super–structure and cranes, as well as the wire antennas of other experimenters, all within the near fields of the antennas. Therefore, the system gain for partial reflection measurements was at best marginal and great care was used in the design and installation of each element of the system to assure maximum sensitivity.

The output power of the transmitter is largely dictated by the ratings of the final amplifier tubes and is therefore restricted to a maximum of 50 kW. The transmitter pulse width was adjusted to 50 μs in order to achieve a balance between receiver bandwidth and height resolution of the reflected signals. The bandwidth of the receiver was chosen from the relation:

$$BW = 5/2T = 50 \text{ kHz} \tag{2.6}$$

where

T = length of the rectangular pulse

This relationship has been derived for optimum receiver signal-to-noise ratio and does result in rounding of the pulse in the receiver (Schwartz, 1959). The response of the receiver to a rectangular RF pulse

input therefore resembles a $\cos^2 x$ function, but the amplitude and position characteristics of the pulse are retained at the peak of the output pulse.

The pulse repetition rates of the system were chosen to be between 1/2 and 5 pulses per second so that fading of the ionospheric reflection could be observed. The pulse repetition rate was held to a maximum of 5 pps to minimize interference to other experiments. The mechanical system of the camera dictated one record per second as the maximum data recording speed, (determined by the rate at which the 35 mm film can be changed from one frame to the next) so that all filmed recordings were made at a pulse rate of 1/2 or 1.0 pps. The 5 pps rate was used primarily for visual observation and in adjustment of the transmitter. Measurement of the partial reflections further required that both ordinary and extraordinary modes be recorded on the same frame of film and in rapid succession. Therefore, double pulses, one of each mode, were transmitted and received by the system within 125 ms of each other at a pulse repetition rate of either 1/2 or 1.0 pps. For measurement of vertical incidence absorption, the second pulse was eliminated in the timing and control system.

A further requirement of the system for the ship experiment was that it be tunable over the frequency range from 2.0 to 3.5 MHz so that interference could be avoided by shifting the system frequency and so that measurements could be made at several distinct frequencies.

Therefore, the requirements of the entire system to achieve recording of vertical incidence absorption and low altitude partial reflections were:

1. The transmitter should be capable of delivering at least 50 kw to the antennas during the pulse.

2. The receiver should be capable of receiving a signal of strength 2×10^{-13} watts (3.0 μV across 50 ohms) with a signal-to-noise

ratio of 10 dB minimum. (i.e., a noise figure of approximately 3 dB).

3. The transmitted pulse should be 50 μs long with a pulse repetition rate adjustable between 1/2 and 5 pps.

4. The -3 dB bandwidth of the receiver should be approximately 50 kHz.

5. The antenna system should be capable of radiating either right- or left-hand circular polarizations in a vertical direction. The sense of the polarization should be controlled automatically by the timing system for recording of partial reflection data.

6. The recording of the data should consist of photographing the receiver output as displayed on an oscilloscope. The film should be 35 mm and provision should be included for automatic advancing of the film by the timing system for each transmitted and received pulse. Other pertinent data such as date, time and frame number should be recorded on each frame of film.

7. The entire system should be capable of operation over the frequency range of 2.0 to 3.5 MHz.

8. The mechanical construction of the system should be designed so that the rugged environment of shipboard use would not be detrimental to its operation. All component units should be capable of mounting in shock-mounted relay racks and should be individually shielded to or interference from other experiments also participating in the research expedition. All units of the system with the obvious exception of the antennas and matching networks should be housed in an air-conditioned instrumentation trailer van furnished by NASA.

9. The control system should be so arranged that it can be easily operated for data recording by one individual.

10. Sufficient metering circuits should be included in all units so that servicing time can be kept to a minimum.

The block diagram of the complete system as designed for shipboard measurement of vertical incidence absorption and D-layer partial reflections is shown in Figure 2.1. Figure 2.2 is a photograph of the system as installed in the van.

The following report discusses the design and construction of each major instrument used in the shipboard experiment as well as a brief description

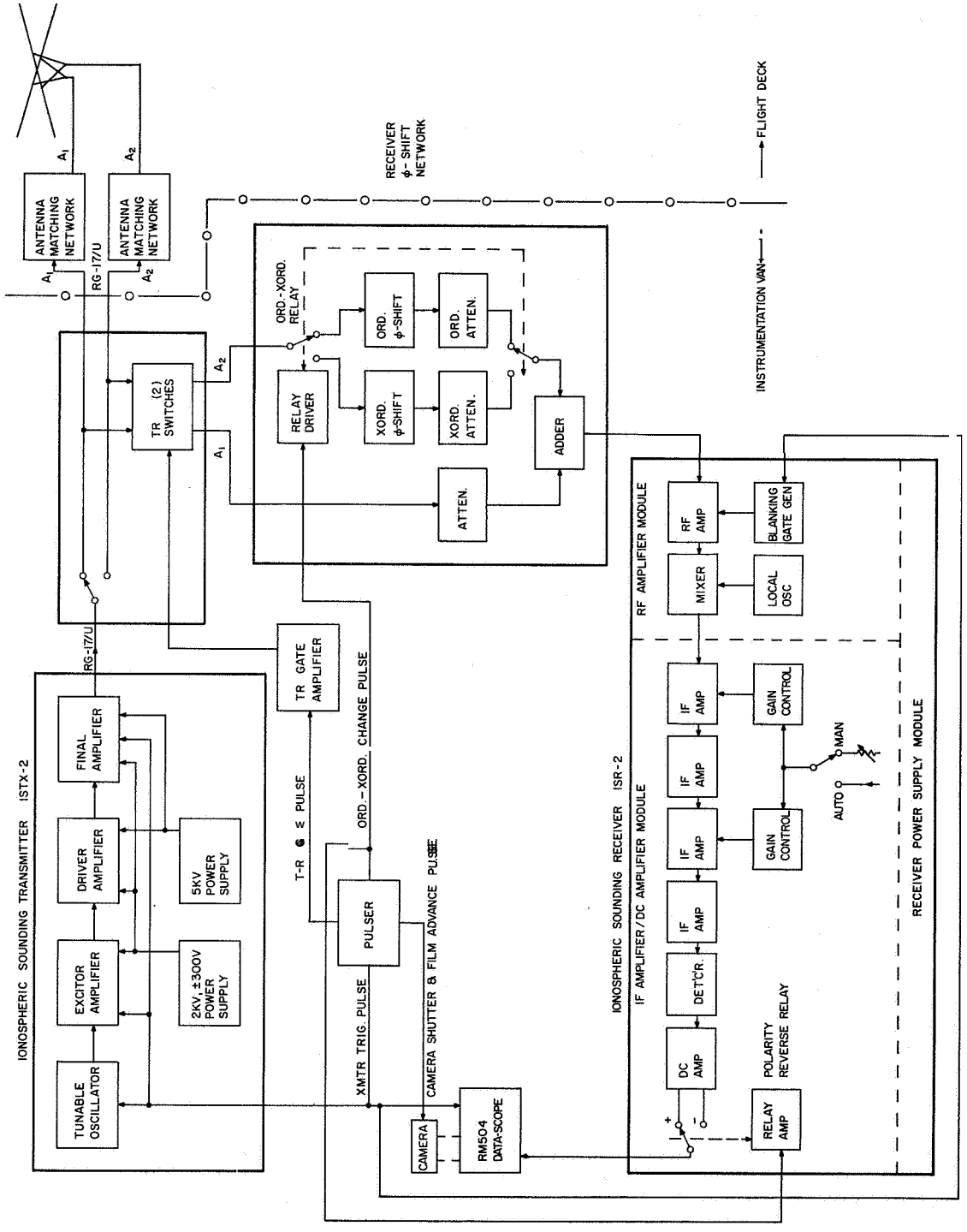

Figure 2.1 Block diagram of the shipboard system.

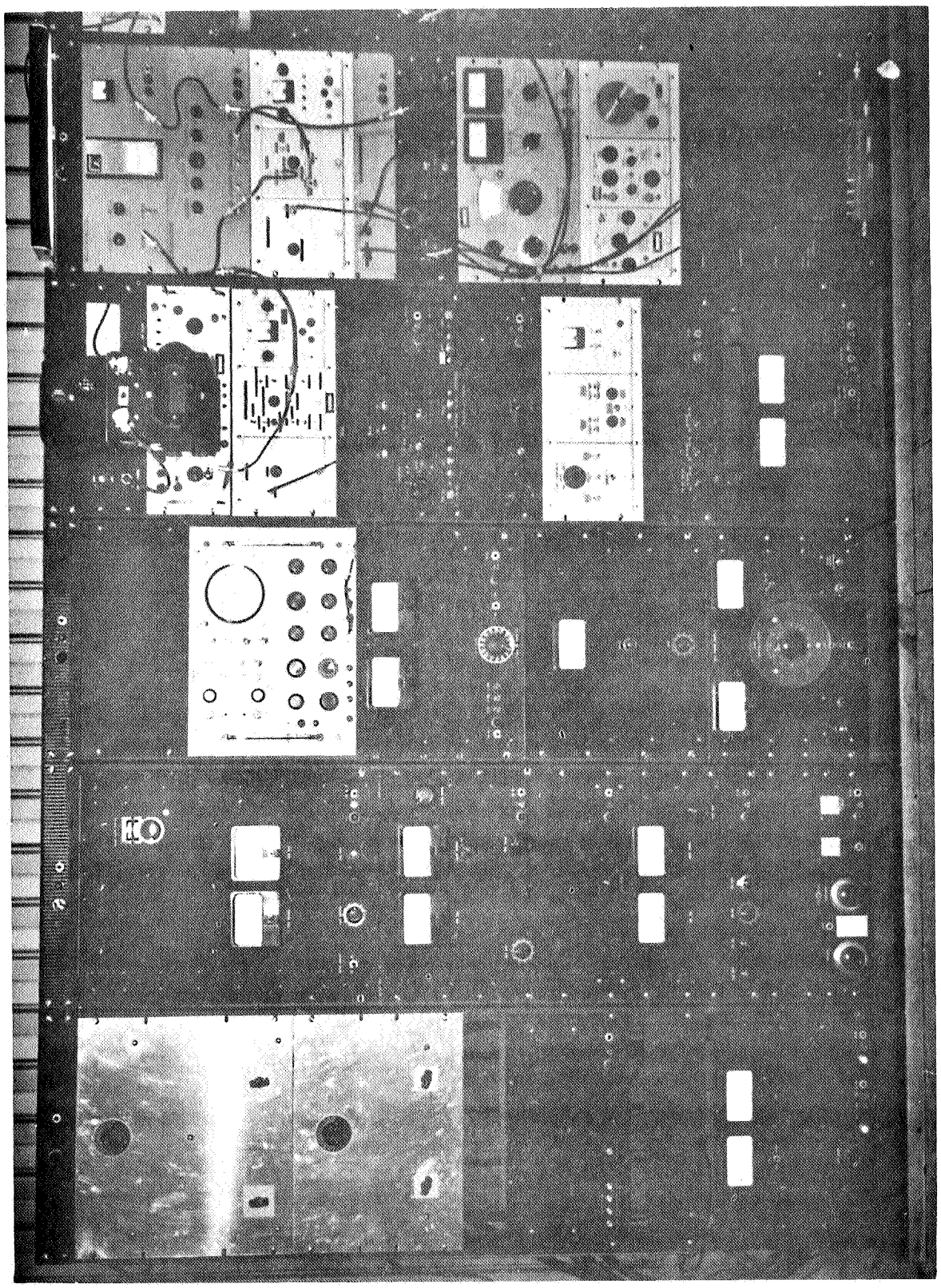

Figure 2 The shipboard system.

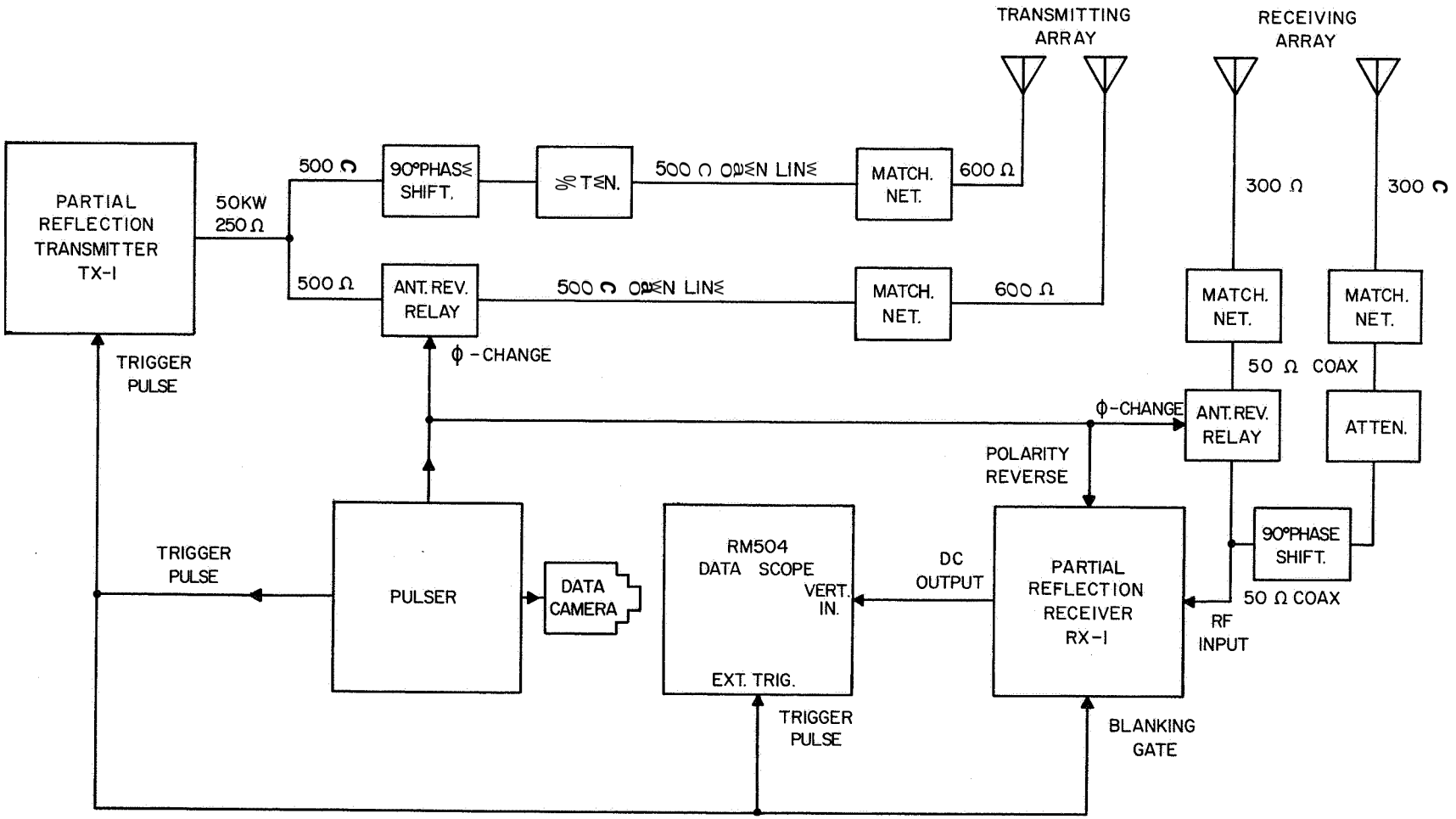

PARTIAL REFLECTION SYSTEM IN USE AT WALLOPS ISLAND VA

Figure 2.3 The Wallops Island system.

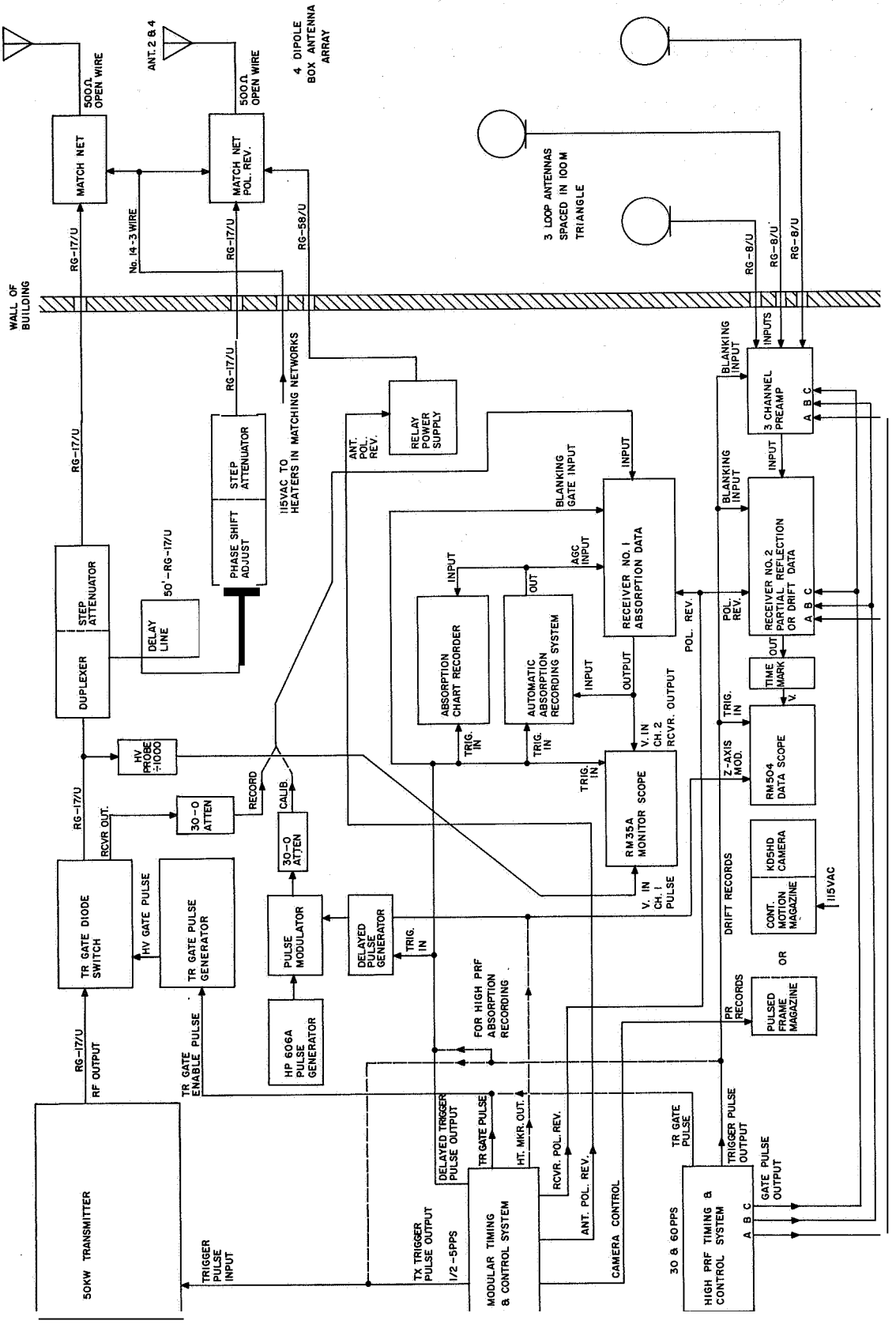

Figure 2.4 The field station system.

of similar instruments in use at the Wallops Island installation and the field station at the University of Illinois. Figure 2.3 is a block diagram of the Wallops Island installation and Figure 2.4 is a block diagram of the field station installation.

3. RECEIVER DESIGN

General Requirements

The receiver requirements of the shipboard ionospheric sounder were as follows:

1.	RF Center Frequencies	Tunable from 2.00 to 3.50 MHz or fixed frequency at 3.030 MHz.
2.	Noise Figure	3 dB maximum.
3.	Bandwidth	50 kHz at -3 dB points on bandpass response curve.
4.	Ripple Within Passband	3 dB overall maximum.
5.	Manual Gain Control	Sufficient to adjust for an input variation over the range of 1.0 microvolt to 1.0 millivolts.
6.	Recovery Time	200 microseconds for receiver to drop into noise after 0.1 volts rms at the signal frequency applied at the input is removed.
7,	Gain Variation	3 dB maximum over the temperature range of 15° C to 35° C.
8.	Power Supply	External to RF portions of receiver, all voltages to the receiver must be regulated to within 0.1% for AC line voltage variations of 10% and over the temperatures of 15° C to 35° C.
9.	RF Input Impedance	50 ohms, unbalanced.
10.	Output Impedance	10,000 ohms maximum, unbalanced.
11.	Output Response	DC to 50 kHz, 10 volts maximum with capability of selecting either positive or negative polarity output externally.
12.	Mechanical Housing	All receiver units to be shielded from external RF fields and housed in a cabinet capable of being mounted in a standard 19 inch relay rack.

The basic design of the shipboard receiver is the same as that previously developed by the author for use in an ionospheric sounding system at Wallops Island in 1964. The design and construction of the tunable RF amplifier section represents the major departure from the original design. The following is a discussion of the design of all receivers from the first used at Wallops to the latest additions for use at the University of Illinois.

The original design concept of the receiver was based upon the use of Clevite ceramic ladder filters as the bandpass determining element. However, laboratory testing proved that the filters are not adaptable to use in a pulse receiver--ringing of the filters after a pulse is applied continued for a time much greater than that expected for the delay in reception of ionospheric echoes. Therefore, the use of many-section filters to determine the bandpass of the receiver was discarded in favor of the more simple system of cascaded single-tuned amplifier stages. A complete description of the filters, amplifiers, and results obtained with the filters is found later in this chapter.

The receiver design finally chosen follows fairly conventional super-heterodyne design techniques. For an input signal of 1.0 microvolt at 50 ohms to produce a 10 volt output at 10,000 ohms, a power gain of at least 117 dB is required in the receiver. To achieve this high gain with optimum stability, the receiver was designed for the following gain per stage:

RF Amplifier	20 dB
Mixer	10 dB
IF Amplifiers	20 dB each, 80 dB total for 4 stages
Detector	-10 dB (loss)
DC Amplifier	20 dB
Maximum Receiver Gain	120 dB

To avoid problems of strong adjacent-channel signal crossmodulation, the gain preceding the bandwidth-determining IF amplifier chain was purposely kept low.

Design and construction of the receiver has followed a two-part program, that of design and development of an experimental prototype receiver and the subsequent design and development of the current series of receivers. The inclusion of a blanking circuit to block the receiver input during transmitter operation and improvements in the power supply and DC amplifier stability were the only major items of electrical change between the prototype and operational receiver. Design and construction of the prototype receiver were accomplished during the months of November and December, 1963 and a portion of January, 1964. The first Ionospheric Sounding Receiver (ISR-1) was constructed during the months of January, February, and March of 1964. Subsequent receivers have been designed and constructed as needed since March, 1964.

Discussion of the design of the receiver is divided into the following sections, in which the various units are described individually:

RF Amplifier, Mixer, and Local Oscillator Unit
IF Amplifier, Detector, and DC Amplifier Unit
Power Supply Unit
Receiver Mechanical Design
Receiver Performance Characteristics
Early Receiver Designs

After each general discussion of the unit design, the individual modules designed for the existing six receivers are discussed and differences between them are outlined. A block diagram and photograph of the complete receiver are found in **Figures 3.1** and **3.2,** respectively.

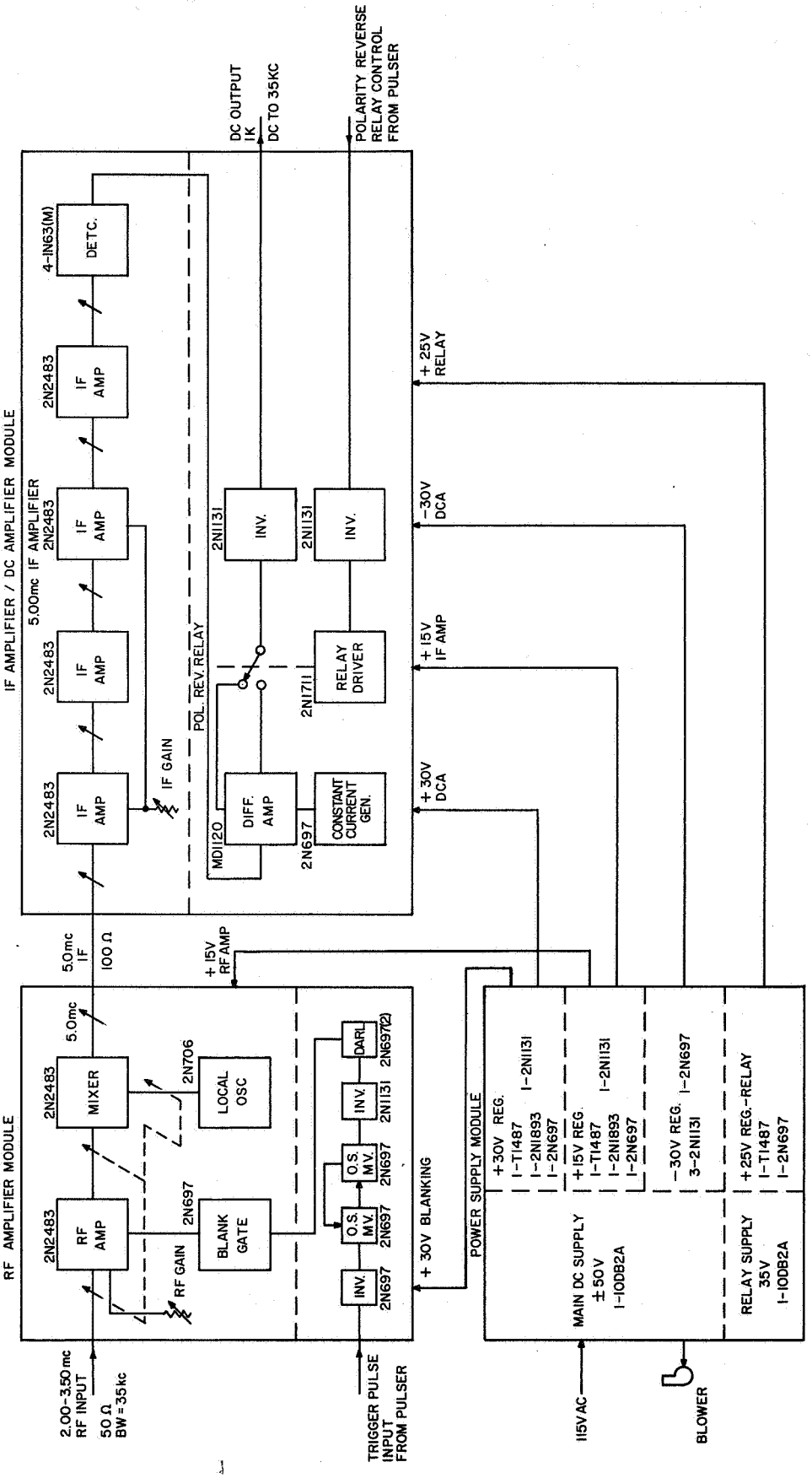

Figure 3 1 Block diagram of the receiver

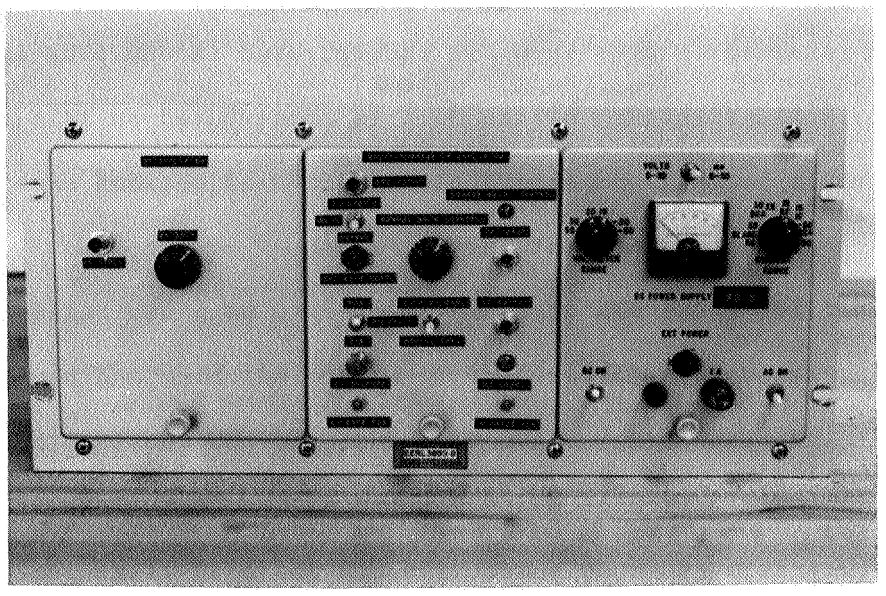

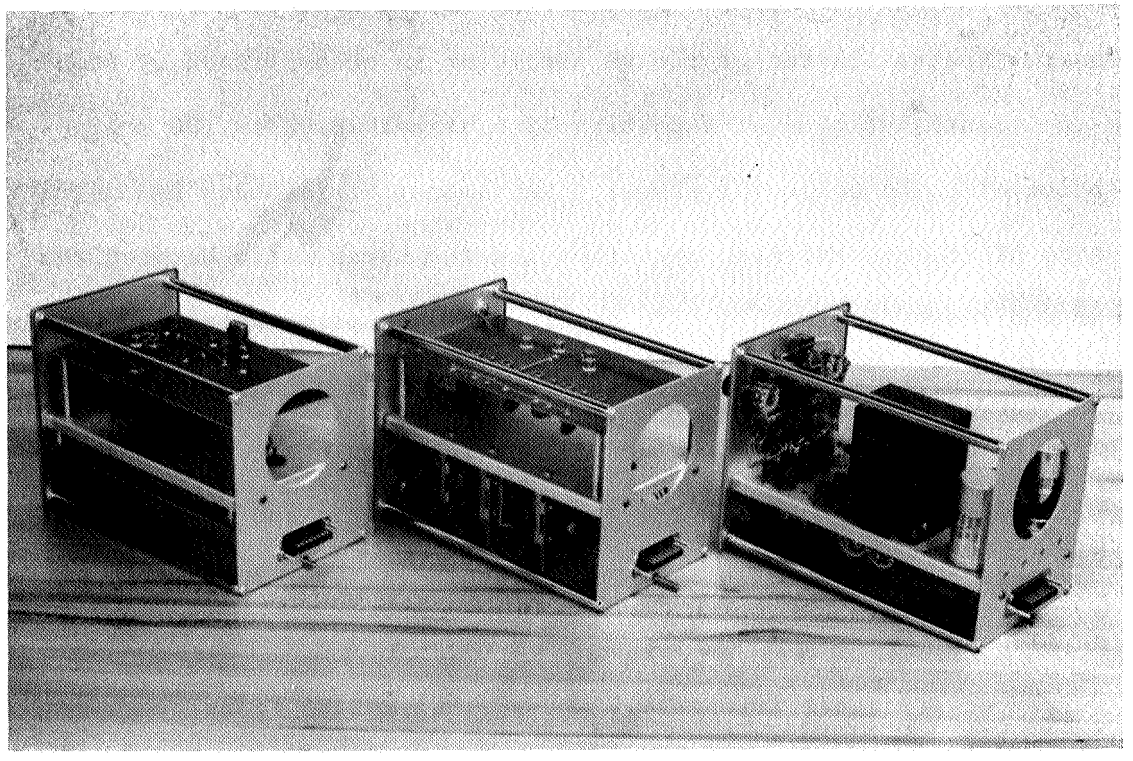

Figure **3.2** The receiver.

RF Amplifier, Mixer, and Local Oscillator Unit

The RF amplifies, mixer, and local oscillator circuits as well as the blanking pulse generator stages were all incorporated in one plug-in unit of the receiver, All circuitry of the unit is constructed on 1/16-inch copper-clad circuit boards, and shield plates are used between each stage to minimize interaction and prevent instability,

The RF amplifier stage was designed to operate as a neutralized tuned amplifier, using tuned transformers for impedance inatching and neutralization feedback'. The transformers have been designed and constructed by University of Illinois personnel using Cambridge Thermionic Corporation type 1181 shielded coil form and core assemblies and no. 5-44 'litz wire, Use of the CTC form, litz wire, and bifilar winding achieved coefficients of coupling of approximately 0.9, making double tuning of the transformers unnecessary. Neutralization of the RF amplifier is accomplished by feedback to the transistor base of a portion of a signal which is 180 degrees aut of phase with the collector signal, The amount of feedback is controlled by the size of the neutralizing capacitor and the turns ratio between the collector and feedback windings, To assure close coupling between these two windings, the neutralization winding is actually wound as a portion of the collector winding!, with the collector DC supply connected to a tap on this winding. To assure close coupling between the collector and output windings, the two are bifilar wound, with the secondary winding starting at the collector DC supply tap.

A survey of available transistors showed that 2N2483 transistors were capable of achieving the low noise figure required in the 2 to 10 MHz frequency range and were therefore chosen for use as the RF amplifier and mixer

transistors in the receiver. In the interest of economy and standardization, 2N2483's are also used in the IF amplifier stages of the receiver,

For optimum gain and noise performance, the 2N2483 transistor base is matched to an input impedance of 7,500 ohms and the transistor itself is operated at I_e = 1.0 mA (DC bias). The input transformer matches the base to a 50 ohm coaxial cable, the input to the receiver. The gain of the RF amplifier stage is controlled over a 25 dB dynamic range by varying the DC base bias of the 2N2483.

The mixer stage also employs a 2N2483 transistor matched for a base impedance of 7,500 ohms and DC biased for I_e = 1.0 mA. The RF input signal is injected to the base of the mixer transistor by the output transformer of the RF amplifier stage. The IF output is transferred from the collector of the mixer by means of a tuned transformer that matches the IF signal to a 100 ohm coaxial cable for transmission to the IF amplifier module. The local oscillator signal is injected in the emitter circuit of the mixer by means of an isolating emitter follower that shares a common emitter resistance with the mixer transistor. This emitter follower stage again uses a 2N2483 transistor at a DC bias of I_e = 1.0 mA. Use of the emitter-follower stage minimizes the possibility of the local oscillator being "pulled" in frequency by a very strong signal at the RF input frequency of the receiver.

The local oscillator stage uses a 2N706 transistor in a Colpitts type of circuit. The crystal is operated in its series-resonant mode in series with the feedback path. The amount of feedback is controlled with a capacitive voltage divider system across the collector tuned circuit. Most stable and reliable operation has been achieved with approximately 15% feedback voltage. The oscillator DC collector voltage is doubly regulated, first

by the main +15 volt regulator and then by a 10 volt zener diode, to assure stable operation under all conditions. The local oscillator output signal is also coupled to the emitter-follower stage by means of a capacitive voltage divider. Approximately 1% of the total oscillator collector signal is required to give proper injection to the mixer, affording a still greater degree of isolation for the oscillator.

After initial test of the receiver in a sounding system with a 50 kW pulse transmitter, it was found to be quite desirable to provide some means of disabling the receiver during the transmitter operation time. This is necessary not only to protect the RF amplifier transistor but also to prevent the receiver from saturating completely, a condition requiring approximately 200 μs from which to recover. The receiver blanking circuit prevents these bad effects by shorting out the RF input to the receiver during the transmitted pulse.

A single 2N697 is used as a shunt switch between the RF amplifier base and ground. A 10 volt positive pulse applied to the base of the 2N697 is sufficient to deactivate the receiver to all but signals on the order of 10 to 20 volts. To insure protection against input signals greater than 10 volts, two silicon diodes, HD5000's, are connected directly across the base winding of the input transformer. Under normal operating conditions, the voltage developed across the base winding is much less than the required silicon diode threshold level of 0.7 volts and the receiver operation is unaffected by their presence. However, when voltages greater than 0.7 volts are present across the base winding, the diodes conduct and effectively short out the signal.

The blanking gate generator itself is simply a monostable multivibrator that is triggered by the same pulse that triggers the transmitter. The blanking gate is normally set up for a nominal operation time of 150 μs, but any time from 50 μs to several milliseconds is readily obtainable. An inverter stage is used ahead of the "one-shot" so that the circuit will trigger from a standard positive pulse. A Darlington-connected emitter follower couples the blanking pulse from the "one-shot" to the gate transistor.

Construction of the RF amplifier, mixer, and local oscillator stages follows conventional construction practices for high frequency designs; all signal leads are kept as short as possible, extensive shielding is used to separate each RF circuit from the others, all DC and control lines are by-passed with as short leads as possible. The RF circuitry board is mounted in the upper compartment of the module, the regular module chassis being mounted in the middle of the module to act as both a shield and mechanical support for the circuit boards. The pulse circuitry of the blanking gate generator is constructed on another copper-clad circuit board which is mounted below the module chassis.

The RF input to the receiver and the RF gain control are mounted on the upper portion of the front panel and are the only controls or connectors on the front panel. The required DC voltages as well as the IF output and blanking gate trigger pulses are distributed by means of the connector on the rear of the module. Various models of the RF amplifier module constructed to date are:

RF-1

The RF-1 module was the first module constructed and is therefore the most similar to the prototype model. It was originally designed and built

for an input frequency of 2.325 MHz and was used at that frequency in the Wallops Island system for 6 months. At this time, it was converted to operate at a frequency of 3.030 MHz by changing the tuning of the two transformers assosciated with the RF amplifier stage and the tuning of the oscillator as well as changing the crystal from 7.325 MHz to 8.030 MHz. The RF-1 was used on board the USNS Croatan Mobile Launch Facility in a partial reflection and vertical incidence absorption sounding system.

RF-2

The BF-2 module as originally constructed was identical to the RF-1, and was to serve as a back-up module for the Wallops Island partial reflection system. It, too, was initially designed and constructed for operation at 2.325 MHz, but has since been converted to 3.030 MHz for use in a modified partial reflection sounder at Wallops Island. The schematic diagram of RF-1 and BF-2 modules is found in Figure 3.3.

RF-3

The BF-3 module represented the first major departure from the prototype design. The RF-3 module is a tunable unit covering 2.00 to 3.50 MHz. Three tuned circuits are required to track in the 2.00 to 3.50 MHz range: the RF input tuned circuit, the mixer input tuned circuit, and the oscillator tuned circuit. A three gang, 365 pf per section air variable capacitor is used as the tuning device.

Tunable operation also required redesign of the oscillator circuit. Since the frequency range was so wide, it was no longer feasible to use a capacitive voltage divider to obtain the feedback voltage. A tuned transformer of the type used in the other RF circuitry was used with a tap to obtain the necessary feedback voltage. The crystal in the feedback path was

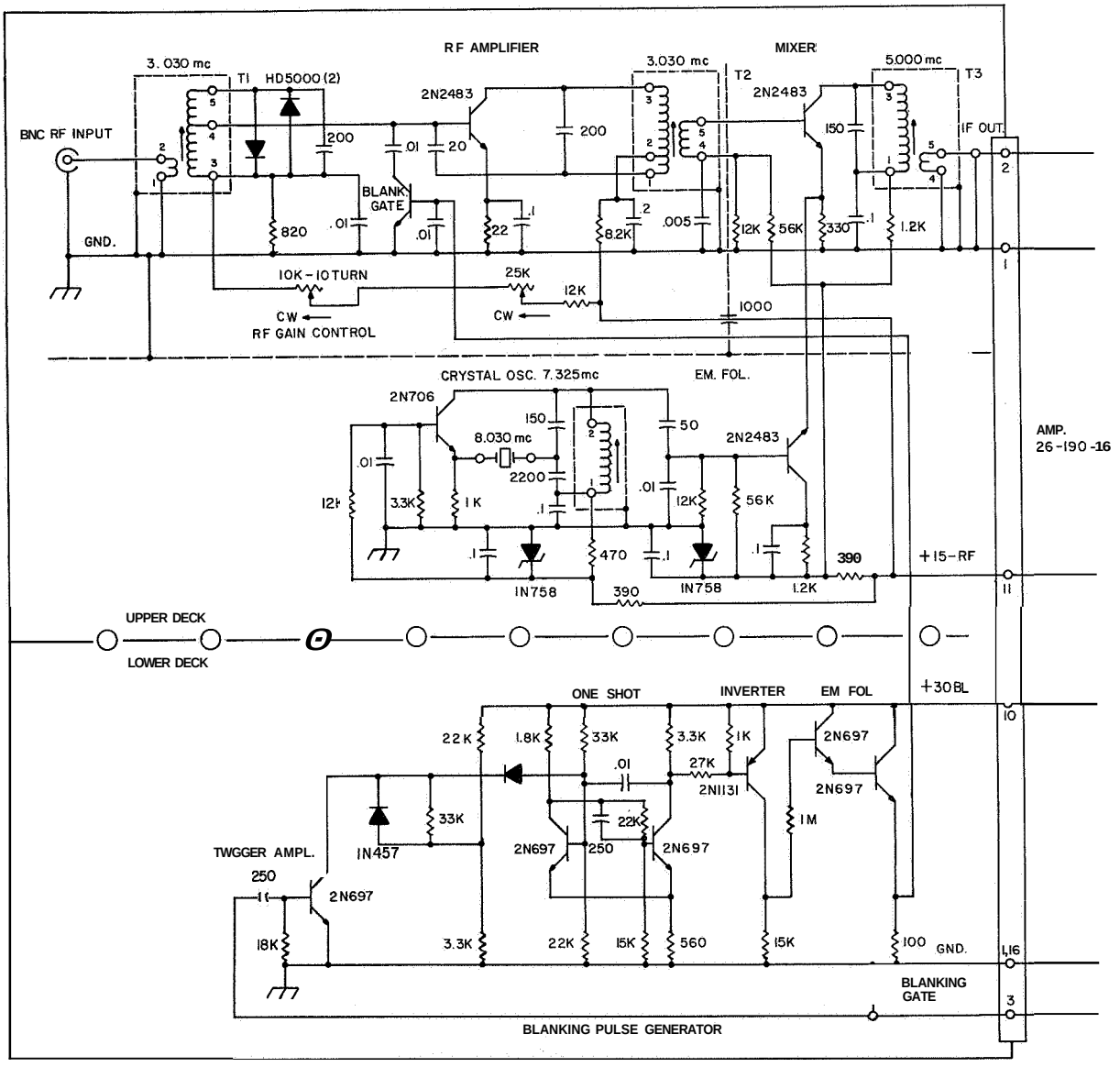

Figure 3.3 The RF-1 and RF-2 modules.

replaced with a resistance, the value of which controls the feedback current, A secondary winding on the oscillator coil provides the injection signal to the mixer. Because of the wide bandwidth of the receiver, it has not been found to be necessary to stabilize the oscillator beyond the precautions already outlined. The emitter follower stage was also deleted for this reason. The biggest problem with a tunable receiver without any form of automatic gain control has been that the gain of the RF amplifier varies with frequency, as well it should, since gain of the amplifier is proportional to circuit Q.

The tunable unit is vastly different mechanically from earlier models in that it is constructed on 1/8-inch thick copper-clad circuit board and the components are arranged in an entirely different layout, The physical configuration of the tuning capacitor requires a stage-by-stage layout so that each circuit is near its own section of the tuning capacitor. This results in a much more compact though less easily serviced layout than that of previous modules, The circuit board of the RF-3 is mounted vertically in the module instead of in the usual horizontal mounting. The blanking gate generator of the RF-3 is located at the rear of the RF circuit board. The controls and connectors located on the front panel of the RF-3 are the tuning dial, RF gain control, and the RF input. Tne RF-3 was used on board the **USNS** Croatan Mobile Launch Facility.

RF-4

As with the RF-2, the RF-4 is identical to the RF-3, designed to serve as a back-up module. It, too, was aboard the USNS Croatan. The schematic diagram of the RF-3 and RF-4 modules is found in Figure 3.4.

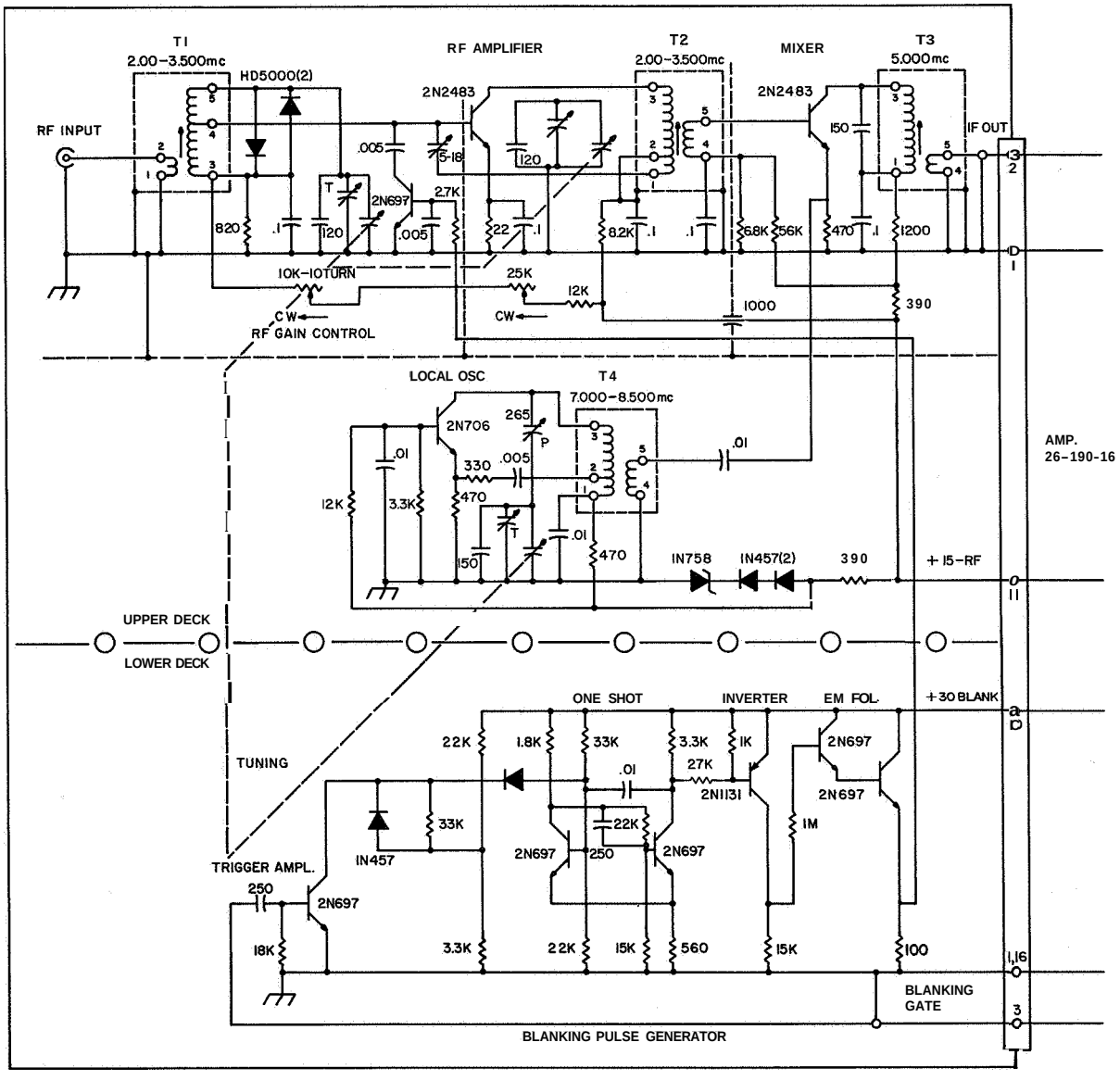

Figure 3.4 The RF-3 and RF-4 modules.

RF-5

The RF-5 represents a complete redesign of the receiver system because of the need for a receiver to cover from 3.00 to 8.00 MHz. This frequency range dictated that the IF frequency be changed from 5.00 MHz to 11.5 MHz and that all RF amplifier, mixer, and oscillator circuitry be modified accordingly,

The RF-5 is a tunable RF amplifier module designed in the same manner as RF-3 and RF-4. It is capable of tuning the range of 3.30 to 8.30 MHz. It incorporates the same type of 365 pf three gang air variable capacitor as used previously. The blanking gate generator is deleted from this unit and the 2N697 blanking transistor input is connected directly to the blanking connector on the rear of the manifold of the receiver. The tuning dial, RF gain control, RF input, and oscillator output connectors are located on the front panel. Since the receiver local oscillator signal is required for synchronizing purposes, an additional emitter-follower stage is incorporated for isolation purposes. The RF-5 is currently in use in a pulse compression sounder at the University of Illinois. The schematic diagram of the RF-5 module is found in Figure 3.5.

RF-6

The RF-6 module is a unit designed for a 7.9225 MHz sounding receiver for use in conjunction with a differential absorption rocket experiment at Ft. Churchill, Canada in the spring of 1966. Ionospheric sounding is used in the differential absorption experiment as a means of correctly aligning the transmitting antennas for ordinary and extraordinary modes of circular polarization. The circuitry of the RF-6 module is identical to that used in RF-1 and RF-2 with the change, in center frequency noted above. The RF amplifier

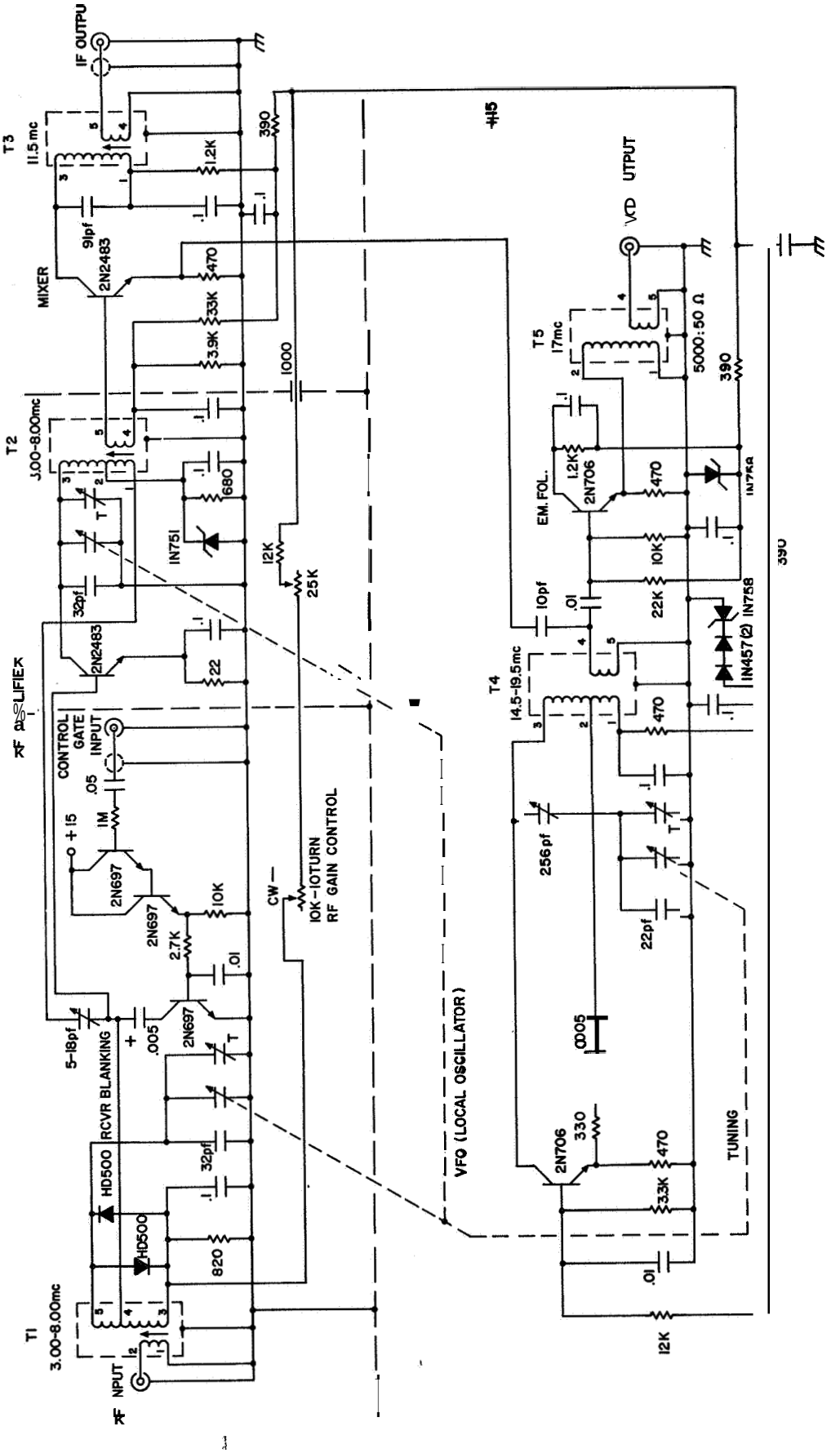

Figure 3 5 The RF-5 module.

input and mixer input tuned circuits are resonated at 7,9925 MHz and the crystal oscillator is tuned to 12,9225 MHz. Since the circuitry of RF-6 is the same as that of RF-1 and RF-2, a separate schematic diagram is not included for this unit.

Future planning indicates that one more receiver is required for use in conjunction with the differential absorption experiment, Two RF amplifier modules are required for this receiver--one with a center frequency of 2.225 MHz and one with a center frequency of 3.385 MHz. These units will be constructed in the near future.

IF Amplifier, Detector, and DC Amplifier Unit

The IF amplifier, detector, and DC amplifier stages, as well as an output polarity reversing relay and relay driver circuit, are all incorporated in one plug-in unit of the receiver. All circuitry of the unit is constructed on 1/16-inch copper-clad circuit boards and is divied so that the IF amplifier stages and detector stage are constructed on the upper board and the DC amplifier and polarity reversing stages are constructed on the lower board,

The IF amplifier portion of the receiver consists of four neutralized tuned amplifier stages again using single-tuned transformers to achieve neutralization and impedance matching. The input transformer matches the 100 ohm coaxial cable from the RF amplifier module to the base of the first transistor amplifier, Three interstage coupling transformers are used, one between each amplifier stage, The output transformer matches the collector of the output transistor amplifier to the detector system,

A frequency of 5.0 MHz was chosen for the IF frequency because of the wide bandwidth required of the reciever. If a frequency of approximately 1.0 MHz were used, the loaded Q of each tuned circuit would have to be much

too low (15 or less) to allow for any skirt selectivity. The overall IF bandwidth is 50 kHz. Using five single-tuned, isolated transformers, the bandwidth of each transformer must be 50/.386 = 130 kHz (Landee et al., 1957). At a center frequency of 5.0 MHz, a loaded Q of 38 will result in this bandwidth. A Q of 38 is readily obtainable from the CTC coils and allows for fairly steep skirt selectivity.

As in the RF amplifier and mixer stages, 2N2483 transistors were used as amplifier transistors. Use of this transistor simplifies design, reduces to a minimum the number of spare transistors to be kept in stock, and, most important of all, gives a very low noise high gain IF amplifier system. As before, the 2N2483 is DC biased for I_e = 1.0 mA. Gain control of the IF amplifier chain is accomplished by varying the base bias of the first and third amplifiers. The overall dynamic range of the IF gain control is approximately 45 dB.

The detector stage consists of four matched 1N63A germanium diodes connected in a full-wave bridge circuit. This circuit was chosen over the more conventional half-wave detector system because of the inherent reduction in pulse distortion with the full-wave system. The initial detector designs used 1N914 silicon diodes, but the threshold voltage of the silicon diodes (.7 volt typically) was found to be too high for good detector efficiency. Germanium diodes, with their lower threshold voltage (about 0.2 volts) gave a marked improvement in the stage efficiency. Temperature stability of the germanium diodes is not a problem because the relatively high load impedance used (10 kilohms) makes changes in diode forward resistance (100 to 200 ohms) insignificant, and changes in diode reverse impedance are cancelled by the bridge circuit, particularly if the diodes are matched.

The detected signal is of an average level of 0.5 volts, sufficiently high to be easily amplified by the DC amplifier stage.

A standard differential amplifier is used in the DC amplifier stage. The differential amplifier was originally designed for a matched pair of 2N697 transistors. However, providing means for keeping both transistor case temperatures the same, which is necessary to avoid temperature drift problems, was found to be impractical, Temperature drifts of several volts over the period of an hour were measured, due entirely to fluctuations in ambient temperature. This problem has been eliminated almost entirely by using an MD1120 dual matched transistor device in the differential amplifier. The MD1120 consists of two closely matched (all parameters within 1%) NPN silicon transistors in one TO-5 case. Since both semiconductors are in one package, differential temperature drifts are nearly impossible. A 2N697 is used as a 1.0 ma constant current source in the emitter circuit of the differential amplifier to assure high common-mode rejection. A 2N1131 transistor is used as an inverter and DC level-shifting stage following the differential amplifier. The requirementsof the partial reflection system are such that it must be possible to invert the receiver output. This is very simply achieved by switching the input of the 2N1131 stage from one collector of the differential amplifier to the other. A relay is used for this switching function, since the polarity reversal is electronically controlled by the timing and control system. To avoid any problems that might arise from relay switching transients, a relay driver system is built into the receiver. This circuit consists of a 2N1711 series switch transistor and a 2N1131 amplifier/inverter stage. External control is accomplished by simply connecting the base of the

2N1131 to common ground. The relay may also be activated by a panel-mounted switch, thus providing manual control of the receiver output polarity.

Front panel controls and connectors on the unit are the IF gain control, DC output connector, and output polarity switch. The IF input, relay control circuit, and all supply voltages are supplied through the connector at the rear of the module. The various models of the IF/DC Amplifier module constructed to date are:

IF-1

The IF-1 module was the first of the modules constructed and is therefore quite similar to the prototype receiver. It is presently in use at Wallops Island in a partial reflection system.

IF-2

The IF-2 module was constructed at the same time as IF-1 to serve as a back-up for IF-1 at Wallops Island, where it was used until July, 1964. At this time, IF-2 was returned to the University of Illinois to be used as a test module in conjunction with the design and development of the tunable RF Amplifier modules, RF-3 and BF-4. It is still being used at the University as a general test module. The schematic diagram of the IF-1 and IF-2 modules is found in Figure 3.6.

IF-3

The IF-3 module is the first departure from the original design and construction as used in IF-1 and IF-2. The changes were all mechanical in nature and were made to facilitate servicing and operation. The parts lay-out of IF-3 remained essentially the same as before, but the two circuit boards were rotated 90 degrees so that they are both vertical in the module, but are still separated by the horizontal module chassis. This arrangement

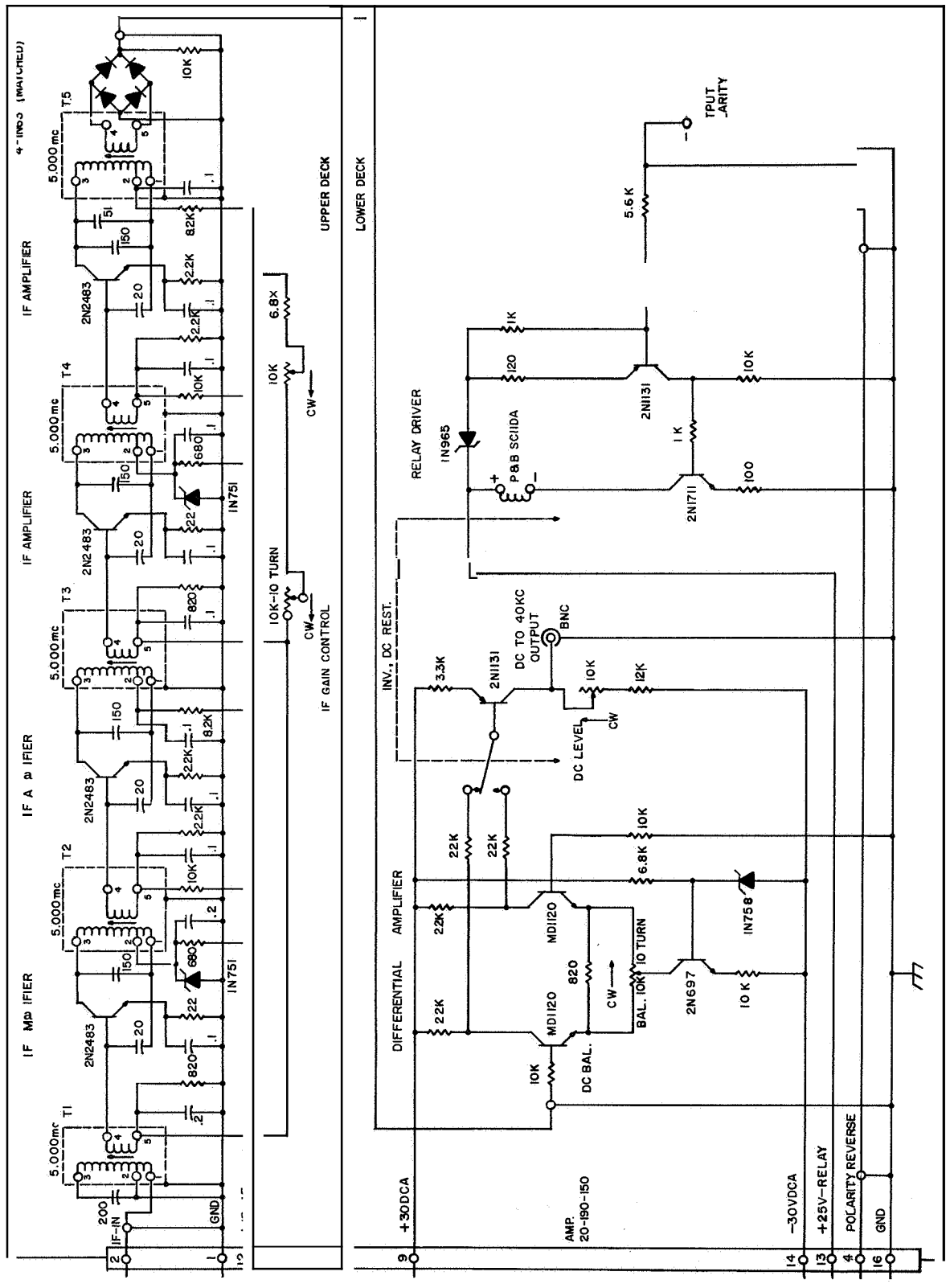

Figure 3.6 The IF-1, IF-2, IF-3, and IF-4 modules.

allows access to either side of the circuit board, making it unnecessary to remove the boards when servicing *or* modifying. Additionally, the DC balance control and the DC level controls were changed to ten-turn trimmer potentiometers and mounted on the front panel. Use of the ten-turn trimmers allows a much more accurate adjustment of these controls, and placing them on the front panel makes it unnecessary to remove the module from the manifold to adjust the DC amplifiers. This is especially important since all DC amplifier adjustments must be made under operating temperature conditions, a condition chat cannot be realized unless the module is in the manifold. Since the boards are vertically mounted in the module, it was necessary to drill ventilation holes in the boards themselves to allow the ventilating air stream to flow through the module. The IF-3 module was used on board the USNS Croatan Mobile Launch Facility.

IF-4

The IF-4 module was constructed to serve as a back-up to IF-3 aboard the ship. The schematic diagram of the IF-3 and IF-4 modules is the same as that of IF-1 and 'IF-2 and is also found in Figure 3.6.

IF-5

As with RF-5, the IF-5 module represents a major departure from the design of the original IF amplifier module. The required center frequency of 11.50 MHz and new bandwidth of 100 kHz necessitated a complete redesign of the tuned transformers and their tuning components. Other than the above transformer and tuning changes, the IF amplifier stages are the same in design and construction as in previous modules. The IF amplifier strip is constructed on copper-clad circuit board and this board is mounted horizontally above the module chassis as was the case in IF-1 and IF-2. The lower

deck portion of the IF-5 is used for a mixer and bandpass filter system for the pulse compression system. The detector, DC amplifier, and relay and relay driver circuits are deleted from this module because they are not needed with this system. The IF-5 is currently in use in a pulse compression system at the University of Illinois. The schematic diagram of the IF-5 module is found in Figure **3.7.**

IF-6

The IF-6 module is the latest receiver module constructed and incorporates many improved circuits over those used in the original IF amplifier modules. These improvements are:

(a) Incorporation of a gain control system that is easily controlled with an AGC voltage.

(b) Modification of the gain control circuitry and operating points of the IF amplifier stages to minimize gain variation with temperature.

(c) A completely new DC amplifier system that incorporates feedback stabilization and improved bandwidth.

(d) Incorporation of a relay system so that three consecutive pulse traces can be displayed at different positions on the oscilloscope screen.

The gain control system used in the original receiver provided an adequately wide dynamic range but presented serious drawbacks in a number of later applications. The biggest disadvantages of the base-bias gain control system were the distortion of the signal waveform at low gain settings and variation of amplifier gain stability with temperature. Additionally, the bias control system was not readily adaptable for control by an AGC system, as is required for use in the automatic absorption recording system (Appel and Bowhill, 1965). The gain control circuits developed for use in IF-6 are shunt attenuators connected across the input to the first and third IF amplifier stages.

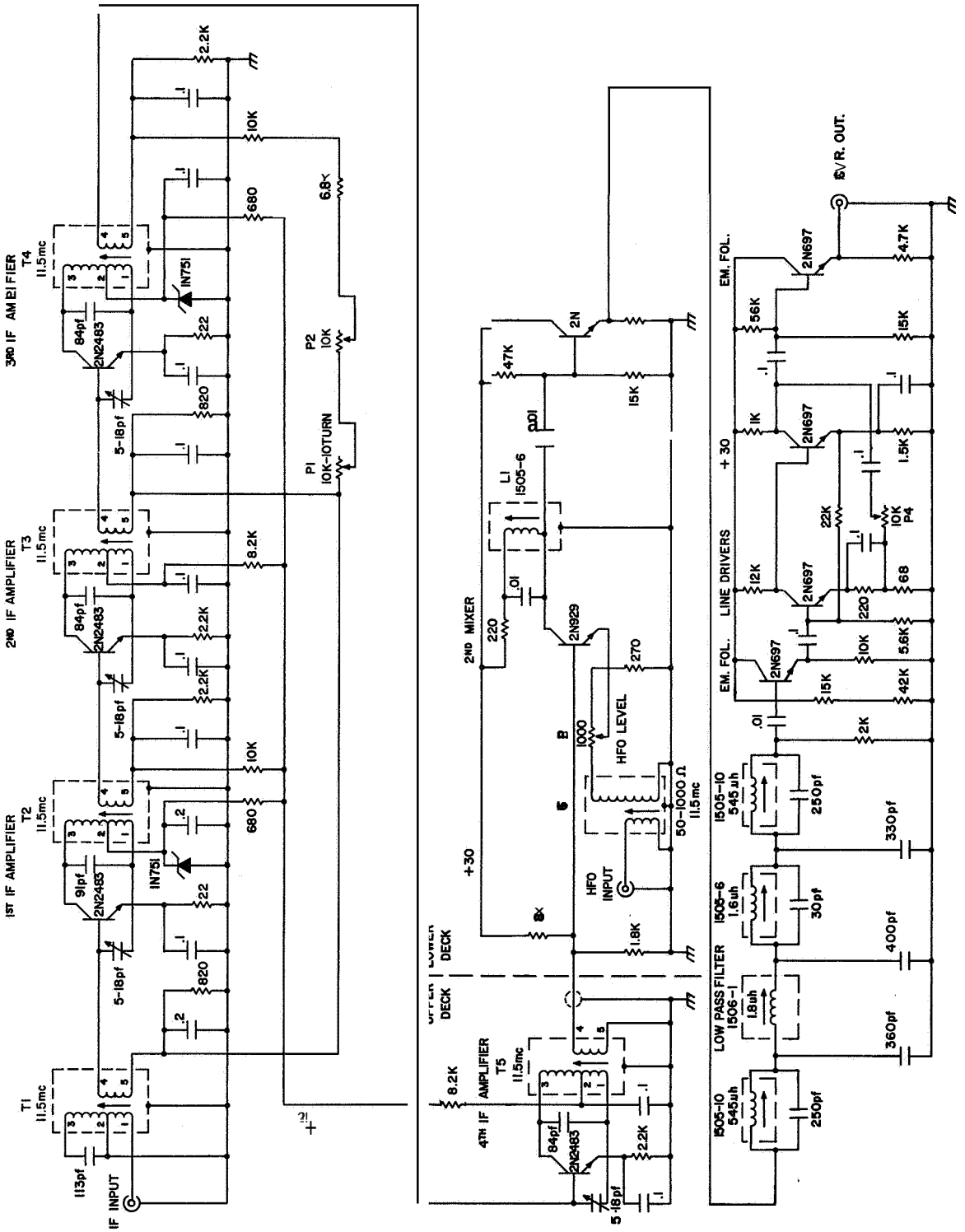

Figure 7 The IF-5 module.

The maximum gain of the IF amplifier chain is still controlled by the base-bias control used previously and its setting is chosen for optimum gain-temperature stability of the overall IF amplifier gain. Variation of the control bias supplied to the shunt attenuators permits the IF amplifier overall gain to be varied from maximum to approximately 40 dB of attenuation below maximum gain,

The temperature instability of the base-bias control system previously used was traced to temperature instability of the h_{fe} of the amplifier transistors at very low collector currents. This is particularly true of a high h_{fe} transistor such as the 2N2483. Experimentation with the 2N2483 transistor amplifiers showed that maximum temperature stability is achieved with collector currents on the order of 1.0 to 1.5 ma. Since the optimum noise figure of the 2N2483 is achieved at collector currents around 1.0 ma, the bias for all IF amplifier transistors is adjusted to obtain collector currents in this range. The bias on the first and third amplifiers is adjusted by means of the Coarse Gain Control for best temperature stability and noise figure of the entire IF amplifier chain, and this setting determines the maximum gain of the IF amplifier. Reduction of IF gain from the maximum gain is controlled by shunt attenuators on the first and third amplifier stages.

A 2N697 transistor is used as the shunt attenuator--the collector to emitter resistance and therefore the shunt resistance across the signal path is controlled by varying the base bias of the 2N697. A 2N697 constant current source in series with the emitter DC return of the shunt transistor minimizes the effects of h_{fe} variations of the shunt transistor with temperature. Control of the bias voltage to the shunt transistor from 5.5 to 15 volts varies the gain of the IF amplifier from maximum to approximately 40 dB

below maximum gain. Two attenuators circuits are required to achieve this dynamic range. The gain of the IF amplifier is varied by means of either a panel-mounted 10 turn potentiometer or an external control voltage of the range mentioned above.

The DC amplifier circuit used in the original receiver design was stabilized as mentioned previously with a matched dual transistor, but further improvement in temperature stability and bandwidth has been found to be quite desirable. A differential DC amplifier using complementary transistors in feedback pairs (Beneteau, 1961) was chosen because of its greatly improved temperature characteristics. Use of the complementary circuit allows the amplifier output to be independent of transistor h_{fe} and dependent only on the collector load resistors and the variations in base-to-emitter voltages between the two NPN transistors (first order approximation). Use of the MD1120 dual transistor for the two NPN transistors reduced the variation of base-to-emitter voltages of the two to a minimum and therefore minimized gain variations of the amplifier with temperature. As before, a 2N697 constant current source is used in the emitter return of the differential amplifier to assure high common-mode rejection. Since the output DC level of the receiver should be referenced at zero volts DC for zero signal input, it was necessary to include a second differential amplifier system. This function could have been performed by a simple inverting amplifier as in the original DC amplifier circuit, but degrading of the temperature stability of the amplifier would have resulted. Therefore, the inversion and DC level-shifting function is performed by a differential amplifier very similar to the input stage except with PNP instead of NPN transistors as the amplifier stages. The zero-signal DC reference of the

amplifier is adjusted by varying the emitter current of the second amplifier. Without feedback, the two stage differential amplifier has an open-loop voltage gain of 750. Twenty-four dB of overall feedback was used to reduce the gain of the amplifier to 45 and extend the frequency response to 100 kHz ($\pm$1.0%). Symmetrical feedback is used from the two differential outputs to the inputs of the amplifier to assure complete amplifier balance. The polarity of the output signal is chosen by selecting with a relay one or the other of the second differential amplifier outputs. The relay driver circuit is the same as used in the original receiver design.

Use of the receiver in an ionospheric drift system required that the reference level of the receiver output be switched to three different voltages so that three concurrent signals could be displayed on an oscilloscope screen and photographed. This function is provided by means of two relays and their associated relay driver circuits. These level-shifting relays change the reference voltage to the differential amplifier from zero volts, as is the case normally, to one of two predetermined bias voltages, thereby shifting the output zero-signal reference voltage and displacing the trace on the oscilloscope. With both relays unenergized, the receiver functions normally with the output voltage referenced to dc ground. Energizing either relay shifts the output reference to either a positive or negative voltage depending upon the setting of the A-Trace or C-Trace Position potentiometers, thus giving a possibility of three distinct output levels on the oscilloscope. An improvement of this system worthy of consideration is replacement of the relays with electronic switching circuitry to improve system reliability.

The schematic diagram of the IF-6 module is found in Figure 3.8. The IF-2 and IF-3 modules have been modified to include the improved gain control circuitry used in IF-6, but these units do not at present incorporate any of the other modifications developed in IF-6.

Power Supply Unit

The third module of the receiver houses the power supplies and regulator circuits for the entire receiver. All voltages supplied to the receiver are electronically regulated and provision is provided for monitoring of all voltages and currents of each unit of the receiver. The following list outlines the voltages required by the various units of the receiver:

+30 volts	Blanking gate generator in RF amplifier unit.
+30 volts	DC amplifier in IF amplifier unit.
+25 volts	Relay driver circuits in IF amplifier unit.
+15 volts	RF amplifier, mixer, and local oscillator circuits in RF amplifier unit.
+15 volts	IF amplifier and gain control circuits in IF amplifier unit.
-30 volts	DC amplifier in IF amplifier unit.

Although both of the +30 volt and +15 volt lines are supplied from one 30 volt and one 15 volt electronic regulator, they are divided in the power supply so that the current to each unit can be monitored separately for maintenance purposes. The original receiver did not incorporate the +25 volt supply, and power for the relay circuits was supplied from the +30 volt regulator. It was found that the switching transients from the relay were causing instability in the blanking and DC amplifier circuits. The addition of a separately regulated +25 volt power supply eliminated this problem.

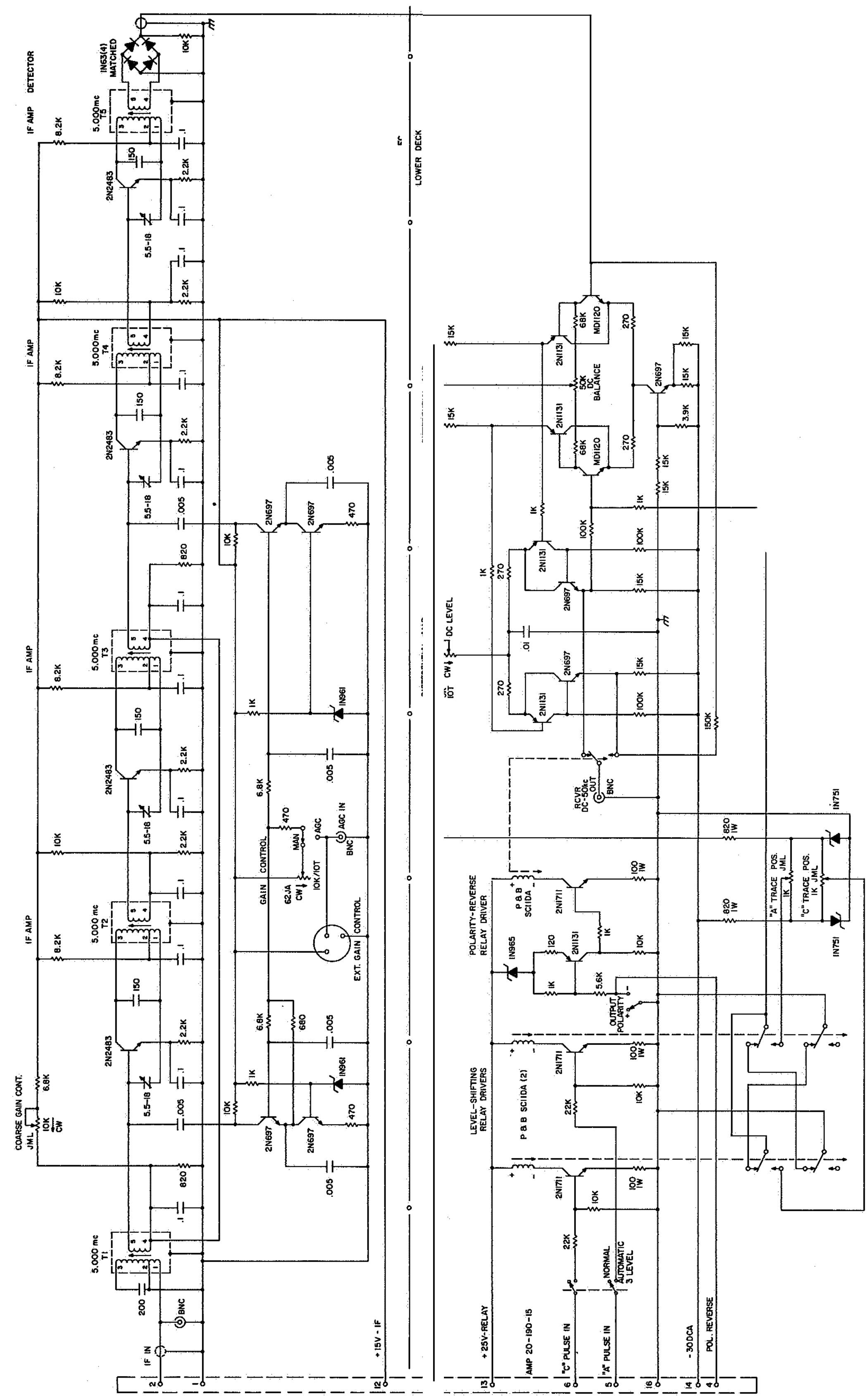

Figure 3.8 The IF-6 module.

The DC voltages for all regulators except the +25 volt circuit are supplied from a single full-wave bridge rectifier circuit. By grounding the center-tap of the power transformer, voltages of +40 volts and -40 volts are obtained from the bridge rectifier. These unregulated voltages, although not used in the receiver at present, are supplied to both the RF and IF amplifier units for versatility in future designs.

The electronic regulator circuits used for the +30, +15, and -30 volt supply voltages are all nearly identical in design. The -30 volt regulator uses equivalent PNP transistors instead vi' NPN transistors as in the positive regulators, but is otherwise identical, A TI487 power silicon transistor is used as the series control element of the regulator. A 2N2102 or 2N697 transistor is used as a Darlington amplifier to control the TI487. A 2N697 is used as the error sensing-amplifier and compares a sample of the output voltage with a zener-regulated voltage. A 2N1131 PNP transistor is used in a preregulator circuit to achieve greater line-voltage regulation and reduction of 120 Hz ripple.

The regulator for the +25 volt line is sitnilar to those discussed above, but is much simpler. because of Lhe less stringent requirements of the relay-driver circuits. A single TI487 is the series control transistor and a 2N697 is the error sensing transistor.

Separate filter circuits are provided for the +40 volt, -40 volt, and +30 volt unregulated voltages. All voltages except the relay energizing voltage are controlled oy the DC-ON switch to provide ease of servicing.

All components of the power supplies art? mounted on the module chassis. All transistors are mounted in stud-mounting heat sinks on the chassis. The 115 volt 60 Hz supply voltage as well as all regulated voltages to the

receiver are carried in the connector in the rear of the power supply unit. Additionally, an external power socket on the front panel of the supply makes all regulated and unregulated voltages available for experimental use or other equipment. These voltages are not monitored by the current meter of the power supply. Metering of the voltages and currents for each circuit of the receiver is provided by one meter that can be switched for use as a current meter or voltmeter. The two series of power supply modules designed and constructed to date are discussed below.

PS-1, PS-2

The PS-1 and PS-2 modules were originally constructed for receivers at the Wallops Island installation in 1964. These units differ from the current models in that an adjustable autotransformer was included in the primary circuit of the power transformer to assure that the peak inverse voltage ratings of the 1N1220 diodes in the bridge rectifier were not exceeded on line voltage surges. Use of the 10DB2A bridge rectifier in the later versions eliminated this problem and the need for the space-consuming autotransformer. The regulator circuits of the PS-1 and PS-2 modules were less sophisticated than those of the present power supplies and did not include the preregulator circuits. In other respects, the PS-1 and PS-2 are very similar to the current series. The schematic diagram of the PS-1 and PS-2 modules is found in Figure 3.9.

PS-3, PS-4, PS-5, PS-6

All four of these modules are identical in electrical design and have minor variations in physical construction. Elimination of the autotransformer used in PS-1 and PS-2 allowed extensive circuit rearrangement for greater ease of servicing. All of these modules incorporate the improved regulator

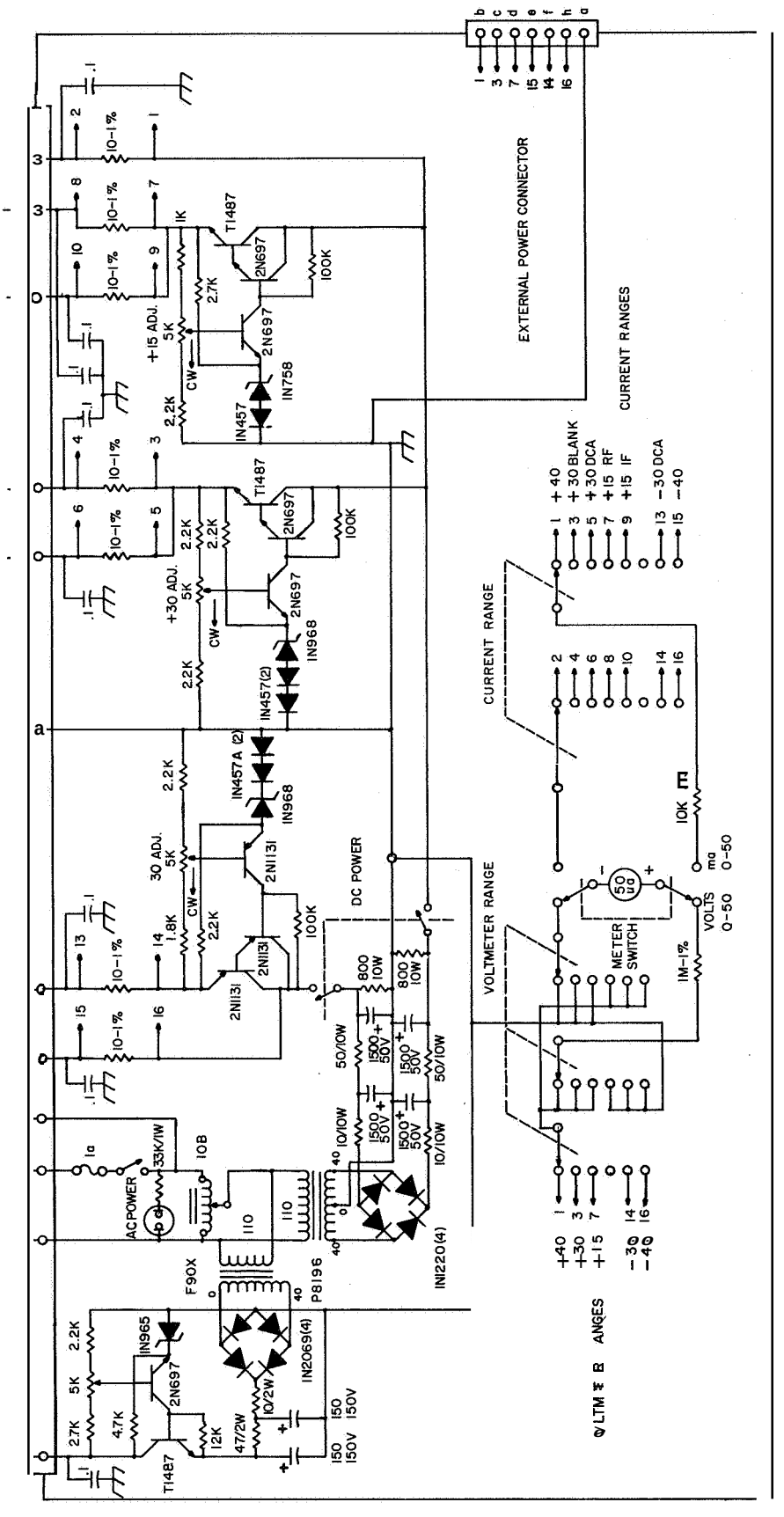

Figure 3.9 The PS-1 and PS-2 modules.

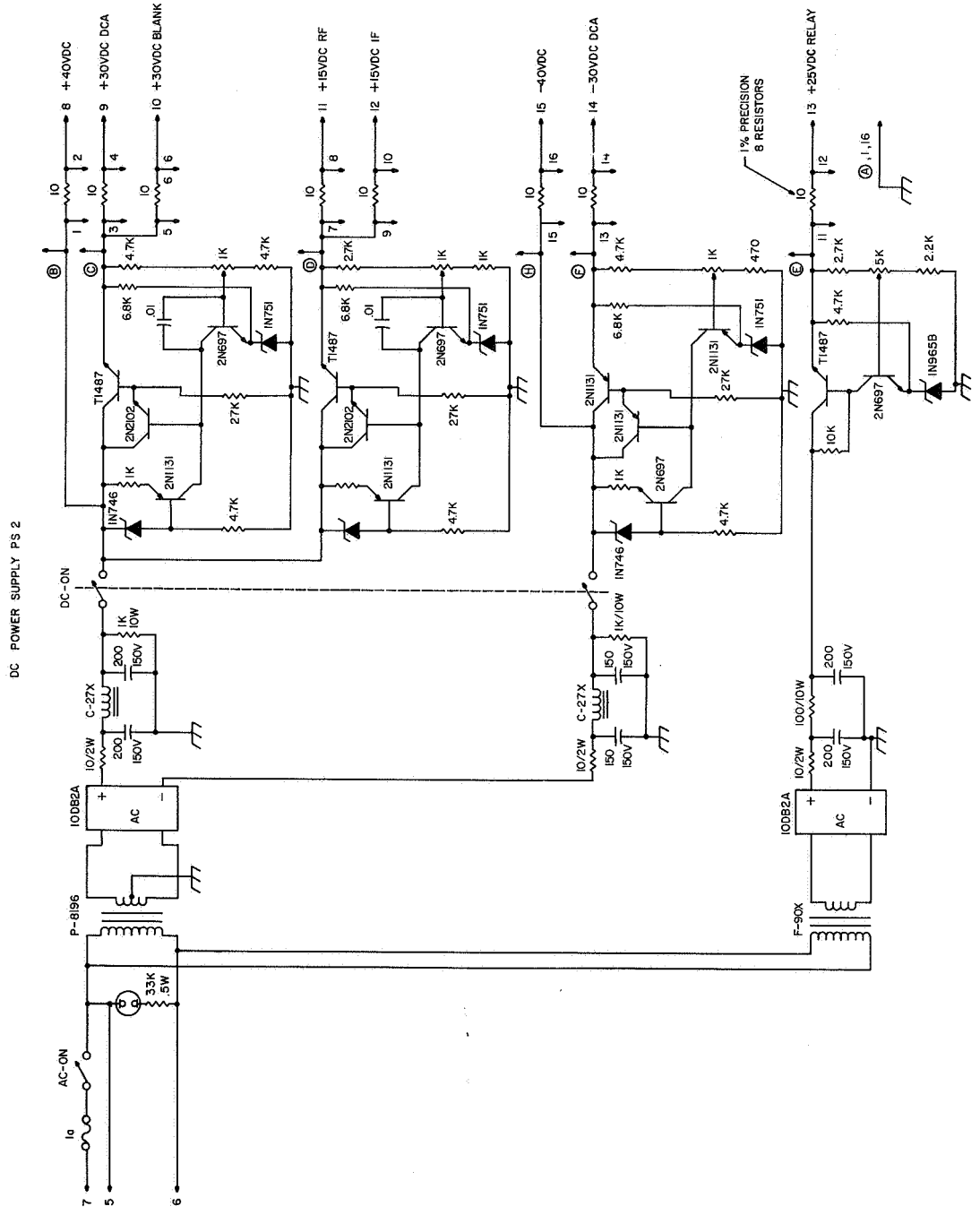

Figure 3.10a The PS-3, PS-4, PS-5, and PS-6 modules--regulator circuitry.

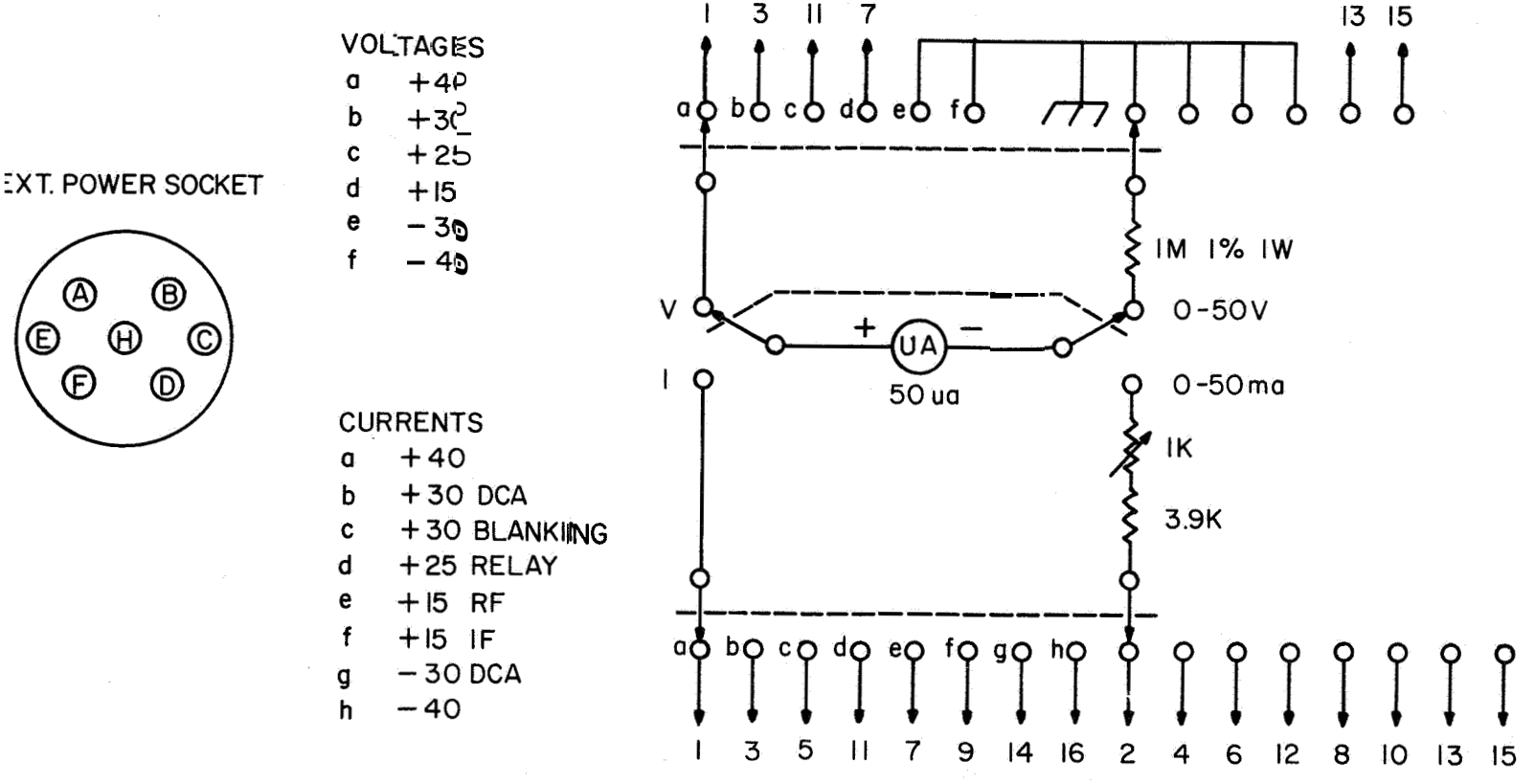

Figure 3 10b The PS-3, PS-4, ⊏⊐-5, and PS-6 modules--metering circuitry

circuits and improved heat sink mounting techniques for the transistors. The PS-5 and PS-6 modules have all four voltage regulator controls mounted on the front panel to permit adjustment of the regulated voltages with the module plugged into the manifold. The schematic diagram of the PS-3, PS-4, PS-5, and PS-6 modules is found in Figure 3.10a and Figure 3.10b.

Receiver Mechanical Design

Since complete shielding of the receiver from external RF fields was a prime requirement of the receiver design, considerable thought was given to the housing and construction of the receiver so that the shielding could be maintained and still have the receiver in such a mechanical arrangement that it is easily serviced and the input center frequency can be easily changed. A plug-in module arrangement can satisfy all of these requirements and does not require appreciably more construction time than a single chassis unit would, The Tektronix Company has used plug-in modules for oscilloscopes for some time with a great degree of success and offers blank plug-in modules for custom amplifier design, as well as storage racks to hold three spare oscilloscope plug-in amplifiers. These storage racks are designed for rack mounting, but are not supplied with any form of shielding. Shielded panels were added to ends of the cabinet and between each of the three sections. The same type of connector as used in the oscilloscope units was used for interconnection of the three receiver units, but they are physically inverted to prevent accidental insertion of oscilloscope units into the receiver or vice versa. All wiring of the unit connectors is enclosed in a shielded cable raceway at the rear of the cabinet, and all power supply leads are individually bypassed at the connector for each module.

The three-module capacity of the cabinet or manifold dictated the division of the receiver circuitry into three units. These three, as described previously, are (1) the RF amplifier unit that includes the RF amplifier, mixer, local oscillator, and blanking gate generator circuits, (2) the IF amplifier unit that includes the IF amplifier, detector, DC amplifier, and relay switching circuits; and (3) the power supply unit that provides all power for the first two units. Although a further subdivision of the modules, particularly the IF amplifier unit, would be quite desirable, this arrangement has worked quite well and provides the needed isolation between the various portions of the receiver. A wiring diagram of the receiver manifold is found in Figure 3.11.

Receiver Performance Characteristics

Calibration of RF and IF gain controls:

Since measurement of ionospheric absorption of the reflected signal requires normalization of the receiver gain over a run of data, an accurate gain control system for the receiver is necessary. As mentioned previously, the gain controls for the RF and IF amplifier stages are 10-turn potentiometers with a dial calibrated from 000 to 1000. The calibration procedure involves the use of a signal generator of known output voltage and an oscilloscope to monitor the detected receiver output. With the control to be calibrated set at maximum gain, the signal generator and remaining control are set so as to give an oscilloscope trace of known amplitude that can easily be measured and reset. The signal generator output voltage is then noted and all further measurements are referenced to this input voltage to the receiver. The output of the signal generator is then increased in

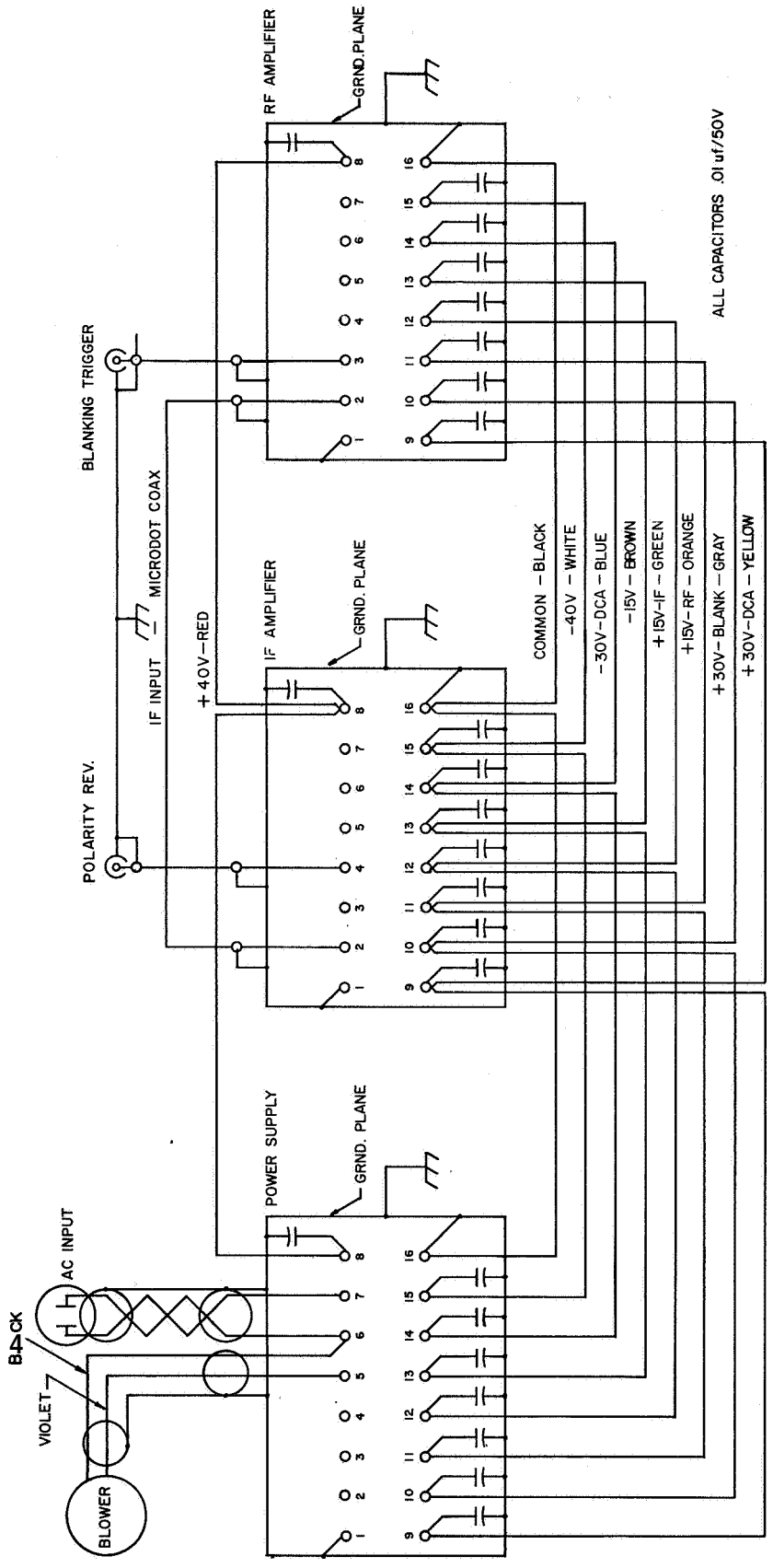

Figure 3.11 The receiver manifold.

constant steps (in this case 2 dB steps were chosen) and the gain control to be calibrated is adjusted to produce the same oscilloscope deflection as originally set up. The gain control dial reading is noted for each step and the characteristic curve of the gain control is plotted from this data. The control characteristics of the RF gain control of the receiver are shown in Figure 3.12. Note that whatever may be the other faults of the base-bias gain control system it is, after all, quite linear. The control characteristics of the original IF gain control are shown in Figure 3.13. This curve is also fairly linear, but shows the effect of controlling two stages simultaneously with the base-bias method. The control characteristics of the improved IF gain control circuit are shown in Figure 3.14. Since this control circuit is used with both the panel-mounted control and an external control voltage, both are plotted as a function of receiver gain. While the characteristics of the control dial reading vs receiver gain is fairly linear, the voltage control curve is far from linear and approaches a logarithmic curve. This characteristic has resulted in compression of one end of the calibration of the automatic absorption system (Appel and Bowhill, 1965) and expansion of the other as shown in Figure 3.15. As long as signals are in the large-signal portion of the curve, the data is easily reduced with great accuracy. However, reduction of data that fails in the low-signal portion of the chart is very difficult. By manual shifting of the RF gain control, the operator can usually keep the recorded signal in the optimum range of the chart, but this is not desirable in a supposedly automatic system. The curve can be linearized with a system of diodes, but a control voltage range of approximately zero to 100 volts would be required, thus requiring stable high-voltage DC amplifiers to be compatible with the present automatic recording system. The voltage

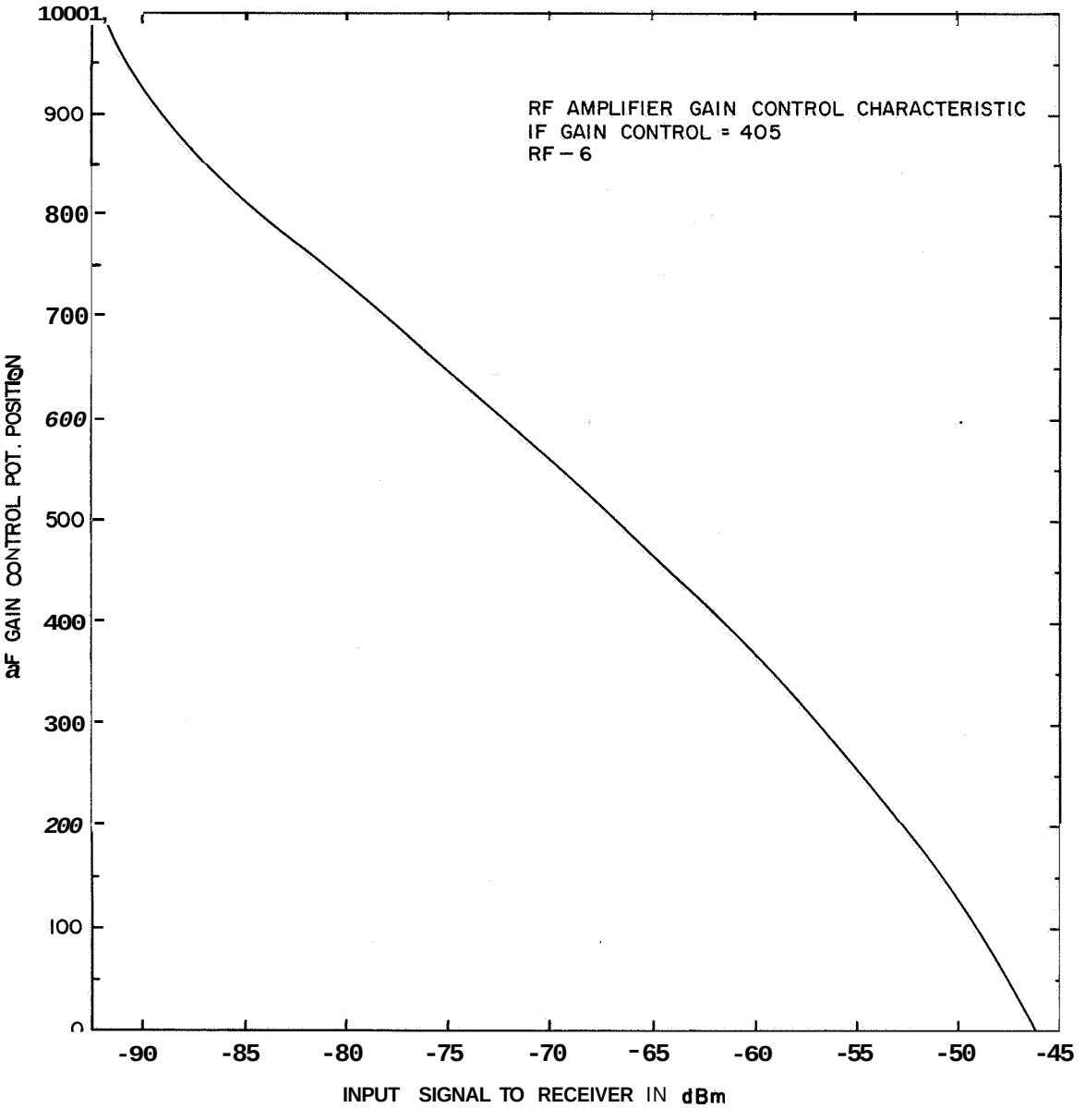

Figure 3.12 Control characteristics of RF Gain control.

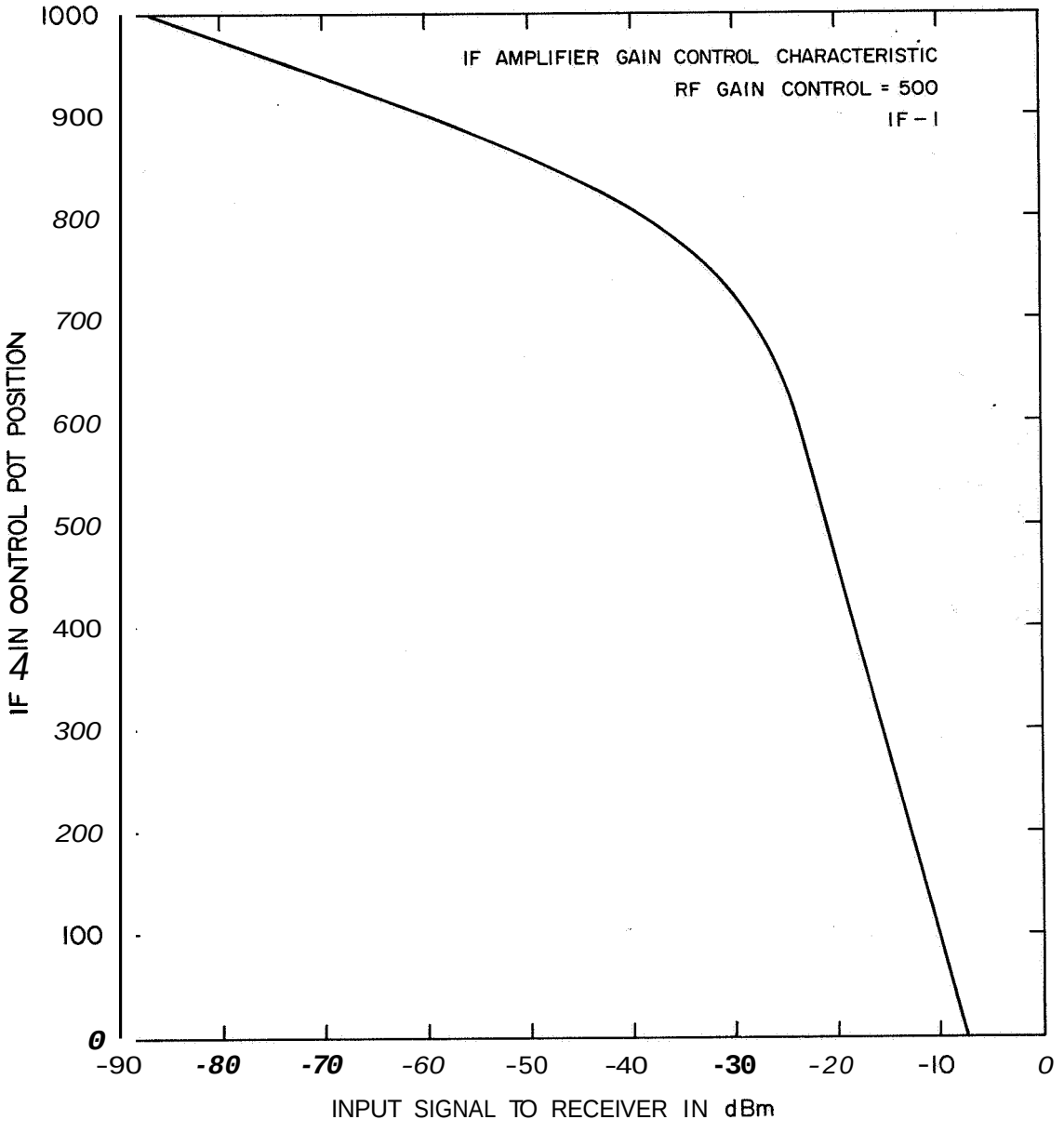

Figure 3.13 Control characteristics of IF Gain control--IF-1.

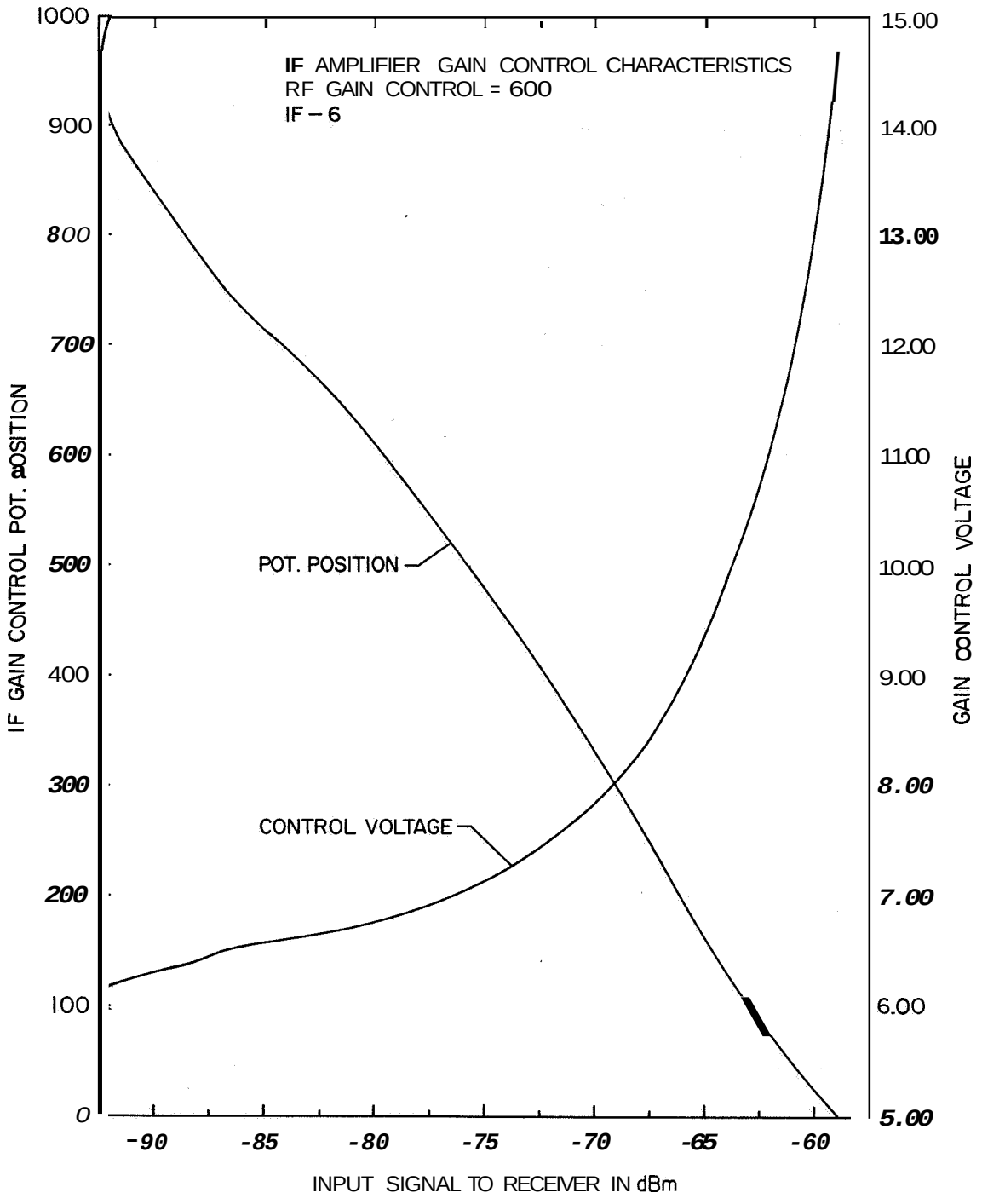

Figure **3.14** Control characteristics **of** IF Gain control--IF-6.

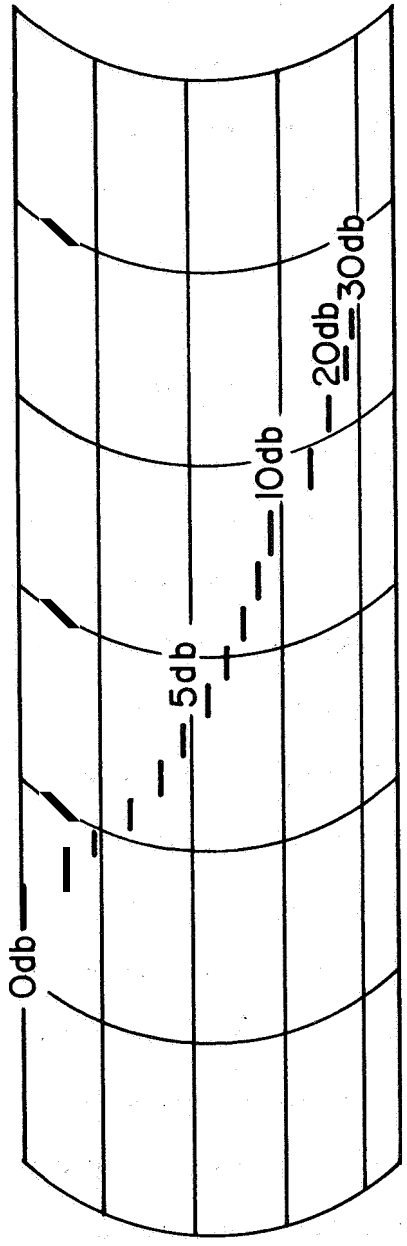

Figure 15 Typical calibration chart of absorption recording system.

control characteristics of field effect transistors are much more easily linearized and consideration is being given to their use in the receiver instead of the 2N2483 transistor presently used. Additionally, the value of the automatic absorption recording system would be greatly increased if a larger dynamic range of receiver gain control were available. Application of the AGC voltage to the RF amplifier stage would achieve this larger dynamic range and assure that there is no condition under which overloading of the RF amplifier stage can occur.

Receiver response characteristics:

The bandpass curve of the receiver (Figure **3.16)** was obtained in a manner similar to the gain control calibration. Since all tuned circuits of the receiver are single-tuned transformers isolated by amplifiers and all are peaked at the center frequency of the receiver, the bandpass curve of the overall receiver is gently rounded at the top with no measureable ripple within the receiver bandpass. Since the IF amplifier frequency is greater than the RF input frequency, the tuned circuits in the RF amplifier and mixer stages appreciably effect the receiver bandpass characteristic. The bandwidth of the IF amplifier chain is actually 75 kHz at the -3 dB points and the effect of the RF and mixer circuits is to reduce it to approximately 55 kHz. This effect also tends to reduce the steepness of the skirts of the receiver bandpass, but this has not been found to be objectionable. Since the transistor device reactance varies with control bias, there is a 5 kHz narrowing of the bandpass curve when the RF gain control is reduced 10 dB from maximum gain position. Below this level, little change in the bandpass response is measured. This problem does not exist with the IF amplifier gain control since the amplifier

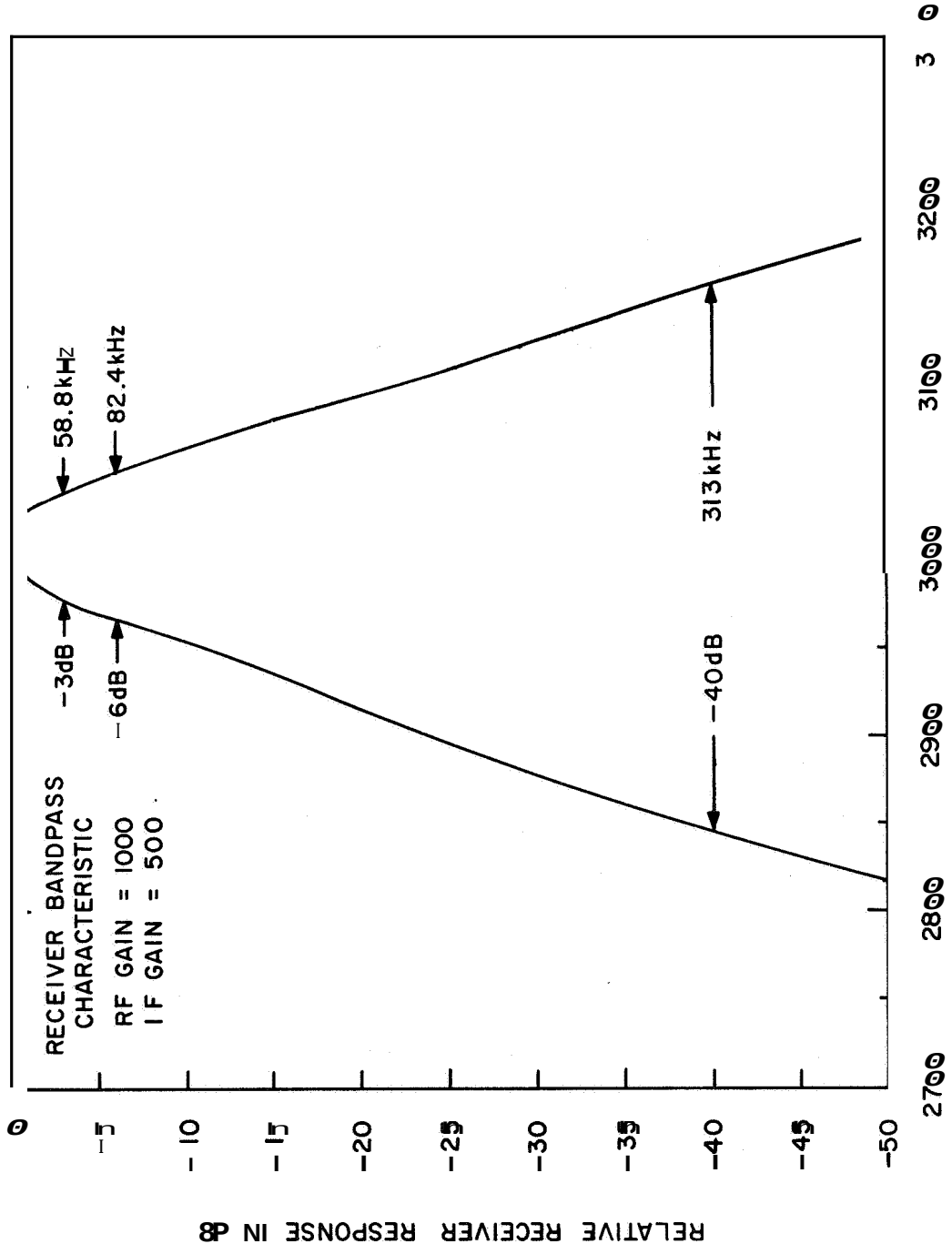

Figure 3.16 Bandpass response of the receiver.

transistors operate with a constant bias while the shunt attenuator transistors control the gain. However, as would be expected with a shunt resistance across the tuned circuit, the bandwidth of the IF amplifier tends to increase as the shunt resistance is lowered and therefore as the IF amplifier gain is lowered. This does not effect the receiver overall bandpass as much as first might be expected since, as previously mentioned, the tuned circuits of the RF amplifier and mixer essentially govern the overall response of the receiver. This bandwidth variation of the receiver with IF amplifier gain has been measured to be less than 5 kHz, increasing as the gain is varied from maximum to 40 dB less than maximum IF amplifier gain. Preliminary tests indicate that the field effect transistor, while not completely immune to Miller-effect capacitance variations with control bias, is considerably better than the bipolar transistor presently used in the RF amplifier and does not show the shunting property of the present IF amplifier chain. The use of the field effect transistor is being given further consideration at this writing.

Since the receiver is intended for use in reception of pulsed RF signals, its response to a pulsed signal is definitely of interest. Figure **3.17** shows the typical output obtained from the receiver with a square RF pulse input (the RF input pulse is the upper trace and the receiver output is the lower trace). Since the receiver bandpass of 50 kHz is only sufficient for the 5th order sidebands of a 50 μsecond square pulse, the output pulse is rounded and has a Gaussian shape. The time delay between the input pulse and the output pulse represents the actual time delay of the receiver. As long as the phase shift of the receiver is a linear curve within the receiver bandpass and the time delay does not

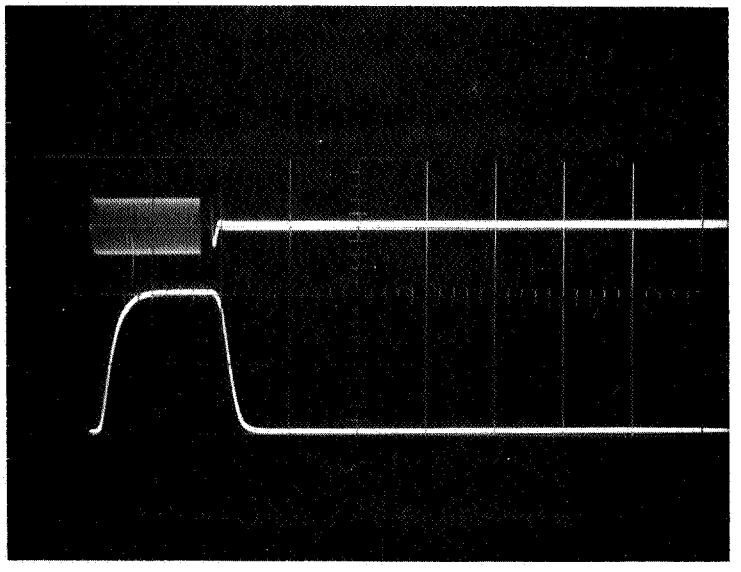

Figure 3.17 Receiver response *to* a pulsed RF signal.

change with receiver gain, this delay is easily cancelled out in the data reduction process or, in the case of filmed recording, the oscilloscope trace is simply delayed by an amount equal to the time delay of the receiver., The most recent timing and control systems designed include a provision for a delayed trigger to provide compensation for both receiver and transmitter-originated delays.

The measured receiver sensitivity is 0.4 μvolt of signal for an observed signal-to-noise ratio of 1.00. Taking into consideration bandwidth of the receiver, the noise figure was calculated to be approximately 2.0 dB, depending upon the accuracy with which a signal-to-noise ratio of 1.00 can be measured. In practice, this sensitivity has proven to be more than that required, because of the high level of man-made and atmospheric noise at the frequencies of interest (2 to 5 MHz).

The gain of the receiver has been measured as constant within 1.5 dB over an eight hour period of operation in a sounding system. This gain change has been traced to h_{fe} variations of the RF amplifier transistor with temperature and, to a smaller degree, to drift of the power supply regulator voltage. Experiments with field effect transistors ind'icate that they do not exhibit these gain variations with temperature. The use of temperature compensated reference diodes in the power supply should prevent voltage drift.

The crystal-controlled local oscillator stability was measured to be within 500 Hz of center frequency 15 minutes after turning the receiver on and within 100 Hz throughout the remainder of an eight hour operation schedule. The tunable oscillators used in the RF-3 and RF-4 modules have a short-term stability of ±3 kHz and a long term stability of ±250 Hz. While more stable tunable oscillators are fairly easily achieved with temperature

compensation techniques, the wide bandwidth of the receiver and the signals to be received do not require stabilization beyond this point.

Past and Future Receiver Designs

Receiver Design Using Ceramic Ladder Filters:

As mentioned previously, the initial design of the receiver involved the use of ceramic ladder filters in the IF amplifier stage to determine the receiver bandpass, These filters, constructed by the Clevite Corp. are composed of seventeen ceramic discs in an electromechanically resonant system. The filter chosen for the receiver was the TL-50D-75C and has the following parameters:

Center frequency	500 kHz $\pm$2 kHz
Bandwidth at -6 dB	50 kHz
Bandwidth at -60 dB	75 kHz
Shape factor	1.5:1
Insertion loss	3 dB
Ripple within passband	3 dB maximum (peak-to-valley)
Input and output impedance	1200 ohms resistive

The most attractive feature of the filter is the very steep skirt selectivity which is in fact considerably better than that achieved in the final version of the receiver. The input and output impedances of the filter are ideally suited for use in transistor circuitry, as is the physical size. A block diagram of the proposed receiver design using these filters is shown in Figure 3.18. Since the phase response of the receiver had to be as linear as possible throughout the passband, the IF amplifiers were designed to be very wide band video amplifiers and all selectivity and phase response were therefore controlled by the filters. A schematic diagram of the IF amplifiers designed and constructed for use with these filters is shown in Figure 3.19. This IF amplifier uses three

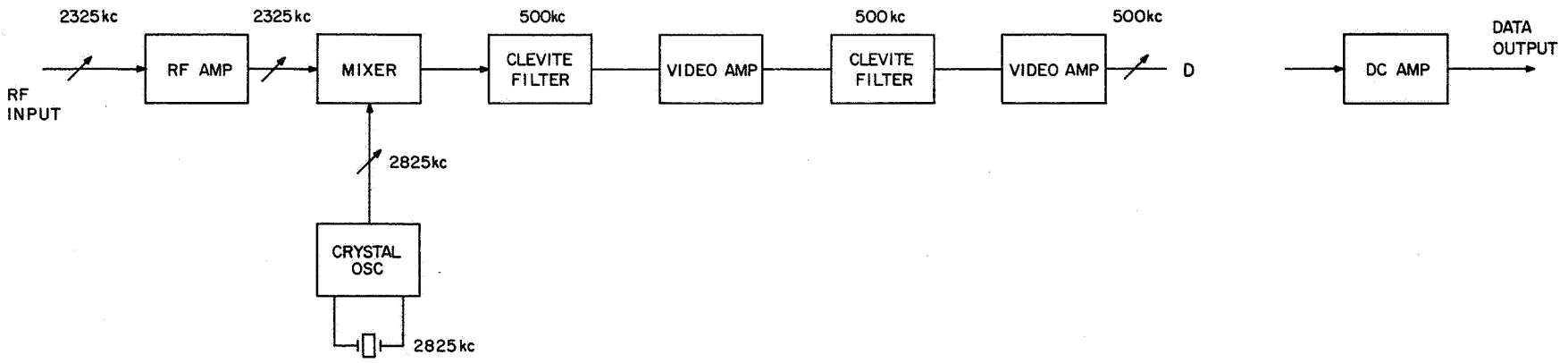

Figure 3.18 Block diagram of receiver with ceramic filters.

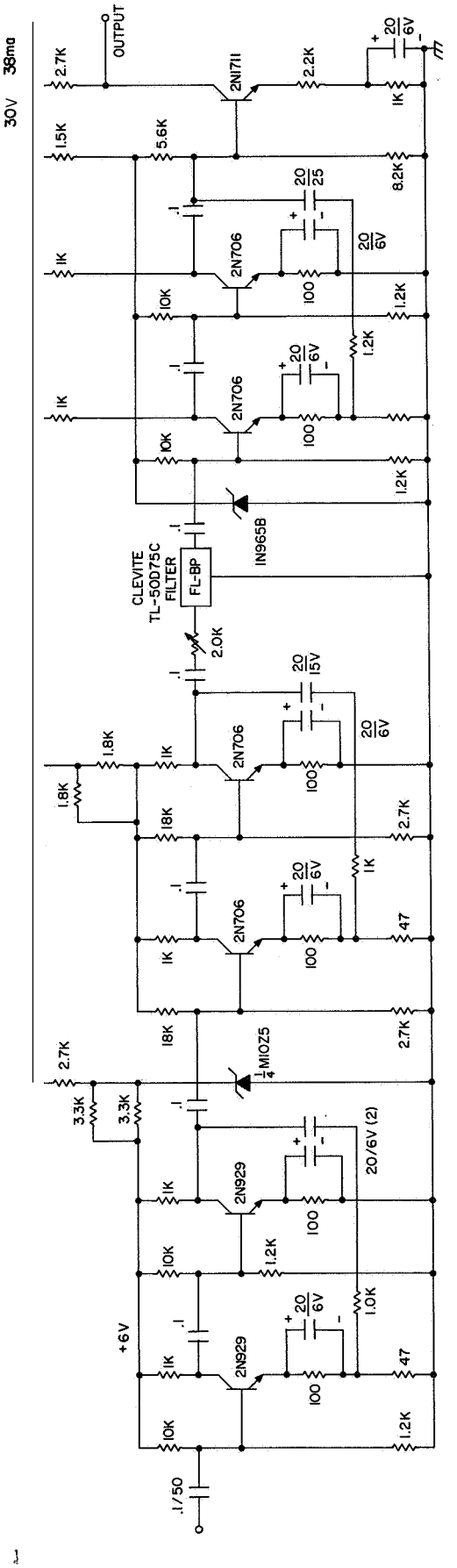

Figure 3.19 Amplifiers used with ceramic filters.

two-transistor video amplifiers, (Texas Instruments, 1963) two ahead of the filter and one after. Each video amplifier has a typical response from 50 kHz to 15 MHz ±3 dB. The overall gain of the circuit is 67 dB at 500 kHz and the bandpass response of the amplifiers and filter is shown in Figure 3.20. The 2,000 ohm potentiometer at the input of the filter provides a means of adjusting the filter feed impedance.

Upon testing of this circuit with a pulsed RF signal, it was discovered that the filter generated serious spurious signals of the same order of magnitude as the original signal in the form of ringing. Adjustment of both feed and load impedances of the filter reduced this problem somewhat, but not sufficiently to give acceptable results. The response of the filter to a pulsed RF signal is shown in Figure 3.21. After much experimentation, it was determined that this ringing was due to mismatch of the filter's input and output impedances. Measurements of the filter itself showed that the intrinsic impedance was not at all constant throughout the bandpass. Use of several filters in series reduced the ringing still further, since the filters all exhibited similar impedance characteristics, but no more than 20 dB of rejection of the ringing was obtainable. The behavior of the filter has been likened to that of an incorrectly terminated transmission line in that, due to mismatch at both the input and output, a pulse is reflected at both ends of the filter, producing the ringing observed. Short of a very complex termination and feed network or an infinite chain of identical filters, these units are not adaptable for use in a pulse receiver. This ringing effect has since been noticed in receivers using other varieties of mechanical filters and seems to be inherent in all such filters. For the above reasons, the receiver design incorporating

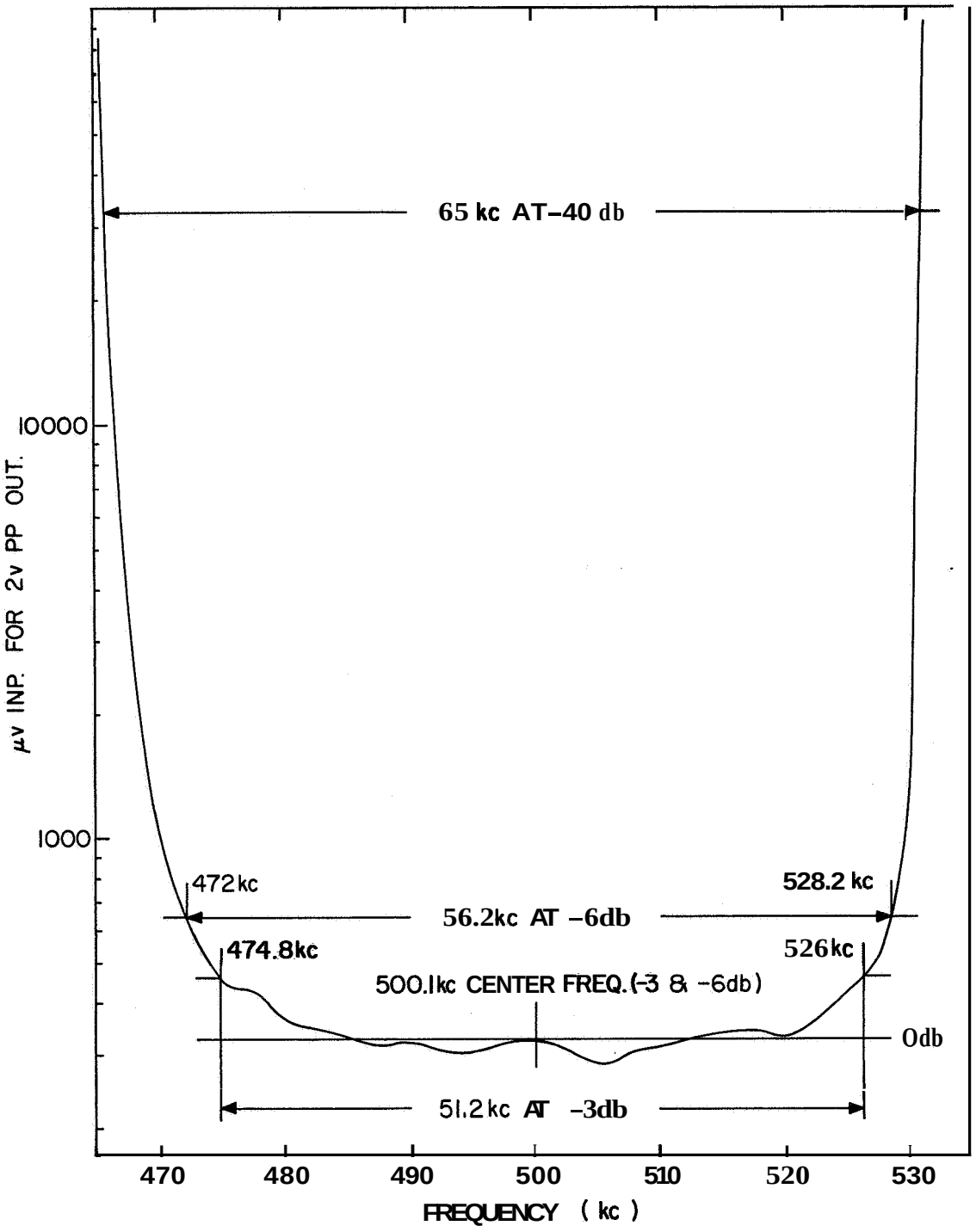

Figure 3.20 Bandpass response of ceramic filter.

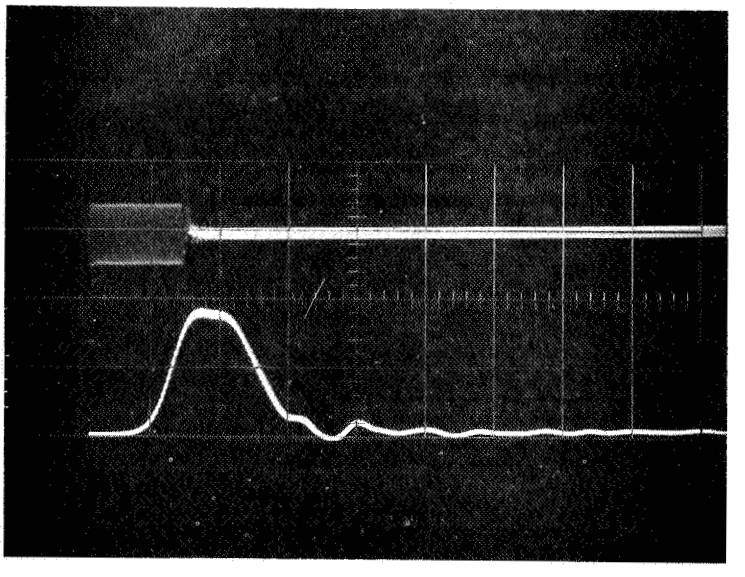

Figure **3.21** Response of ceramic filter to a pulsed RF signal.

the ceramic filters was finally abandoned in favor of the more conventional tuned transformer system used in the present receivers.

An Electronically Switched RF Preamplifier:

The use of the receiver in an ionospheric drift experiment necessitated the design and construction of an electronically switched preamplifier that would select one of three spaced antennas upon command from the timing and control system. Although this unit was not used in the shipboard experiment, a brief explanation of it is included in this report so that a complete description of all electronic instrumentation currently in use for ionospheric sounding measurements will be available for future reference.

The switched preamplifier uses three RF amplifier stages, all very similar in design to that used in the receiver itself. The output tuned circuit of each amplifier is designed to drive a 50 ohm coaxial cable instead of the mixer input, as is the case in the receiver. The input transformer of each amplifier is identical to that used in the receiver input circuit. All components of the three amplifiers, particularly the transformers and transistors, have been matched as closely as possible to assure that the gain and phase characteristics of each channel are nearly identical. The channel switching operation is accomplished by gating the base bias circuitry of each amplifier. A positive pulse applied to the 2N697 gate transistor applies a positive pulse to the amplifier bias circuit. The amplitude of this pulse is limited to 10.0 volts by a 1N961 zener diode to assure that the amplifier gain is the same for each gate pulse. A blanking gate generator that is identical to that designed for the receiver is included to provide blanking of all three amplifiers during the transmitter pulse. The power supply and regulator

circuits are patterned after those designed for the receiver. To provide a means of calibrating the three amplifiers for identical gain, a test switch is included. This switch allows each of the amplifiers to be separately connected to a standard signal source (usually a signal generator).

In using the preamplifier for drift measurements, the three spaced antennas are connected to the three inputs of the unit. Three gate pulses, generated by the timing and control system, gate the preamplifiers on and off in sequence. The outputs of the three switched amplifiers are mixed and connected to the input of the receiver previously described in this chapter. The sequencing of the gate pulses to the switched amplifier and those applied to the three-level switching circuit in the receiver DC amplifier is such that the "A" trace occurs first in time and is displayed at the top of the oscilloscope screen with the "B" and "C" pulses appearing in sequence thereafter. Each amplifier is capable of a maximum gain of 20 dB and a gain control dynamic range of 35 dB. Since the amplifiers are identical to the RF amplifier stage of the receiver, the noise figure of the combination is still approximately 2 dB at maximum gain. The bandwidth of each preamplifier is approximately 200 kHz and some reduction of the overall preamplifier-receiver bandwidth has been noted. The schematic diagram of the electronically switched preamplifier is found in Figure 3.22.

Field Effect Amplifier:

As mentioned in the above discussions of the RF and IF amplifier stages of the receiver, consideration has been given to the use of field effect transistors instead of the 2N2483 bipolar transistor presently employed. A breadboard circuit in the form of a single stage preamplifier has been designed and

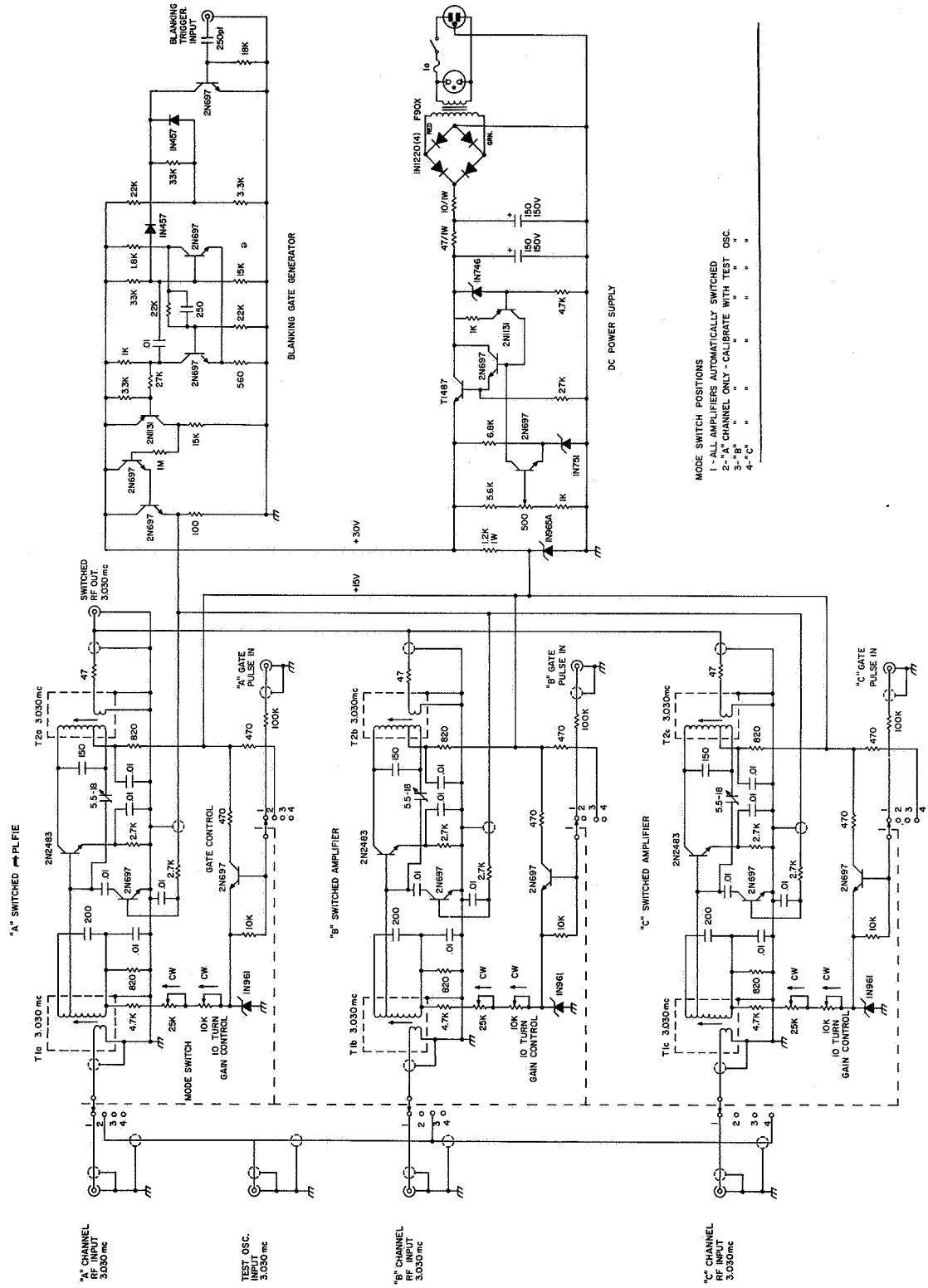

Figure 3 22 Electrically switched preamplifier

constructed for testing of the FET. The schematic diagram of this breadboard amplifier is found in Figure 3.23.

A 3N126 tetrode field effect transistor was chosen for this test amplifier because of its excellent noise characteristics in the 2 to 5 MHz range and because of the ease with which its transconductance and therefore gain can be controlled. The amplifier is a common drain circuit with signal injection on gate 1 and AGC control on gates 1 and 2. The FET is a high impedance device (50 kilohms typical input and output resistance in the 2 to 5 MHz range) and therefore impedance matching with the input and output transformers is not attempted. The bandwidth of the amplifier is determined primarily by the unloaded Q of the two transformers. Although no resistive loading of either transformer was included in this amplifier, it would probably be necessary to include some form of loading to achieve the same bandwidth as that of the original receiver. The primary purpose of the breadboard design was to investigate the low-signal, temperature stability, and AGC performance of the FET. The maximum measured gain of the FET amplifier at 3.030 MHz was 24 dB and the noise figure of the amplifier at maximum gain was 2.1 dB. The dynamic range of the gain control was found to be 52 dB if both gates of the transistor were varied from zero to 3.4 volts.

Since linearity of the gain control circuit of the present receiver has proven to be less than optimum, considerable experimentation was carried out on the FET amplifier circuit to obtain the best possible voltage vs dB attenuation characteristic curve. As can be readily seen from Figure 3.24, the characteristic control of the gate bias of the FET (point "X" in Figure 3.24) is far from linear. In fact, the curve exhibits a very sharp knee at approximately 3.2 to 3.3 volts. The shape of this knee is very similar

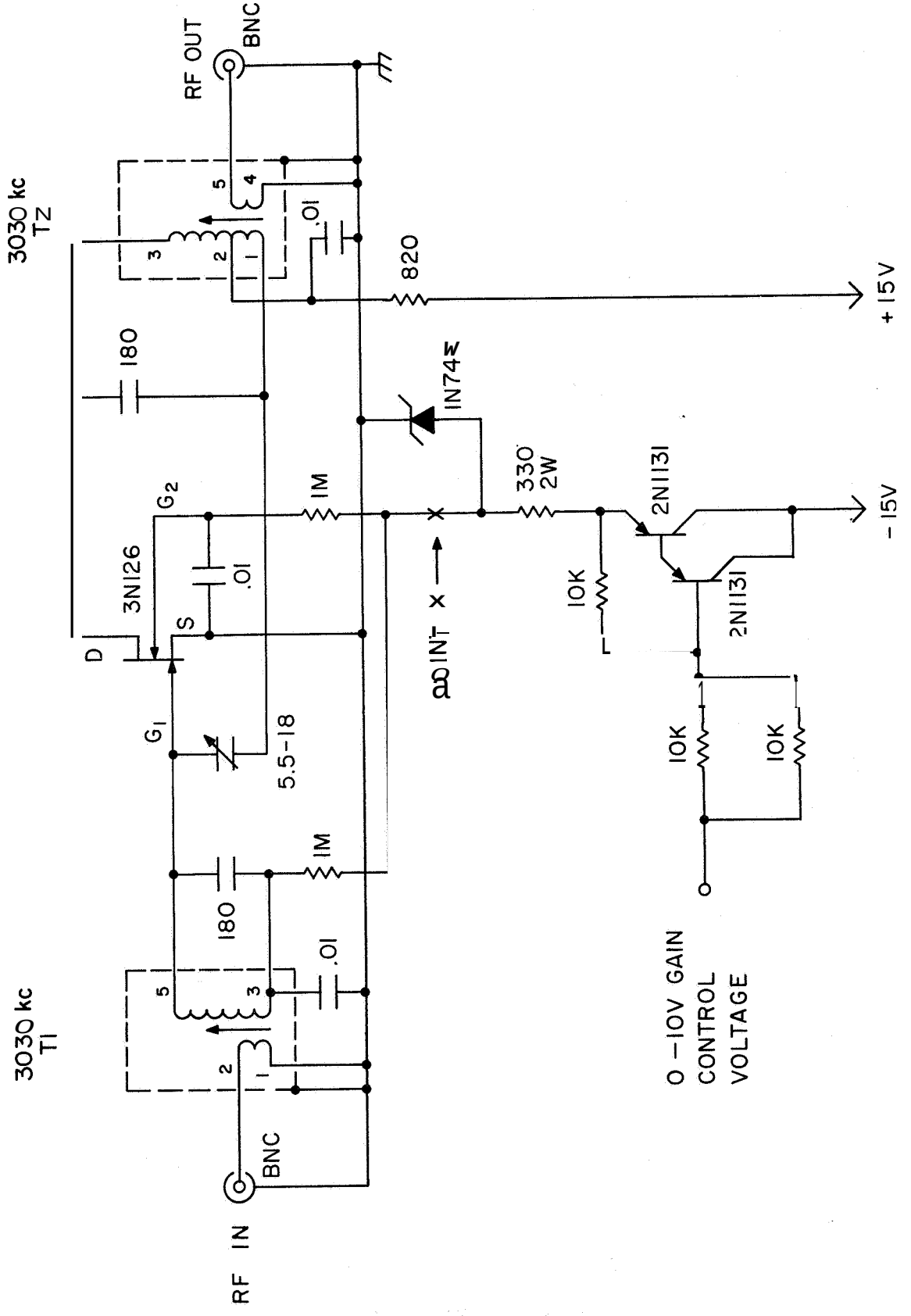

Figure 23 Breadboard FEM amplifier

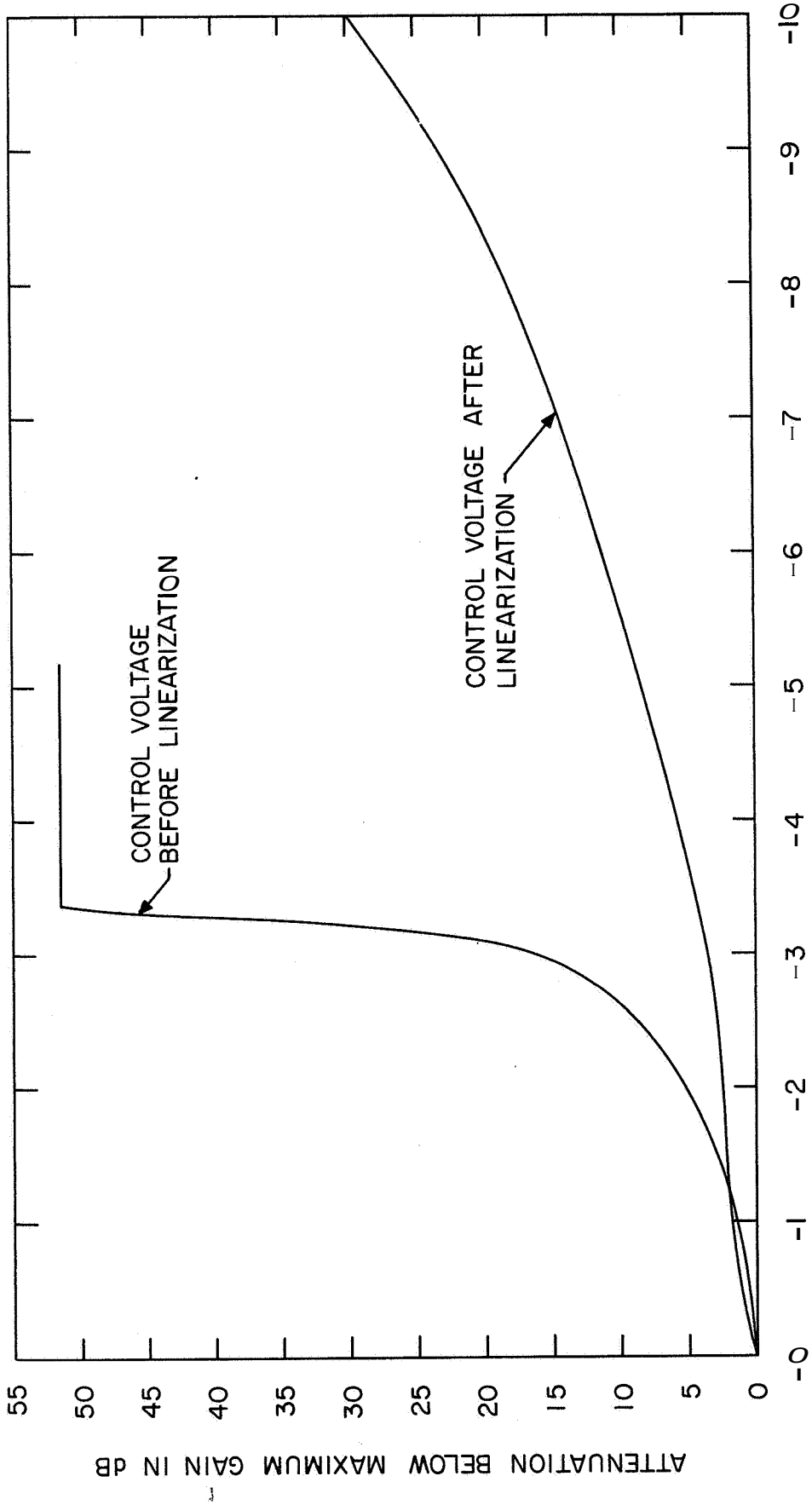

Figure 24 Control characteristics of FET amplifier.

to the voltage-current curve of a zener diode with a 3.3 volt firing voltage. In fact, the use of a zener diode across the gate bias circuit resulted in a much more linear curve. Because the driving point impedance of the zener-compensated control circuit is on the order of 500 ohms, it was necessary to include a Darlington amplifier to control the circuit with the existing AGC amplifiers in the automatic absorption recording system (Appel and Bowhill, 1965). Adjustment of the resistor in series with the zener varies both the control voltage range and shape. The 330 ohm resistor shown in Figure 3.23 was chosen as a compromise between the maximum control voltage range of 10 volts, the best linearity of the curve, and the requirement of at least a 30 dB dynamic control range. As can be easily seen from Figure 3.24, the resulting control curve is much more linear than any other control circuit previously used in the receiver. A stability check of the FET amplifier showed 1 dB of gain variation over the temperature range from 0° to 100° C--significantly better than any previous amplifier designs. Serious consideration is being given to the use of this FET amplifier in both the RF and IF amplifier stages of the receiver. An unfortunate aspect of the FET amplifier is that its DC control. voltage range is not compatible with the AGC range of the present IF amplifier. In fact, the two are inverted with respect to each other. This problem could easily be resolved with a one-stage DC amplifier, but a great deal of attention must be paid to temperature stability of such an amplifier to avoid degrading the stability of the entire system. Since the FET seems to be an inherently more temperature-stable device than the bipolar transistor, it is thought that a one-stage P-channel DC amplifier might fulfill the requirements (Sevin, 1965). The versatility of the FET gives rise to many

intriguing possibilities for application in future receiver designs (Mergner, 1966).

4. TRANSMITTER DESIGN

General Requirements

The transmitter requirements of the shipboard ionospheric sounder were as follows:

1.	Power Output	50,000 watts during pulse
2.	Pulse Width	50 microseconds
3.	Pulse Repetition Rates	1/2, 1, 2, and 5 pps
4.	Center Frequency	2.00 to 3.50 MHz
5.	Output Impedance	50 ohms, unbalanced

6. All transmitter units to be completely enclosed in shielded cabinets to prevent interference to other equipment.

The basic design of the transmitter closely follows the design of an ionospheric sounding transmitter designed by A. B. Gschwendtner in 1964 for use in land-based measurements at Wallops Island, Virginia. The major differences between the two transmitter designs are the tunable feature of the shipboard transmitter, complete shielding of all units in the shipboard transmitter, 50 ohm unbalanced output impedance of the shipboard transmitter as Compared to the 250 ohm balanced output impedance of the Wallops transmitter, and major improvements in the design of the shipboard transmitter driver-amplifier stage to assure adequate RF driving power to the final amplifier stage. The following discussion of transmitter design has been restricted to the design of the shipboard transmitter only, but all schematics and a brief discussion of the Wallops transmitter are included in the pages following this discussion.

All units of the shipboard transmitter were constructed in completely enclosed cabinets mounted on standard 19-inch relay rack panels. The entire transmitter occupies a total of 96 inches of vertical rack space.

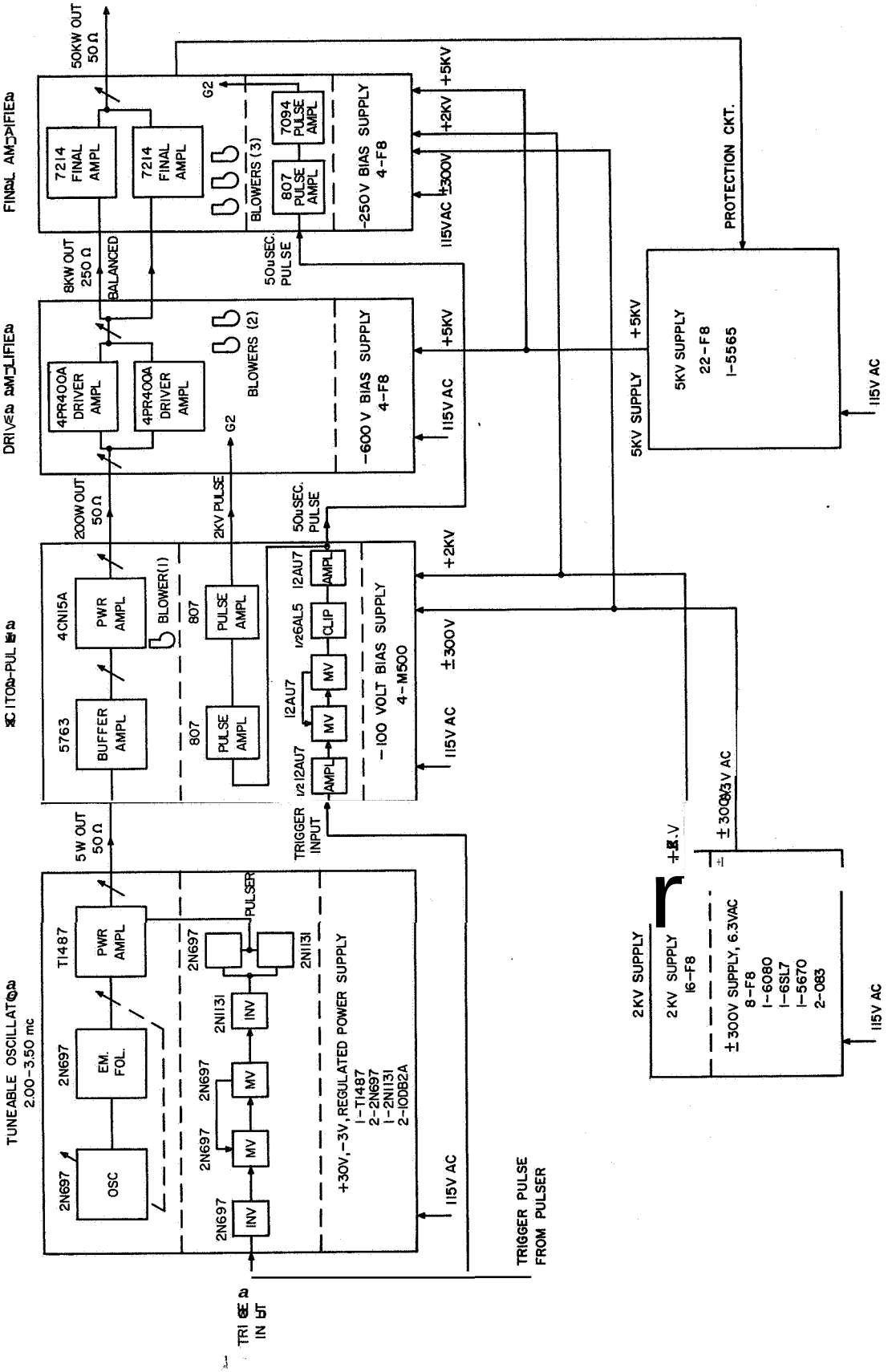

Figure 4.1 Block diagram of transmitter.

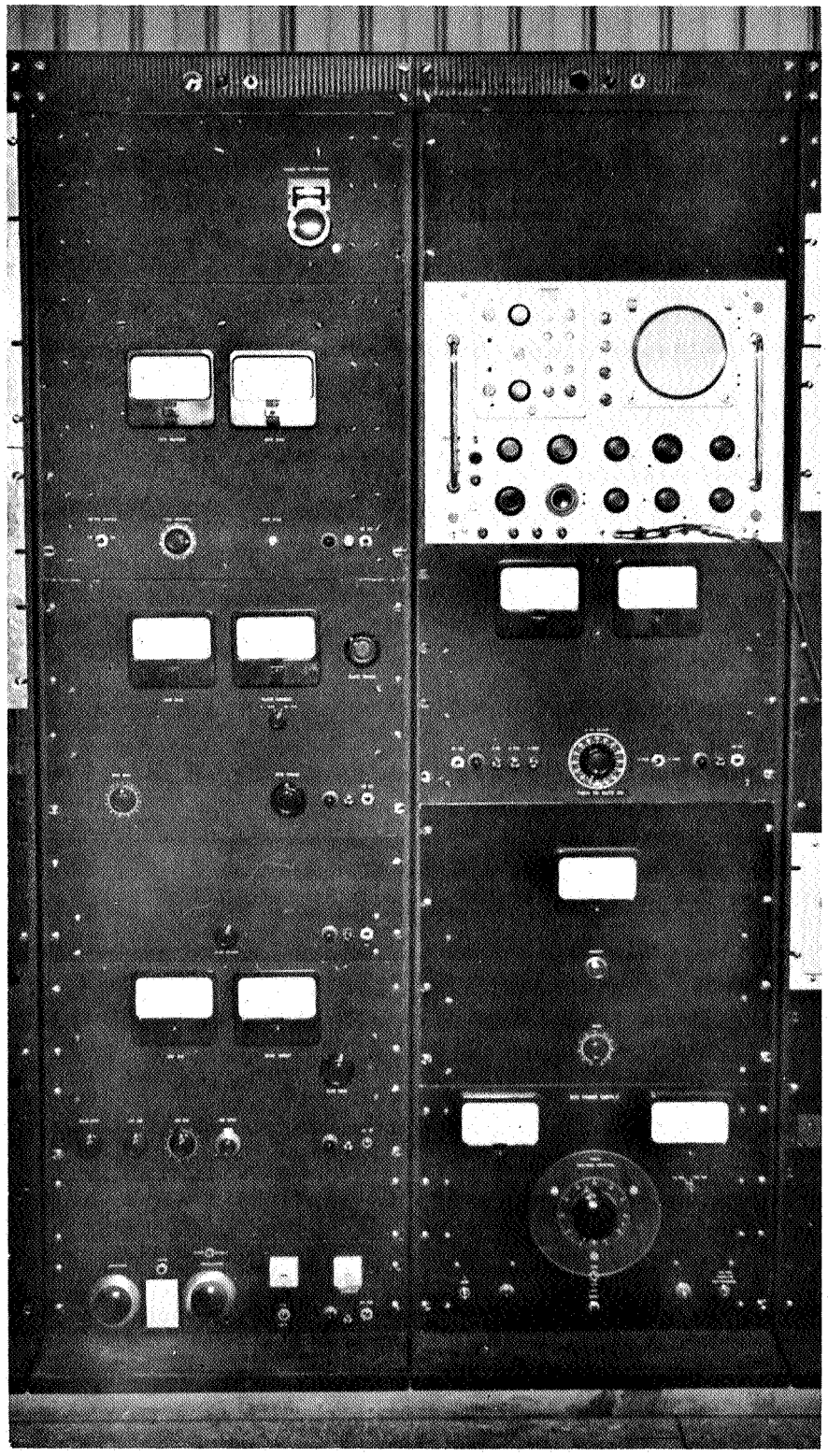

Figure 4.2 The transmitter.

Discussion of the transmitter design is divided into the following sections, in which the various units are described individually:

Tunable pulsed oscillator unit

Excitor and pulse modulator unit

Driver and amplifier stage

Final amplifier stage

Improved final amplifier stage, bias supply, and pulse modulator stage

Low-voltage power supply

High-voltage power supplies

Wallops Island transmitter

A block diagram and a photograph of the complete shipboard transmitter are found in Figures 4.1 and 4.2, respectively.

Tunable Pulsed Oscillator Unit Design

The tunable pulsed oscillator unit is composed of an oscillator stage, buffer amplifier stage, power amplifier stage, pulse generator and pulse modulator stages, and low-voltage power supply stage. All circuitry of this unit is transistorized to achieve best" frequency stability and to minimize heat generation. To further guarantee frequency stability, the entire unit is housed in a shielded enclosure fabricated from 1/8-inch thick brass plate and the circuitry is constructed on 1/8-inch thick epoxy-fiberglass copper-clad board. Also, all power supply voltages to each stage are electronically regulated. The schematic diagram of this unit is found in Figure 4.3.

A single 2N697 transistor in a Hartley oscillator circuit generates a continuous wave signal at the desired frequency of operation. The operating frequency of the transmitter is determined by the resonant frequency of the

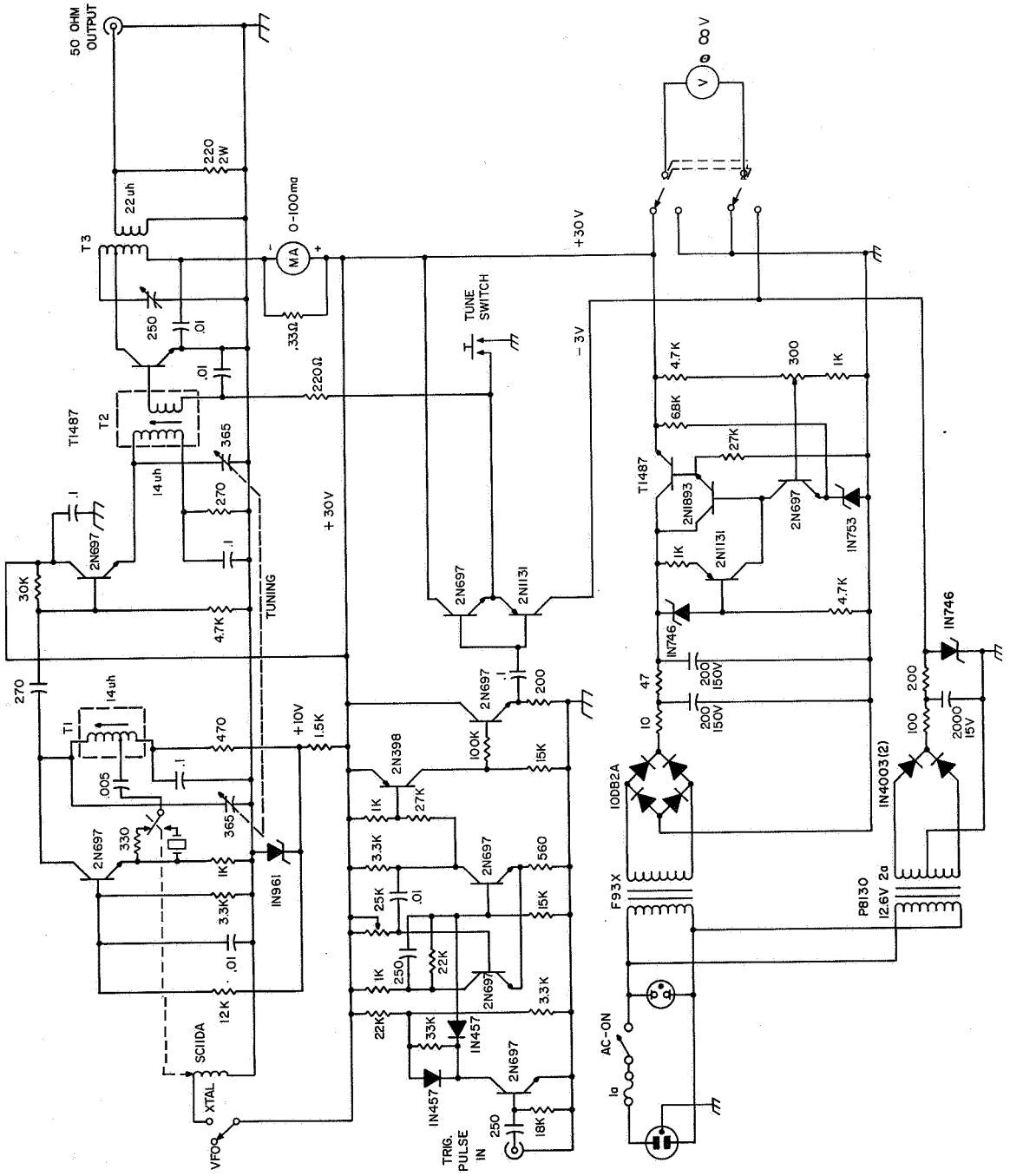

Figure 4.3 The tunable pulsed oscillator.

collector tuned circuit of the oscillator and is variable from 2.00 to 3.66 MHz. Provision for fixed frequency, crystal-controlled operation of the transmitter is included in the oscillator stage. The crystal is operated in its series resonant mode in the emitter feedback path of the oscillator stage. A small frequency variation of ±200 Hz from the center frequency of the crystal can be achieved by varying the collector tuned circuit, but the most stable operation in the crystal-controlled mode is achieved when the collector circuit is tuned to the crystal frequency. The long-term stability of the oscillator stage has been measured to be ±1 part in 10^4 in the tunable mode and 1 part in 10^5 in the crystal-controlled mode, either of which is sufficient for the pulsed measurements for which the system is designed. The collector and base bias supply voltage for the oscillator is regulated with a 10 volt 1N961 zener diode to prevent frequency instability due to supply voltage variations.

The oscillator stage is followed by a 2N697 emitter-follower buffer amplifier to eliminate frequency instability caused by the variable nature of the pulsed load presented by the pulsed amplifier stage. The tuned circuit in the emitter of this stage is necessary to reduce "cross-over" distortion of the RF waveform and to provide an impedance transformer to match the input impedance of the pulsed amplifier stage. The transformer has a turns ratio of 4:1 and, therefore, an impedance ratio of approximately 16:1. (Note: The exact impedance ratio of the transformer depends upon the coefficient of coupling between primary and secondary, but experimentation with the Cambridge Thermionic shielded coil form assembly 1181 has shown that bifilar winding of primary and secondary on these forms permits very high coefficients of coupli'ng to be achieved.) The input impedance of the pulsed amplifier stage is approximately 100 ohms during the pulse. The emitter impedance of the buffer amplifier stage is therefore approximately 1600 ohms. The input impedance of an emitter-follower

stage is approximately h_{fe} times the emitter impedance (first-order approximation), or 150,000 ohms at 3.00 MHz in parallel with the base-bias resistors. Therefore, the load on the oscillator stage changes from 18,000 ohms between pulses to 16,500 ohms during the pulse, a change that has proven to produce little frequency variation of the oscillator.

The pulsed amplifier stage uses one TI487 transistor in a common-emitter, base-pulsed RF amplifies circuit. Adequate shielding of the base and collector circuits and the low gain of this stage permitted design without neutralization. The class B amplifier delivers approximately 5 watts of pulsed RF energy at the operating frequency into a 50 ohm load. The base of the TI487 transistor is normally biased to -3 volts between pulses and to a DC base current of 18 ma during the pulse to achieve on-off keying of the amplifier.

The tuned circuit in the collector of the TI487 provides impedance matching from the collector to the 50 ohm output load. In order to achieve a loaded Q of 20 or more in this tuned circuit, it was necessary to tap the collector down on the primary. The output of the amplifier is coupled through a four turn link on the bottom of the tuned circuit. The TI487 transistor is stud-mounted to the circuit board to provide the small amount of heat transfer required for operation at CW or high repetition rates, Metering of the collector current is provided to aid in tuning of the amplifier output circuit. A push-button in the base circuit of the TI487 permits the amplifier to be operated in the CW mode for further aid in tuning.

A seven transistor circuit generates the 50 microsecond pulse to gate the base of the pulsed amplifier stage. A 2N697 transistor inverts the positive trigger pulse generated by the timing and control unit and triggers a two

transistor (2N697) monostable multivibrator circuit that generates a 50 microsecond pulse for each trigger pulse. A two stage amplifier incorporating one 2N398A and one 2N697 transistor shapes the pulse and couples it to the two transistor pulse modulator stage (2N697 and 2N1131) which pulses the base of the output amplifier.

An electronically regulated 30 volt supply powers all stages of the pulsed oscillator unit and a -3 volt zener regulated supply generates the bias voltage necessary to cut off the output amplifier between pulses. A voltmeter is switchable between the 30 volt and -3 volt supplies for continuous monitoring purposes.

The entire pulsed oscillator unit is constructed in the brass box previously mentioned and is mounted on a 5 1/4-inch rack panel. The tuning capacitor for the oscillator and buffer amplifier stages is a standard two-gang 365 pf per section variable capacitor. Tuning of the output amplifier stage is accomplished with a separate capacitor, necessitating two adjustments for each change in frequency. This approach was chosen in preference to using a three gang capacitor because of the difficulties associated with achieving proper tracking of the three gangs.

A future improvement planned for the oscillator stage is to generate the operating frequency by heterodyning a crystal-controlled frequency with a variable frequency and gating the mixer and crystal-controlled source to achieve on-off keying. A much higher degree of rejection of the signal frequency between pulses may be achieved with this technique, reducing shielding requirements and making possible the use of this same oscillator unit for receiving system calibration.

Excitor and Pulse Modulator Unit Design

The excitor and pulse modulator unit is composed of a 5763 RF amplifier and a 4CN15A power RF amplifier stage that is capable of delivering approximately 150 watts during the pulse to a 50 ohm unbalanced load. Also included in the unit is a pulse generator circuit and high-voltage pulse modulator circuit. The entire unit is constructed in a shield enclosure mounted on a 10 1/2-inch relay panel. The schematic diagram of this unit is found in Figure 4.4.

The output of the pulsed oscillator unit is coupled directly to the grid of a 5763 class C amplifier stage. Although drive requirements for the 5763 would be much less if impedance matching had been used in the grid circuit, the problems of additional tuning adjustments and neutralization of a tuned-plate tuned-grid circuit more than offset any advantages of impedance matching. Moreover, by designing all circuits to provide more than adequate drive for the following stage, all amplifiers are operated well below their maximum ratings, improving the long-term reliability of the system. The output of the 5763 amplifier, and therefore the drive to succeeding stages, is controlled by varying the screen voltage to the tube (RF Drive Control). The tuned circuit in the plate of the 5763 is the tuning adjustment for both the 5763 stage and the grid circuit of the 4CN15A amplifier stage (Grid Tuning Control).

The excitor power amplifier stage uses one Eimac 4CN15A tube in a tuned RF amplifier circuit. (The 4CN15A is a version of the 4CX300A designed specifically for pulse operation at low duty cycles.) This stage is keyed by a 1000 volt pulse applied to the plate and, through a dropping circuit, to the screen. The screen grid is operated at 300 volts during the pulse by using two OA2 gas regulator tubes to limit the pulse amplitude. Experimentation with these gas regulator tubes has shown that they will ionize and regulate within 4

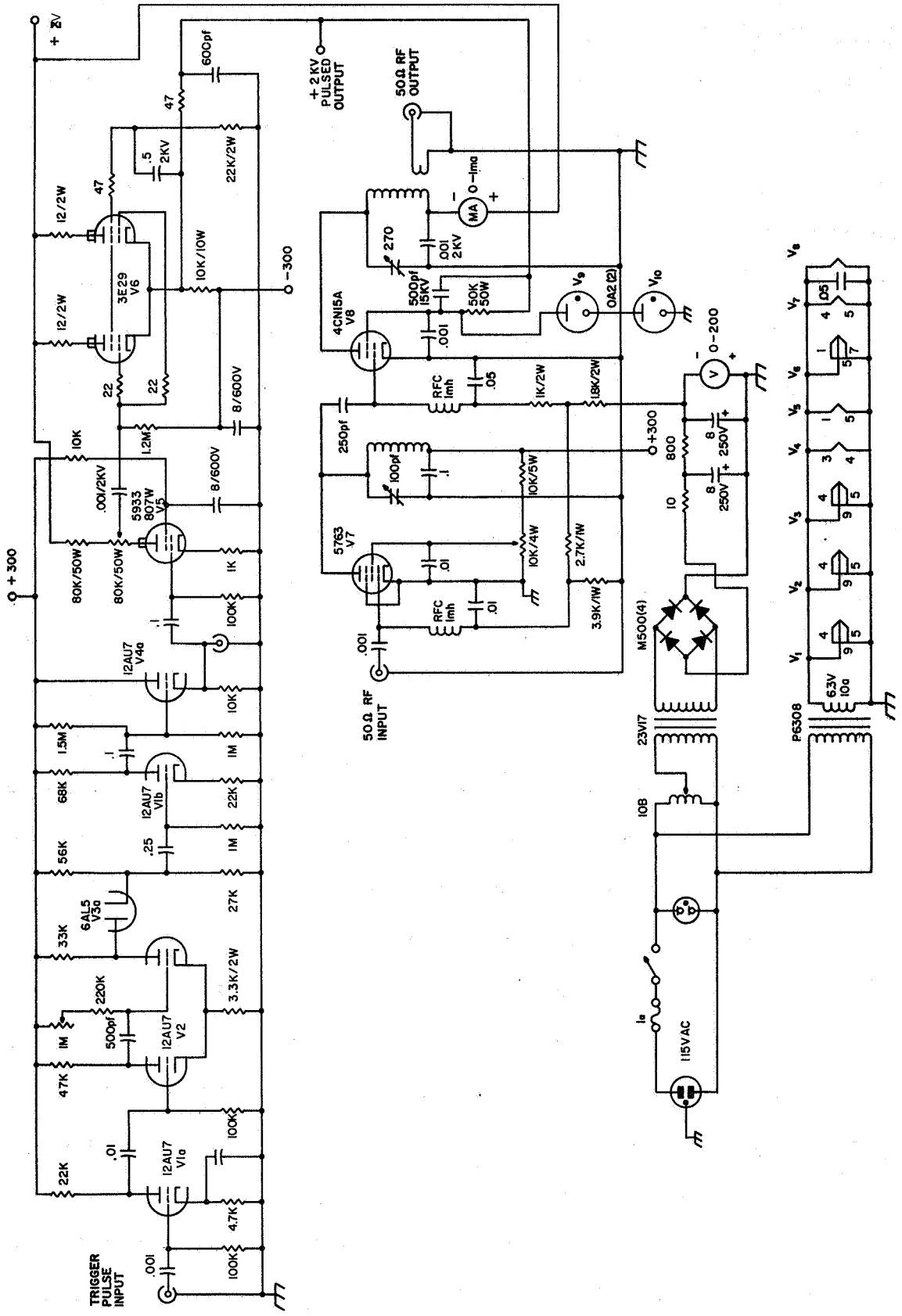

Figure 4.4 The exciter and pulser.

microseconds with a maximum overshoot of approximately 75 volts. The overshoot requirement is particularly important because of the 400 volt DC rating of the screen by-pass capacitor built into the Eimas SK-700 socket used. The manufacturer rates the capacitor at 1000 volts DC tests, but experience has shown that this rating is the absolute maximum voltage the capacitor can handle before breakdown occurs. The gas tubes greatly improve the reliability of the 4CN15A amplifier stage.

The tuned output of the 4CN15A amplifier (Plate Tuning Control) is coupled to the 50 ohm coaxial cable output by means of conventional link coupling, The impedance transformation ratio was determined empirically with a Wayne Kerr B601 impedance bridge.

An adjustable bias supply constructed on the same chassis as the 5763 and 4CN15A stages provides -100 volts of fixed bias for these stages.

Also constructed on the same chassis is the pulse generator circuit and pulse modulator circuit. The trigger pulse generated by the timing and control unit is inverted in a 12AU7 stage and applied to a 12AU7 50 microsecond monostable multivibrator, The pulse width is adjusted with a potentiometer in the grid circuit of the second triode of the "one-shot?' (Pulse Width Control). This pulse is shaped and amplified in the following stages of the 6AL5 and 12AU7 tubes, The resultant 60 volt negative pulse gates the pulse modulators for the excitor, driver, and final amplifier units of the transmitter (50 μsec pulse output).

The pulse modulator circuit for the excitor and driver stages uses an 807W/5933 tube as a pulse amplifier and a 3329 tube as a pulse modulator to provide a +1000 volt pulse for keying of the plate and screen-gride circuits of the 4CN15A and the screen-grid circuit of the 4PR400A driver tubes. The output

of the pulse modulator is clamped at –300 volts under conditions of no pulse input to assure complete cut–off of the keyed stages.

Filament requirements of these pulse tubes as well as those of the 5763 and 4CN15A tubes are supplied by a single 6.3 VAC filament transformer also located on the excitor chassis. The f300 volts required for the pulse and 5763 stages is supplied by the Low–voltage Power Supply unit.

4CN15A 100 Watt Excitor Amplifier Design Notes

DC plate supply voltage, E_{bb} (during pulse) = 1,000 volts

DC screen supply voltage, E_{c2} (during pulse) = 300 volts

DC control grid bias voltage, E_{cc} = –100 volts

RF Drive is adjusted so that:

Max inst. plate current, i_b max = 0.800 amps

Min inst. plate voltage, e_b min = 75 volts

Max inst. grid voltage, e_c max = +2.5 volts

The 5–point "Chaffee" [1936] approximation technique is used to obtain the following parameters for the tube during the pulse.

DC plate current, I_{bb} = 200 mA

DC screen current, I_{c2} = 20 mA

DC control grid current, I_{cc} = 14 mA

Peak fundamental RF plate current, i_{b1} = 360 mA

Peak fundamental RF grid current, i_{c1} = 25 mA

RF power output, P_o = 167 watts

DC plate power input, P_{in} = 200 watts

Plate circuit efficiency, η_p = 83.5%

RF driving power, P_d = 1.28 watts

RF plate load resistance, R_{pl} = 2,560 ohms

RF grid driving resistance, R_g = 4,100 ohms

The plate tuned circuit was empirically designed with the Wayne-Kerr impedance bridge to match the 2500 ohm plate load to the 50 ohm coaxial line. The primary winding is designed for a minimum loaded Q of 10 with an inductance of 30 µhy. A single section 30 to 250 pF variable capacitor tunes the output tank.

The grid input resistance is sufficiently close to that of the 5763 plate circuit that no matching system is required. The grid tuned circuit is likewise designed for a minimum loaded Q of 10.

A future improvement planned for this stage is to remove the pulse circuits to a chassis separate from the RF circuitry. .Some trouble has been experienced with spurious triggering of the "one-shot" by stray RF generated by the 4CN15A stage. Extensive shielding of both circuits has reduced the problem considerably, but physical separation is the logical solution, .Additionally, some thought has been given to the possibility of transistorizing both the 5763 and 4CN15A stages. Current advances in semiconductor construction indicate that 100 watts of pulsed RE' power at 2.00 to 3.50 mc/s is fairly easily and economically achieved. The principal advantages of such a design would be reduction of heat, elimination of filament transformers, and elimination of the need for a high-voltage power source.

Driver Amplifier Stage

The driver amplifier stage is a push-pull class C power amplifier capable of delivering approximately 5,000 watts of RF energy during the pulse to the' grids of the final amplifier tubes, A bias supply is constructed in the same

unit as the driver, but all other voltages are furnished by separate power supplies. The entire unit is constructed in a shield enclosure and mounted on a 14-inch rack panel. The schematic diagram of the driver amplifier stage is found in Rgure 4.5.

Two Eimac 4PR400A tetrodes are used in a class C, push-pull amplifier stage. These tubes are designed specifically for use in pulsed service and incorporate larger cathode elements to withstand higher pulse currents than would be expected in continuous-wave operation. The 4PR400A tubes easily provide sufficient driving power to the final amplifier without exceeding any of their ratings.

The tubes are keyed by pulsing the screen supply with the same pulse modulator used to key the 4CN15A stage of the excitor. The screen voltage is approximately 1000 volts during the pulse and -300 volts between pulses.

The 100 watt output of the excitor stage is link coupled to the push-pull grid tuned circuit. Control grid bias is furnished by the -600 volt supply constructed on the same chassis as the driver stage. The bias supply is completely adjustable from 0 to -850 volts and is metered for monitoring purposes.

An Eimac SK-410 air-system socket and chimney is used for each 4PR400A. Separate 15 cfm blowers are used to cool each tube. Since the duty cycle of the transmitter is very low, cooling requirements are minimal.

The plate circuit of the amplifier is a conventional push-pull balanced tuned circuit designed for a loaded Q of approximately 12. The secondary winding drives the grids of the final amplifier tubes directly. The plate circuit is tuned with a large 100 pF variable capacitor (Plate Tuning Control). A meter in series with the cathode leads of the tubes provides continuous indication of combined plate, screen and control grid current. Since the DC plate current of

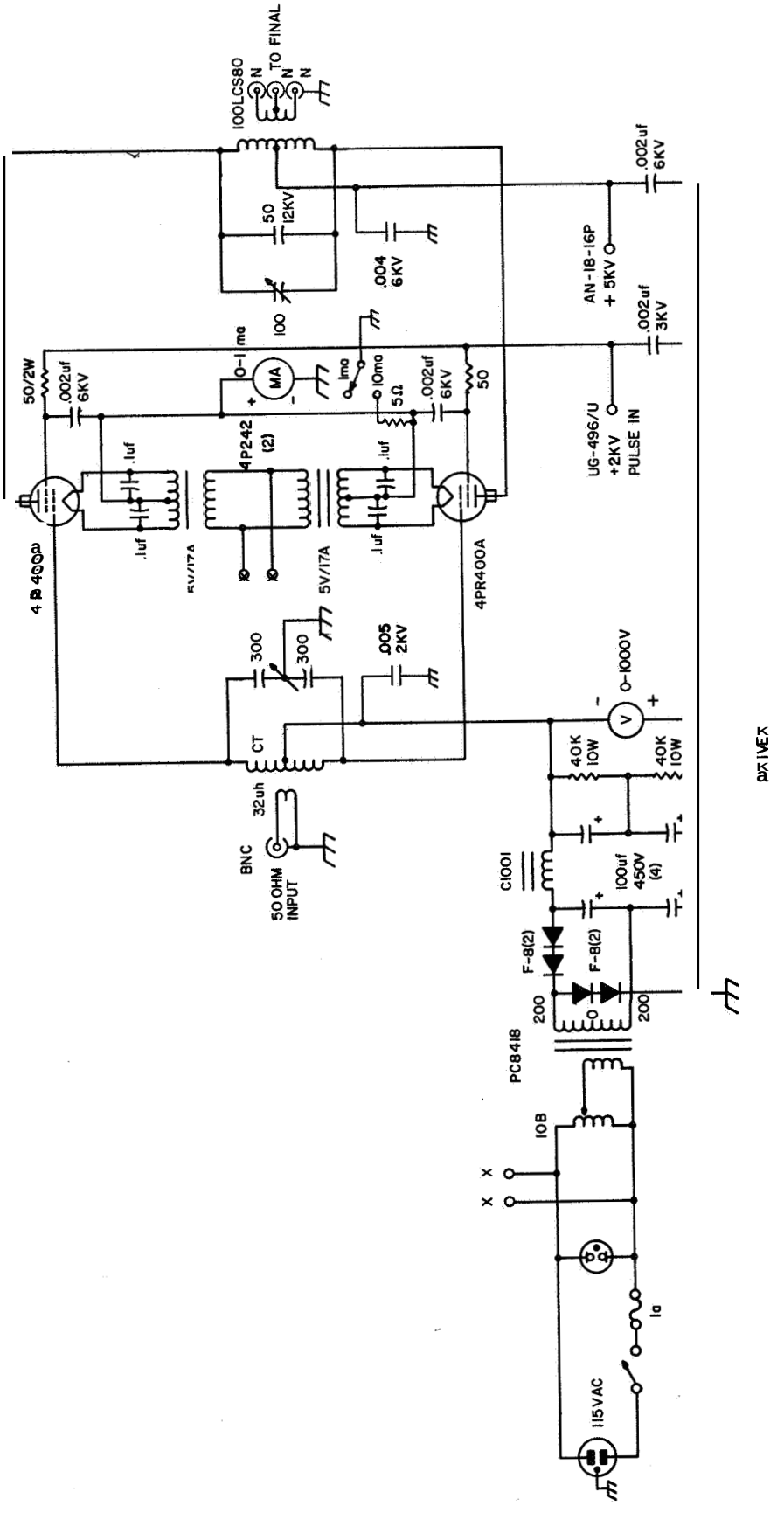

Figure 4.5 Driver amplifier.

the tubes is an order of magnitude greater than combined screen and control grid DC currents, the meter indicates primarily plate current, with 10% accuracy. A 10:1 shunt and switch are provided so that plate current can be monitored at either high or low pulse repetition rates. The DC plate voltage of the driver tubes is 5,000 volts provided by the high-voltage power supply.

4PR400A 5,000 watt Driver Amplifier Design Notes

DC plate supply voltage, E_{bb} = 5,000 volts

DC screen supply voltage, E_{c2} (during pulse) = 1,000 volts

DC control grid bias voltage, E_{cc} = -600 volts

RF Drive is adjusted so that:

Max inst. plate current, i_b max = 3.00 amps

Min inst. plate voltage, e_b min = 1,000 volts

Max inst. grid voltage, e_c max = 80 volts

The 5-point "Chaffee" [1936] approximation technique is used to obtain the following parameters for one tube during the pulse:

DC plate current, I_{bb} = 0.800 amps

DC screen current, I_{c2} = 70 mA

DC control grid current, I_{cc} = 10 mA

Peak fundamental RF plate current, i_{b1} = 1.35 amps

Peak fundamental RF grid current, i_{c1} = 18 mA

RF power output, P_o = 2,700 watts

DC plate power input, P_{in} = 4,000 watts

Plate circuit efficiency, η_p = 67.5%

RF driving power, P_d = 63 watts

RF plate load resistance, R_{pl} = 2,960 ohms

RF grid driving resistance, R_g = 3,900 ohms

For two tubes in push-pull, these parameters become:

I_{bb}	= 1.60 amps
I_{c2}	= 140 mA
I_{cc}	= 20 mA
P_o	= 5,400 watts
P_{in}	= 8,000 watts
P_d	= 126 watts
R_{pl}	= 5,920 ohms
R_g	= 7,800 ohms

Since the range of the tuning capacitance for the plate circuit is restricted to 60-150 pF, it is necessary to use two plug-in coils to cover the entire range of Prequencies from 2.00 to 3.50 MHz, An E. F. Johnson 1000LCS80 coil, with an inductance of 45 μHy, is used for frequencies from 2.00 to 2.70 MHz, resulting in loaded Q's between 15 and 10. An E. F. Johnson 1000HCS80 coil with an inductance of 27 μHy, is used for the 2.50 to 3.50 MHz frequency range, also achieving loaded Q's between 10 and 15. The secondary winding was empirically determined by use of the Wayne Kerr B601 balanced impedance bridge to match the 6,000 ohm plate-to-plate impedance of the 4PR400A's to the 240 ohm grid-to-grid impedance of the 7214's.

The grid tuned circuit is likewise designed for a range of loaded Q's between 10 and 20 over the frequency range from 2.00 to 3.50 MHz. The tuning capacitor used in the grid circuit has a sufficient adjustment range to permit use of one coil for the entire frequency range. This tank was also designed empirically with the impedance bridge.

Future improvements desirable for this unit include construction on a larger chassis and relay rack panel (24 inches wide), replacement of the large

air-insulated variable plate circuit tuning capacitor with a vacuum-variable capacitor, and replacement of the blowers with unitshaving a larger cooling capacity and high reliability.

Final Amplifier Unit

The final amplifier stage employs two RCA 7214 ceramic tetrode tubes in a push-pull configuration to deliver 50,000 watts of RF energy to the antenna. The type 7214 was chosen because of its small size, high performance at low plate voltages, and relatively high power gain. The schematic diagram of the final amplifier unit is found in Figure 4.6.

The grid input circuit of the amplifier is a secondary winding on the output coil of the driver amplifier stage. In order to preserve system shielding, short lengths of coaxial cable are used to connect the grids of the final tubes to the grid winding. The lengths are much too short to cause any impedance transformation because of mismatch and do not have sufficient shunt capacitance to affect the tuning of the driver plate circuit. The DC grid bias voltage for the tubes is generated in a bias supply constructed on the same chassis as the final amplifier and connected to the center tap of the grid winding through another length of coaxial cable. The nominal grid bias voltage for the 7214 tubes is -200 volts, although some improvement in pulse shape at the expense of output power can be realized by increasing the bias voltage to -300 volts.

As was the case in the driver amplifier stage, the filaments of the 7214's have a rather high current requirement (17.5 amperes per tube), necessitating the use of separate filament transformers for each tube. The filament voltage of

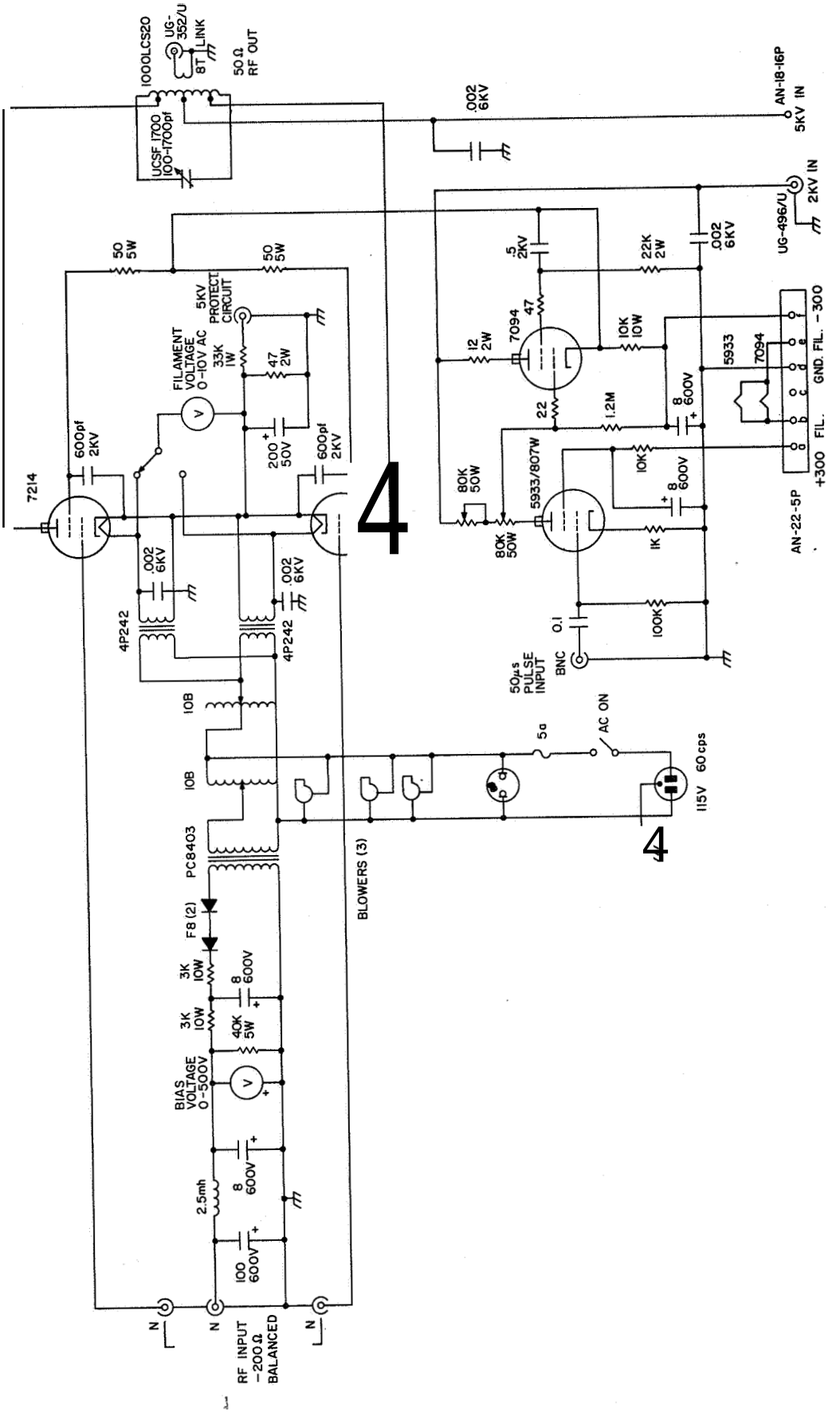

Figure 4.6 The final amplifier.

each tube is completely adjustable from 0 to 5.6 VAC to permit gradual application of filament voltage, Monitoring of either filament voltage is provided with a panel-mounted meter and meter and meter switch.

Three blowers are used to cool the 7214 tubes and other components inside the final amplifier cabinet. Originally, two 15 cfm blowers were installed, one for each 7214 tube, but it was found that these blowers were insufficient to cool the tubes and that heat generated by other components in the same cabinet was excessive, Installation of a single rotary fan at the top of the cabinet resulted in improved cooling of the final amplifier unit.

The 7214, designed for very high and ultra-high frequency operation, uses concentric rings for all element connections. In high frequency applications, these rings are ideal for use in tuned-line or cavity circuits, However, at the lower radio frequencies such as those desired for this application, connection to the tube elements presents a problem. Custom-made sockets are available for this tube, but are quite expensive and require long delivery times, The sockets used in the shipboard transmitter were constructed at the University of Illinois by soldering lengths of number 14 copper wire around the concentric element rings of the tubes and mechanically mounting the tubes and the terminals for each element in 3/8-inch thick plexiglass boxes, These sockets function quite well, but present serious drawbacks when tube replacement or testing is required, In addition, some trouble was experienced with tube instability due to inadequate screen-grid bypassing, This latter problem was cured by insertion of a low value of resistance in series with each screen inside the tube socket.

The screen grids of the 7214's are keyed with a 1000 volt pulse generated by a pulse modulator similar in design to that described previously in connection

with the excitor stage. The pulse modulator uses a 5933/807W amplifier tube and 7094 pulse modulator tube. The screens are held at a voltage of -300 volts between pulses to assure complete cut-off of the final amplifier tubes. This pulse modulator stage is located on the same chassis as the final amplifier and was one of the causes of the cooling problem.

The plate circuit of the final amplifier stage is a balanced push-pull tuned circuit designed to have a loaded Q of approximately 15 at the final output plate-to-plate impedance of 550 ohms, A high capacitance (1700 pF maximum), 15,000 volt vacuum-variable capacitor (Jennings UCSF - 1700) is used to tune the plate circuit (Plate Tuning Control), The output link is very closely coupled to the plate winding by locating it physically inside of the latter winding. The link size was empirically adjusted with the impedance bridge to reflect the correct plate-to-plate impedance with a 50 ohm load on the link. The circuit, when set up in this manner, will only provide the correct plate-to-plate impedance (and therefore the full output power of 50,000 watts) when loaded with 50 ohms. For this reason, great care is required to assure that antennas are closely matched to 50 ohms.

The +2,000 volts, and f300 volts and 6.3 VAC for the pulse-modulator circuit are supplied through shielded cables from the low-voltage power supply unit. The +5,000 volts for the final amplifier plate circuit is supplied through a shielded cable from the high-voltage power supply unit. Since the energy storage capacitors for the plate supply are located in the high-voltage supply, it was necessary to use wire large enough to handle the DC pulse current and insulated to withstand at least 10,000 volts.

7214 50,000 Watt Class C Power Amplifier Design Notes

DC plate supply voltage, E_{bb} = 5,000 volts

DC screen supply voltage, (during pulse) = 1,000 volts

DC control grid bias voltage, E_{cc} = -200 volts

RF Drive is adjusted so that:

Max inst. plate current, i_b max = 22 amps

Min inst. plate voltage, e_b min = 1,000 volts

Max inst. grid voltage, e_c max = +270 volts

The 5-point "Chaffee" [1936] approximation technique is used to obtain the following parameters for one tube during the pulse:

DC plate current, I_{bb} = 8.34 amps

DC screen grid current, I_{c2} = 1.50 amps

DC control grid current, I_{cc} = 2.25 amps

Peak fundamental RF plate current, i_{b1} = 14.4 amps

Peak fundamental RF grid current, i_{c1} = 4.00 amps

RF power output, P_o = 28.8 kW

DC plate power input, P_{in} = 41.6 kW

Plate circuit efficiency, η_P = 69.2%

RF driving power, P_d = 940 watts

RF plate load resistance, R_{pl} = 274 ohms

RF grid driving resistance, R_g = 120 ohms

For two tubes in push-pull, these parameters become:

I_{bb} = 16.68 amps

I_{c2} = 3.00 amps

I_c = 4-48 amps

P_o = 57.6 kW

P_{in} = 83.2 kW

P_d = 1860 watts

R_{pl} = 550 ohms

R_g = 240 ohms

The plate tank of the final amplifier matches the 50 ohm, unbalanced RG-17/U coaxial cable to the balanced 550 ohm plate-to-plate impedance of the tubes. An E. F. Johnson 1000LCS20 coil tuned with a Jennings UCSF - 1700 vacuum-variable capacitor is used as the final amplifier plate-tank circuit. In order to preserve a minimum loaded Q of 10 and provide the correct impedance ratio at frequencies from 2.00 to 3.50 MHz, it is necessary to tap the plate connections down one turn from each end of the Johnson coil. A six-turn link constructed inside the Johnson coil provides the correct impedance ratio for most of the frequency range, but an eight turn link for frequencies between 2.00 and 2.50 MHz results in more efficient operation at these lower frequencies. Coupling between the plate and output windings is sufficiently great that any leakage reactance contributed by the secondary can be corrected with the plate tuning control. The parameters of the plate tank were determined empirically with the Wayne Kerr B601 balanced impedance bridge. The voltages present in the plate-tank circuit are sufficiently low that no problem has been experienced with insulating the output winding from the plate winding; the 1/2-inch air gap between the two windings is quite adequate.

As discussed previously, the grid RF circuit is simply a closely coupled secondary winding on the driver stage output tuned circuit.

Possible future improvements for the final amplifier stage are numerous, Incorporation of commercially constructed tube sockets would be a very worthwhile

improvement. The pulse modulator circuit should be constructed on a separate chassis to prevent RF retriggering problems, reduce heat sources in the final amplifier cabinet, and reduce the physical component crowding. This latter problem could be greatly reduced if the final amplifier stage were constructed on a larger chassis and 24-inch wide relay rack panel. Placement of the high voltage energy storage capacitors inside the final amplifier cabinet would reduce lead inductances, lead resistances, and the size of the cable to the high-voltage supply, Larger blowers for each tube with a filament interlock system are quite desirable. Replacement of the present unregulated bias supply with a shunt regulated supply would eliminate the "self-bias" effect that now occurs at high pulse repetition rates because of the charging of bias supply capacitors by grid current pulses.

The Final Amplifier Unit - Addendum

Operation of the original final amplifier unit at high pulse repetition rates (30 and 60 pps) resulted in serious cooling problems and eventual failure of the final amplifier. The additional heat generated at the high repetition rates was sufficient to oxidize and partially melt the solder on the connections to the 7214 tubes, An attempt was made to offset this problem by using high melting-point solder and clamp-type connections, but proved to be insufficient. A complete re-analysis of the cooling requirements of the 7214 tubes resulted in the redesign of the final amplifier stage and its bias supply and pulse modulator. The redesigned final amplifier incorporates commercially designed sockets for the 7214 tubes and much larger blowers, thus requiring considerably more physical space than the original final amplifier stage. It was therefore necessary to reconstruct the bias supply and pulse modulator circuits for the final amplifier

on a separate chassis. The design and construction of these three units are discussed in the following paragraphs.

Reconstruction of the final amplifier stage was planned so that maximum utilization of the original cabinet, rack-panel, and vacuum-variable capacitor mounting could be realized, thereby reducing construction time to a minimum. Electrically, the improved final amplifier stage is identical to the original circuit--the changes were all in the mechanical arrangement of components and in the cooling system. The schematic diagram of the improved final amplifier unit is found in Figure 4.7. A photograph of the improved final amplifier is found in Figure 4.8.

Special sockets designed and constructed for the 7214 tubes by RCA (designated the Y-102 socket) were purchased for installation in the final amplifier stage. These sockets incorporate beryllium-copper rings for connection to the tube elements and are designed to direct all air flow around the tube concentric rings and through the plate cooling fins for optimum cooling of the tubes. The RCA sockets and tubes together present a much higher pressure load on the cooling blowers (approximately **0.3** inches of water at 40 cfm) than the previous arrangement and necessitated the use of larger blowers. The blowers selected are Incor **B-3** blowers capable of delivering **30** to 40 cfm of air flow through the tube sockets at this high static pressure. Air ducts constructed of sheet metal direct all of the available blower air output through the socket and tubes. Separate blowers and ducts are provided for each 7214 tube. An air-flow switch is installed in the air duct to provide interlock protection of the tubes should the air flow stop.

Great care has been taken to assure complete RF grounding of the cathode and screen grid elements of the tubes. All four of the cathode terminals of

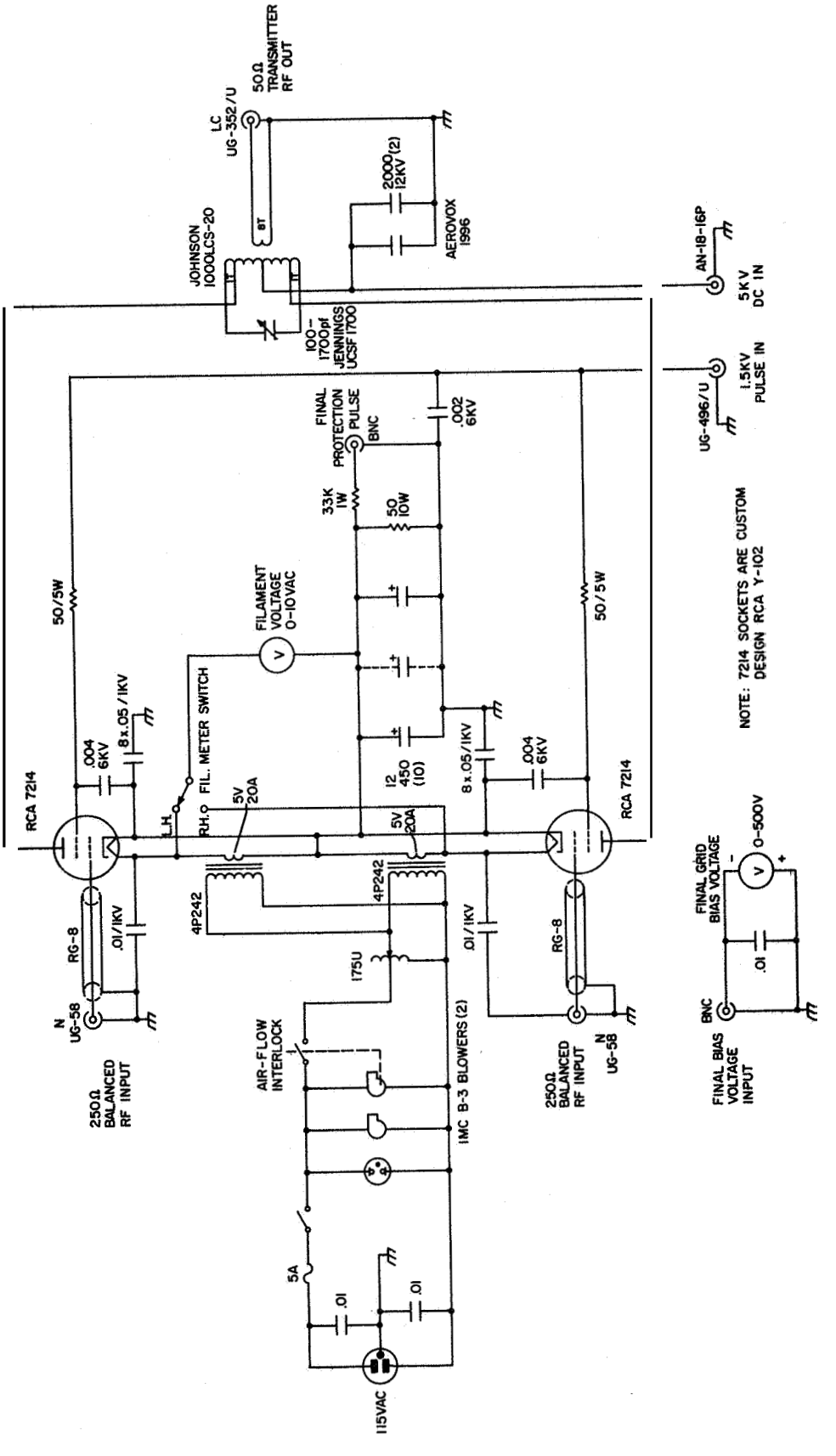

Figure 4.7 The improved final amplifier.

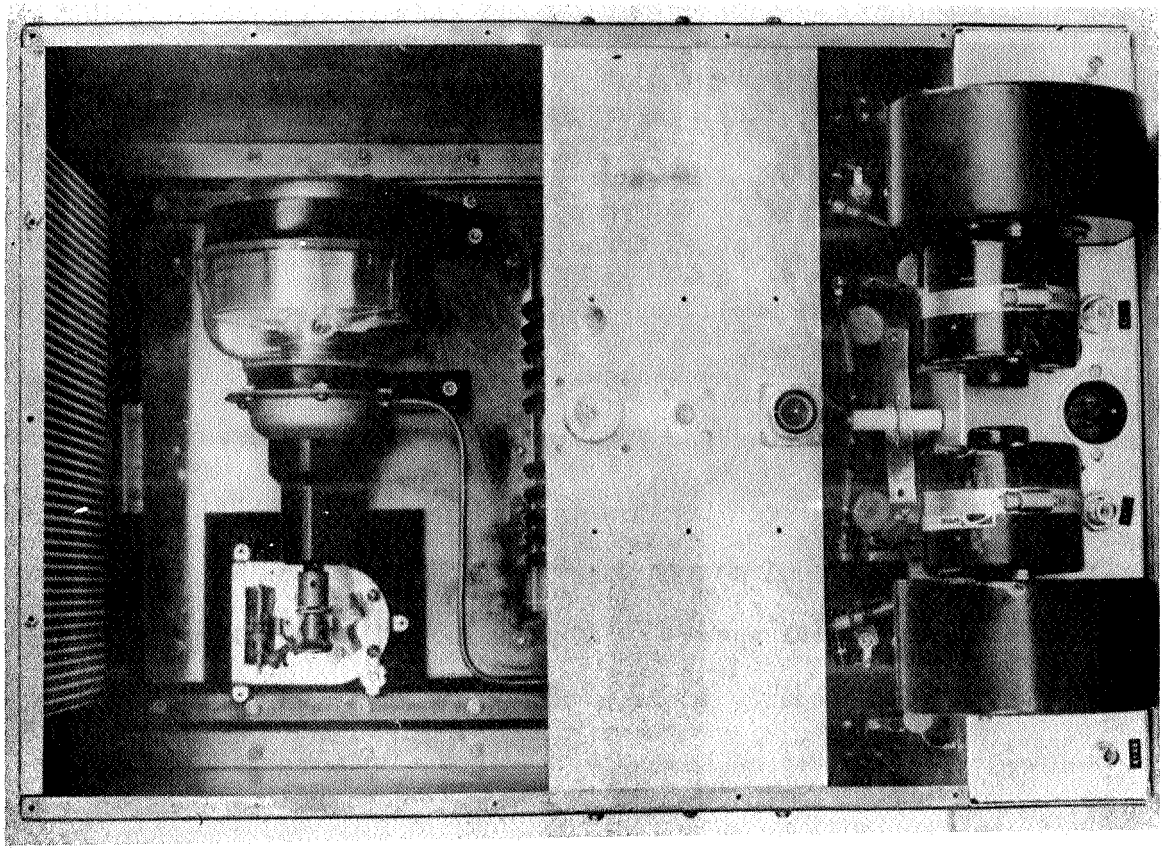

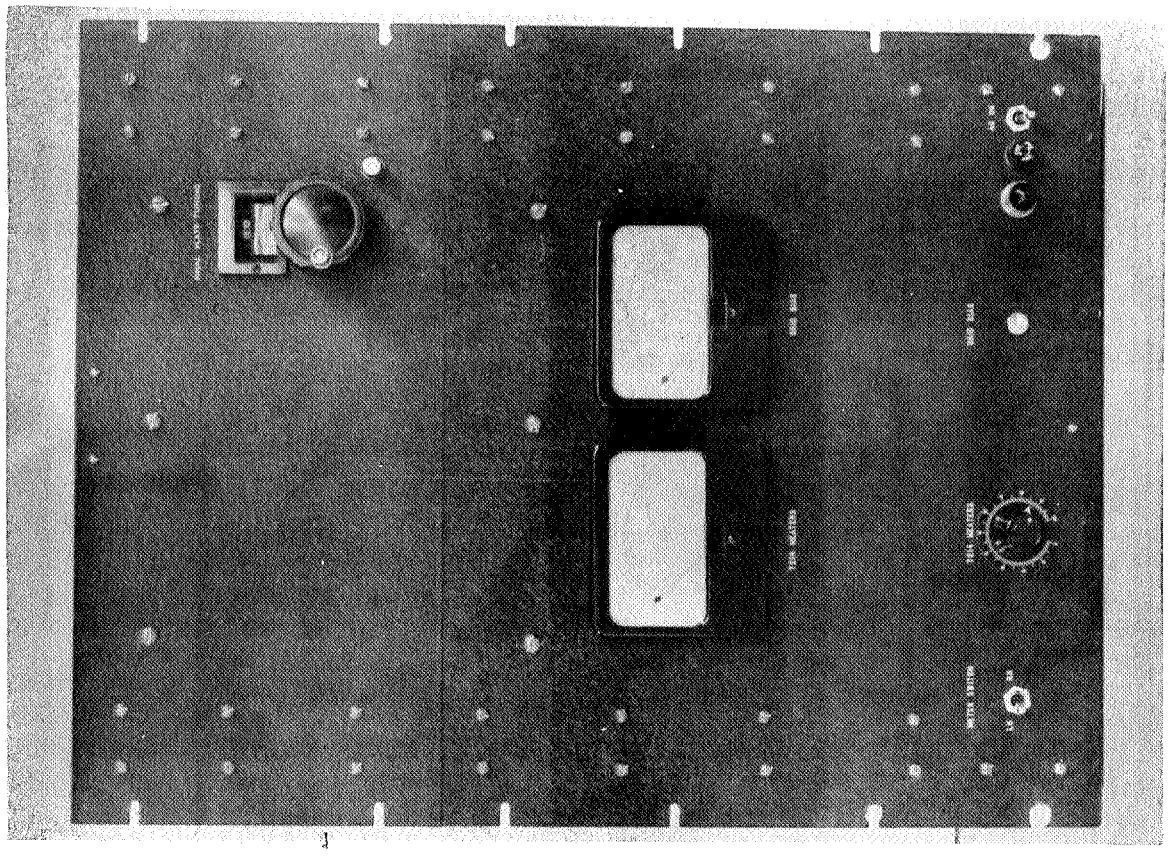

Figure 4.8 The improved final amplifier.

the socket are tied together with a 1/2-inch wide copper strap and four bypass capacitors to chassis ground are spaced around the strap. The screen terminals are bypassed directly to the cathode at the socket, Copper straps are used throughout the improved final amplifier for all plate circuit and ground connections in order to minimize lead inductance.

Since space limitations required construction of the final amplifier bias supply as a separate unit, it was decided to revise the bias supply to provide the additional regulation required for operation at high repetition rates, The circuit is an electronic shunt regulator much like that used by Belrose et al. (1964) in a similar application. A single 6DC6 tube operates as the shunt regulator device, The tap switch in the grid circuit allows adjustment of the output voltage from –200 to –350 volts DC. (Grid Bias Adjust Control). Metering of the bias voltage is accomplished with a voltmeter located on the final amplifier unit as it was originally. The schematic diagram of the final amplifier bias supply is found in Figure 4.9.

Space limitations in the final amplifier also required reconstruction of the screen pulse circuits on a separate chassis. Because of the problems associated with the RF triggering of the pulse circuits located on the excitor chassis, it was decided to reconstruct all transmitter pulse circuits on one chassis to take the place of the pulse circuits on the excitor chassis, It was also decided to construct separate pulse modulators for the 4CN15A stage, the 4PR400A stage, and the final amplifier stage.

The pulse modulator unit therefore incorporates the 12AU7 - 6AL5 monostable multivibrator and amplifier circuits identical to those originally used on the excitor chassis as well as three identical high–voltage pulse modulator stages similar in design to that originally used in the final amplifier unit. Each

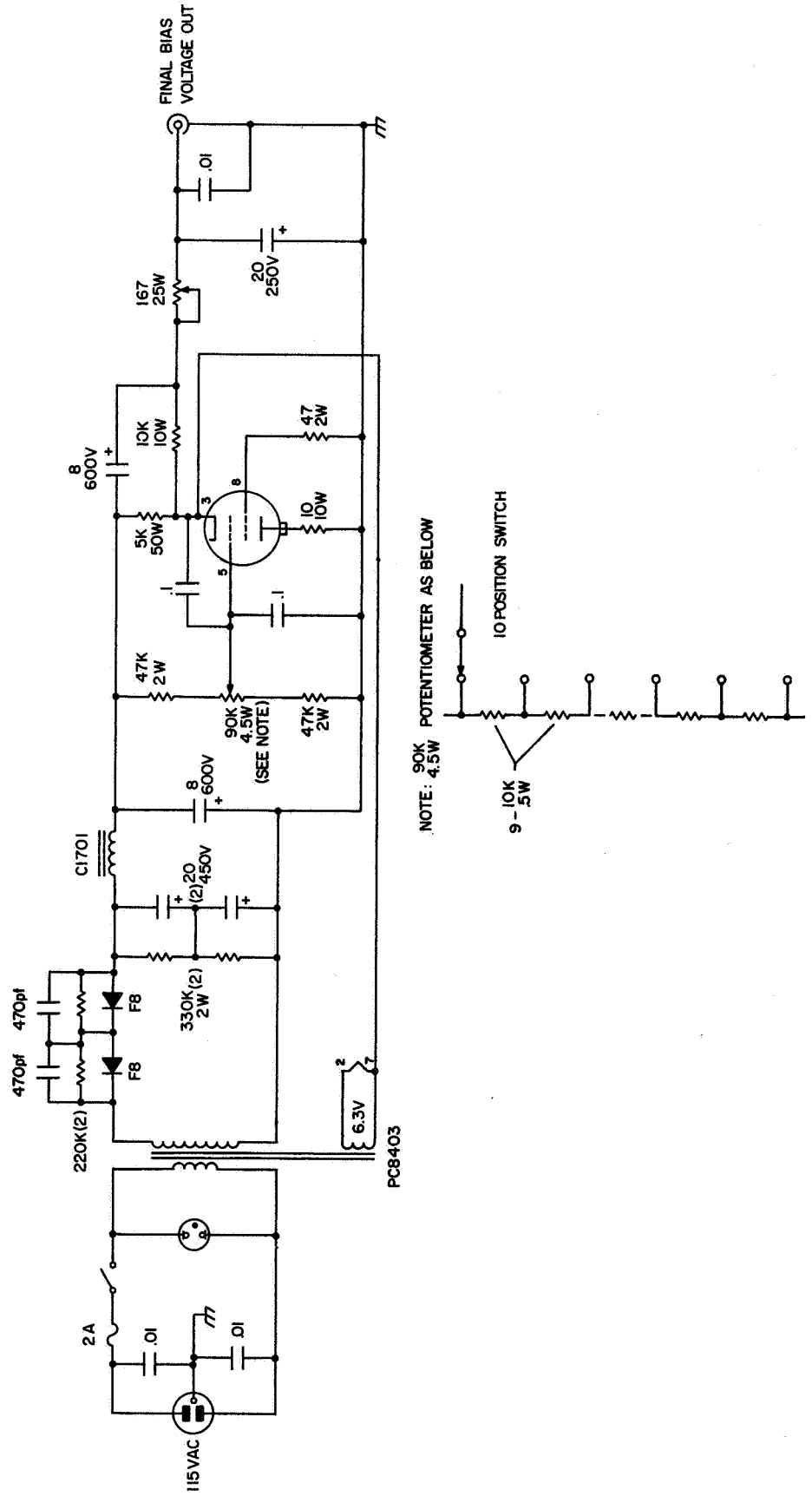

Figure 4.9 Final amplifier bias supply.

pulse modulator uses one 5933/807W tube and one 7094 tube. Additionally, a 6 μF 3000 volt capacitor is included in the pulser to assure that adequate storage capacitance is available to prevent voltage droop of the high-voltage pulse (approximately 1200 volts positive during the pulse). For the convenience of testing, monitor points are provided for the multivibrator output and for each of the three high-voltage pulse modulator outputs. The monitor outputs are derived from voltage dividers so that the output pulse in each case is within a 10 to 20 volt range when all circuits are functioning correctly. Future plans are to extend this technique to other stages of the transmitter to facilitate adjustment and maintenance of the transmitter. The schematic diagram of the pulse modulator unit is found in Figure 4.10.

Low-Voltage Power Supply

The low-voltage power supply delivers the following voltages to transmitter units:

1. 0 to 92,000 volts @ 200 mA max, adjustable.
2. +300 volts @ 100 mA max, electronically regulated.
3. -300 volts AC @ PO amps max.

The 2,000 volt supply uses an adjustable autotransformer in the primary circuit of the plate transformer to achieve voltage control. The rectifier system is composed of 16 type F8 diodes in a full-wave-circuit, The F8 silicon diode was chosen because of its relatively high peak inverse voltage (800 volts), Pow forward voltage drop (1.0 volt each at 500 mA), and lack of heat generation or requirement of filament transformer. Eight diodes were used in each leg of the rectifier system to achieve the required peak inverse voltage rating,. Shunt capacitors and resistors are used to equalize reverse capacitances of the diodes and therefore equalize the peak inverse voltage across each diode. The resistors have been chosen purposely high agd the' capacitances low. to prevent any degrading

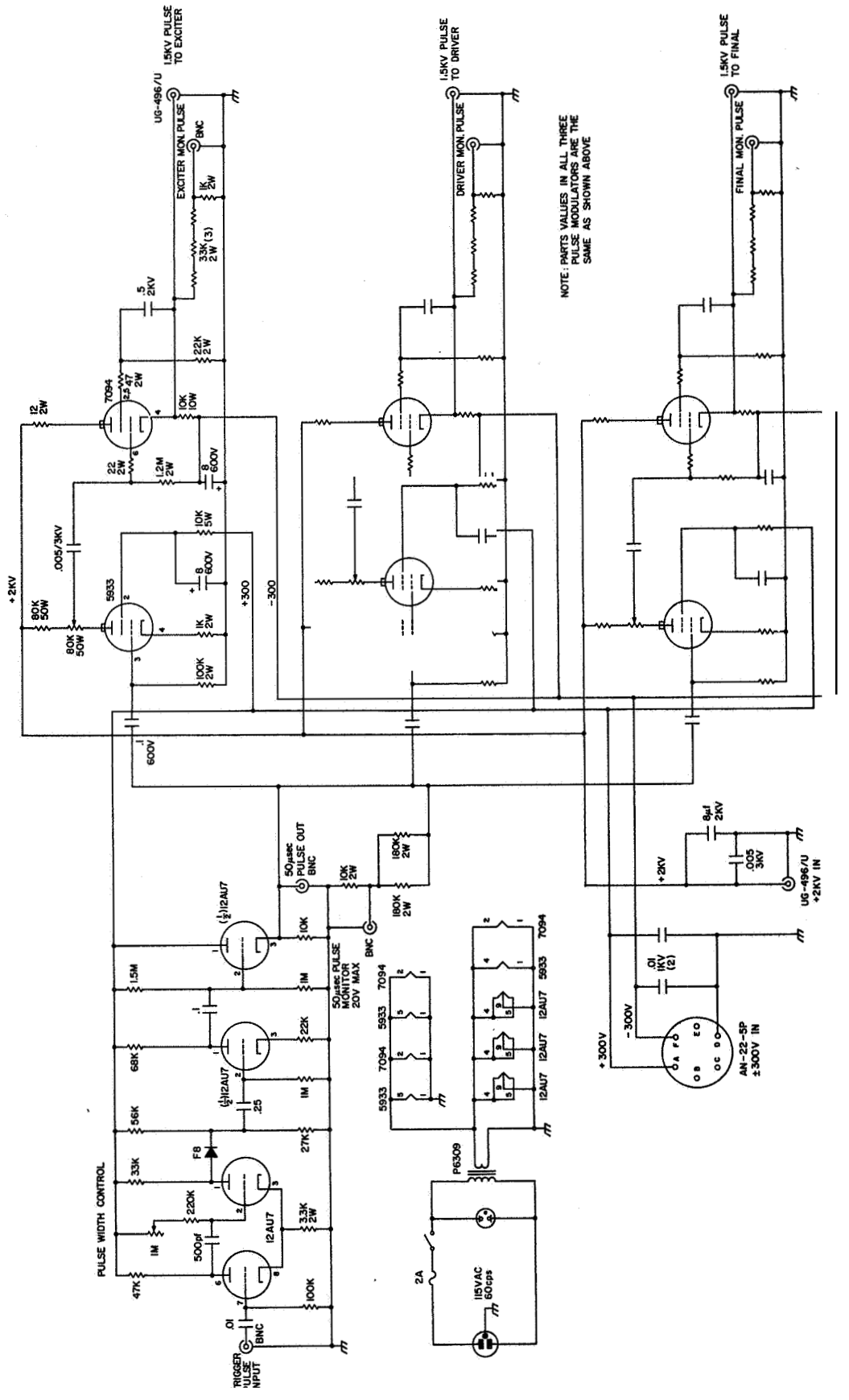

Figure 4.10 Pulser modulator.

of rectifier performance. A choke-input, single section filter is used on the output of the rectifiers, The output voltage of the 2,000 volt supply is monitored with a panel meter.

The positive and negative 300 volt supplies both use a 450 volt silicon rectifier supply before the regulators. Four F8 rectifiers are used in each supply, and both supplies incorporate a capacitor-input filter. The -300 volt Supply uses two type OA2 gas regulator tubes to deliver the shunt regulated -300 volts. The operating range of these tubes is 5 to 35 mA, restricting current drain from this supply to 30 mA maximum.

The +300 volt supply uses a standard series electronic regulator circuit, The 6080/6AS7G tube is the series control element and a twin triode 6SL7 serves as a reference comparator and control amplifier. The 5651 gas tube is used as the reference voltage source. Filaments of the 6080 and 6SL7 are operated from the filament transformer that also furnishes all 6.3 VAC power required by other units of the transmitter. The +300 volt and -300 volt supplies are voltage monitored with a single meter and meter switch. The schematic diagram of the low-voltage power supply-is found in Figure 4.11.

Possible future improvements on the low-voltage supply are numerous. The development of 400 volt, 75 watt silicon transistors has made possible the design of both series and shunt regulator circuits for the +300 and -300 volt supplies that are entirely composed of transistors, thereby eliminating, filament supplies and heat, and improving regulation. The -300 volts supply could be redesigned for currents up to 100 mA with greatly improved regulation. The +300 volt supply could realize a much higher degree of stability and regulation than is possible with the tube circuitry.

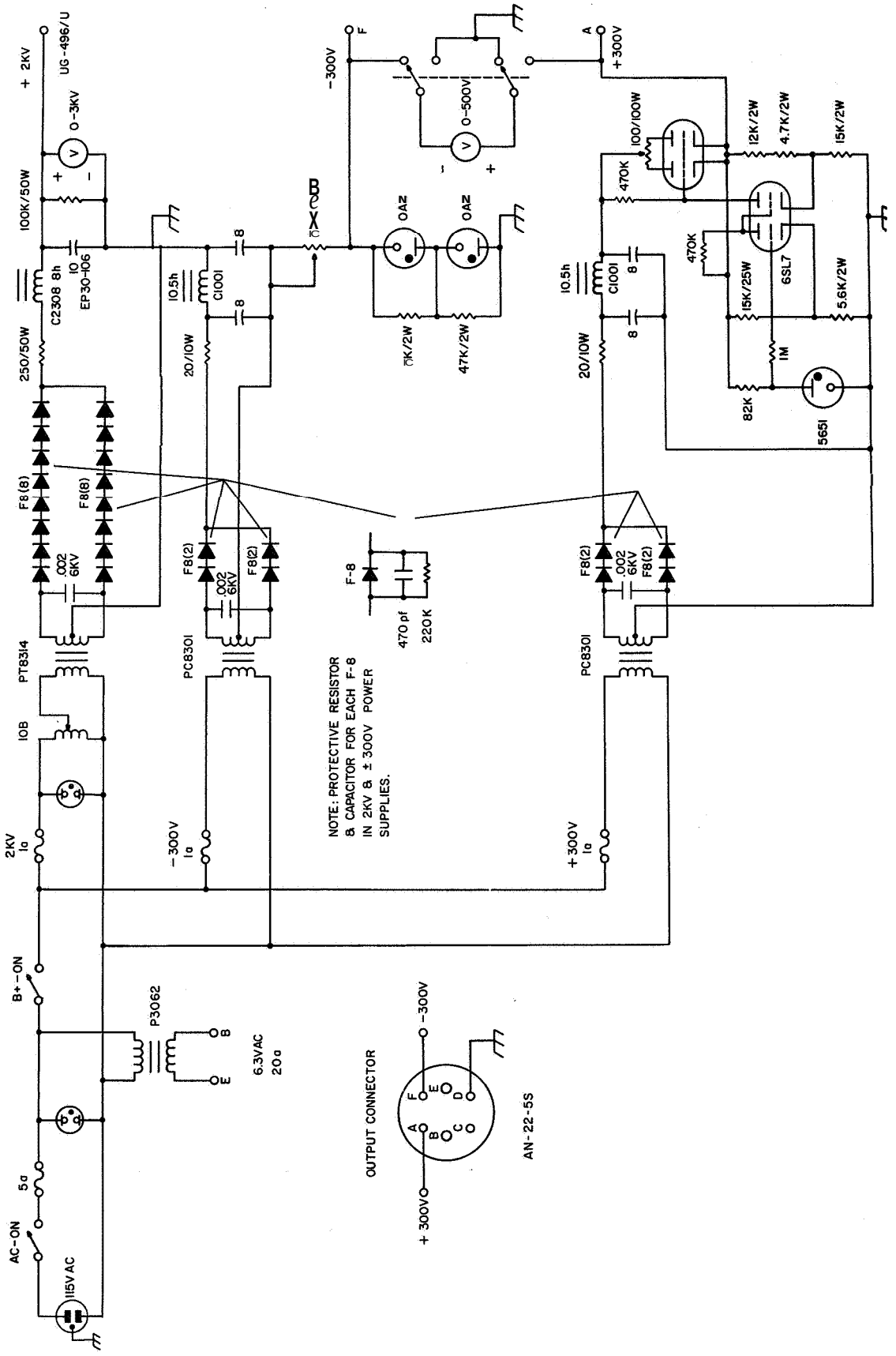

Figure 4 11 Low-voltage power supply

In order to reduce weight of the unit, it would be advisable to separate the ±300 volt supplies from the 2,000 volt supply. This isolation would result in greater ease of servicing of each unit than is now possible. Filament transformers should be located on the same chassis as the tubes which they supply to keep voltage drop in cables to a minimum.

High-Voltage Power Supply Design

Two high-voltage power supplies have been designed and constructed for use with the shipboard transmitter. The original power supply, designated HV power supply I, is capable of delivering 5,000 volts DC at currents up to 20 mA. This supply will handle the 5,000 volt requirements of the transmitter if the maximum pulse repetition rate does not exceed 5 pps. For operation of the transmitter at 30 and 60 pps, it has been necessary to construct a larger 5,000 volt supply capable of delivering currents up to 100 mA, designated HV power supply II.

HV Power Supply I Design

This power supply is constructed around a commercially available high-voltage power supply unit, the Del PS 5-30-2. The Del power supply uses 16 silicon rectifiers in a half-wave voltage doubling circuit to generate the 5,000 volt output from the 3,000 VAC winding of a plate transformer. The diodes as originally supplied by the manufacturer would withstand neither the peak current requirements of the storage capacitors nor the heat and were therefore replaced with 16 F8 silicon diodes. The output voltage of the supply is controlled by a variable autotransformer in the primary circuit of the plate transformer.

Since the current requirements of the final amplifier and driver amplifier are very high only for the duration of the pulse, energy storage capacitors are

used to supply the current required. The high voltage supply simply charges the capacitors between pulses. Two 8 μF capacitors in parallel are sufficient to reduce the output voltage droop during the pulse to 100 volts or less. The 50,000 ohm series resistor from the Del power supply to the storage capacitors limits the maximum output of the Del supply to 20 mA and determines the average charging current to be approximately 5 mA for operation at 5 pps. A high-voltage thyratron crow-bar circuit is used to rapidly discharge the storage capacitors should a fault occur in the final amplifier, The crow-bar circuit also provides a rapid means of removing the high voltage from all circuits when the AC power to the Del supply is turned off. An RCA 5563A thyratron is used as the crow-bar tube. A latching relay in series with the thyratron cathode circuit provides interlock features to insure that the thyratron be returned to an "off" state before the high-voltage supply can be reactivated. Protection of the final amplifier tubes from current faults is provided by monitoring the cathode currents of the tubes. If an excessive current surge should pass through the final amplifier cathode circuit, the positive pulse generated triggers the thyratron and shuts off the 5,000 volt plate supply. The crow-bar circuit also functioned quite well as a positive transmitter interlock necessary for range safety operations aboard the ship. Grounding of the grid circuit of the thyratron insured non-operation of the transmitter. The schematic diagram of the high-voltage power supply I is found in Figure 4.12.

High-Voltage Power Supply 11 Design

Operation of the transmitter at pulse repetition rates of 30 and 60 pps requires a power supply capable of higher average power output and hence higher current output than the previous supply. The actual peak power required during

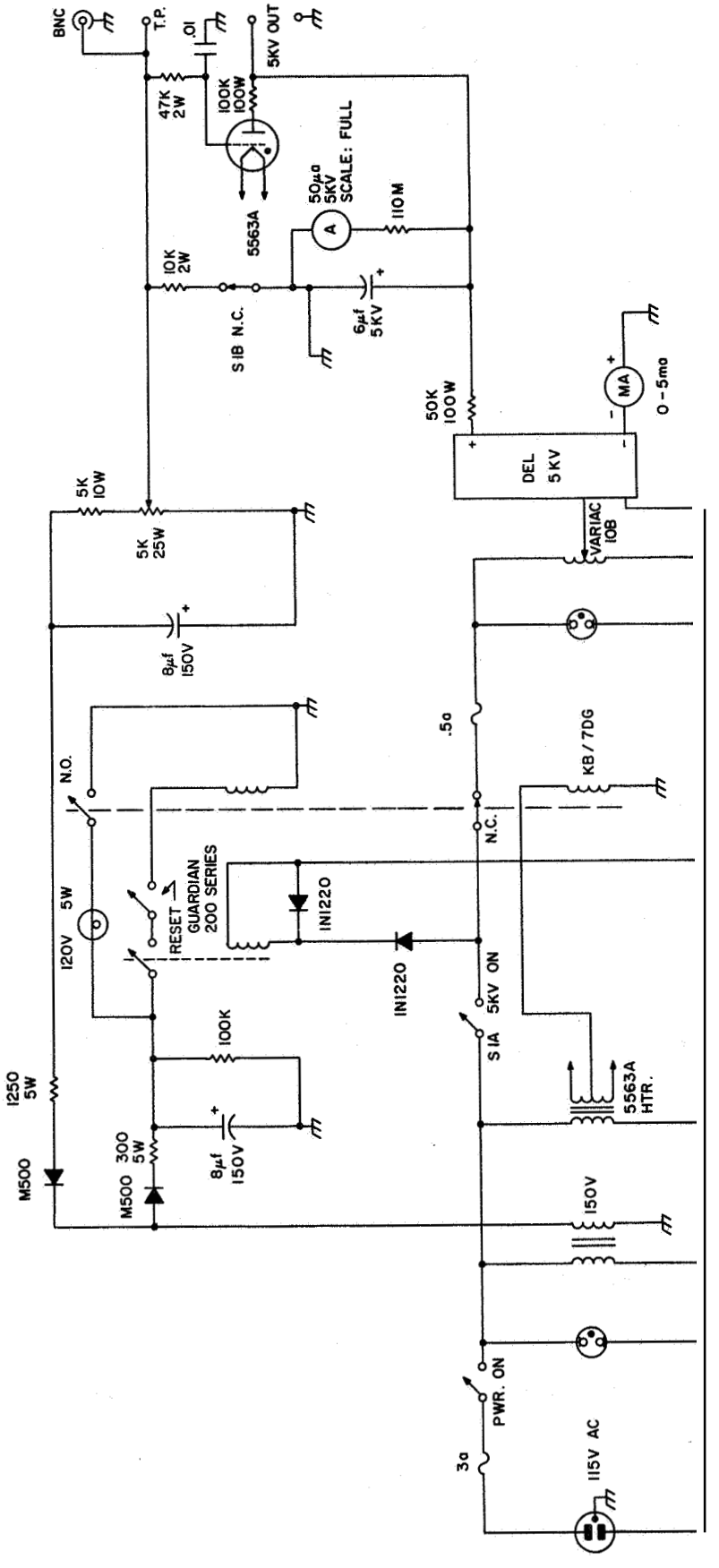

Figure 4.12 High-voltage power supply I.

the pulse does not change, so these are changes in the storage capacitor requirements. To increase the average power output of the supply, the Del power supply unit is replaced with a conventional plate transformer and full-wave rectifier circuit. The rectifier is constructed with 40 F8 silicon diodes to achieve the high peak reverse voltage rating required. Equalizing resistors and capacitors are used to minimize any diode-to-diode variations in PIV or reverse capacitance parameters, A conventional single section choke-input filter provides sufficient filtering of the rectifier output to charge the storage capacitors. Filtering requirements are not too stringent, since the charging' network for the storage capacitors also behaves as a filter section.. The thyratron crow-bar circuit for this supply is identical with that previously described.; The major difference between this power supply and HV power supply I is the increased size of the higher current supply. The large physical size of the plate transformer and rectifier bank required construction of the supply on two separate chassis with interconnecting cables, One chassis holds the plate transformer and rectifier bank; the other contains the storage capacitors and crow-bar circuit, The current meter on the supply is provided with a 10:1 shunt and range switch to permit use of the supply at all pulse repetition rates. The schematic diagram of the high-voltage power supply II is found in Figure 4.13.

Wallops Island Transmitter

As mentioned previously, the shipboard transmitter represents an extension and improvement in design over a transmitter designed by A. B. Gschwendtner in 1963-1964 for use in an ionospheric sounding installation at N.A.S.A. Wallops Island, Virginia. The following is a brief discussion of each unit of the Wallops transmitter and how the shipboard and Wallops designs differ,

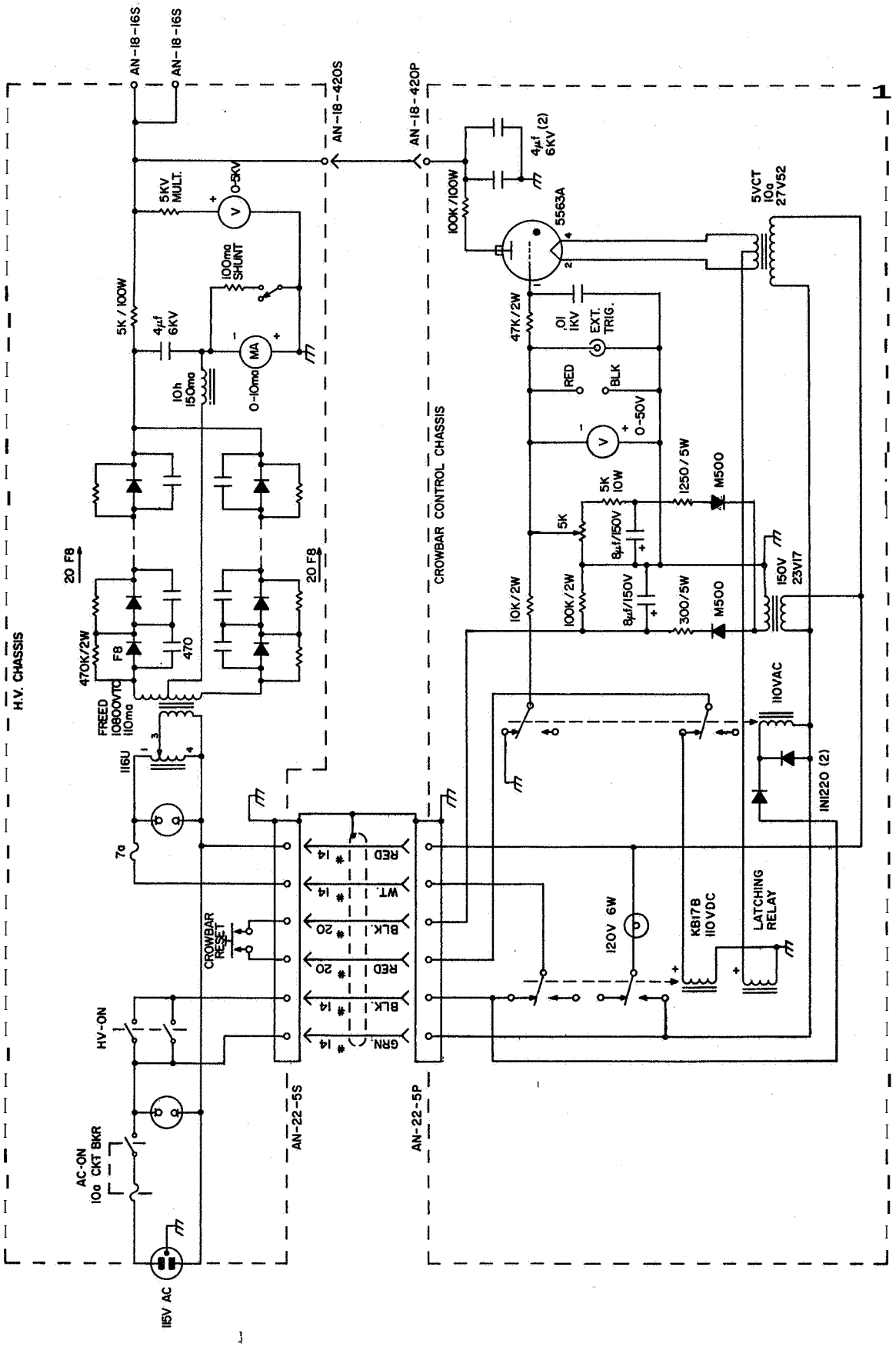

Figure 4 13 High-voltage power supply II

The 50,000 watt Wallops transmitter was actually constructed in two steps, The initial design of the transmitter was first tested and modified in a prototype transmitter, This transmitter was constructed at the University of Illinois in Urbana, Illinois and used in a temporary installation south of Bondville, Illinois in the spring of 1964 to test not only the transmitter design, but also the entire system performance, When satisfactory performance of the prototype transmitter was achieved, a second transmitter was constructed that incorporated all of the improvements installed in the prototype transmitter. This second transmitter was transported to Wallops Island, Va, where it is currently in use. The Wallops transmitter was constructed in a much more compact form than the shipboard transmitter and is completely housed in one six-foot enclosed relay rack cabinet. The individual units of the Wallops transmitter were not constructed in separate shield enclosures as those the shipboard transmitter were--the enclosed relay rack served as the shield enclosure for the transmitter. Considerable problems were encountered at the Wallops installation with spurious RF retriggering of the pulse generating circuitry and for this reason the shipboard design incorporated individual shielding of all units of the transmitter. The other differences between the shipboard and Wallops transmitters are outlined below in a unit-by-unit description. The block diagram of the entire transmitter is found in Figure 4.14.

Like the shipboard transmitter, the final amplifier of the Wallops transmitter uses two RCA 7214 tetrodes in a push-pull class C power amplifier,, The plastic box tube sockets used in the shipboard transmitter were designed and developed for the Wallops transmitter, Since the Wallops transmitter was designed for fixed frequency use only, the plate tank circuit is tuned with fixed high-voltage mica capacitors and no provision for adjustment is provided, The output

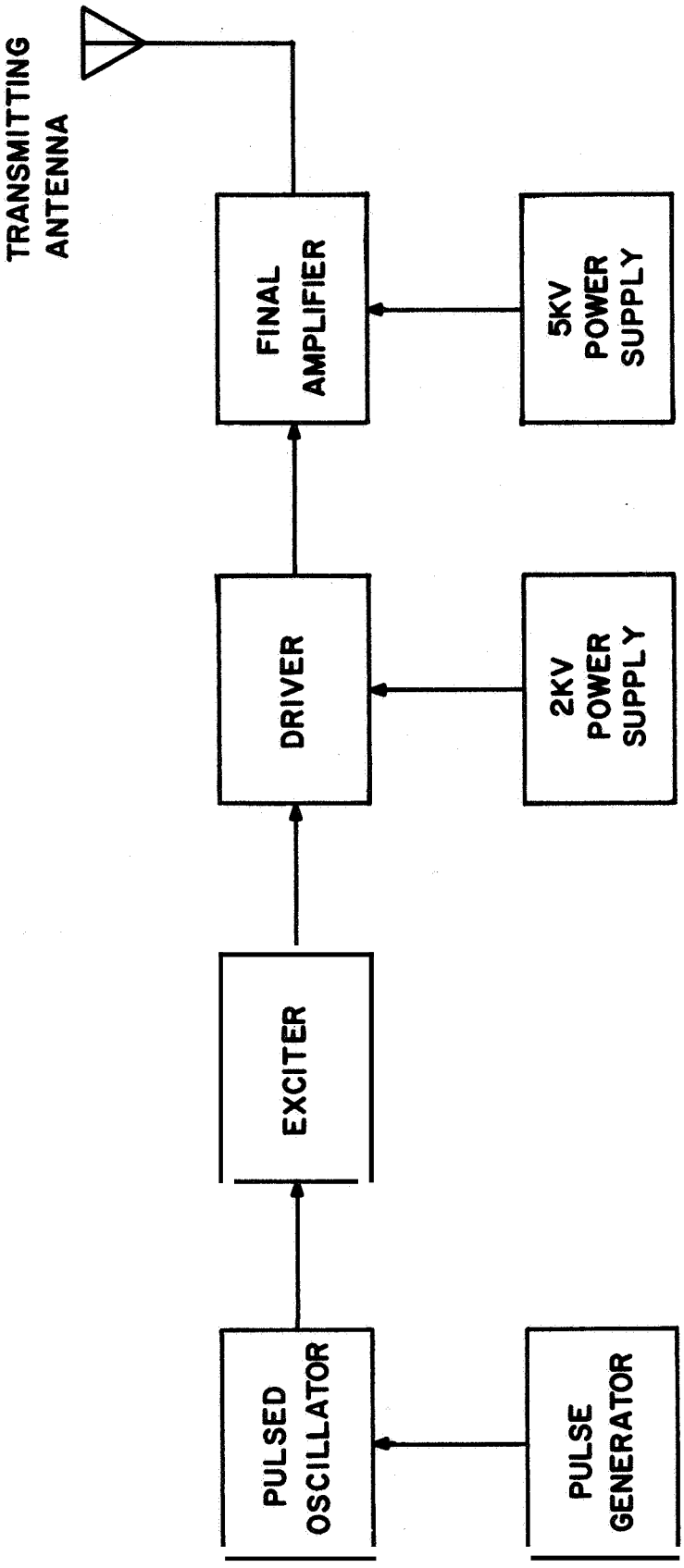

Figure 4.14 Wallops Island transmitter

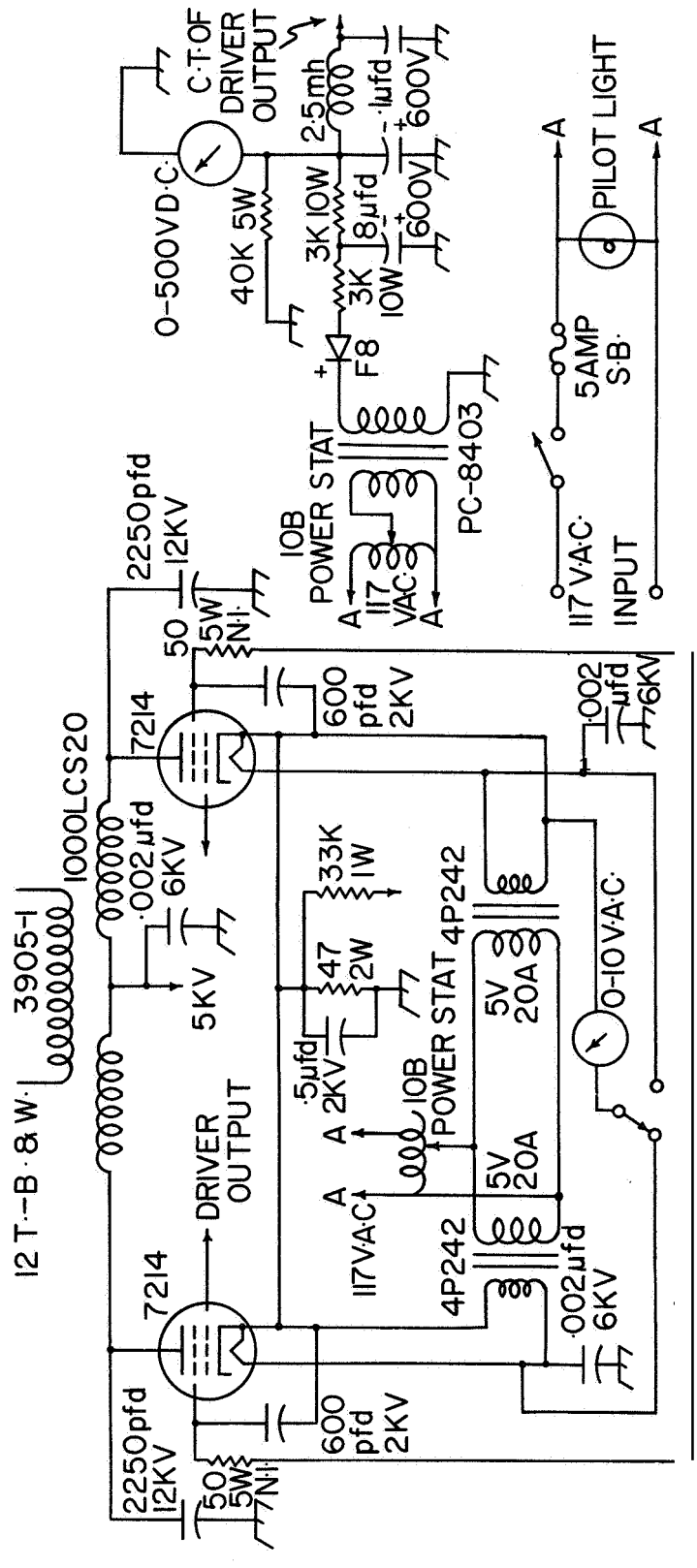

Figure 4.15 Wallops final amplifier.

link of the final plate tank is designed to feed a balanced 250 ohm load because of the high-impedance feedline'network used at Wallops, As mentioned previously, the final amplifier unit is not constructed in a shield enclosure, In other respects, the final amplifier at Wallops is identical to that used on board the ship. The schematic diagram of the Wallops final amplifier is found in Figure **4.15.**

The circuitry of the driver amplifier units of the two transmitters represents one of the major departures between the two transmitter designs. The Wallops transmitter uses two RCA **7094** tubes in push-pull to drive the final amplifier tubes, Two **6AG7** tubes are used in parallel to drive the **7094's.** The pulse circuits in this unit are identical to those used in the excitor-pulser unit of the shipboard transmitter. The **7094** tubes in push-pull deliver approximately 2,000 watts of RF driving power during the pulse to the final amplifier tubes. This level of RF drive has never been quite adequate to fully drive the final amplifier tubes and the **7094's** are operated somewhat over the manufacturer's recommended ratings. The life of the **7094** tube has therefore been less than would normally be expected and the reliability of the Wallops transmitter has not been as great as that of the shipboard transmitter. The schematic diagram of the driver unit is found in Figure **4.16.**

The low-voltage and high-voltage supplies of the two transmitters are very similar to each other in design and construction. The major difference between the low-voltage power supplies is in the use of silicon rectifiers in the shipboard transmitter in place of mercury-vapor and high-vacuum tube rectifiers. Additionally, the electronic regulator circuit of the shipboard +300 volt supply has been modified from the original circuit used in the Wallops transmitter to achieve better regulation.

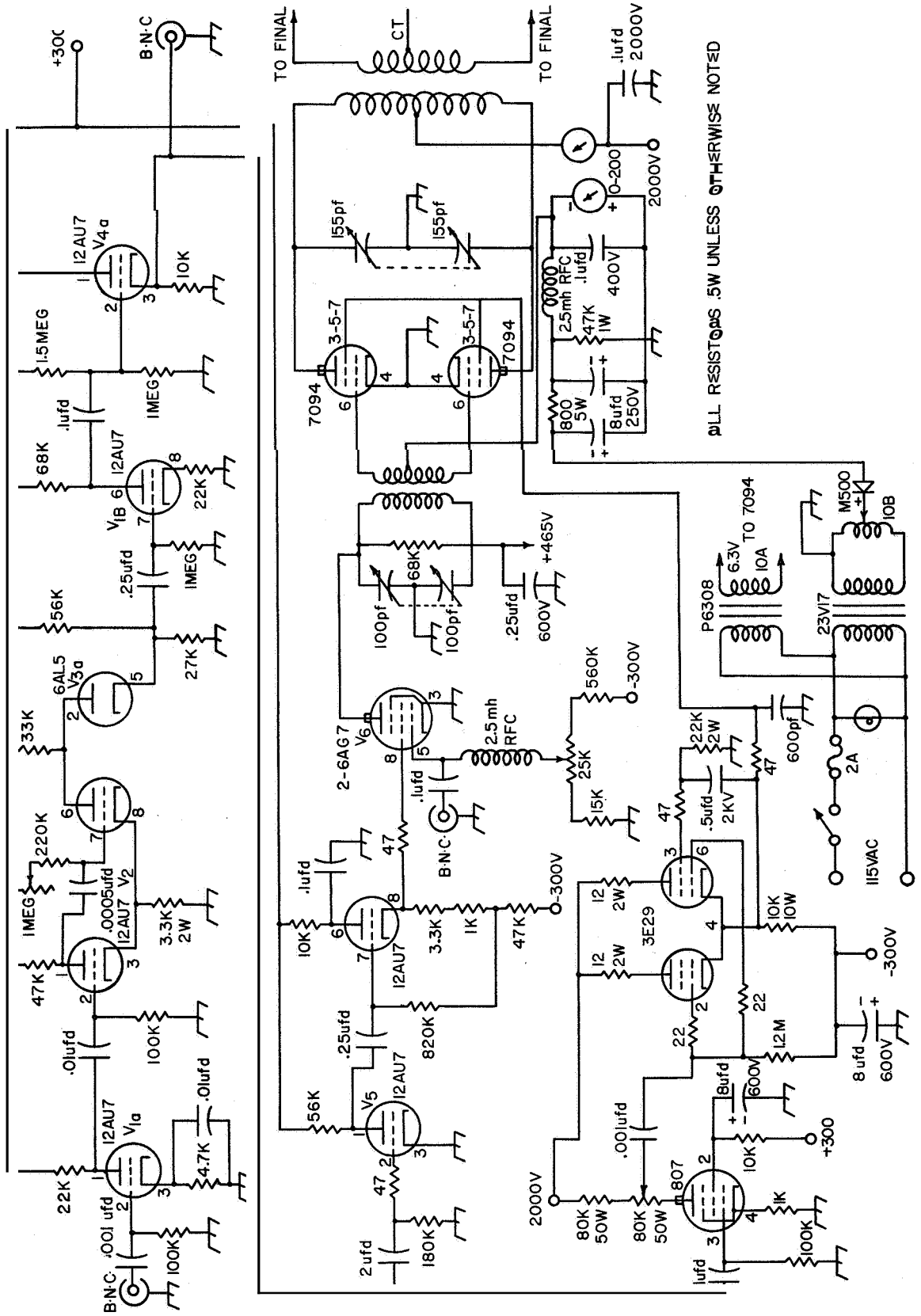

Figure 4.16 Wallops driver amplifier.

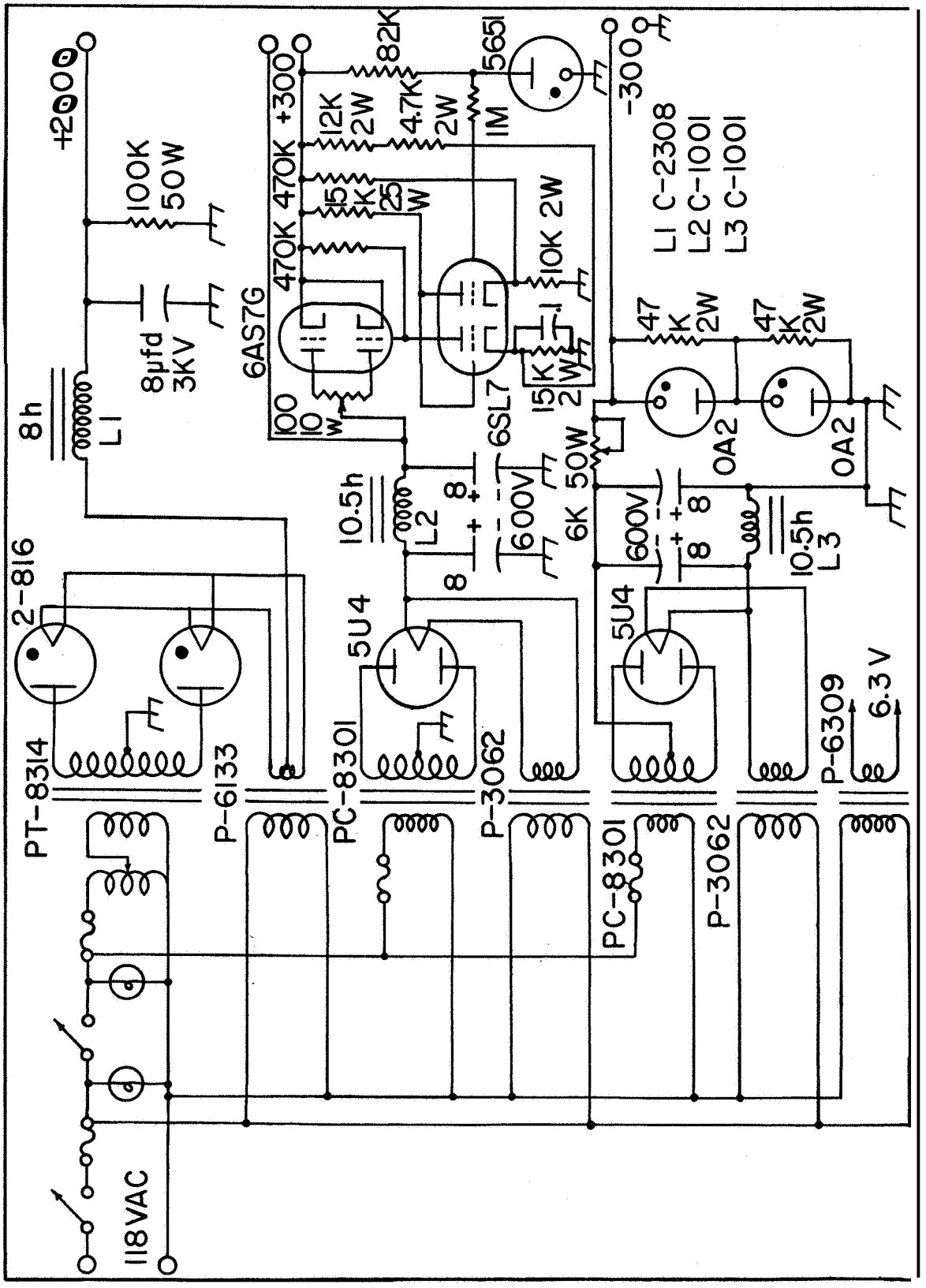

Figure 17 lloqs 1 -voltage power supply

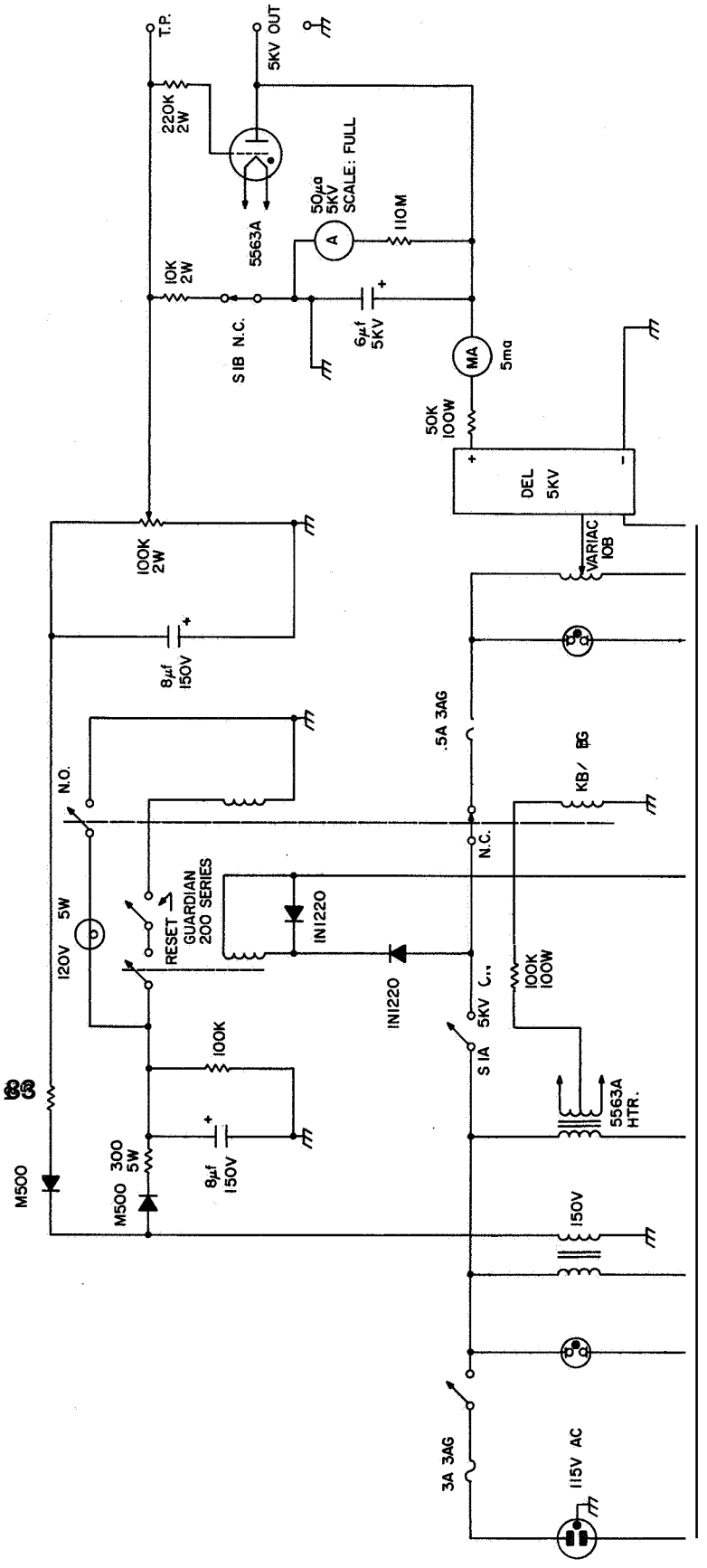

Figure 4.18 Wallops High-voltage power supply

The high-voltage supplies of the two transmitters are identical with the exception of a minor change in the crow-bar triggering circuit of the shipboard transmitter to prevent accidental firing of the crow-bar under conditions of high ambient temperature and humidity.

The schematic diagram of the low-voltage power supply is found in Figure 4.17 and that of the high-voltage power supply in Figure 4.18.

The pulsed oscillator unit in use at Wallops Island is a fixed-frequency version of that used on the ship. The only difference in the two oscillator units is in the lack of tuning facilities in the Wallops version. The schematic diagram is therefore not reproduced since the diagram for the shipboard unit is correct for the Wallops unit with the above exceptions in mind.

5. ANTENNA SYSTEM DESIGN

Because of the limited space available on the ship for antenna system installation, the same antenna system was used by both the differential absorption rocket experiment (Knoebel et al., 1965) and the partial reflection/absorption sounder described in this report. Both of these experiments were designed and operated by the personnel of two University of Illinois research groups under the overall scientific direction of Dr. S. A. Bowhill. Initial study of the antenna design for shipboard use was therefore performed for both groups by Dr. K. G. Balmain, who is the author of the first portion of this chapter. Dr. Balmain investigated extensively the effects of the ship and its superstructure on the radiated polarization of the antenna by means of scale model studies made in cooperation with the Antenna Laboratory of the University of Illinois. Also investigated by Dr. Balmain were alignment techniques for adjustment of the phase and amplitude of signals fed to each dipole to assure radiation of either mode of circular polarization. Since Dr. Balmain's work represents a cooperative effort between both research groups (Coordinated Science Laboratory and the Aeronomy Laboratory), references to the specific requirements of both experiments are included. Use of the shipboard antenna system was divided so that the rocket experiment used the antennas for the first half of the cruise, during which time all five rockets were fired, and the ionospheric sounder used the antennas for the remainder of the cruise. The design of the antenna feedline system and matching networks used in the rocket experiment are included in a final project report by the Coordinated Science Laboratory of the University of Illinois (Knoebel et al., 1965). With the

exception of Dr. Balmain's discussions of precruise experiments and study, all references to antenna system design in this chapter apply only to the ionospheric sounder experiment.

Radiation of a Prescribed Polarization from a Large Irregular Platform

During the past two years, the University of Illinois has been engaged in a program of ionospheric measurements with emphasis on the region between 50 and 120 kilometers from the earth's surface (the D and E regions). Due to the presence of the earth's magnetic field in the ionosphere, two characteristic electromagnetic waves may exist there, each with its own velocity, polarization, and attenuation factor; these waves are designated "ordinary" and "extraordinary". The differences between the two characteristic waves are utilized in order to determine experimentally some of the properties of the ionosphere.

The quantities which can be determined using radio wave techniques are the electron density N and the electron-molecule collision frequency (above the E region, collisions between electrons and ions also are significant). The quantities which can be measured directly are the attenuation and phase shift of the characteristic waves from which N and ν may be calculated. Since there are two Characteristic waves, measurement of the difference in attenuation and the difference in phase shift is possible, leading to improved accuracy in the determination of N and ν. The difference in attenuation is referred to as "differential absorption" and the difference in phase gives rise to a rotation of the polarization ellipse which is called "Faraday rotation". The differential absorption and Faraday rotation may be measured in the ionosphere with a rocket-mounted antenna receiving signals transmitted

from the ground. Attenuation and phase-shift measurements also may be carried out on signals reflected from the ionosphere. The measurement of the differential amplitude of characteristic waves reflected from the D region is referred to as the "partial reflection" technique. The measurement of differential phase of reflected signals is possible but the techniques for carrying out this measurement are as yet undeveloped.

In order to use the measurement techniques described above, it is necessary to transmit vertically and receive the two characteristic polarizations which can be determined knowing the strength and direction of the earth's magnetic field. The transmission of a specified polarization from an antenna over a flat earth is relatively easy since the presence of the earth has no effect on the polarization of the vertically radiated wave, However, the mobile rocket launcher program carried out by NASA as a contribution to the International Quiet Sun Years required that antennas be mounted on the aircraft carrier "Croatan" and used by University of Illinois staff for the differential absorption, Faraday rotation and partial reflection experiments. The radiated polarizations clearly would be affected by the presence of the aircraft carrier, especially since the dimensions of the ship are comparable to a wavelength (the dimensions are roughly $1/4\lambda$ x $1/4\lambda$ x $1\ 1/2\lambda$ for frequencies in the vicinity of 3 mc).

The purpose of this discussion is first to show that the ship's hull and superstructure have a strong effect on the radiated polarization. This is done by carrying out measurements on a 450:1 scale model of the aircraft carrier and antenna system. The second objective is to describe various techniques which can be employed in order to set up the antenna system for

any prescribed polarization, The basic requirement is the efficient, independent radiation of two different polarizations with a wide range of relative amplitude and phase. This requirement is satisfied by the crossed-dipole arrangement shown in Figure 5.1; crossing the dipoles at a 90^{o} angle minimizes mutual coupling and orienting the dipoles at 45^{o} to the ship's axis permits each dipole to be a half-wavelength long (with any excess length bent downward near the masts), Attenuators and phase-shifters are inserted in the feedlines next to the transmitter (or receiver). The so-called "Y" match is used to connect the feedlines to the dipoles.

Model Studies

The flight deck of the aircraft carrier "Croatan" is approximately 500' long, 80' wide and 70' off the water. A simplified scale model with a scale factor of 450 was constructed and a flat metal plane was used to represent the surface of the sea. A rotating dipole antenna was mounted directly above the model in order to obtain voltage polarization patterns, examples of which are shown in Figures 5.2 and 5.3, The experimental frequencies ranged from 1.0 to 1.5 GHz corresponding to a range from 2.2 to 3.3 MHz on the full-scale aircraft carrier,

The primary purpose was to find out how much the ship's hull and superstructure affect the polarization of a straight dipole antenna hung horizontally 70' above the deck. For one particular frequency the patterns in Figures 5.2 and 5.3 show that the ship's hull has a pronounced effect on the polarization and that the addition of superstructure to the model produces an equally strong additional effect. Furthermore the addition of the superstructure destroys the mirror symmetry between the patterns of antennas 1 and 2.

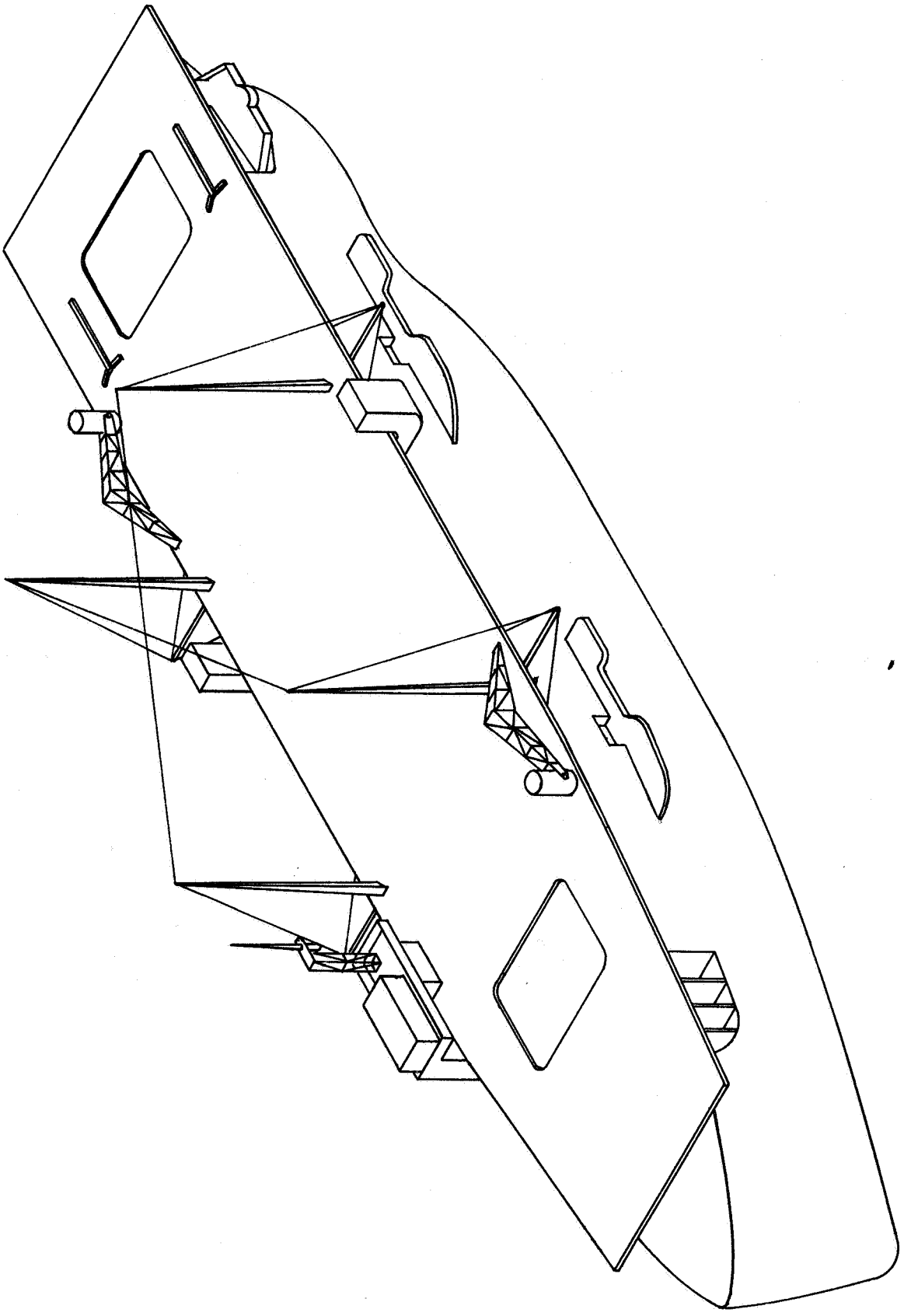

Figure 5.1 The crossed-dipole aircraft carrier antennas

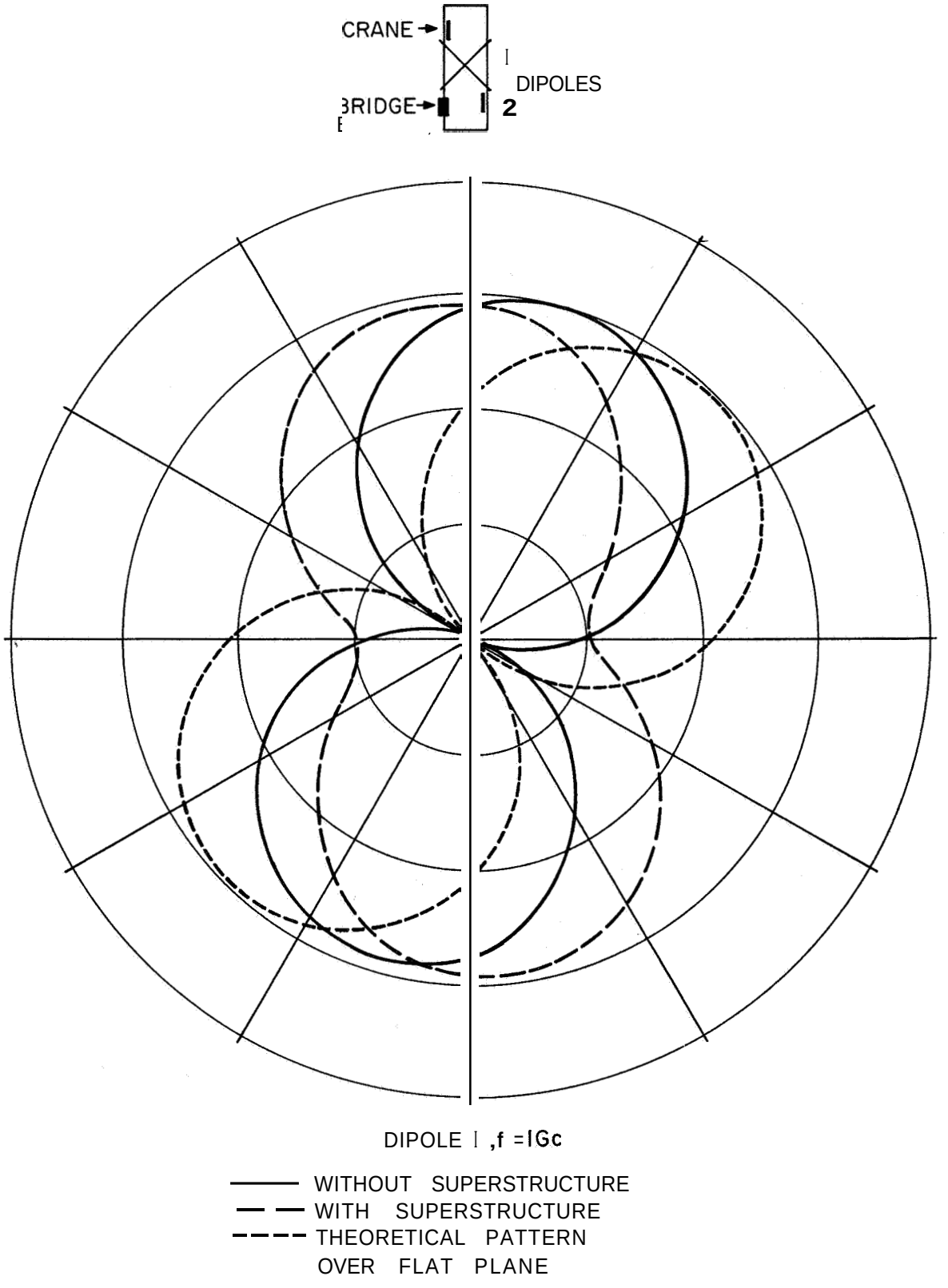

Figure 5.2 Polarization patterns for dipole no. 1.

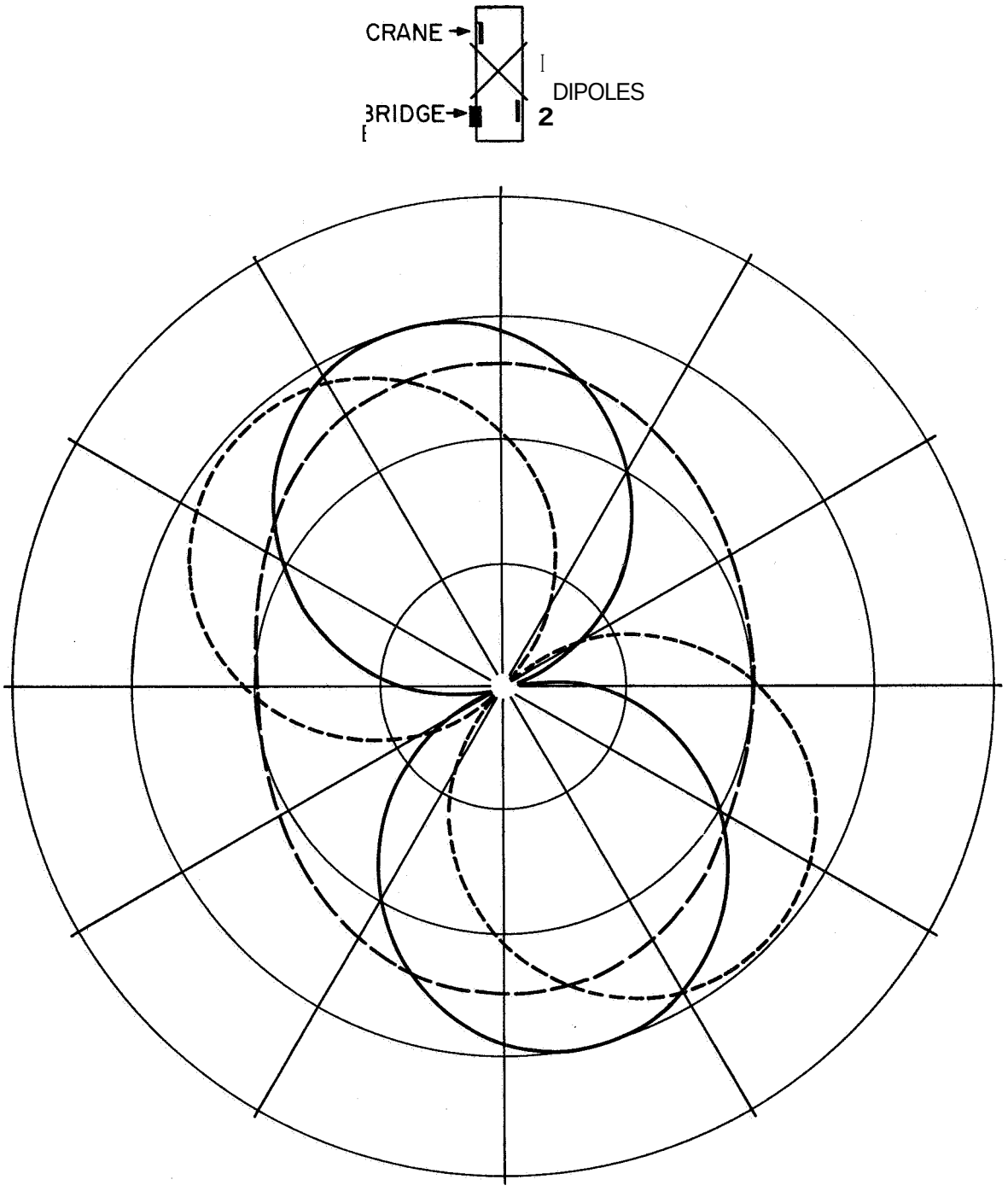

Figure 5.3 Polarization patterns for dipole no. 2.

When a number of polarization measurements is carried out, it is convenient to plot the polarizations as points on a surface. One such surface is the surface of the Poincare' sphere (Ramsey et al., 1951 and Papas, 1965); the "poles" of the sphere correspond to right and left circular polarization while the points of the "equator" correspond to all possible orientations of linear polarization, The points on the curved spherical surface may be mapped onto the flat equatorial plane by some projection, a very useful one being the stereographic projection. This projection consists of drawing a line from the paint on the sphere to one of the poles; the intersection of this line with the equatorial plane determines the projected point, Thus points on one hemisphere (one sense of polarization) fall inside the equator while points on the other hemisphere (the other sense of polarization) fall outside the equator.

A complete set of polarization measurements is represented in Figure 5.4 as stereographic projections on the equatorial plane, the equator being indicated by the large circle, In the experiments the sense of polarization was not measured and for this reason all the polarizations have been plotted inside the equator, Without the superstructure it is clear that the hull very strongly influences the polarization and that the polarization is strongly dependent on frequency. As would be expected, the polarizations from the two antennas exhibit nearly perfect mirror-image symmetry, With the superstructure attached, a strong non-symmetrical influence is evident.

From the experiments it is clear that the antenna environment (the ship and its superstructure) exerts a controlling influence on the polarization of the vertically radiated wave. In order for scale model studies to provide

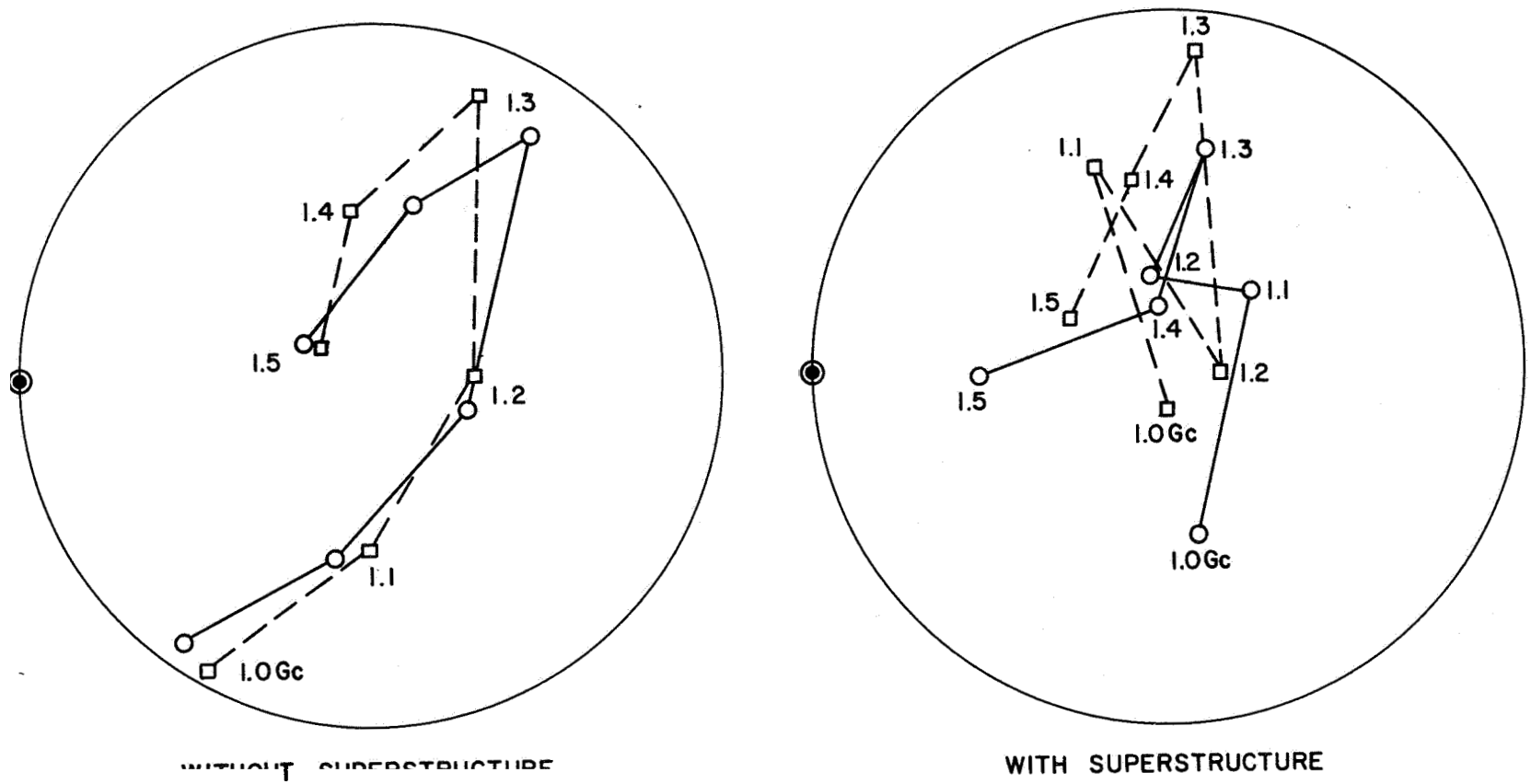

Figure 5.4 Model carrier polarization measurements using stereographic projection from the Poincare' sphere.

an accurate prediction of polarization, it would be necessary to construct a very precise scale model. Even if a sufficiently precise model could be constructed, difficulties would arise due to last-minute changes in the arrangement of objects mounted on the deck. Thus it is necessary to be able to carry out polarization measurements at sea shortly before the antenna is to be used for ionospheric sounding,

Shipboard polarization measurements

Helicopter overflight:

The most direct and accurate general method of measurement is the use of a spinning magnetic dipole suspended below a helicopter hovering over the carrier. It is convenient to use a rocket payload for this purpose since the payload contains all the necessary equipment (antenna, receivers, and telemetry). The axial ratio and the orientation of the polarization ellipse can be measured by causing the payload to rotate, However, in practice, the rotational speed is too slow to permit measurements of the senses of polarization.

Deck-mounted spinning dipole:

A spinning magnetic dipole mounted on the deck directly beneath the center of the antenna array can be used to measure the polarization, The axial ratio and orientation of the polarization ellipse can be measured as in the case of the payload suspended from a helicopter. In addition, the rotational speed of the spinning dipole can be made great enough so that sense of polarization can be measured. The method is simply to measure accurately the frequency of the received signal; the received signal frequency differs from the transmitted frequency by the frequency of rotation and the sign of the frequency difference gives the sense of the polarization,

Due to the irregular nature of the antenna platform, the fields measured at any one point on the deck are not representative of the far field and thus the polarization measured by the deck-mounted spinning dipole is necessarily inaccurate. In practice, however, it was found that the deck measurement of polarization was surprisingly close to the helicopter measurement, provided that the deck beneath the antenna was cleared of all metallic objects and also provided that the feedlines were arranged symmetrically. Under these conditions it proved possible to calibrate the deck measurement in terms of the helicopter measurement so that the continued use of the helicopter became unnecessary.

Post-launch rocket measurement:

Telemetry pickup from a rocket shortly after launch provides a check on polarization. Between the time of launch and entry into the ionosphere, the rocket provides an excellent spinning mount for the magnetic dipole contained in the payload. As in the helicopter measurements, the axial ratio and orientation of the polarization ellipse are easy to measure. As with the other spinning dipole techniques, the measurements are easiest when the polarization is nominally circular (for high-latitude ionospheric sounding). Measured post-launch axial ratios were always less than 1.5 for nominal circular polarization.

Ionospheric reflections:

Reflections from the ionosphere may be used to set polarization because, during the day, the extraordinary wave is strongly absorbed in the D region while the ordinary wave is reflected from the E and F regions. Thus the adjustment of the attenuator/phase-shifter (on either the transmitter or the receiver)

for minimum received signal corresponds to adjustment for extraordinary polarization.

Accurate adjustment for ordinary polarization is considerably more difficult. It can be done with the help of an auxiliary spinning dipole measurement or by the use of special procedure utilizing ionospheric reflections. One such reflection procedure has been used to set up the receiver attenuator phase-shifter for partial reflection measurements. If T and R stand for the transmitter and receiver attenuator/phase-shifter and if "e" and "o" denote extraordinary and ordinary the procedure may be outlined as follows:

1. Set R_e by adjusting for minimum received signal.
2. Retain R_e and set T_e by adjusting for maximum.
3. Retain T_e and set, R_o by adjusting for minimum,
4. Perform experiments with T arbitrary.

This procedure has been carried out successfully. However, step 2 has an alternative which may be more precise. It may be expressed as follows:

2. (alt) With R arbitrary set T_e by adjusting for minimum.

The suggested alternative has the advantage of a minimum or "null" adjustment.

In practice, the equatorial and low-latitude attenuator/phase-shifter adjustments proved very difficult to make. This was expected since the equatorial absorption of the extraordinary wave is not high enough to permit precise nulling procedures of the type outlined above. In addition, difficulties are to be expected at intermediate latitudes since the characteristic polarizations are dependent on the electron density for propagation in directions neither parallel nor perpendicular to the magnetic field.

Theoretical study

The practical difficulties involved in setting the antenna system for a given polarization (especially ordinary polarization) gave cause for a study of the parameters involved. Suppose that p denotes complex polarization ratio, x and y denote the rectangular components of electric field strength and β denotes the attenuator/phase-shifter setting. Furthermore let subscripts "1" and "2" denote the two crossed dipoles and "e" and "o" denote "extraordinary" and "ordinary". These quantities are related by the following equations:

$$x_e = x_1 + \beta_e x_2 \qquad p_1 = y_1/x_1$$

$$y_e = y_1 + \beta_e y_2 \qquad p_2 = y_2/x_2$$

$$x_o = x_1 + \beta_o x_2 \qquad p_e = y_e/x_e$$

$$y_o = y_1 + \beta_o y_2 \qquad p_o = y_o/x_o$$

If the x's and y's are regarded as unknowns and if the other quantities are regarded as parameters, then the above constitute eight linear, homogeneous equations in eight unknowns. Setting the determinant of the coefficient matrix equal to zero gives the following equation:

$$\beta_o (p_1 - p_e)(p_2 - p_o) = \beta_e (p_1 - p_o)(p_2 - p_e)$$

Evidently any one of the parameters may be obtained if all the others are known.

In general p_o and p_e are known, and p_1 and p_2 can be measured. Thus if β_e can be determined from ionospheric reflections, then β_o can be calculated using the relation

$$\beta_o = \beta_e \frac{p_1 - p_o \quad p_2 - p_e}{p_1 - p_e \quad p_2 - p_o}$$

The usefulness of the above formula may be extended provided that an auxiliary polarization p_a can be measured for some arbitrary attenuator/phase-shifter setting β_a. Writing the subscript "a" in place of "o", we have

$$\beta_e = \beta_a \frac{p_1 - p_e}{p_1 - p_a} \frac{p_2 - p_a}{p_2 - p_e}$$

For the auxiliary measurement it would be possible to make $\beta_a = 1$ by setting the phase-shift and attenuation to zero. Thus with p_e and p_o known, measurement of p_1, p_2, and p_a make possible the computation of β_e and β_o.

Polarization measurements are usually made in terms of the sense, orientation and axial ratio of the polarization ellipse, A Smith chart graphical technique has been devised (Bamsey et al., 1951; Mayes, 1965) to obtain the polarization rate p from these quantities. This technique requires the definition of the quantity S:

$S = jp$ for the right-hand sense of polarization
$S = -jp$ for the left-hand sense of polarization

It can be shown that S is related to another quantity Γ through the transformation

$$S = \frac{1 - \Gamma}{1 + \Gamma}$$

The magnitude of Γ can be found from the axial ratio, and the argument of Γ can be found from the orientation of the polarization ellipse as shown in Figure 5.4, Furthermore, the transformation between S and Γ is identical to the transformation between admittance and voltage reflection coefficient in transmission line theory. Thus the Smith chart may be used to obtain S from Γ as shown in Figure 5.5.

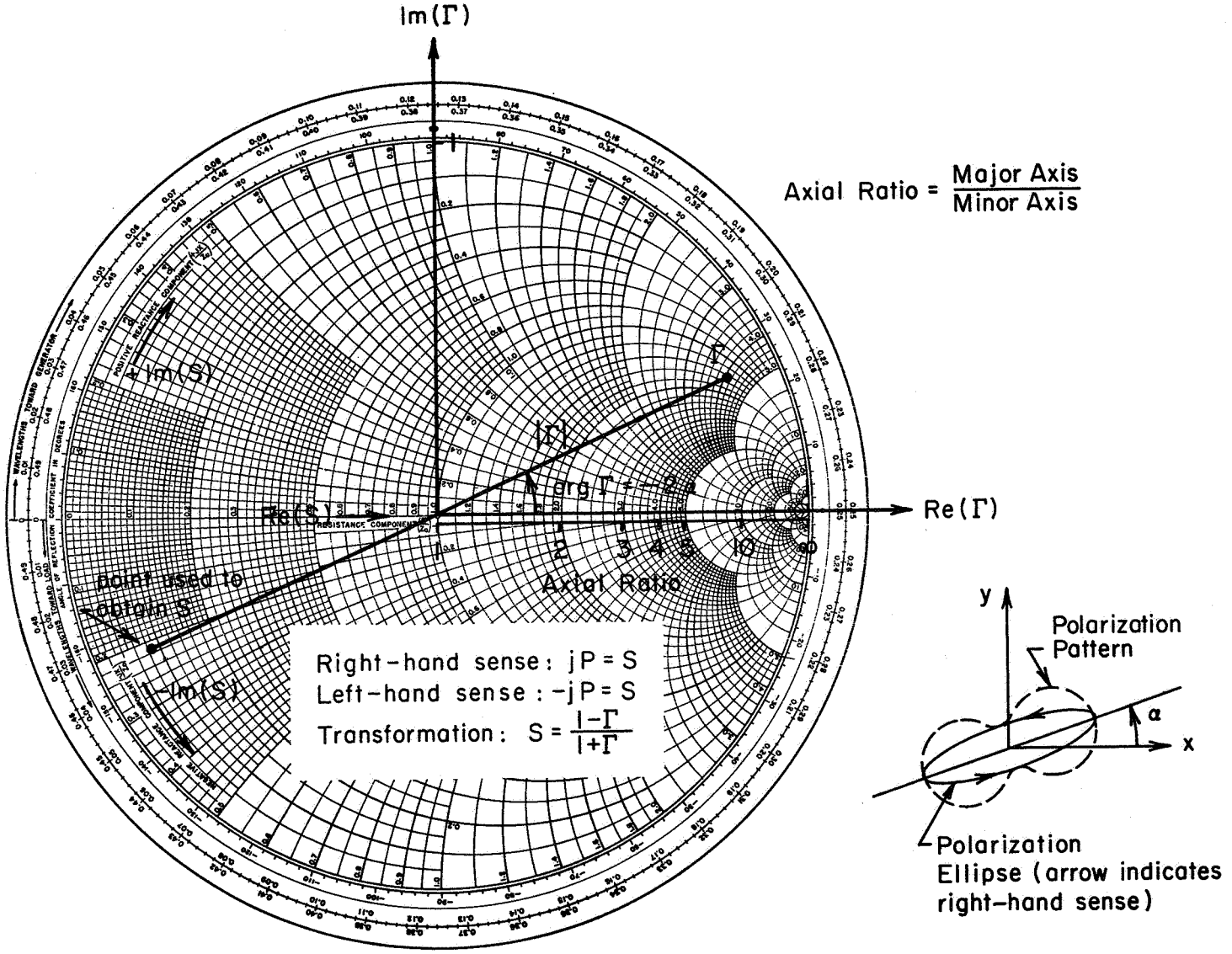

Figure 5.5 Smith chart determination of the polarization ratio P.

It is important to note that the above theoretical discussion is exact (at least within the terms of reference). Thus the theory may be applied with confidence provided that the polarization measurements and attenuator/phase-shifter calibration are accurate.

Model studies show that the aircraft carrier's hull and superstructure both have a strong influence on the polarization of a vertically radiated wave, For frequencies in the megaherz range the radiated polarization is markedly frequency-dependent. For these reasons, shipboard measurement of polarization is a necessity.

Measurement of polarization is possible using helicopter overflights, a deck-mounted spinning dipole, ionospheric reflections or post-launch rocket measurements. As far as antenna system adjustment is concerned, all the above methods have serious drawbacks but adequate accuracy can be obtained by employing two or more of the experimental methods. These methods have the advantage of not requiring attenuator/phase-shifter calibration.

With adequate attenuator/phase-shifter calibration it is possible to calculate the settings necessary to produce both extraordinary and ordinary polarization. To do this it is necessary to make three polarization measurements. These are the two polarizations radiated by the dipoles excited individually plus the polarization radiated with some arbitrary (but known) attenuator/phase-shifter setting,

Antenna, Matching Network, and Phase-Shifter Design

Antenna:

The antenna requirements of the ionospheric sounder on board the ship were:

1. The antenna system must be capable of vertically radiating either ordinary or extraordinary modes of circular polarization.

2. The antenna system must be capable of handling peak pulse powers of approximately 50 kw.

3. The antenna system must be matched to a 50 ohm coaxial cable at 3030 kHz.

4. Space limitations imposed by the ship were maximum dimensions of a rectangle 110 feet by 72 feet.

5. To be compatible with the rocket experiment, the antenna system should be composed of two mutually perpendicular dipoles of a length of 100 feet, at a height of 60 feet above the flight deck of the ship, and preferably fed with 72 ohm twin-lead balanced feedline.

Operation of the 50,000 watt transmitter and antenna system in the salt and stack gas saturated environment of the ship presented a number of problems not previously encountered in land installations. Testing confirmed the fact that the 72 ohm twin-line, while adequate for the 1000 watts radiated in the rocket experiment, would not withstand the high voltages generated by the 50,000 watt transmitter. Simple replacement of the 72 ohm lines with 470 ohm open-wire transmission lines still resulted in feedline breakdown because of the high standing wave ratio on the lines. The final solution of the transmission line problem was found in the use of the "delta" or "Y-match" dipole feed system (ARRL, 1960). The delta matching system is a combination of tapered-line and folded-dipole impedance transforming techniques. The dimensions of the delta matching network have been empirically derived for optimum match to a 600 ohm transmission line. However, the height of the shipboard antennas was insufficient to achieve the recommended dimensions of the delta match and the dimensions were experimentally adjusted with the assistance of an impedance bridge so that a resistive impedance of

750 ohms was achieved at the feedpoint on the deck of the ship. Use of the delta matching network required extension of the dipoles themselves to a half-wave resonant length of approximately 157 feet overall. This was achieved by extending the ends of the antenna downward toward the flight deck at each corner. Resolution of the feedline breakdown problem allowed still another antenna breakdown to occur. With the full 50,000 watts applied to the antenna system, corona developed at the ends of each antenna, It was found that the heavy accumulation of soot from the ship's stacks and the salt-saturated air gave rise to a much lower air corona voltage than has been observed for land installation. Four inch diameter anti-corona rings were fashioned for each insulator and installed. These rings ended antenna breakdown problems, but required daily cleaning to prevent buildup of soot and re-occurrence of corona, Another problem associated with the radiation of the very strong RF field was that corona formed on several wires in the near vicinity of the antennas and required use of anti-corona paints to eliminate the wide spectrum of radio interference generated. The diagram of the antenna system used for ionospheric sounding measurements is shown in Figure 5.6.

Matching Network:

The design of the antenna matching network also evolved from experimental work on board the ship. As stated previously, the original intention was to use the antenna with the 72 ohm feedline to achieve compatibility between the rocket experiment and the sounder experiment, With this in mind, the initial matching work incorporated an L-network for impedance matching and a 4:1 balun to transform the unbalanced 50 ohm coax to 200 ohms balanced impedance. Using

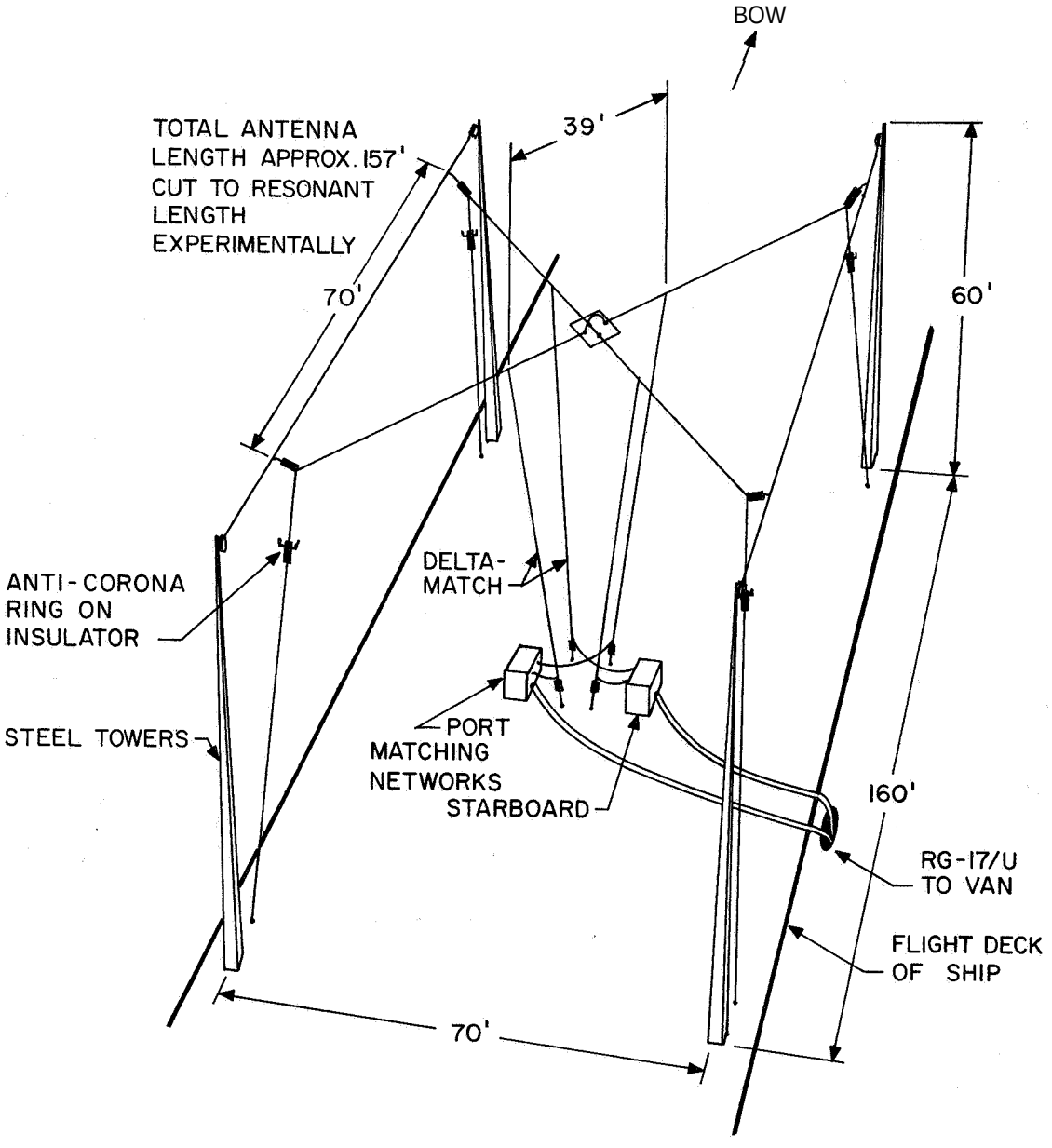

Figure 5.6 Shipboard antenna system.

a design similar to that used by Gooch (Knoebel et al, 1965) for the rocket experiment, a set of balun coils were constructed. These balun coils were one foot in diameter and were wound with the center conductor plus the polyethelyene insulation of RG-8 coaxial cable in a bifilar coil two feet in length. The dimensions of the polyethelyene are such that the two wires side by side have a characteristic impedance of approximately 110 ohms. Two of these bifilar coils were required for each antenna--four total were constructed. The baluns did achieve the balanced to unbalanced transformation, but it was determined that they also contributed considerable reactance and were very susceptable to other radiated fields. It was also determined that to match the antenna feedlines, a much greater range of impedance adjustment was desirable. Experiments with these balun coils were conducted during the shakedown cruise in November, 1964 and it was determined at this time that a redesign of the matching system as well as the antenna feed system would be required. The schematic diagram of the balun matching network is shown in Figure 5.7.

Impedance measurements made on the antennas during the cruise in November showed the need for a network capable of matching balanced impedances ranging from 100 to 1500 ohms to the 50 ohm unbalanced cable. The matching network designed to achieve this is based on a tuned transformer identical to the final output tank of the transmitter. This tuned tank transforms the unbalanced 50 ohm coaxial line to 500 ohms balanced. A rotary inductor across the 500 ohm transformer output is used as an adjustable autotransformer to achieve an impedance matching range of 50 to 1250 ohms. A variable capacitor in parallel with a 10 μH coil provides means of compensating either

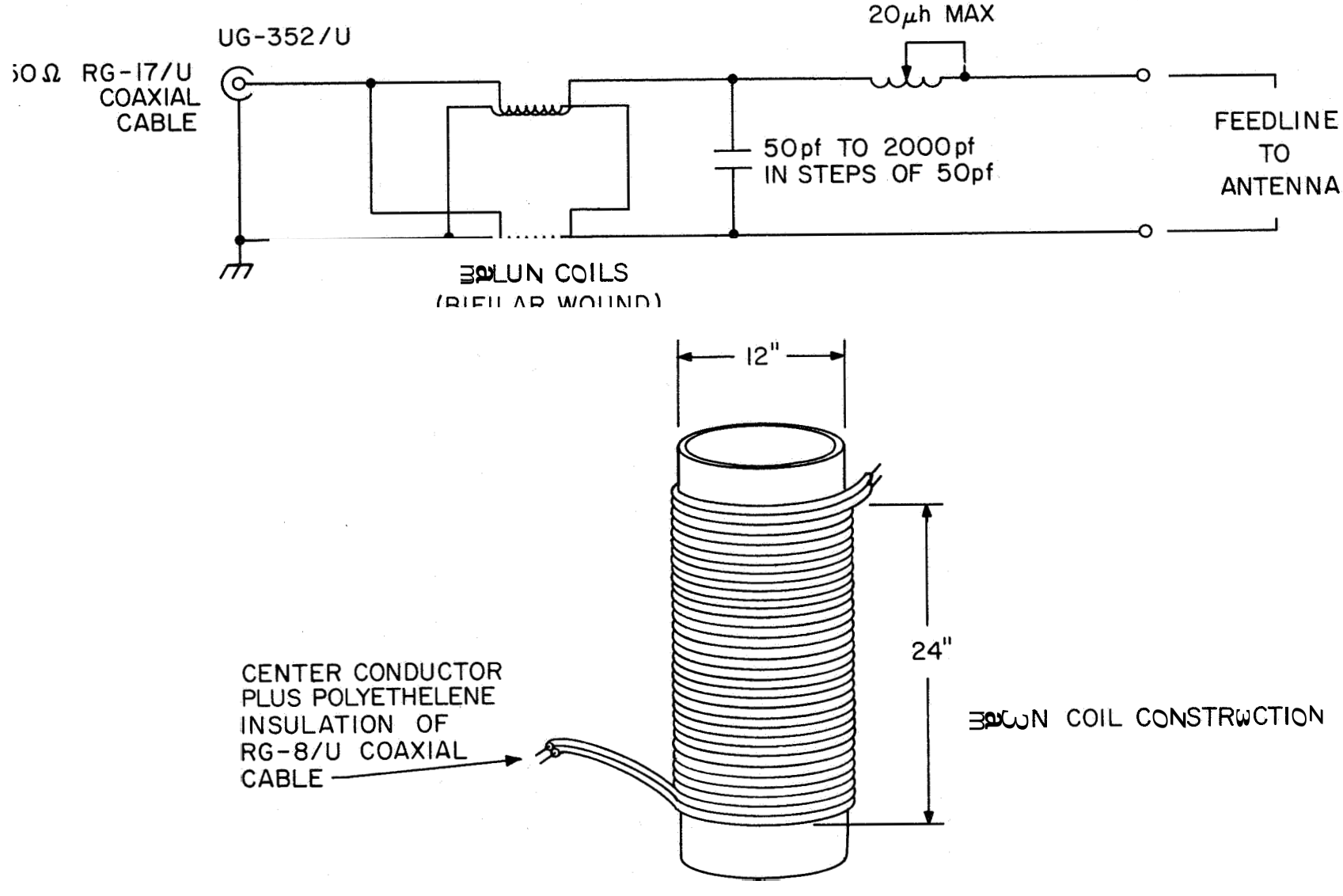

Figure 5.7 Balun-coil matching network.

capacitive or inductive reactances of the antenna. This capacitor also tunes out any leakage reactance contributed by the autotransformer. The schematic diagram of this unit is found in Figure 5.8. Adjustment of the matching network involves resonating the tuned transformer to the operating frequency and adjusting the autotransformer and reactance compensation to achieve a 50 ohm impedance at the input with the antenna connected. All three controls interact and the alignment procedure requires the use of an impedance bridge. The relay is included in one of the two networks to provide the antenna line reversal necessary to change from one mode of circular polarization to the other. These matching networks were used throughout the second portion of the ship cruise and are presently in use at the University of Illinois field station in an fonospheric sounder.

Phase-Shift Network:

In order to generate circular polarization with two mutually perpendicular dipoles and no other radiating elements in the near field, it is necessary to introduce a phase-shift of 90 degrees in one of the feedlines (Offutt et al., 1961). The use of 90-degree phase shift networks has given very good circular polarization at the Wallops and University of Illinois land installations. However, because of the ship's superstructure, cranes, and antenna wires for other experiments, many elements capable of reradiation were within the near field of the shipboard antenna system. The model studies discussed earlier proved this point and demonstrated the need for a phase-shift network with a wide range of adjustment to compensate for the distorted polarization pattern of the antennas. A phase-shift system for the transmitter was designed and tested during the November cruise that was capable of achieving any prescribed

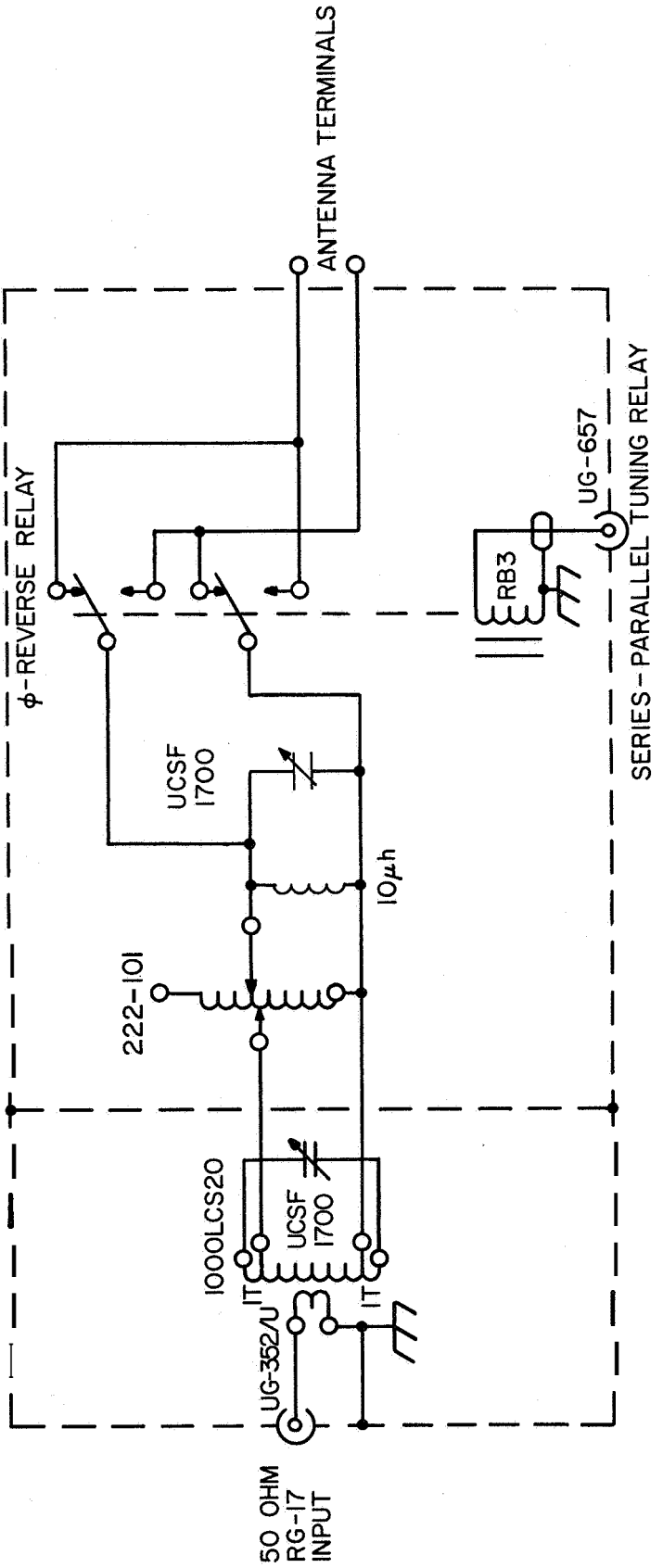

ANTENNA MATCHING NETWORK
50 TO 1250 OHMS BALANCED TO 50 OHM COAX

Figure 5.8 Tuned transformer matching network.

phase shift between the two feedlines over the range from zero to 360 degrees. The schematic diagram of this system is shown in Figure 5.9. The basic phase shifter elements are T-networks, designed for 500 ohms input and output impedance, Phase shift is adjusted by changing both inductive arms and the capacitive shunt arm, Practical considerations dictated that the minimum phase shift easily achieved with this form of network is 45 degrees. Therefore, a fixed 45 degree network is inserted in one of the feedlines to the antenna. The variable phase-shift network is adjustable between 45 and 135 degrees or, zero to 90 degrees relative to the other antenna terminal. By simply reversing one of the feedlines, 180 degrees of phase shift is introduced and the range of 180 to 270 degrees relative phase is possible. Interchanging the two antennas provides for the 180 to 90 degree and 360 to 270 degree quadrants. As can be seen from Figure 5.9, separate variable phase-shifters for the ordinary and extraordinary modes are provided to assure complete versatility of adjustment. The entire phase-shift system occupied one six foot rack and used 500 ohm open wire for interconnection of the various units, Operation of the phase-shift system during the November cruise demonstrated the following shortcomings:

1. The use of the high-impedance open wire lines between the units of the phase-shift syetem resulted in radiation of RF fields of sufficient strength inside the equipment van to cause spurious triggering of the timing and control system,

2. The adjustable phase-shifters required three separate adjustments for each change of phase and all three had to correspond to a precalculated chart of values to assure that the phase shift was achieved without an impedance transformation, Alighment of the antennas requires phase shift controls that are easily adjusted over a wide range within the period of one to two minutes--completely impractical with the system as designed,

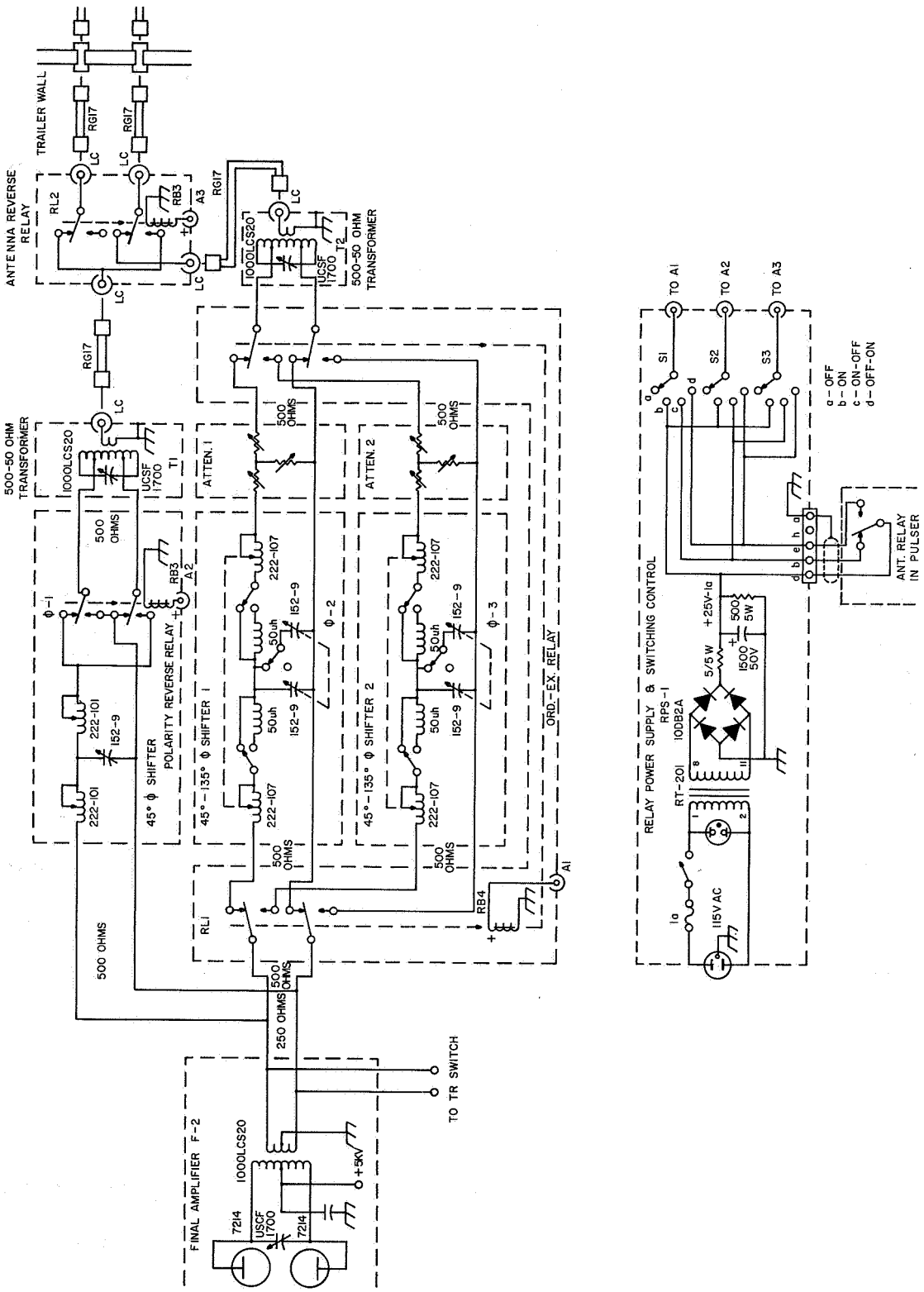

Figure 5.9 High-power, high-impedance phase-shift network.

3. The large number of tuned circuits, relays, and interconnecting feedlines made it very difficult to adjust the system so that losses were low. An error of 5% in the setting of any of the phase-shifters or tuned transformers resulted in a loss of at least 3 dB of radiated power.

For these reasons, it was decided that the transmitter would be connected to only one of the antennas and essentially linear polarization would be radiated. The circular polarization of the antennas would be achieved only in the receive mode in which low power phase-shift systems could be easily designed and operated. The receiving phase-shift system designed and used in the latter portion of the cruise is shown in Figure 5.10. The phase-shift element of this system is a General Radio 314-S86 variable delay line used in a manner similar to that developed for the rocket experiment (Knoebel *et al.*, 1965). This delay line provides a phase shift adjustment range from zero to 540 degrees by rotation of one knob. Impedance matching of the line requires that a loss of 3 dB per line be inserted, but this loss was not found to be enough to appreciably affect the performance of the system. Separate phase-shifters are provided for each mode of polarization as are separate attenuators. Relays driven by the timing and control system determine which mode is received. The disadvantage of this system is that, in addition to the 3 dB of loss introduced by the phase-shifters, the wide-band impedance transformers and the mixing pad on the output contribute losses on the order of 6 dB.

Antenna System Adjustment Procedure:

As stated previously, the phase-shift system for the transmitter proved to be undesirable for use in actual data recording operations. However, in the alignment of the antennas, the transmitter phase-shift system was used

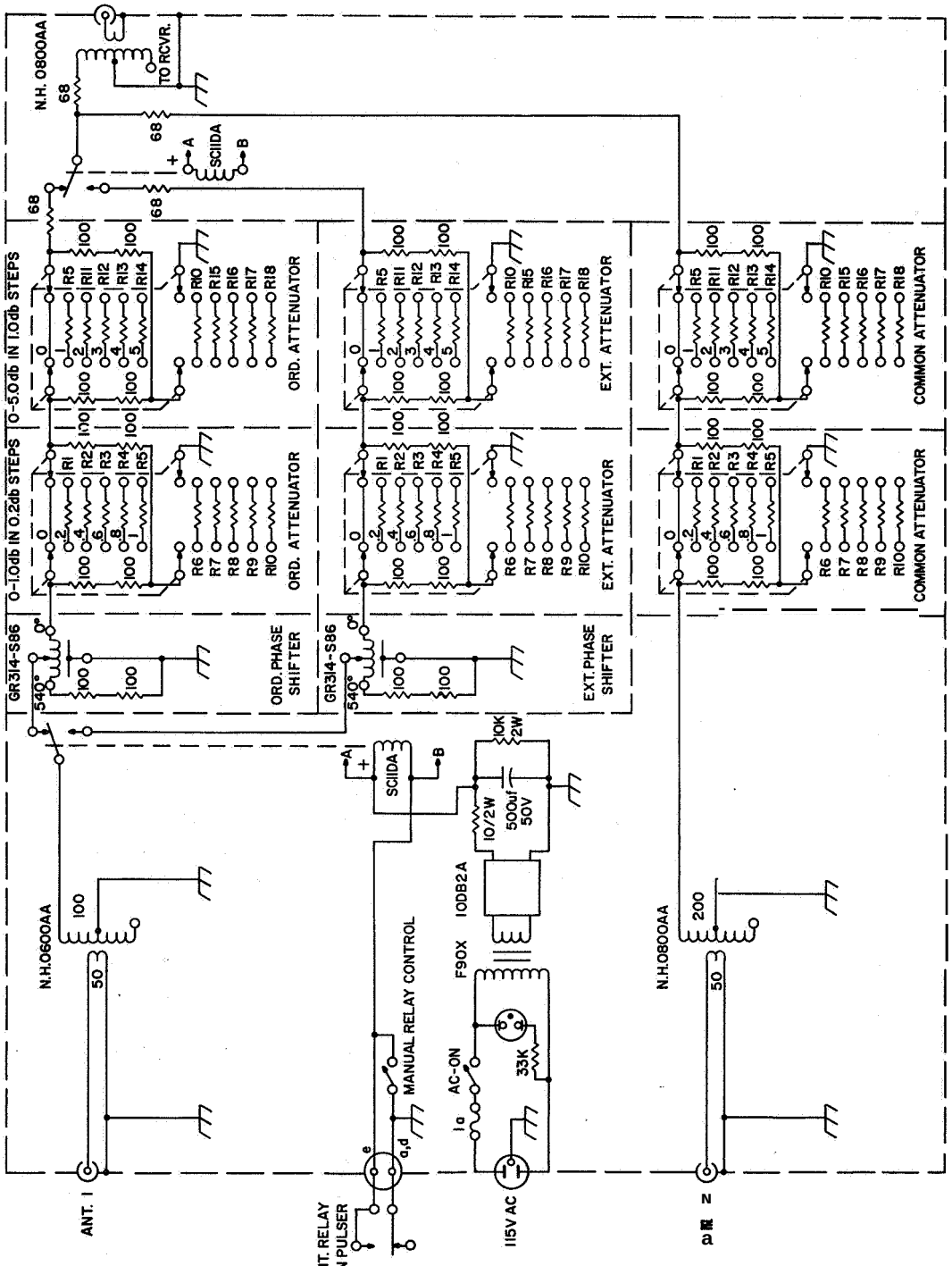

R	VALUE	IN PARA.
R1	4.64	10,10,68
R2	9.45	10,180
R3	14.32	15,330
R4	19.3	22.150
R5	24.4	33,100
R6	8.6K	10K,68K
R7	4.25K	4.7K,4.7K
R8	2.7K	2.7K
R9	2.07K	2.0K
R10	1.64K	3.3K,3.3K
R11	51.8	56,680
R12	82.6	82
R13	117.1	120,5.6K
R14	155.7	180,1.2K
R15	774	820,15K
R16	485	82,1.2K
R17	342	680,680
R18	257	270,4.7K

Figure 5.10 Receiving phase-shift network.

with the driver stage of the transmitter. The alignment of the antenna system involved the following steps.

1. With the transmitter connected to one of the antennas and radiating an essentially linear polarized wave, the receiver phase-shifter was connected to the antennas through the electronic transmit-receive switch and adjusted to receive only the extraordinary component of the E-layer reflected signal. Since absorption of the extraordinary wave is much greater than the absorption of the ordinary wave, this is a nulling operation and can be very accurately determined.

2. With the transmitter and antennas still radiating a linear wave, the receiver phase shifter was shifted to the ordinary mode and adjusted for maximum received E-layer reflection. This adjustment is not as precise as the nulling operation, but it is primarily used to set up the following step.

3. The driver stage of the transmitter was now connected through the transmitter phase-shift network to the antennas and the receiver phase-shift network was set in the ordinary mode determined above.. The transmitter phase shifters were now adjusted for minimum. received E-layer reflection, indicating minimum radiation of the extraordinary wave.

4. With the transmitter radiating extraordinary and the receiver set up to receive ordinary polarization, the receiver phase-shift system was readjusted for minimum reflected signal, assuring true adjustment of the receiver system for both ordinary and extraordinary polarizations.

5. The above procedure was repeated several times to assure accurate adjustments of the received polarizations. The accuracy of the polarizations varied because of the shifting of the antennas and feedlines with ship motion. The antennas were aligned three times each day of observatioq.

Wallops Antenna Systems:

The ionospheric sounding system in use at Wallops Island, Virginia incorporates separate antenna systems for transmitting and receiving. Both antenna arrays consist of four half-wave center-fed dipoles in a square box arrangement. The opposite parallel antennas are fed in phase and the two

sets of dipoles have separate feedlines to the operations room where 90 degree phase shifters are used to achieve circular polarization. The diagram of the transmitting and receiving arrays at Wallops Island is shown in Figure 5.11.

The operating frequency for the installation is 3.030 MHz and therefore both sets of antenna elements are trimmed to a length of approximately 160 feet. The dipoles of the transmitting array use the "delta" matching network described previously in the discussion of the shipboard antenna system. The transmission lines from the transmitter to transmitting antennas are two 450 ohm open-wire feedlines. The 90 degree phase shift and phase-reversal switch necessary to generate either mode of circular polarization are very similar in design to those used on the ship and are diagrammed in Figure 5.12.

The receiving dipoles are folded dipoles fed with two equal lengths of RG-62/U coaxial cable, The center conductors of the coaxial cables are connected to the folded legs of the dipole and the shields of both cables are tied to the center of the upper element to provide mechanical support of the feedline. Heavy-duty 300 ohm twin-lead was used as the feedline in the initial installation, but proved not to have sufficient mechanical strength to withstand the severe weather at Wallops Island. The coaxial cables are considerably stronger and actually provide a better match to the dipoles, as the feed'impedance is actually 200 ohms instead of the predicted 300 ohms because of the relatively low height of the antennas above the ground. Wide-band 100 ohm to 50 ohm transformers are used to match the antenna feedlines to the RG-8/U coaxial cable receiver feedline. The phase-shifting and

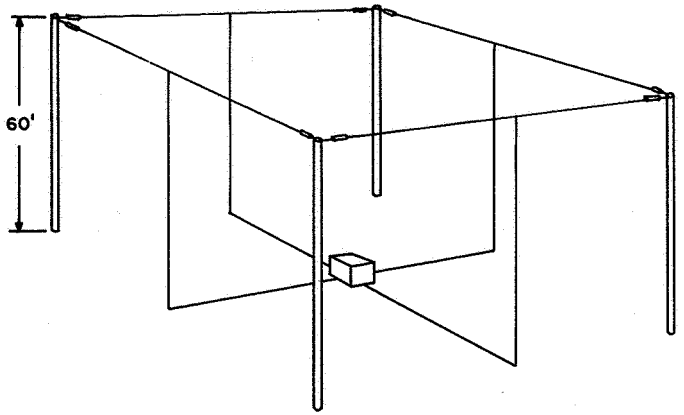

A

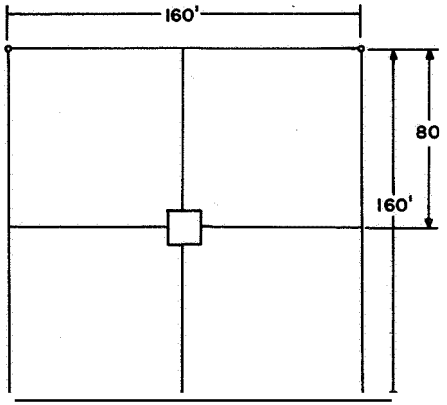

B

TRANSMITTER:
DELTA-MATCHED DIPOLE

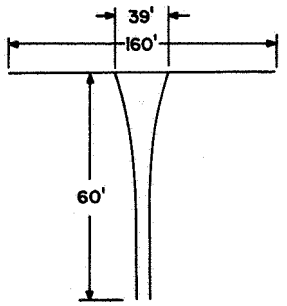

C

RECEIVER:
FOLDED DIPOLE

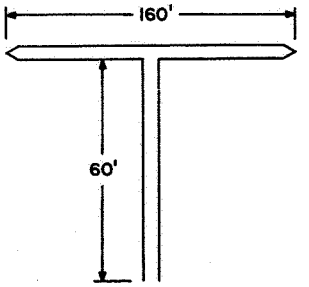

D

Figure 5.11 Wallops Island antenna systems.

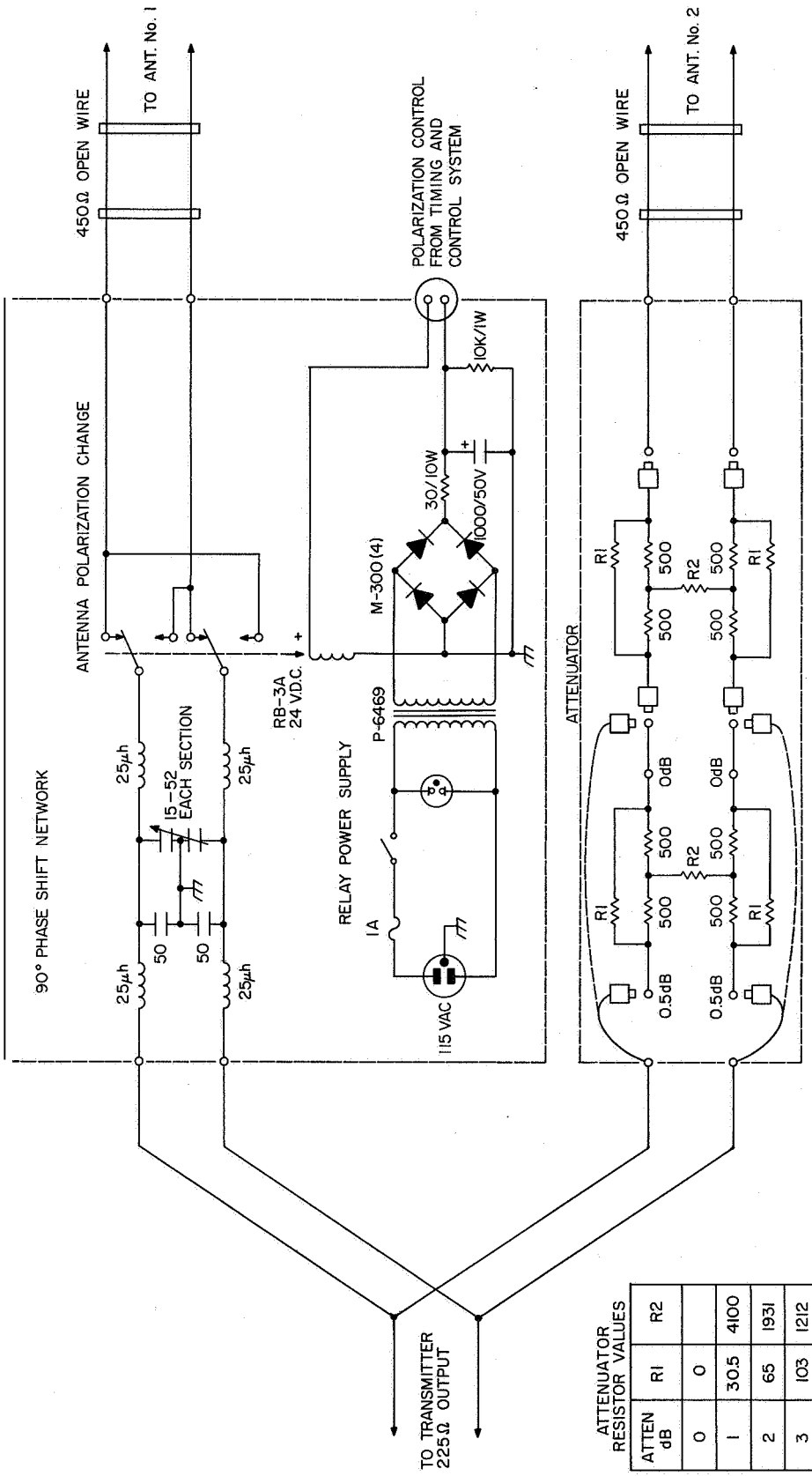

ATTENUATOR RESISTOR VALUES

ATTEN dB	R1	R2
0	0	
1	30.5	4100
2	65	1931
3	103	1212
4	146	855

Figure 5.12 Wallops transmitter phase-shift network.

phase-reversing system for receiving is very similar to that used for the transmitter, but uses a 180 degree phase-shift network to achieve mode change instead of transmission line reversal as is done in the transmitter networks. The schematic diagram of the receiver phase-shifting system is shown in Figure 5.13.

In the original Wallops installation, the transmitter was at its present location, but the receiver was located some five miles away. The receiving antenna system at that time was a system of 18 loops in a spaced array. The diagram of the loop antenna construction is shown in Figure 5.14, and the arrangement of the loop array is shown in Figure 5.15. Problems in synchronizing the receiving and transmitting installations and the lack of sufficient antenna gain prompted the move of the receiving installation to the transmitter site at the north end of Wallops Island with the transmitter where it is presently. Although the vertical directivity of the loop system was considerably better than that of the four dipole box array, an increase in received signal strength of approximately 30 dB was observed upon installation of the box array. This has been determined to be due to the poor efficiency of the loop antenna compare'd to that of a half-wave dipole. The improvement in signal-to-noise ratio was considered to be of more value than the vertical directivity gained with the loop'array in the measurement of partial reflections and ionospheric absorption.

Urbana, Illinois Antenna Systems:

Upon completion of the ship cruise, all instrumentation was returned to the University of Illinois and set up for measurement of partial reflections,

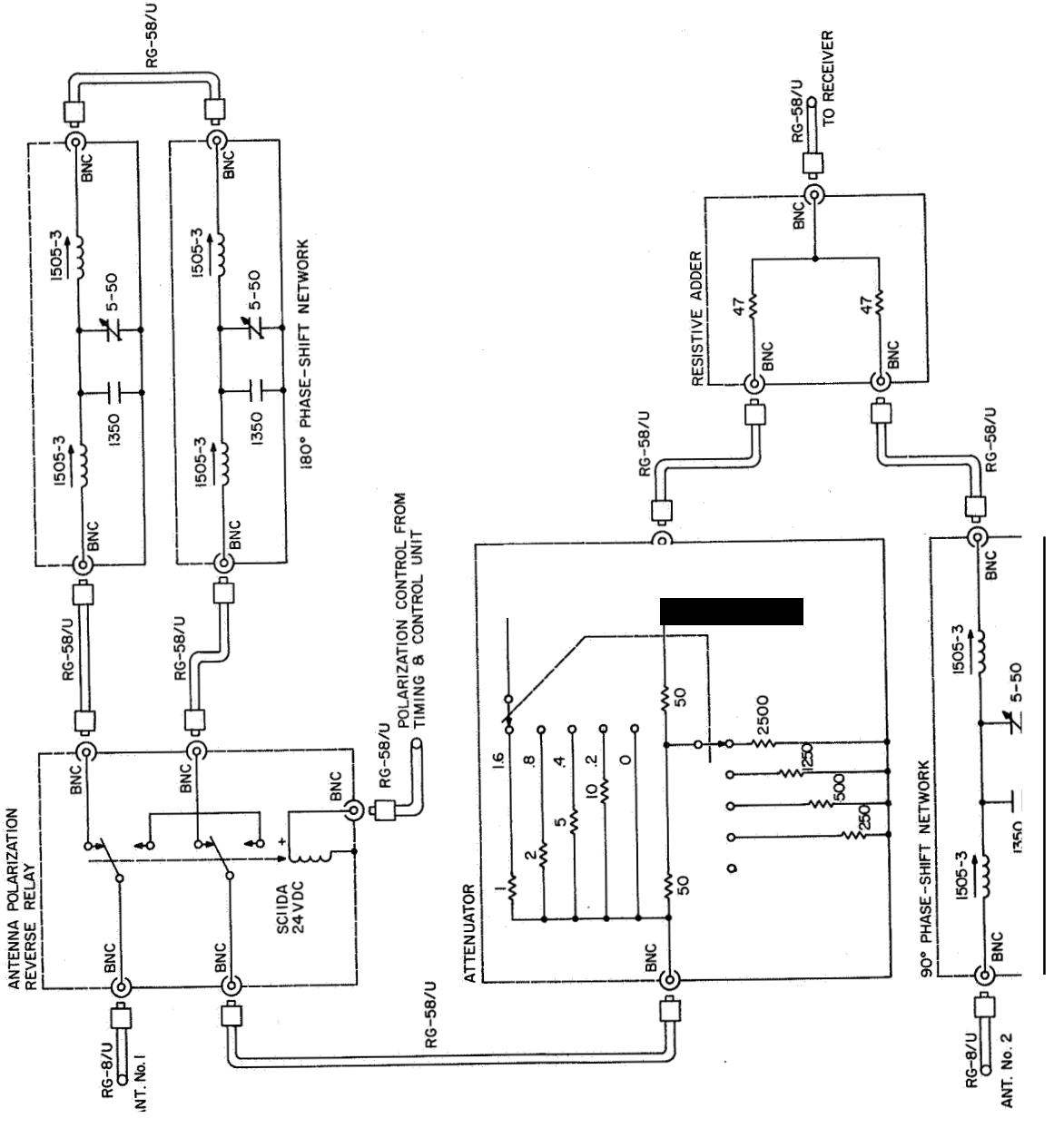

Figure 5.13 Wallops receiver phase-shift network.

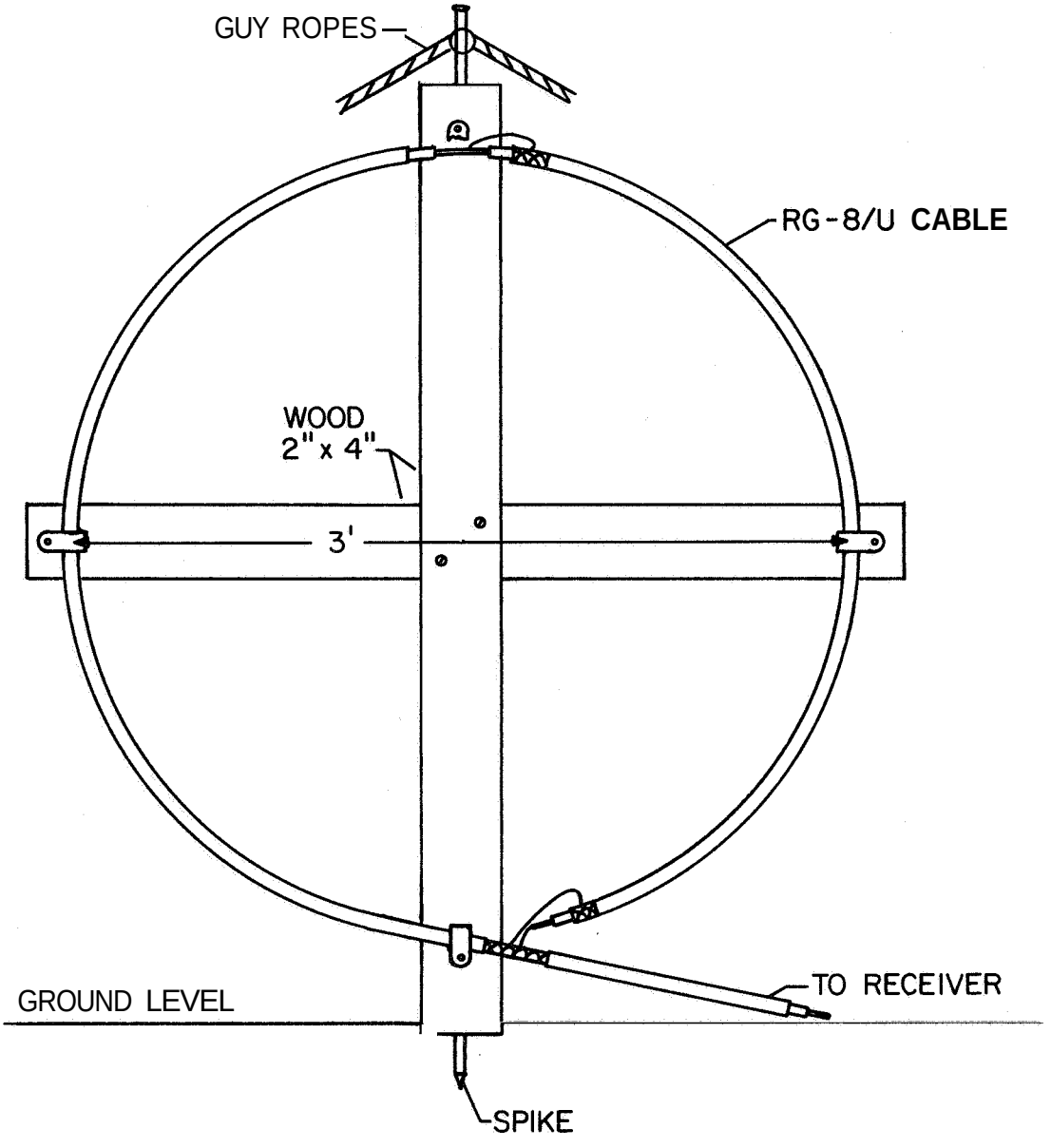

Figure 5.14 Wallops loop antenna.

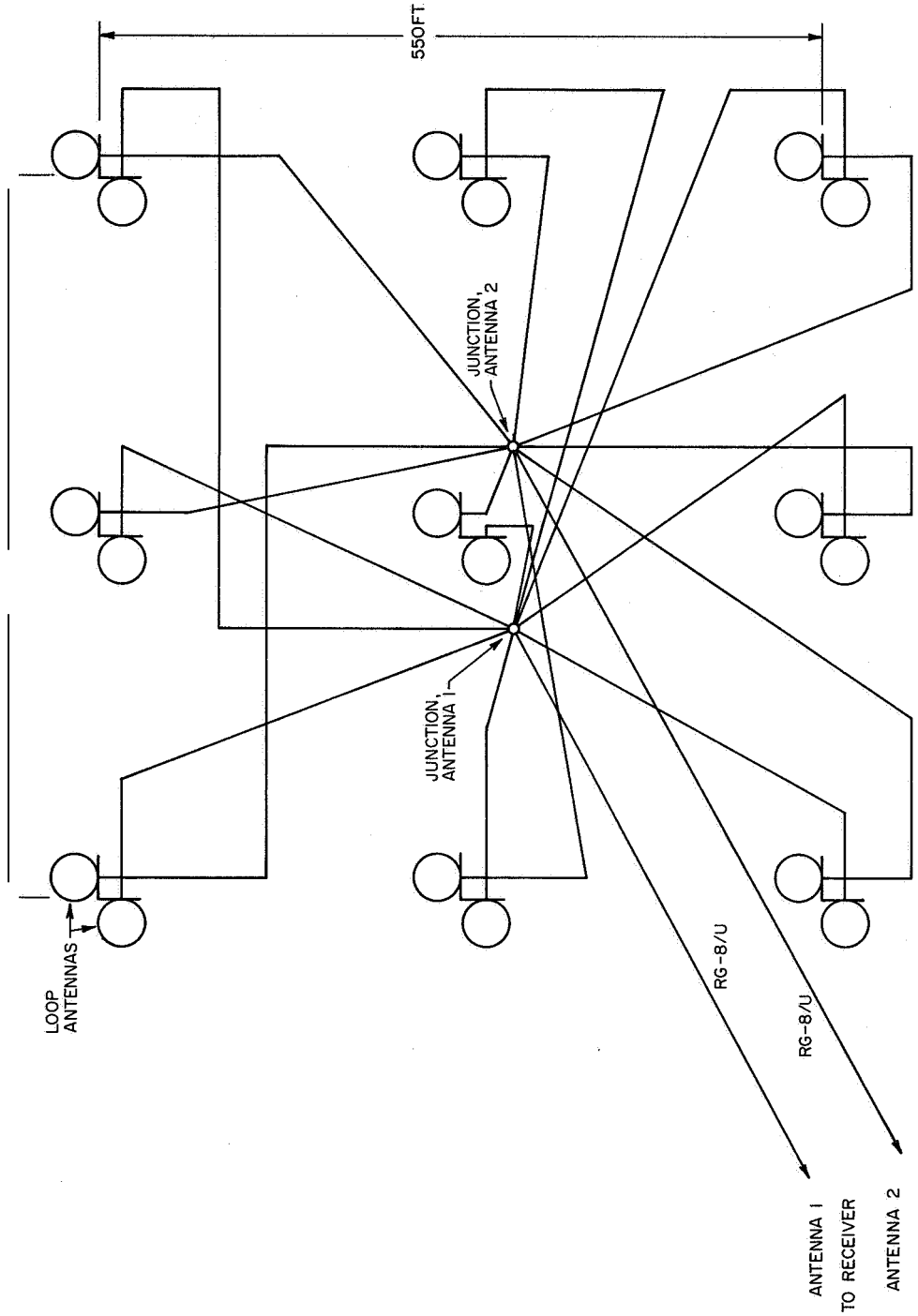

Figure 5 15 Loop array for receiving.

ionospheric absorption, and ionospheric drifts at the Aeronomy Laboratory Field Station northeast of Urbana, Illinois. The antenna system installed for use at the field station is identical in design to that used at Wallops Island and the diagram need not be repeated (see Figure 5.11). The matching networks included in the ship experiment are used in this system to match the 500 ohm antenna feed impedance to the 50 ohm RG-17/U coaxial feedlines. The transmit-receive switch used on board the ship is also incorporated in this installation, eliminating the need for separate transmitting and receiving antenna systems. A new phase-shift system has been designed and installed at the field station that affords considerable improvement over any designed previously and merits some discussion in this report,

Since the transmitter output and the antenna feedlines are both 50 ohms unbalanced, the logical approach to phase-shifter design is to use circuitry with 50 ohms characteristic impedance, The previous phase-shift networks of the T-network design are easily constructed with standard components if the system impedance is 250 ohms or greater. However, a T-network for 50 ohms requires impractically large capacitors and small inductors. The use of a coaxial delay line is a standard means of achieving phase shift, but does not provide any means of adjustment of phase shift short of switching various lengths of transmission line, also impractical with the very large RG-17/U cable. However, a modification of the delay line technique has proven to give very satisfactory performance.

To produce a phase-shift of exactly 90 degrees a coaxial delay line should be one quarter wavelength long, or approximately 53 1/2 feet long at

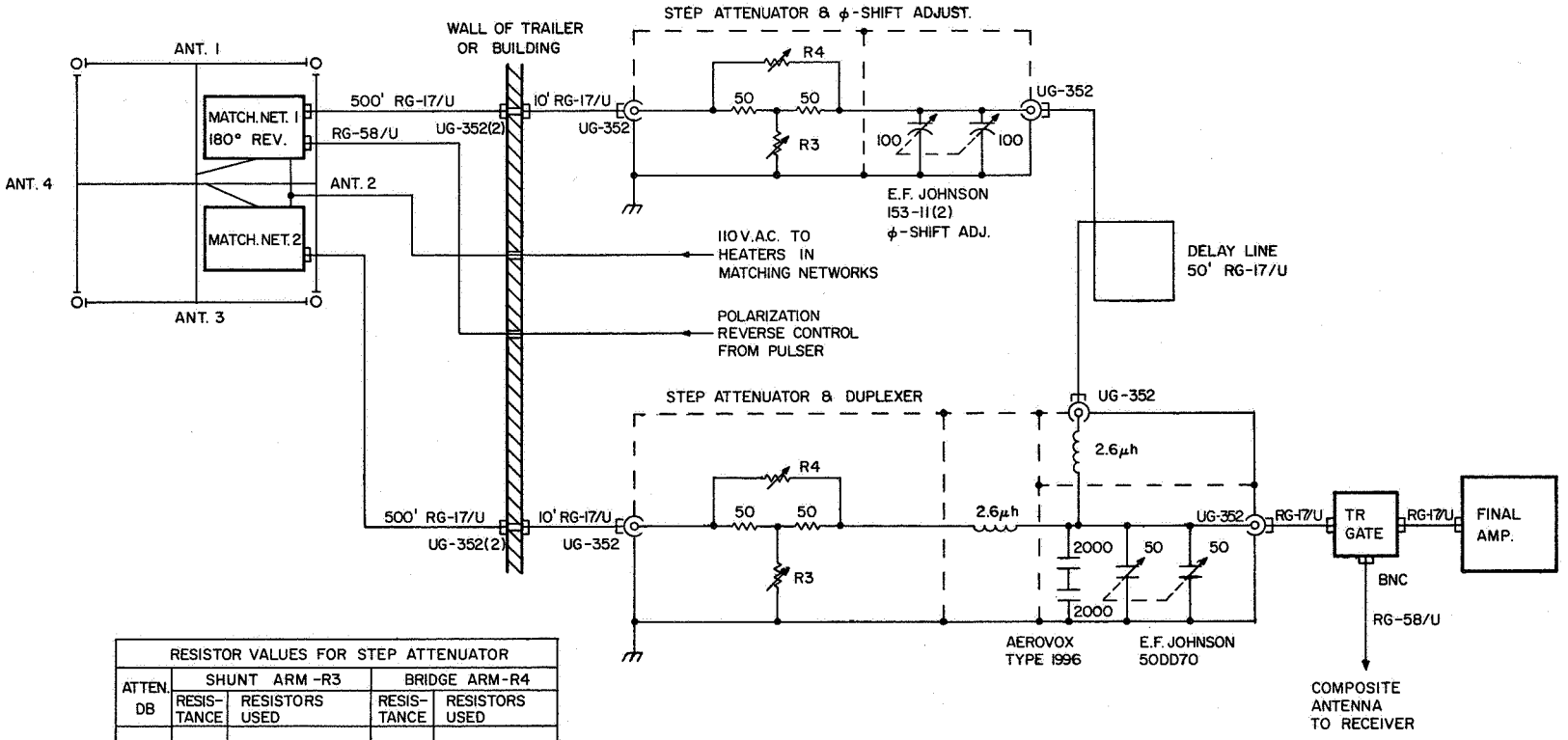

RESISTOR VALUES FOR STEP ATTENUATOR				
ATTEN. DB	SHUNT ARM -R3		BRIDGE ARM-R4	
	RESIS-TANCE	RESISTORS USED	RESIS-TANCE	RESISTORS USED
0db	OPEN	———	0	———
0.5	844	2-150Ω/2w 2-68Ω/2w PLUS ALL BELOW	2.86	2-10Ω/2w 1-12Ω, 1-15Ω IN PARALLEL
1.0	410	4-39Ω/2w PLUS ALL BELOW	6.1	1-10Ω/2w 1-15Ω/2w IN PARALLEL
1.5	254	1-27Ω/2w 1-33Ω/2w PLUS ALL BELOW	9.4	1-10Ω/2w 1-150Ω/2w IN PARALLEL
2.0	193	2-22Ω/2w PLUS ALL BELOW	13	1-18Ω/2w 1-47Ω/2w IN PARALLEL
2.5	150	5-27Ω/2w 1-15Ω/2w	17.15	1-18Ω/2w 1-330Ω/2w IN PARALLEL

Figure 5.16 High-power, low-impedance phase-shift network.

3030 kHz. Experimental work with RG-58/U in the laboratory proved that approximately a 10 degree range of adjustment of phase-shift is possible without appreciably increasing the standing wave on the line if a small variable capacitor is placed across the output end of the delay line. The phase-shift network in use at the field station uses a fifty foot length of RG-17/U coaxial cable and a variable capacitor sufficient to allow the phase shift to be varied from 85 to 95 degrees. Fifty ohm attenuators in series with both antenna feedlines allow adjustment of the amplitude of signals to each antenna pair. Matching of the 50 ohm transmitter output to the two 50 ohm lines is accomplished in the L-network duplexer unit. This phase-shift system is completely shielded and is used for both transmitting and receiving operations. No problems have been encountered with spurious radiation, excessive loss, or in the adjustment of the antennas for circular polarization. The schematic diagram of the phase-shift system is shown in Figure 5.16.

Extensive system measurements at the field station have indicated that insufficient system gain is available to reliably observe partial reflections from the D-layer. Cost analysis has indicated that the most economical as well as the most practical means of achieving this additional gain is by construction of antenna systems capable of greater vertical directivity. Since the electronic transmit-receive switch does not return the system to the receive mode sufficiently fast for partial reflection measurements, two antenna systems are to be constructed, one for transmission and one for reception as in the Wallops installation. Preliminary planning indicates

that these arrays are to use 50 half-wavelength dipoles in a rectangular collinear array. The array consists of five lines of five dipoles each, with one-half wavelength spacing between each line. All twenty-five dipoles are fed in phase, Another twenty-five dipoles at right angles to the above are also fed in phase, but shifted with respect to the first set by 90 degrees to achieve circular polarization. Identical arrays are to be constructed for receiving and transmitting. The calculated 3 dB beamwidth of these arrays is 15 degrees, a considerable gain over the four dipole box array. The preliminary drawing of these antenna arrays is shown in Figure 5.17. Construction of the high-gain antenna arrays is slated to begin during the summer of 1966 and they should be operational by the fall of 1966.

Electronic Transmit-Receive Switch:

The ideal antenna system for use with the vertical incidence absorption and partial reflection sound would employ two separate arrays for transmitting and receiving. This is in fact the case at the Wallops Island and Urbana field station installations. However, as noted above, in the case of the shipboard installation, space was available for only one array. It was therefore necessary to provide a means for rapidly switching the antenna feedline from the transmitter to the receiver. The requirements of a usable switching system to perform this function are as follows;

(a) The maximum switching time between transmit and receive modes should be less than 100 μs, to permit the reception of low-altitude reflections.

(b) The noise generated by the system in the receive mode should not be great enough to degrade the receiving system noise figure.

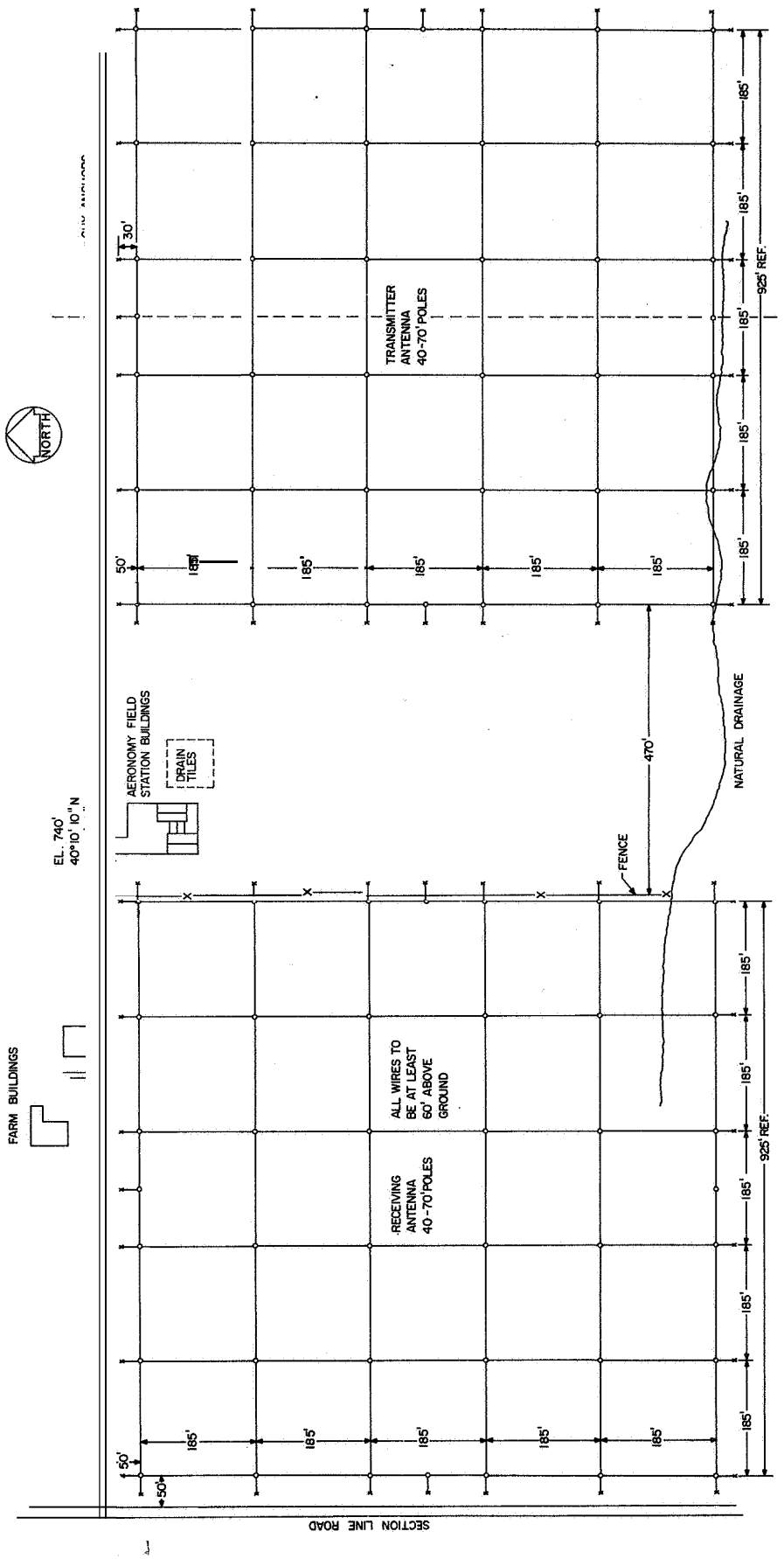

Figure 5.17 High gain antenna array for field station.

(c) The signal leakage to the receiver during transmitter pulses should be less than 2 volts rms.

(d) The system should not have an insertion loss of more than 3 dB.

(e) The unit should be broadband to eliminate the need for adjustment when changing frequency in the 2 to 5 MHz range.

(f) No appreciable reactive or resistive load should be presented to the transmission line during transmitter pulses.

(g) The operation of the unit should be as close as possible to 100% reliable, to prevent reciver damage that could result from a failure.

At the 50 kW power level, conventional vacuum-tube TR switch designs, such as those found in communications systems, are unusable. Several alternative systems were considered. One possibility was to use a quarter-wave length of transmission line, connected in parallel with the antenna feedline at the transmitter, The other end of this line would be connected to the receiver and shorted at the receiver end during transmitter pulses with a high-current diode switch. The quarter-wave line would then act as an impedance transformer, reflecting a very high impedance across the transmitter output. This design is often used in radar installations, but had serious shortcomings for use with the ionospheric sounder. The length of the line would have to be changed with each change in operating frequency, and the diode and the current required to switch it would have to be excessively large, since the RF current at the shorted end of the line would be over 40 amps. Also, the physical size of the quarter-wave line would be a problem, since it would have to be made of RG-17U, the same as the antenna feedline, to withstand the RF pulse voltages and currents.

The most promising system, and the one ultimately adopted, employs a silicon diode in series with the receiver feedline, which is connected in

parallel with the antenna feedline. During the transmitted pulse, the diode is reverse biased by a high-voltage power supply. In the receive mode, the control unit supplies a current of about 50 mA to switch the diode into a conducting state. Figure 5.18 shows the circuitry employed in the final version.

The diode DC supply must be isolated from the transmission line with a capacitor, and the receiver signal path must also be isolated from the DC supply. The latter function could not be performed with an RF choke, since ringing would occur when the DC pulse was applied, so a series of resistors are employed instead. The amount of RF feedthrough to the receiver during transmitter pulses is determined by the reactance of the diode, which acts as a small capacitor when reverse biased. Tests were conducted in the laboratory using a small (800 piv) F8 silicon diode. Impedance bridge measurements showed that the capacitance of a typical diode when reverse biased is small enough to meet the maximum allowable feedthrough requirement, as well as to prevent any appreciable loading of the transmitter output.

A small model of the TR switch was built and connected in the feedline of a pulse receiver in order to measure the noise generated by the diode in its forward conduction state. It was found that the diode did not add measureably to the noise figure of the receiving system. The insertion loss of the diode gate system was also determined to be less than the 3 dB maximum permissible, although the loss was dependent upon the diode forward bias current.

A full-size system was then constructed using an RCA CR212 silicon diode stack, with a peak inverse voltage rating of 12 kV and a maximum forward

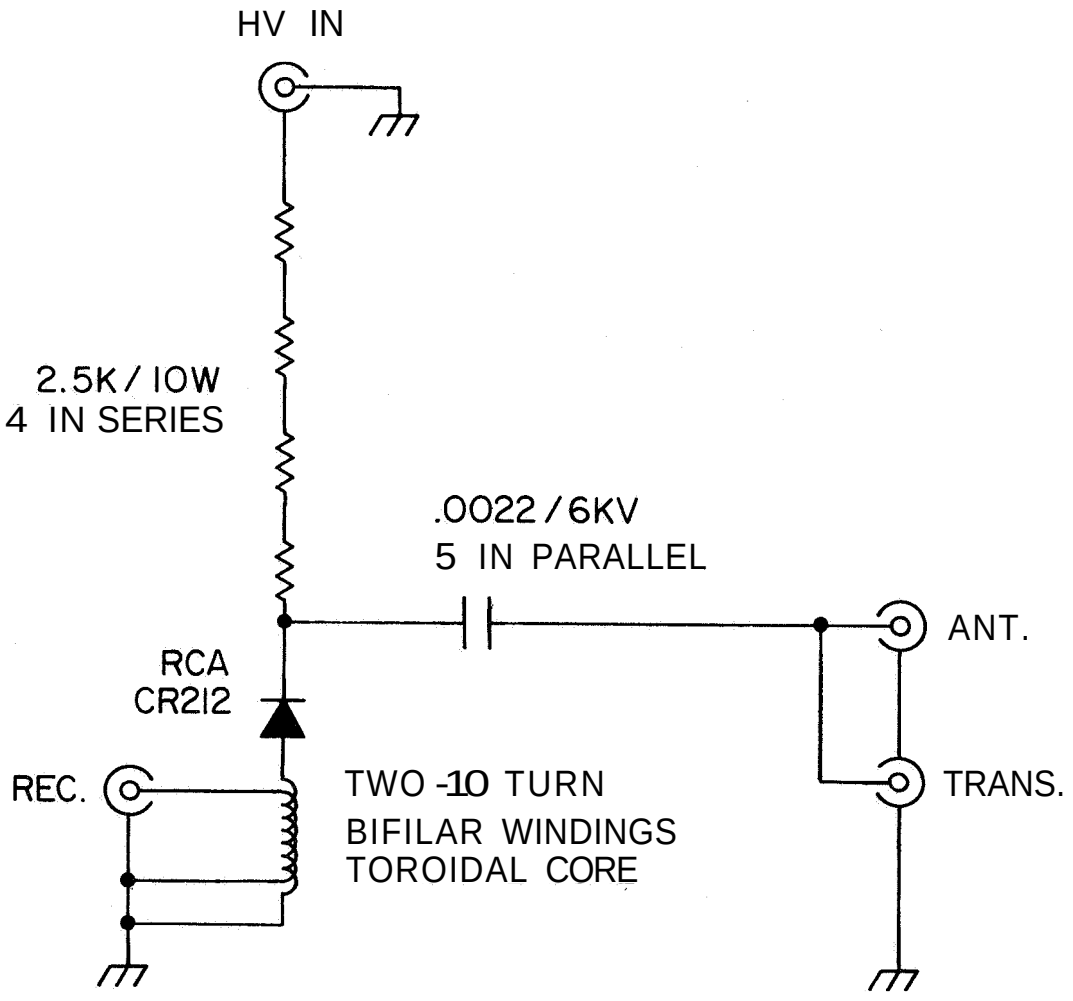

Figure 5.18 Electronic transmit-receive switch--diode unit.

current rating of 300 mA. The capacitor used to isolate the diode DC bias from the feedline was made by placing five 0.0022 μF disc ceramic capacitors in parallel, connected with brass bus strips, The resistance used to isolate the receiver signal from the power supply consisted of four 2.5 kilohm 10 W noninductive wirewound resistors in series. A special toroidal transformer was wound to couple the feedline signal through the diode into the receiver. This transformer was wound with heavy magnet wire, since the diode forward bias current flows through the primarywinding in the receive mode. The number of turns was kept small to prevent saturation of'the core by the bias current flow. The entire unit was packaged in a shielded cabinet. Connectors were provided for the antenna feedline and transmitter output cables, so that the transmitter–to–antenna feed path passes through the TR switch housing.

The control unit designed to actuate the TR switch is shown in Figure 5.19. The normal state of the TR switch is the "off" position; i.e., with the diode reverse biased. This gives maximum protection for the receiver against spurious RF pulses. In this condition, the 3329 control tube grid is biased negatively so that the tube does not conduct. Consequently, there is no load on the 5 kV supply and its 1.08 megohm series resistor, and the diode is biased to 5 kV in the reverse direction.

The command pulse to change the TR switch over to the receive mode is supplied by the timing and control system (see Chapter 6) and is amplified by the 6C4 and 2326 tubes. The'latter amplifier drives.-the grid of the 3329 positive, causing the tube to conduct. The 5 kV supply is now presented with a low impedance to ground, and hence its power is dissipated In the 1.08

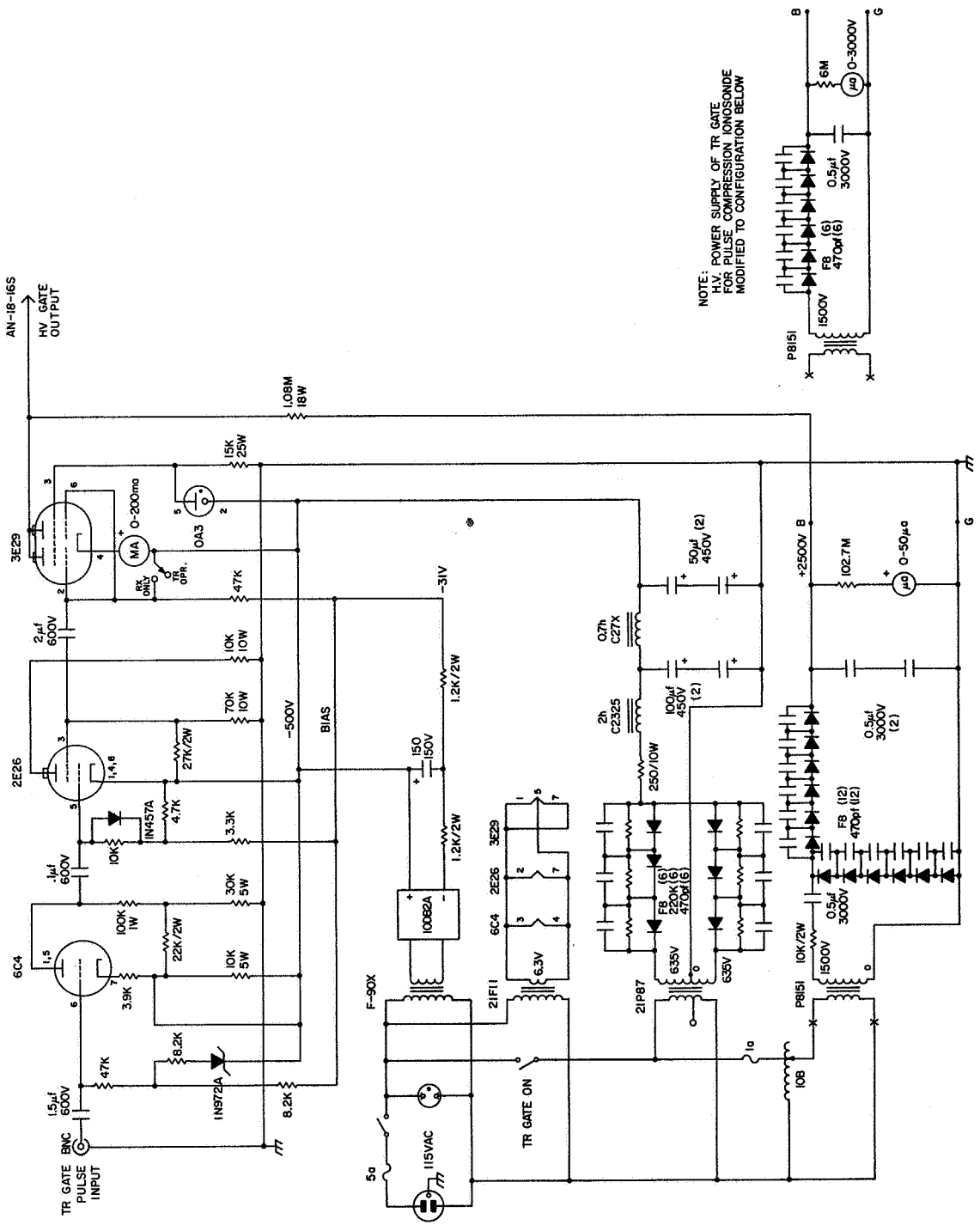

Figure 5 19 Electronic transmit-control unit

megohm series resistor. Since the low-voltage supply positive terminal is grounded, current flows through the toroidal transformer, the switching diode and the 10 kilohm isolating resistor to the plates of the 3329 and through the tube to the supply negative terminal. The 10 kilohm res'istor acts as the plate load resistor for the tube and limits the current through the diode to about 50 ma when the 3329 is saturated. At the end of the enable pulse, the tube is once again returned to its nonconducting state and the 5 kV supply reverse biases the diode. A manually-operated switch has been provided to allow the operator to hold the TR switch in the receive mode, as is necessary when making adjustments to the receiving system.

The maximum voltage to be expected on the transmission line during an RF pulse is about 2300 volts peak. The 5 kV supply is equipped with a variable autotransformer so that the reverse bias may be adjusted to exceed the maximum RE line voltage. However, the recovery time of the TR switch is determined by the RC time constant of the 5 kV supply internal and series resistance, and the diode switch capacitance (contributed mostly by the .011 µF blocking capacitor), so a compromise must be made in adjusting the supply level between certainty of protection against RF transients and maximum allowable recovery time.

This TR switch system has functioned well and met all of the requirements both in the shipboard experiment and at the Urbana field station. A duplicate unit has been constructed for use with a pulse compression sounder at the Aeronomy Laboratory.

6. TIMING AND CONTROL SYSTEM DESIGN

The timing and control system is designed to synchronize and control the operation of the various component units of the vertical incidence sounding system. The functions required of the system are:

(a) to provide pulses to trigger the transmitter, oscilloscope, and associated equipment at pulse repetition rates of 5, 1/2, and 1/10 pulses per second. In addition, the unit must be capable of providing a second trigger pulse 125 milliseconds after the initial pulse of each cycle, so that ordinary and extraordinary propagation modes may be transmitted in quick succession.

(b) to provide relay contacts for actuation of the camera shutter and film advance mechanism. The operation of the relay must be timed to open the shutter prior to the first transmitted pulse of each cycle and to close it after the last of the desired ionospheric reflections has been recorded. The total shutter-open time should be reasonably consistent in duration to ensure proper oscilloscope graticule exposure.

(c) to provide relay contacts for actuation of the switching systems used to change antenna polarization from the ordinary to the extraordinary mode and to reverse the polarity of the receiver output, This relay is to operate only when the second output trigger pulse is employed as outlined in (a). It must actuate 75 milliseconds after the first of the two pulses in each cycle and release 50 milliseconds after the

second pulse. Its period of operation is thus to bracket the occurrence of the second pulse.

(d) to provide a trigger pulse for actuation of the transmit-receive gate system employed when a single antenna is used for both transmitting and receiving, The leading edge of this pulse must occur 200 μs after the initiation of the transmitter trigger pulse, and the duration of the entire pulse must be 10 milliseconds.

Further requirements of the system are that:

(e) all operations of the system must be synchronized with the 60 Hz power line frequency, and must be phase-adjustable with reference to the line, *so* that recurrent line-synchronized interference may be evaded.

(f) the system must be enclosed in a well-shielded housing to prevent stray RF from retriggering the timing circuits. For the same reason, all outputs must be low impedance and shielded,

(g) all output pulses must have a minimum peak amplitude of 20 V to ensure proper triggering of the associated units.

Several timing and control systems were designed prior to the development of the system to be described here. The two earliest models, employing vacuum tubes, were never entirely successful. As the number of functions required of the units was increased, the power supply requirements and physical size of the units rapidly became excessive, The circuitry of these units, which were electronically identical, is shown in Figures 6.1 and 6.2. The use of transistorized circuitry provided the

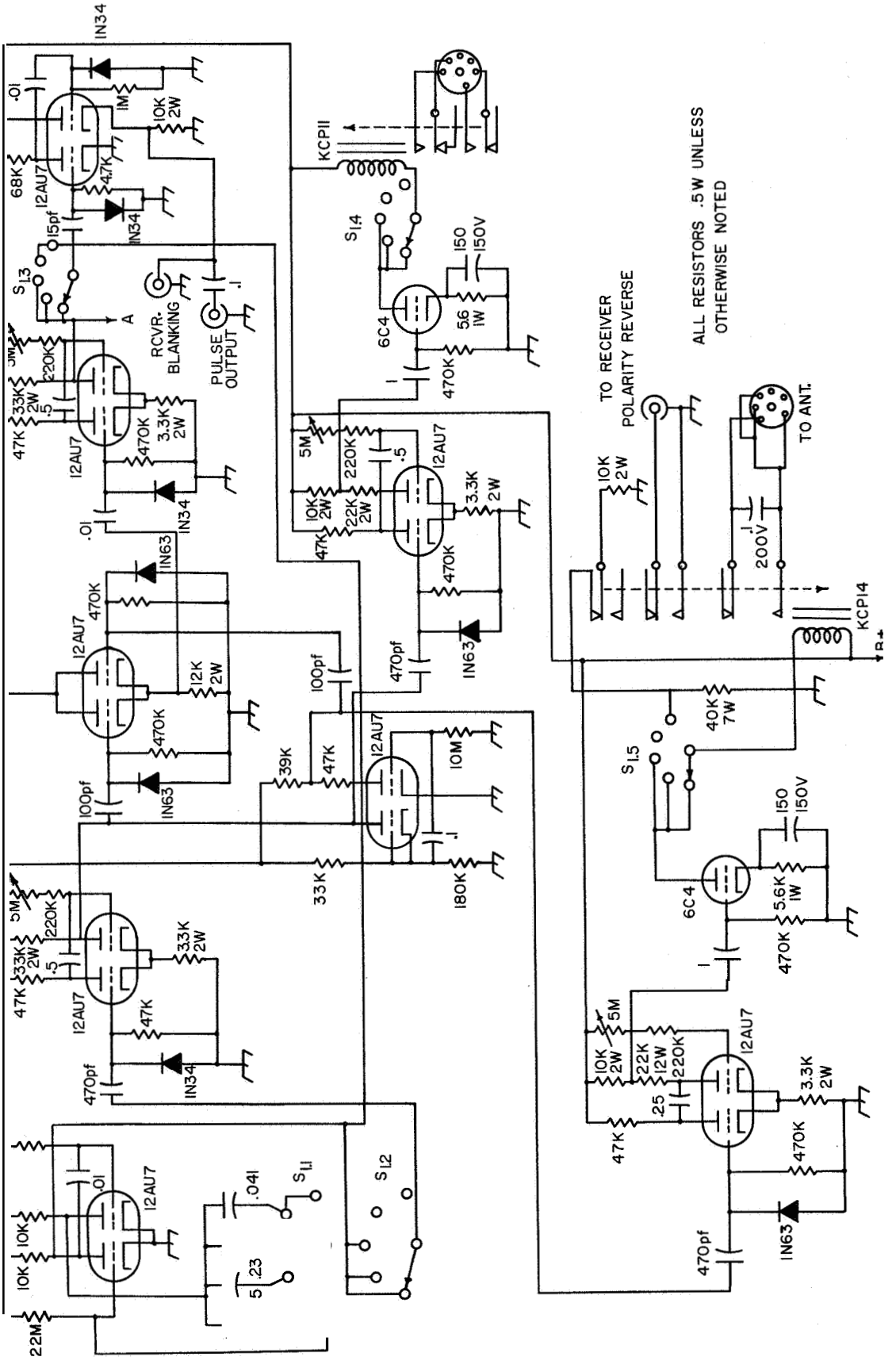

Figure 6.1 Vacuum-tube timing and control system switching circuitry.

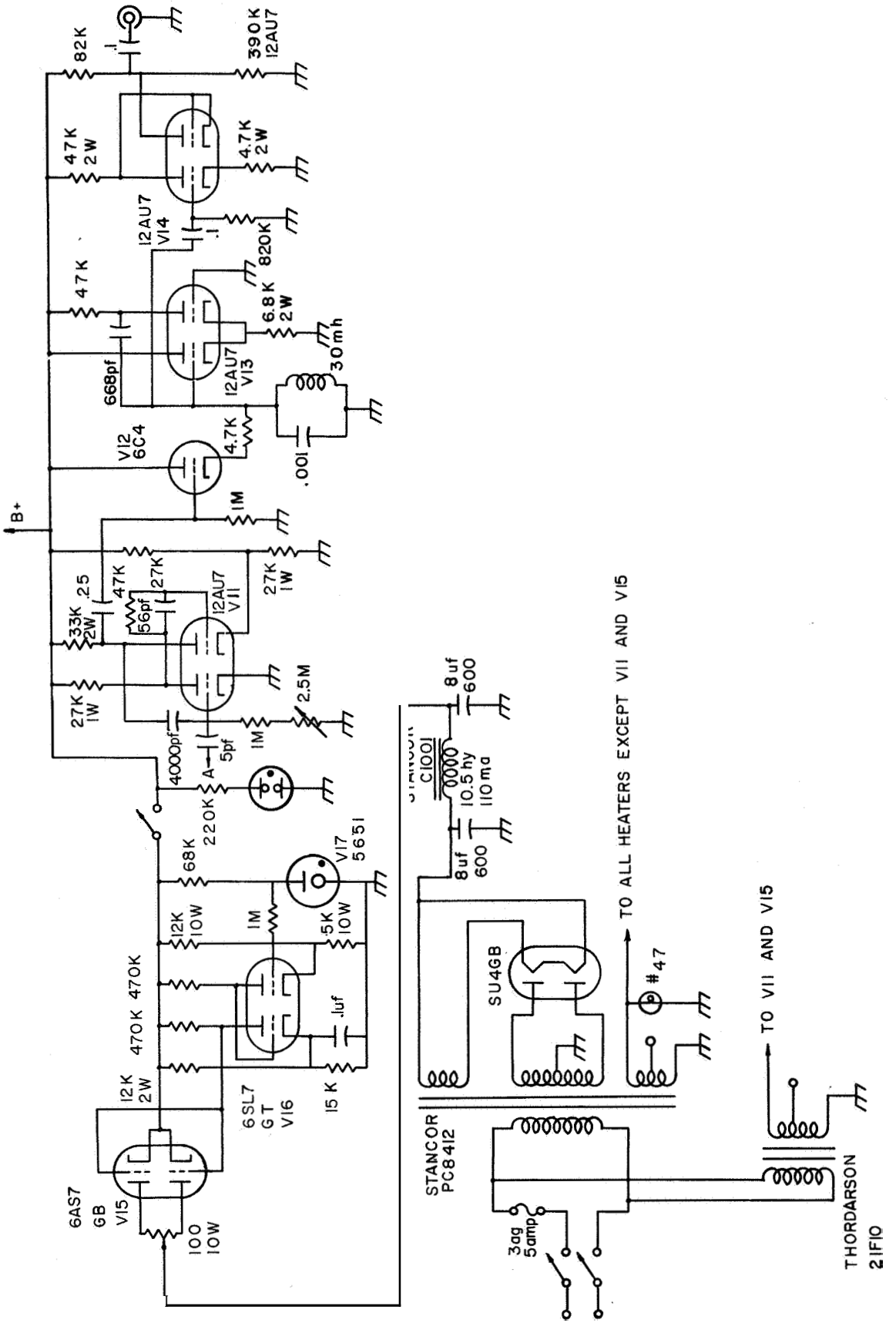

Figure 6.2 Vacuum-tube timing and control system height marker generator and power supply.

obvious remedy for these problems and led to the development of the system shown in Figures 6.3 and 6.4 presently in use with the Wallops Island installation. This early system employed about 30 transistors in conventional timing and switching circuits; it was constructed on 1/16-inch epoxy-fiberglass board mounted to a standard chassis and relay rack panel. No RF shielding was provided for this unit, and some minor retriggering problems were encountered. Timing functions of the system were controlled by a free-running master or "clock" multivibrator, the frequency of which was determined by means of RF time constants. These constants were switch selected for four different pulse repetition rates from 1/2 to 5 pps. No effort was made to provide temperature compensation of the master multivibrator, although the power supply voltage was accurately controlled by means of an electronic regulator.

In all of the above timing and control system designs, circuitry was included to provide accurately spaced marks on the oscilloscope trace. The purpose of these marks was to provide a virtual reflection height reference to be used in scaling the filmed data. This feature has not been included in the most recent modular system design, but space is available in the modules for the addition of such circuits when and if the need arises.

This first transistorized system design was relatively successful and was subsequently duplicated in a shielded version and, with the addition of TR gate control circuitry, in the model used with the shipboard sounder, as shown in Figures 6.5 and 6.6. However, certain additional requirements arose, and the following factors led to the development of the timing and control system to be described in detail here:

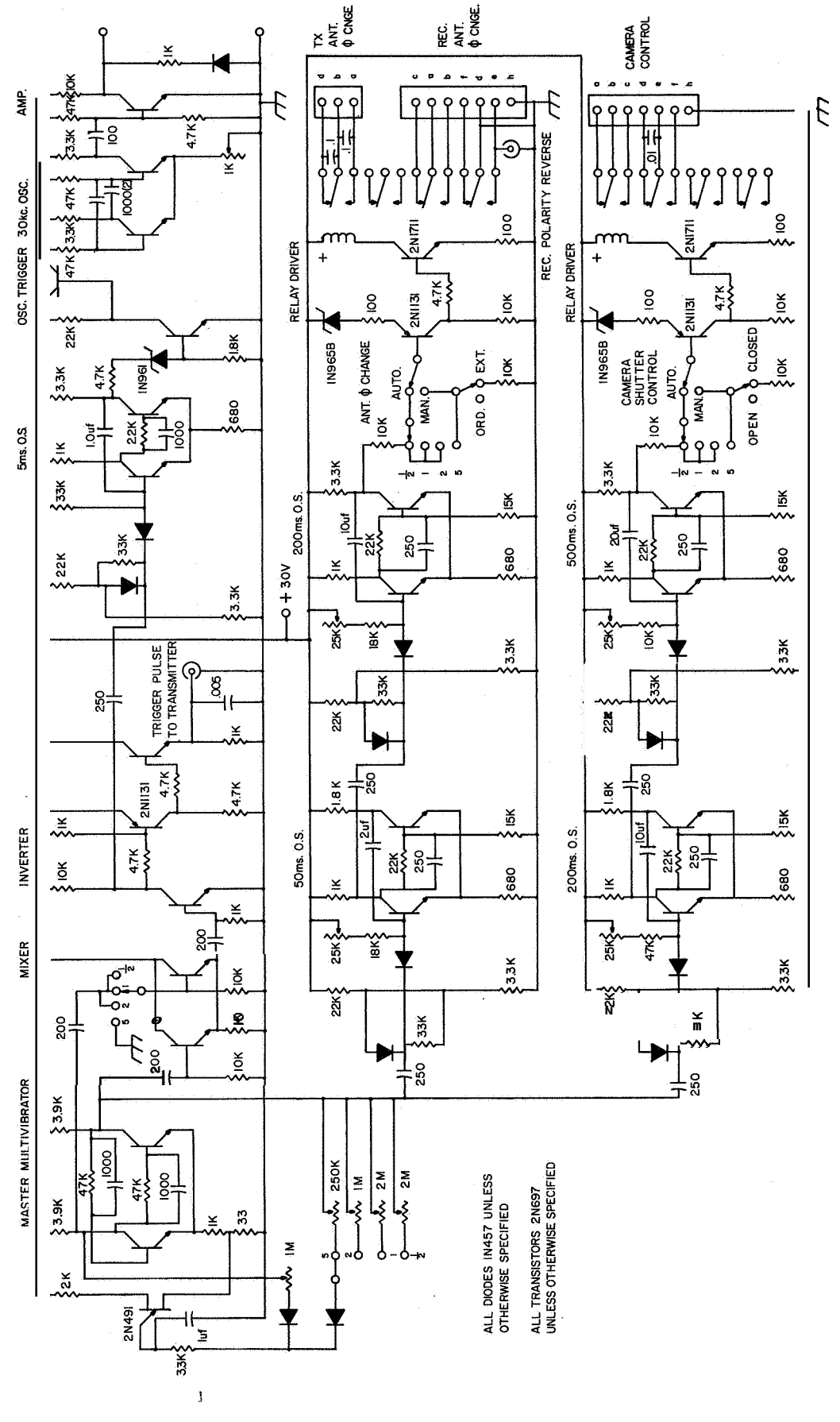

Figure 6.3 Initial transistorized timing and control system circuitry.

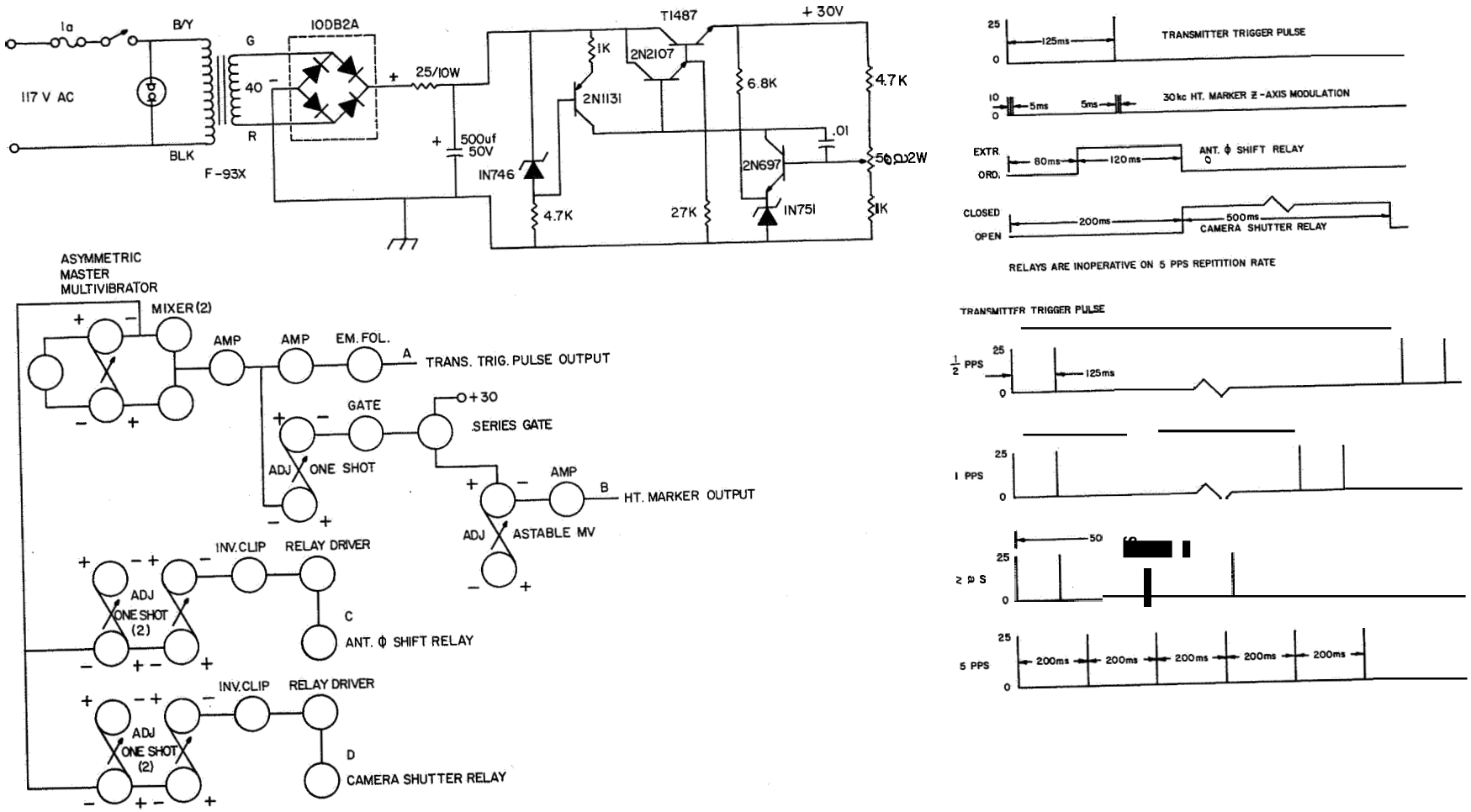

Figure 6.4 Initial transistorized timing and control system power supply, block diagram, and timing sequence chart.

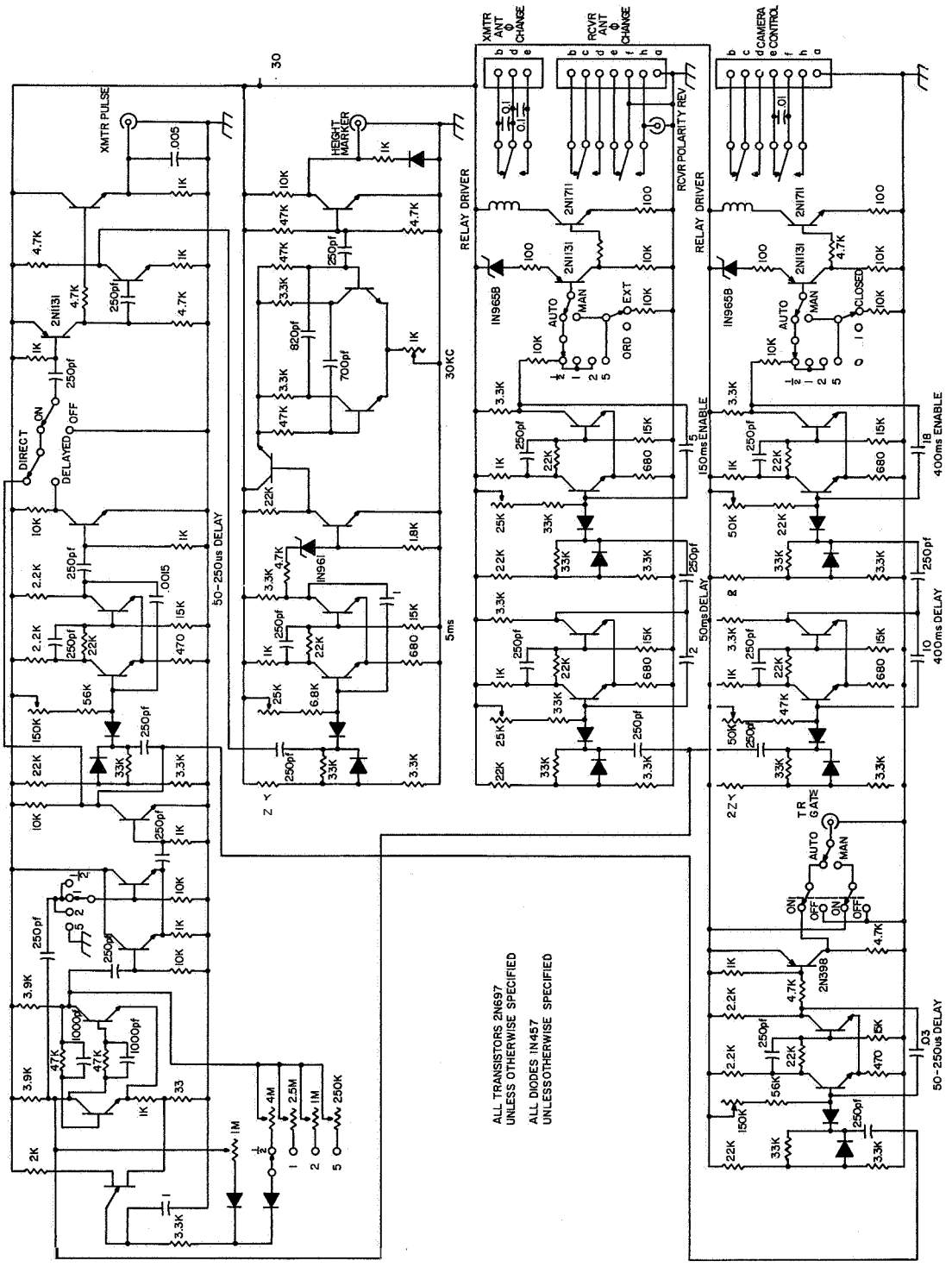

Figure 6 ⊐ Shipboard timing and control ∃ystem.

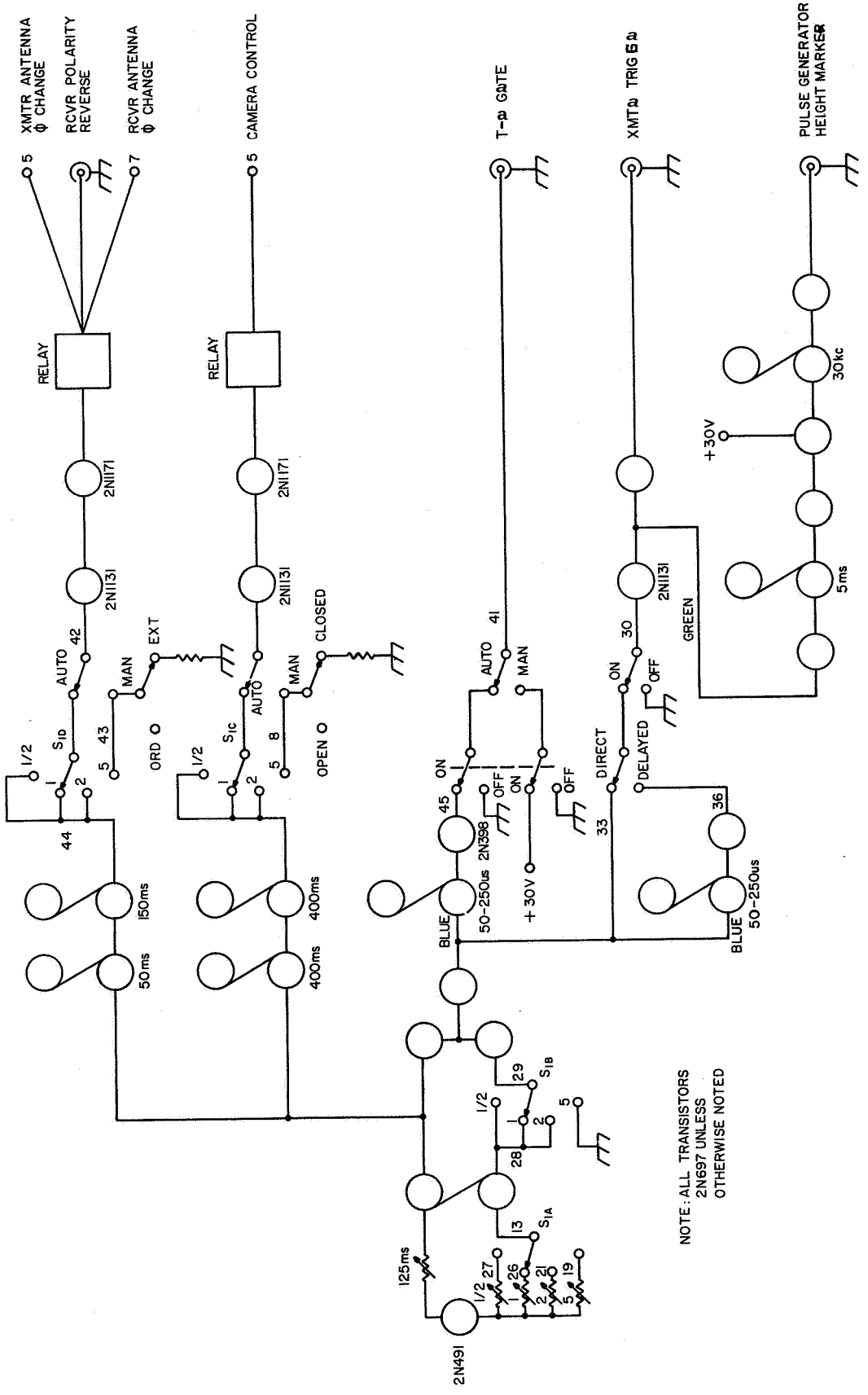

Figure 6.6 Shipboard timing and control system block diagram.

1. The need for good shielding consistent with ease of mechanical disassembly for maintenance purposes,

2. A requirement for greater flexibility of operation, especially with respect to timing duration and sequence, and for ease in incorporating new circuitry as the demand for additional functions becomes apparent.

3. The necessity for reducing "down" time in servicing operations.

4. A desire to synchronize the entire system with the power line to gain timing accuracy and a phase adjustment capability necessary to escape line-synchronized noise pulses.

5. A definite need for a wider range of pulse repetition rates to encompass all foreseeable applications of the sounder, from testing of the transmitter to the taking of long-term absorption records.

6. A foreseeable future need for all-electronic switching of system functions, to allow the operation of the entire sounder to be advance programmed.

In the timing and control system that was designed with the above factors in mind, all transistorized circuitry is constructed on plug-in cards, By relegating the various circuit functions to spearate cards, most of the system parameters may be changed by modifying or rebuilding one or more of the cards, or by adding new cards. In the previous system arrangement, circuit function changes required difficult and time-consuming modifications of an entire chassis. Servicing is also simplified with the card system. Difficulties may quickly be traced to an individual card, which then may either be repaired in the field or replaced with a duplicate while the original is sent back to the laboratory for service.

Shielding requirements were met in the new pulser by mounting the cards and interconnecting wiring in Tektronix plug-in modules, which in turn plug into a Tektronix module storage manifold. This system has also been successfully used in the receiver described in Chapter 3. Provisions

are made for mounting seven cards in each of two modules. Since the present system employs only eleven pulse circuit cards, space remains for the addition of three extra cards when needed. The third module is used to house the power supply components, including two electronic voltage regulator circuit cards. These cards hold all of the regulator circuitry except the series regulator transistors themselves, which are mounted on the module chassis for better heat dissipation. The controls for the circuitry in each module are mounted on the front panel of that particular unit. The modules themselves are not shielded, but are inserted into the manifold, which is modified for complete shielding by the addition of mesh end plates, a shielded cable race-way, and a shielded output connector box. The modules are all keyed so that they cannot be accidentally interchanged with receiver or oscilloscope modules, which are, of course, very similar in appearance.

The basic circuit timing reference in this system is the 60 Hz power line, rather than a free-running "clock" multivibrator. Circuit cards 1-3 contain counting circuits that divide the line frequency by various factors. Card 1, shown in Figure 6.7, is a scaler that divides by 12 to give a 5 pps output. Card 2 (Figure 6.7) divides the output of card 1 by a factor of 10 to give one pulse per two seconds, and card 3 (Figure 6.8) divides card 2 output by five to give one pulse per ten seconds. Each card, in addition to the binary multivibrator counting circuits, holds a Schmitt trigger to square the input waveforms, a 10 μs monostable multivibrator triggered by the output pulses, and an emitter-follower to give a low impedance output. The monostable multivibrator is

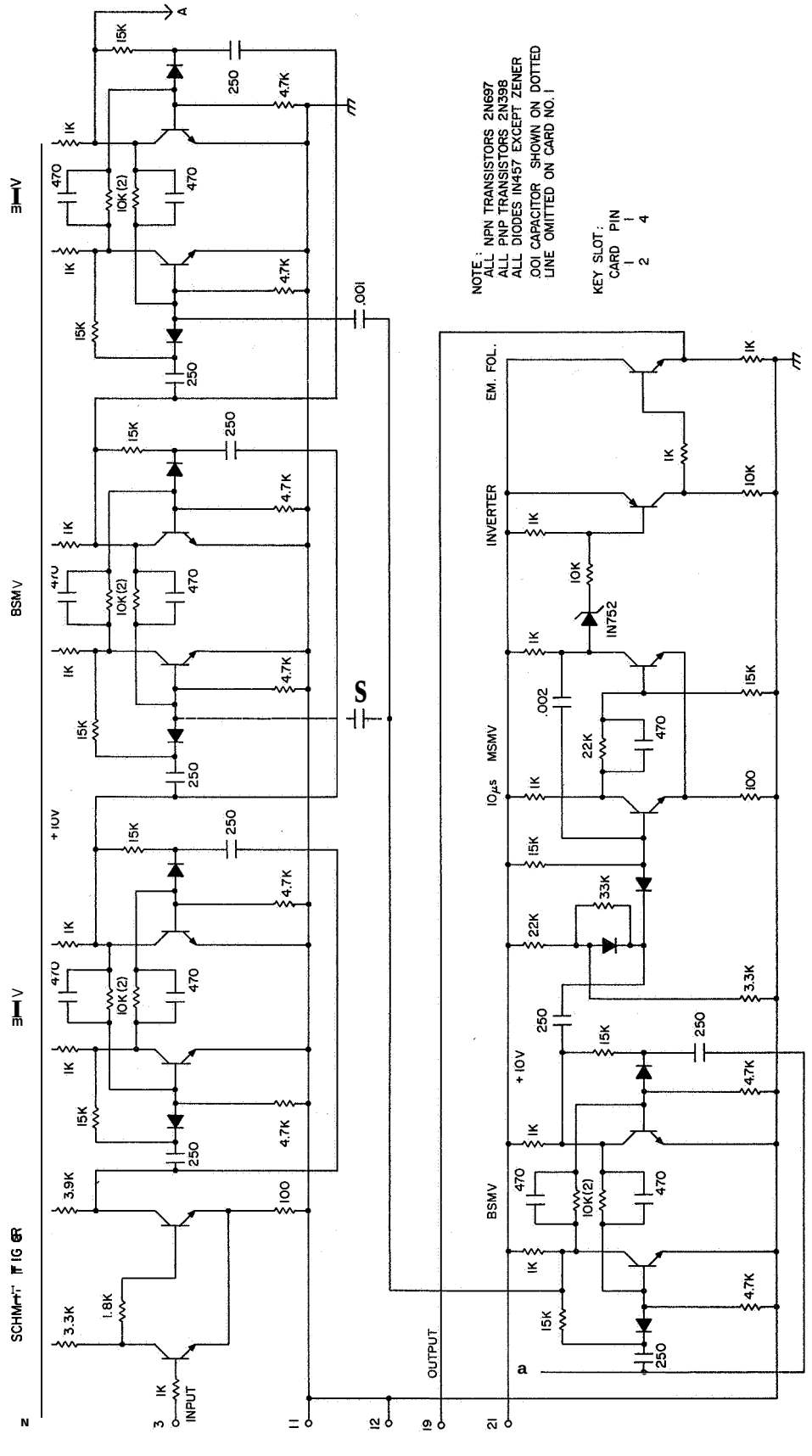

Figure 6.7 Modular transistorized timing and control system (TCS) circuit cards 1 and 2--frequency dividers.

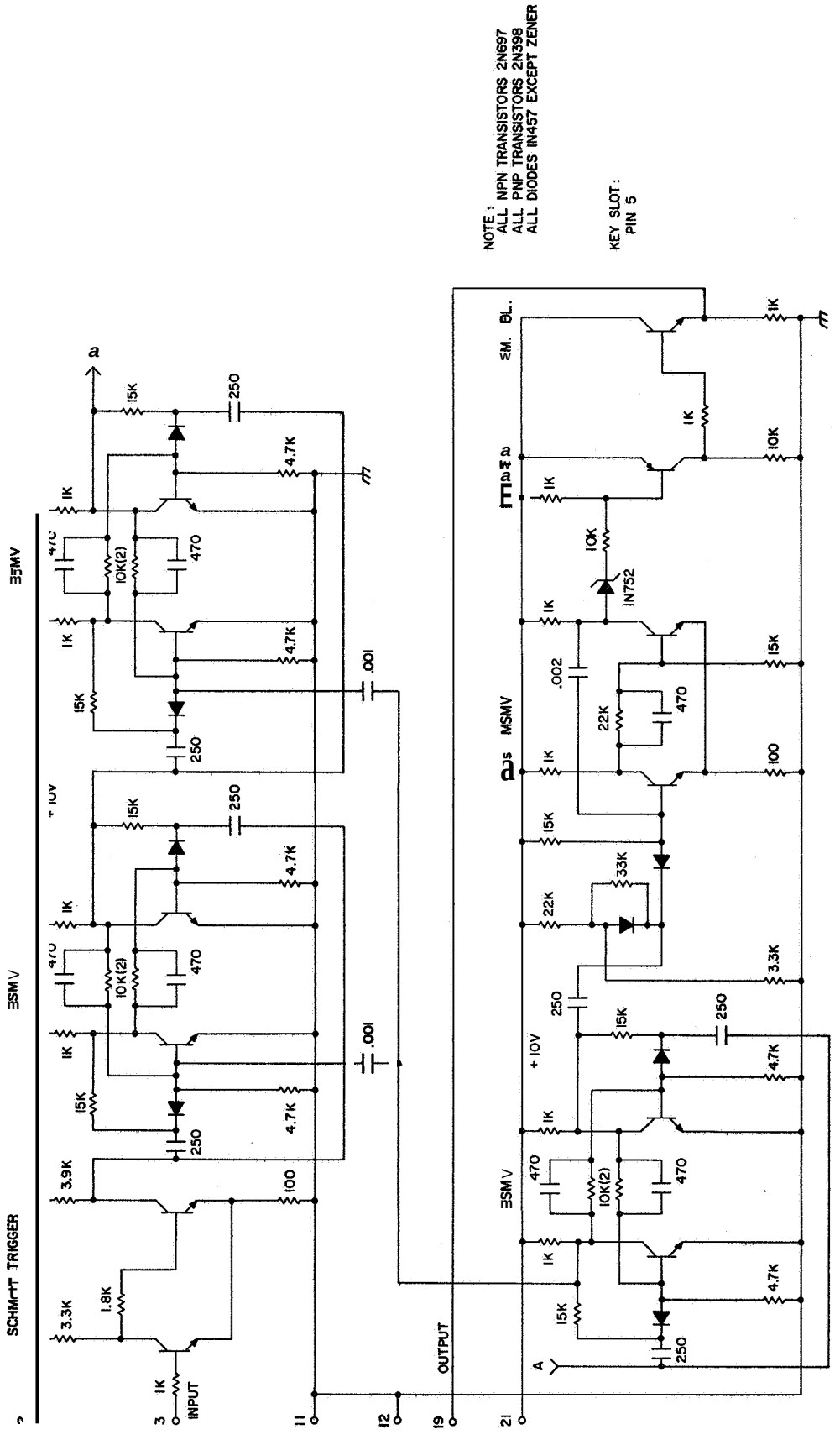

Figure 6.8 Modular TCS card 3--frequency divider.

included so that each card will have a pulse output of a standard width suitable for positive triggering of following circuits.

The 60 Hz source for the counter cards is provided by a small line transformer mounted in the power supply module. It supplies a 10 VAC signal to card 11 (Figure 6.9), which contains a Schmitt trigger, an adjustable delay multivibrator, and an output amplifier. The multivibrator has a pulse width variable over a 1–10 ms range, thereby allowing the output trigger pulses to be delayed through a range corresponding to 180° on the 60 Hz sine wave. This delay, and hence the pulse output phase, is controlled by a front-panel potentiometer, The operator of the system adjusts this control to shift the pulse output phase whenever necessary to avoid line-synchronized interference.

Cards 1, 2 and 3 thus provide outputs, respectively, at 5 pps, used primarily when adjusting the transmitter or in making visual observations of ionospheric reflections, at 1/2 pps, used for making filmed records of partial reflection echoes, and at 1/10 pps, for use in making filmed absorption records. The output of the three cards are fed to card 4 (Figure 6.10), a gate and adder circuit. This card employs three NAND gates, one for each input prf, connected in an OR configuration; i.e., the three gates share a common load resistor so that the output pulses from all of the three gates appear across this resistor. The prf of the system is selected by applying a turn-on bias to the appropriate NAND gate. This bias may be applied either by means of a front-panel switch (PRF Selector) or externally from an automatic programming device if desired, In addition to its primary function

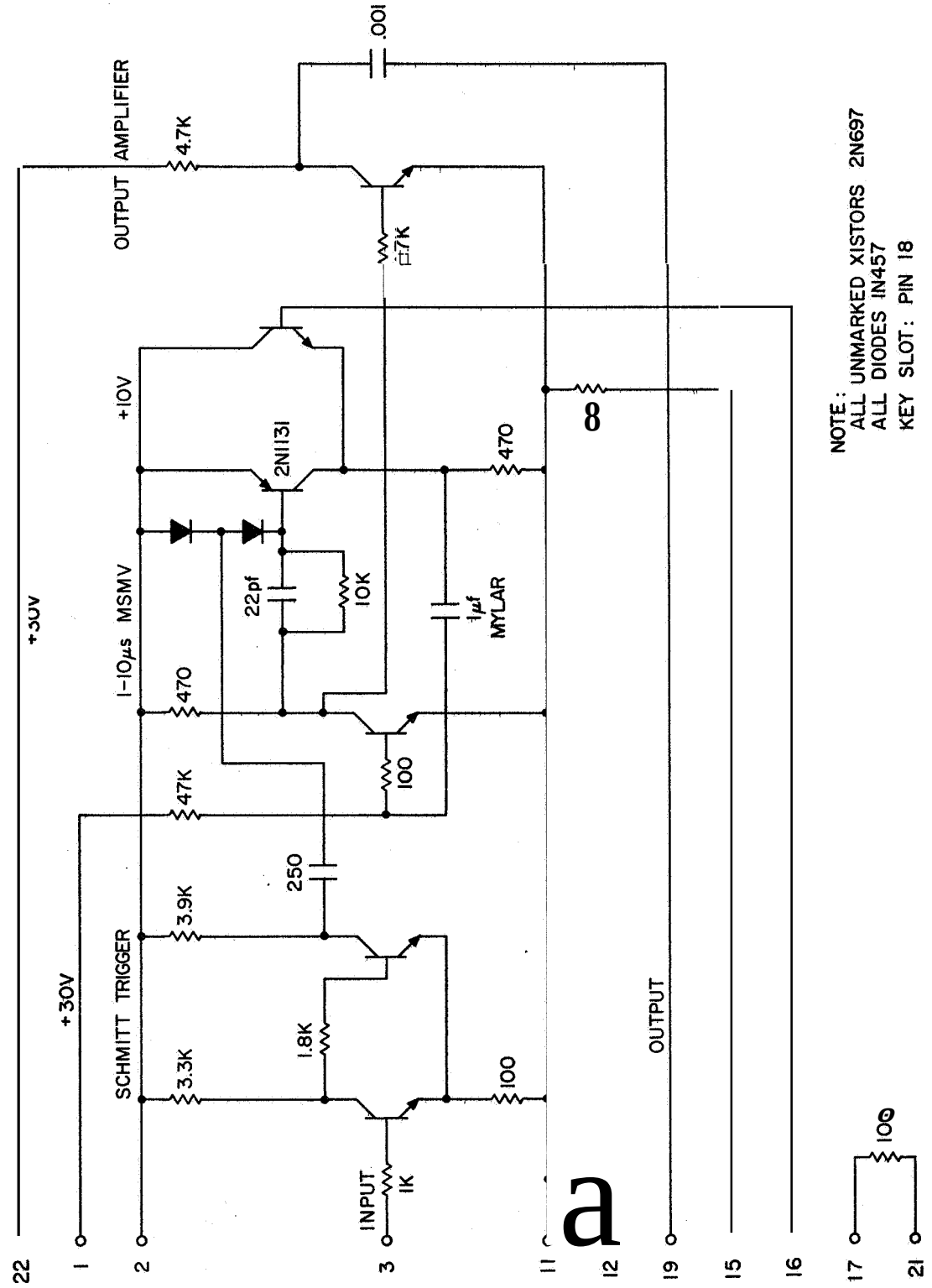

Figure 6.9 Modular TCS card 11--pulse phase delay circuit.

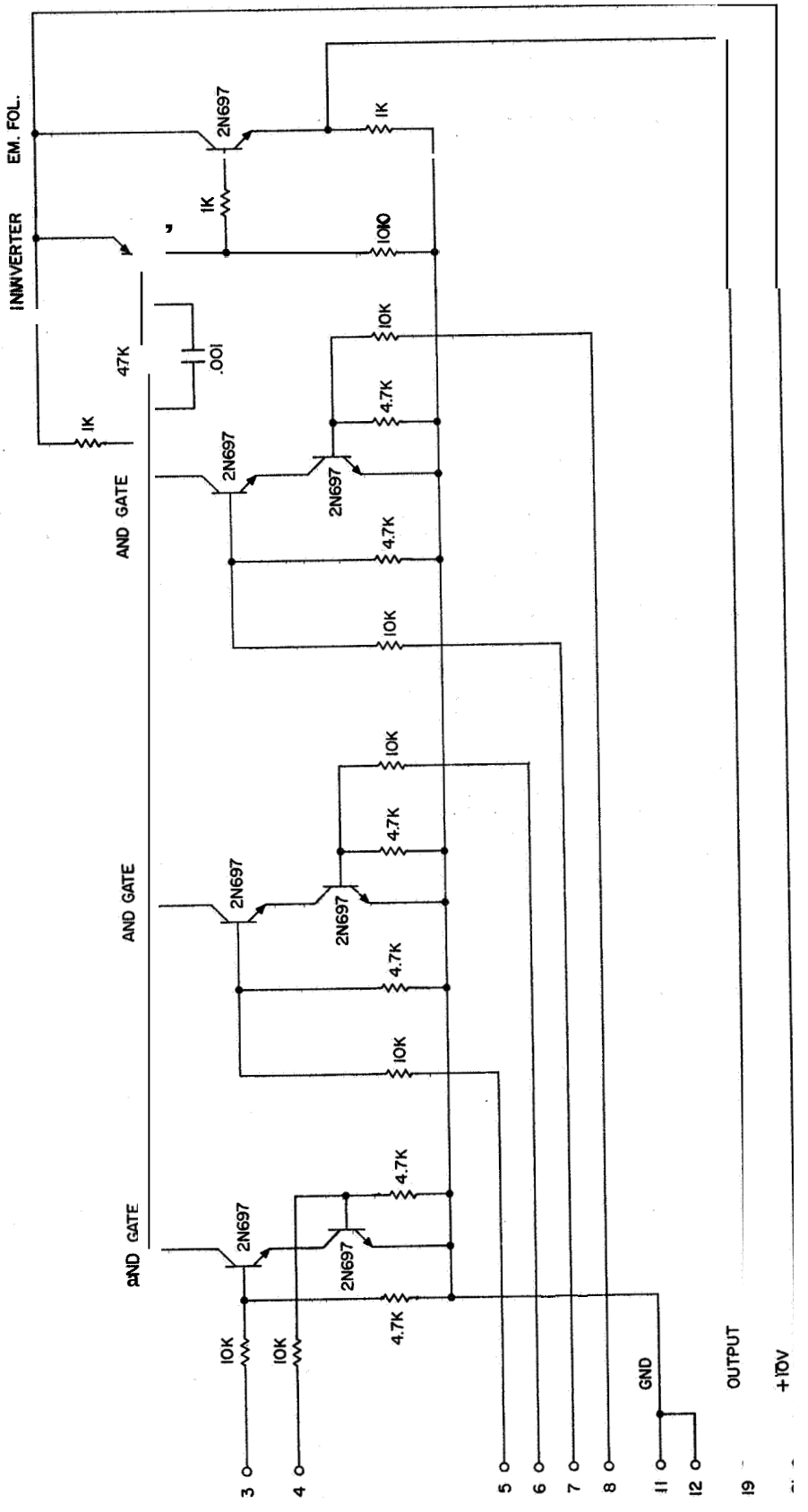

Figure 6 10 Modular TCS card 4--prf selector gate

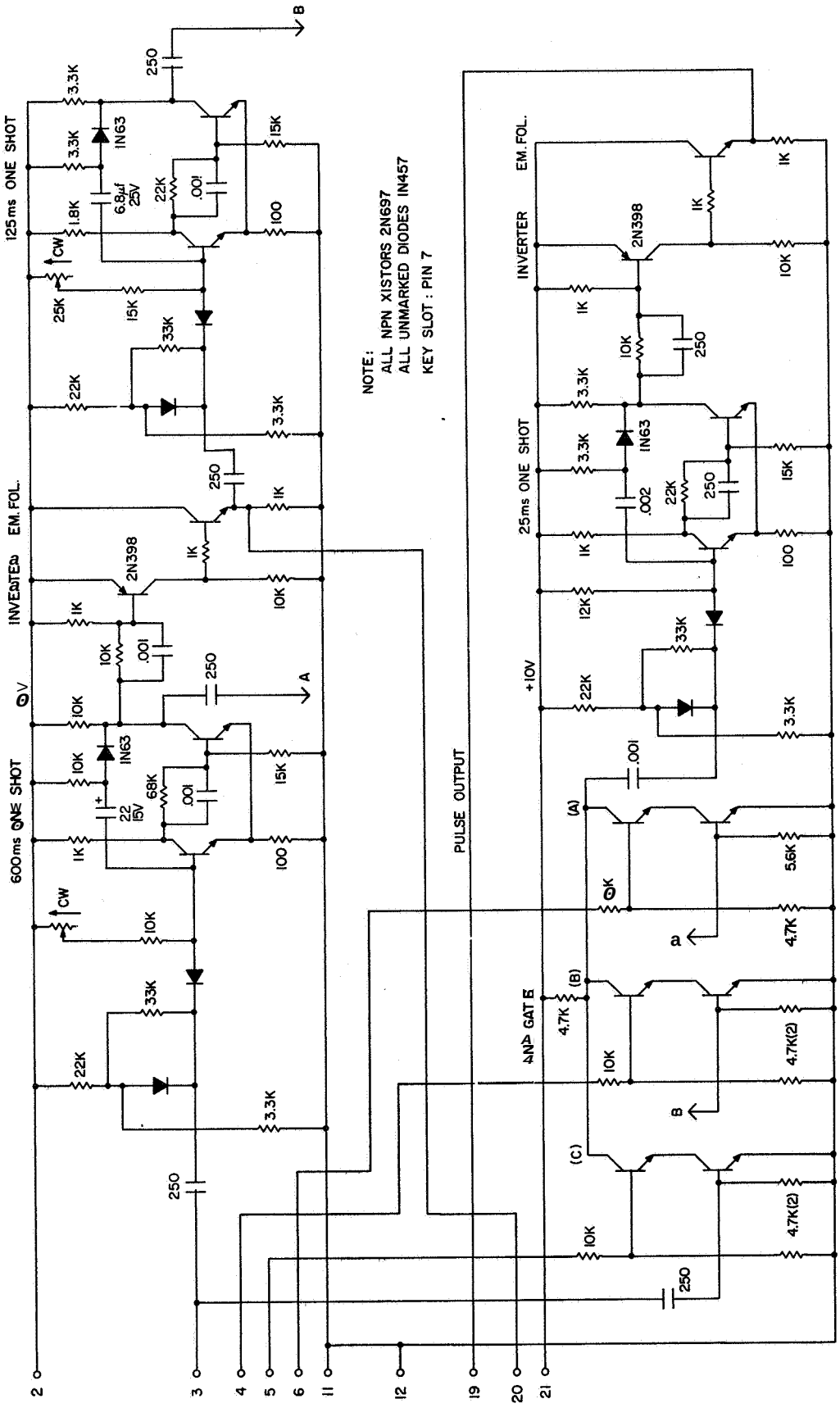

Figure 6.11 Modular TCS card 5--sequencing circuits and second pulse inserter.

described here, the prf selector switch also applies biases to "lock out" certain other circuits at some prf's, as will be explained below.

The pulse output from card 4 is fed to card 5 (Figure 6.11) which holds a rather complex circuit performing several functions, As on card 4, three NAND gates trigger a 25 μs monostable multivibrator (used to shape the output), which in turn drives an inverter and emitter-follower pulse output amplifier., In the simplest case, at 5 pps, the input pulse is fed to gate C, which is actuated by a turn-on bias from the prf selector switch, It is then fed directly to the 25 μs multivibrator. At prf's of 1/2 and 1/10 pps, however, the pulses are not fed directly through to the gates, but drive a 600 ms multivibrator instead. The turn-on spike of the multivibrator is fed to the camera timing control circuit (card 9), causing the camera shutter to open 600 ms prior to the initial output trigger pulse, The turn-off spike is fed (a) to NAND gate A, resulting in the generation of the first output trigger pulse, and (b) to the input trigger of a 125 ms monostable multivibrator. The turn-off spike of this latter multivibrator is fed to NAND gate B, resulting in the generation of a second output trigger pulse 125 ms after the initial one, providing that a gate turn-on bias is applied to gate B. The required bias is controlled by a front-panel switch (Double Pulse On-Off). When this switch is in the "on" position, the second pulse is included in the output, However, an additional switch ganged to the prf selector prevents application of the bias to gates A and B when the system is operated at 5 pps.

One further output of card 5 is generated by the turn-off spike of the 600 ms multivibrator (coinciding in time with the initial output trigger pulse), and is supplied to card 10, which carries the antenna and receiver polarity timing circuits, to be described below.

Card 6 circuitry, shown in Figure 6.12, is designed to actuate the transmit-receive gate (an external unit in the antenna feedline, as described in Chapter 5) after each output trigger pulse, regardless of the prf selected. The TR gate, which normally blocks the feedline energy from the receiver, is activated 200 μs after each trigger pulse, and remains operative until 10 ms after the trigger pulse, to allow observation of received reflections for that length of time.

The output trigger pulses from card 5 are supplied to card 7 (Figure 6.12), where they are applied to a series gate. The gate is activated by a bias controlled with a front-panel switch (Pulse Output On-Off). In the "on" condition, this gate passes the pulses to a 10 Us monostable multivibrator used to ensure that all output pulses are of uniform width and amplitude. The output of the multivibrator drives two Darlington output amplifiers. One of these output amplifiers supplies system output pulses to the transmitter exclusively, while the other (Auxiliary Pulse Output) supplies all associated circuitry requiring synchronization pulses. This arrangement is intended to prevent switching transients generated in other units from causing false triggering of the transmitter.

The pulses from the auxiliary trigger output are also supplied to card 8 (Figure 6-13), which comprises an auxiliary trigger delay circuit.

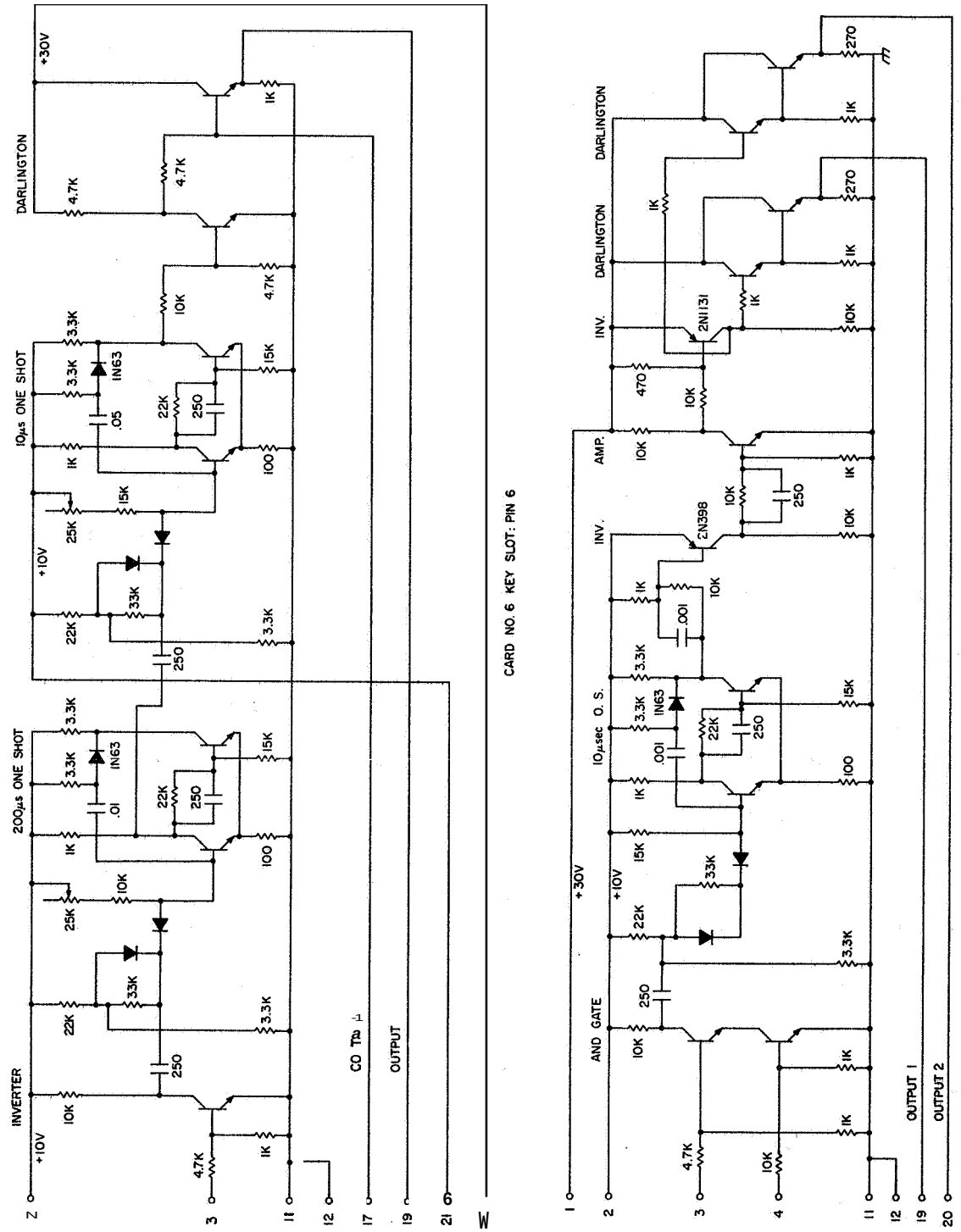

Figure 6.12 Modular TCS cards 6 and 7--TR gate control and pulse output amplifiers.

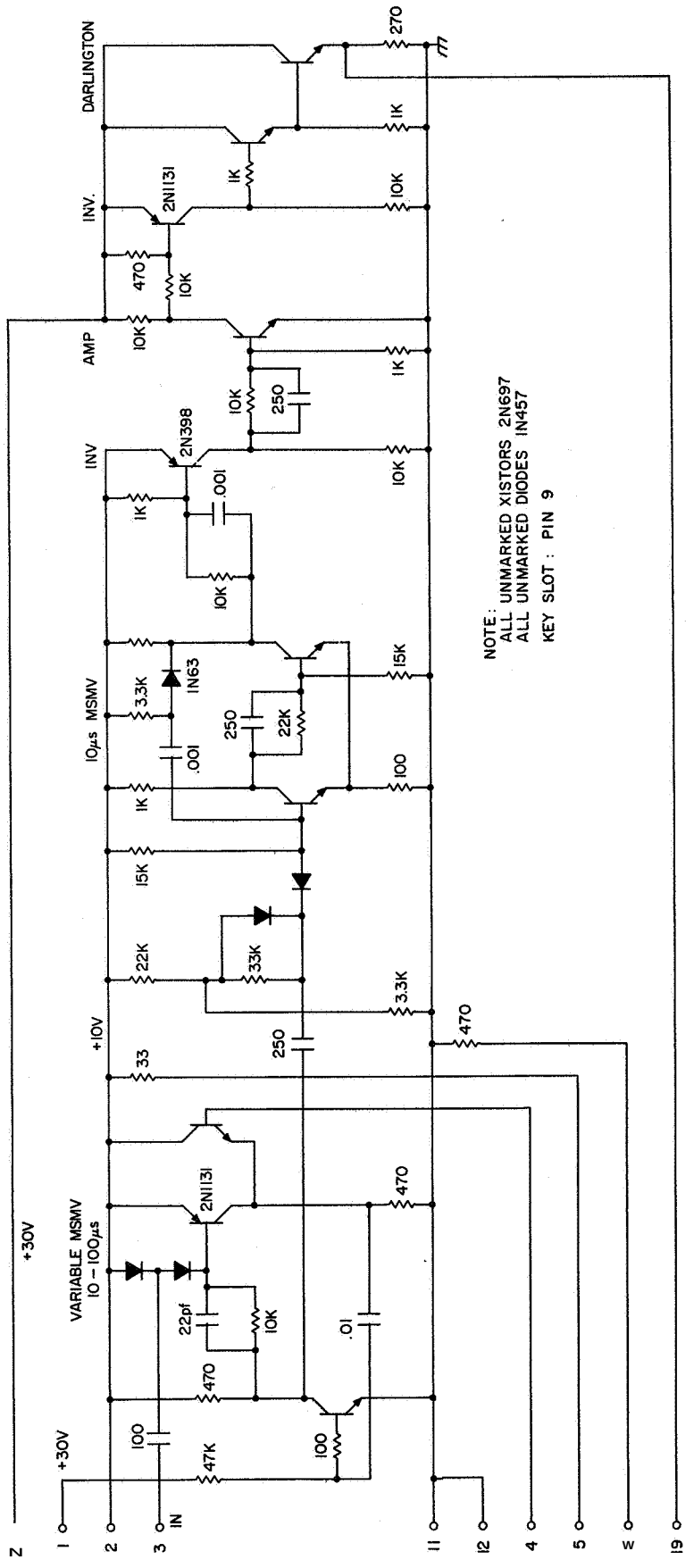

Figure 6.13 Modular TCS card 8--adjustable auxiliary pulse amplifier circuit.

In some cases there is a delay between the transmitter trigger output pulses from the timing and control system and the initiation of the actual transmitter RF output pulse. The adjustable-delay auxiliary trigger output allows the operator to compensate for this delay in the transmitter when triggering other functions, such as the oscilloscope trace. Thus, the beginning of the 'scope trace may be synchronized exactly with the beginning of the transmitter RF output pulse. The delay is adjustable by means of a front-panel control (Auxiliary Trigger Delay).

The data-recording camera shutter is actuated by a relay which is in turn controlled by the circuitry of card 9, shown in Figure 6.14. A lockout provision prevents the camera from operating when the system prf is set at 5 pps. However, at 1/2 and 1/10 pps, a 1600 ms monostable multivibrator is activated 600 ms prior to the initial output trigger pulse and remains active until 1 sec after this pulse. The multivibrator actuates a relay driver and relay that open the shutter during this interval. Front-panel switches are provided to permit manual control of the shutter when desired.

In a similar fashion, the antenna circularity and receiver output polarity are reversed by means of a relay activated by the circuitry on card 10 (Figure 6.15). The initial output trigger pulse of each cycle is supplied to a 75 ms delay multivibrator, the turn-off spike of which triggers a 100 ms monostable multivibrator. This latter stage feeds a relay driver and relay which activates external relays to accomplish the switching functions. The antenna polarity is thus changed to the

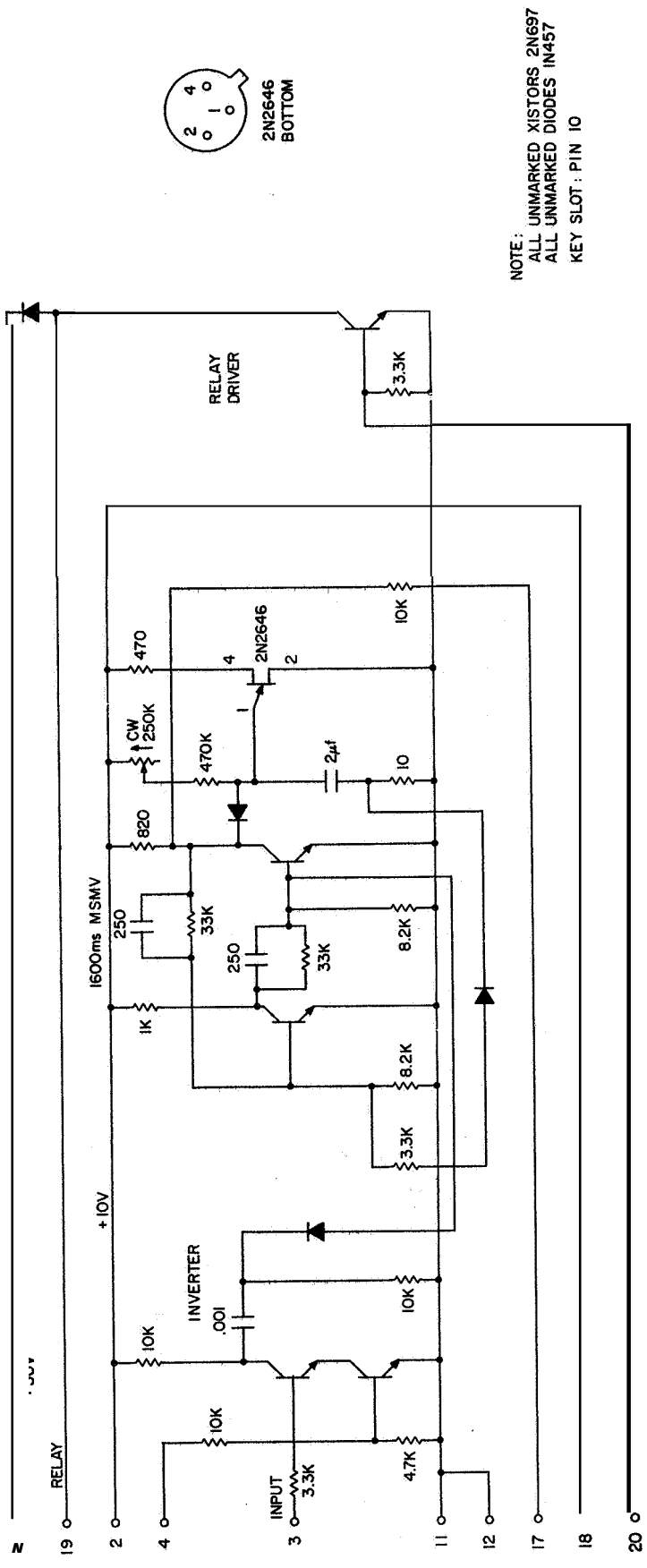

Figure 6 14 Modular TCS card 9--camera control circuit

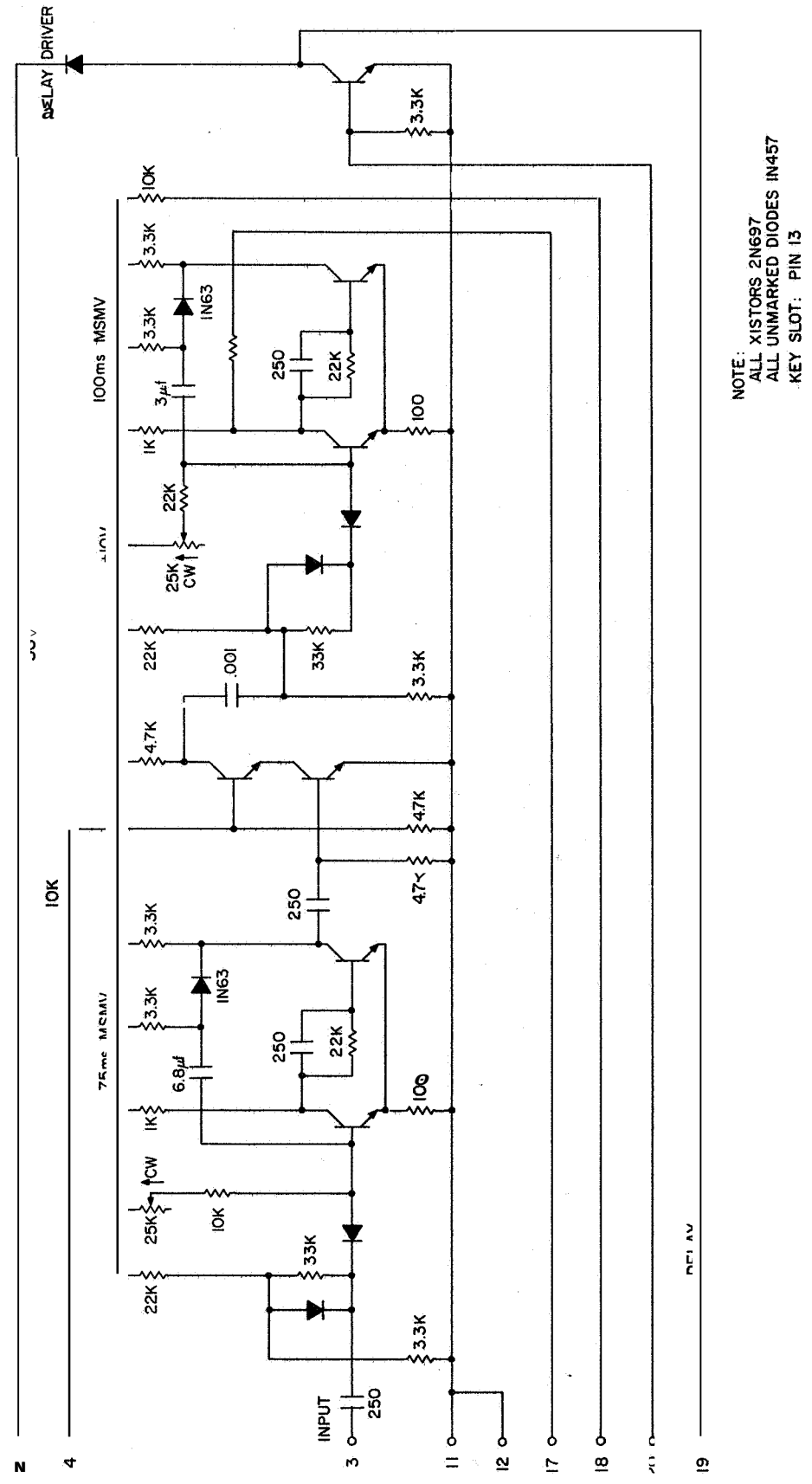

Figure 6 15 Modular TCS card 10--antenna and receiver polarity control circuit.

extraordinary circular mode and the receiver output polarity is switched from positive to negative for this 100 ms interval during which the second transmitter pulse occurs. A lockout feature is also provided to prevent operation of the relay when the system prf is set at 5 pps. As in the case of the camera control circuit, front-panel switches are provided to permit manual control.

In all of the circuits described above, switching operations are performed by the application of bias voltage to the appropriate points of the circuits, There are two reasons for using this technique. First, all functions of the entire sounder system are controlled through the timing and control system during normal operation. The bias control method will allow these functions to be controlled by an external programming device, thereby reducing the requirements for operator attention. Ideally, the system could be self-operating for long periods of time. Secondly, the bias control method prevents switching transients from appearing in the output, since no signal-carrying leads or frequency-determining components are switched directly. Switching transients in earlier systems occasionally proved detrimental to the transmitter.

All of the timing and control system logic circuitry is operated at 10 VDC, but relay drivers and pulse output amplifiers required 30 VDC. The power supply module contains two separate supplies and electronic regulator circuits to provide these voltages. As mentioned above, the regulator circuitry, with the exception of the series regulator transistor, is mounted on plug-in cards as shown in Figure 6.16 for ease of field maintenance. A panel meter is provided and may be switched to monitor current or voltage of either supply.

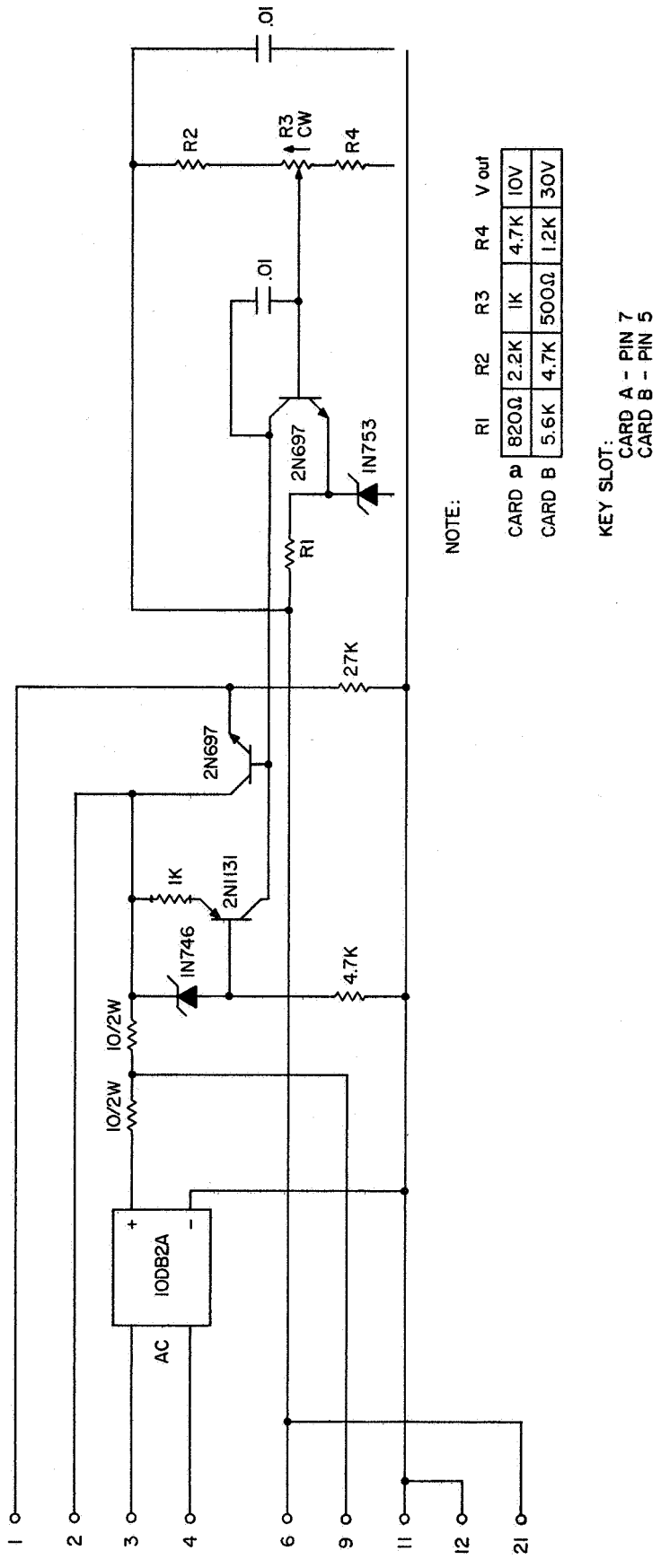

Figure 6.16 Modular TCS cards A and B--power supply voltage regulators.

Figures 6.17, 6.18, and 6.19 illustrate the wiring of the three modules, and Figure 6.20 is a diagram of the manifold wiring. Figure 6.21 is a block diagram showing all of the important logic blocks and their interconnections. Figure 6.22 shows a typical sequence of a single cycle of operation at 1/2 or 1/10 pps pulse repetition frequency,

A High Pulse Repetition Rate Timing and Control System:

In the use of the transmitter and receiver at the University of Illinois after the shipboard experiment, the need arose for a timing and control system capable of operation at pulse repetition rates of 30 and 60 pulses per second. This system is in use for measurement of ionospheric drifts ahd vertical incidence absorption and has proven to be quite useful in observation of partial reflections and in adjustment of the transmitter.

The pulse generating circuitry is very similar in design to the line-synchronized system previously described in this chapter. Because of the high pulse repetition rates generated by this pulscr, it was no longer feasible to include automatic relay switching of antenna polarization, receiver polarity, or the camera :shutter. All of these functions are controlled manually and no provision is provided for their operation by the timing and control system. The requirements of the drift experiment necessitated the inclusion of circuitry to generate three gate pulses for control of the three-channel RF preamplifier and the three-level receiver output switching circuit discussed in Chapter 3. Since the system is in use with the electronic TR switch discussed in Chapter 5, circuitry for generation of the TR gate enable pulse has been included in this pulser.

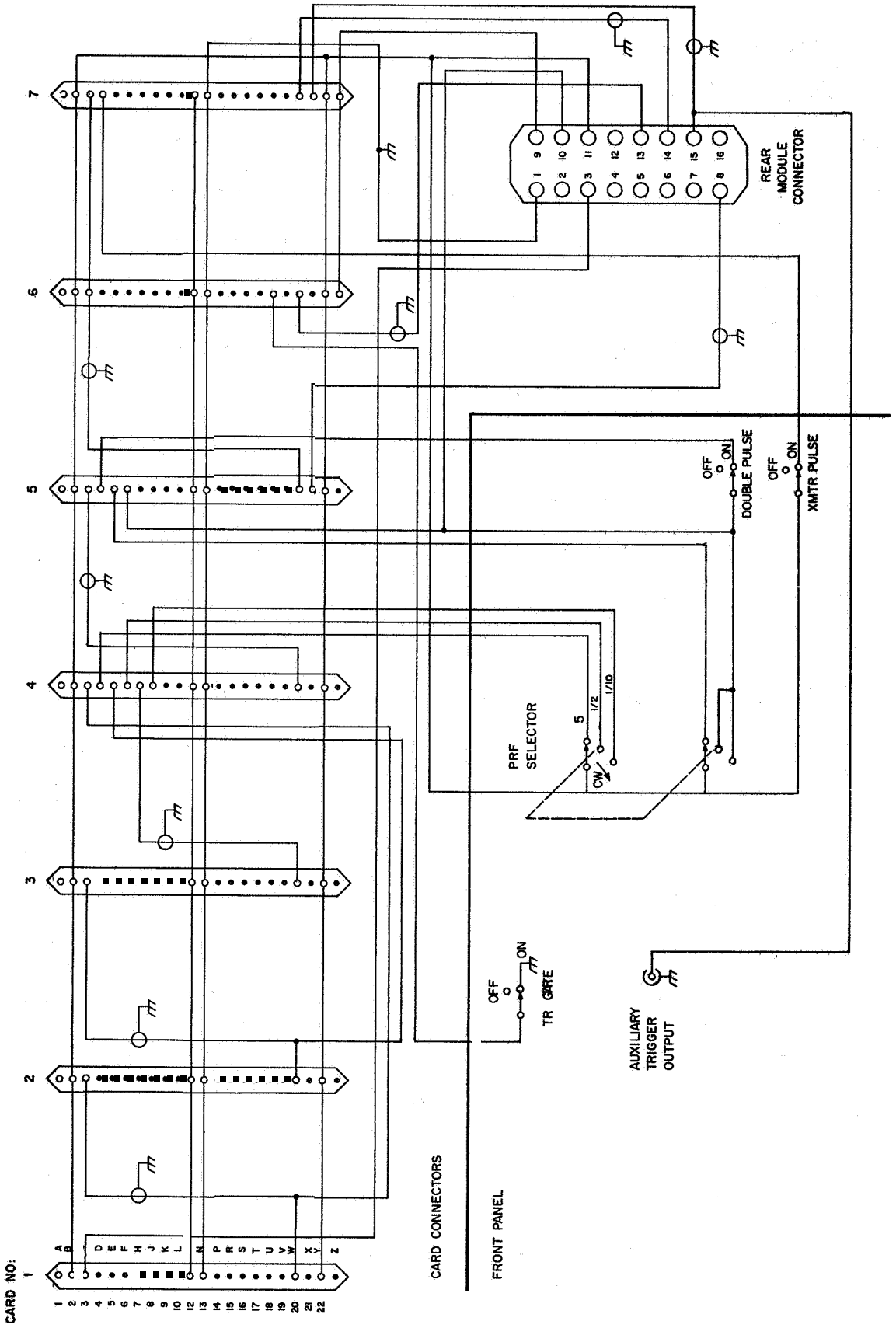

Figure 6.17 Modular TCS--module 1 wiring diagram.

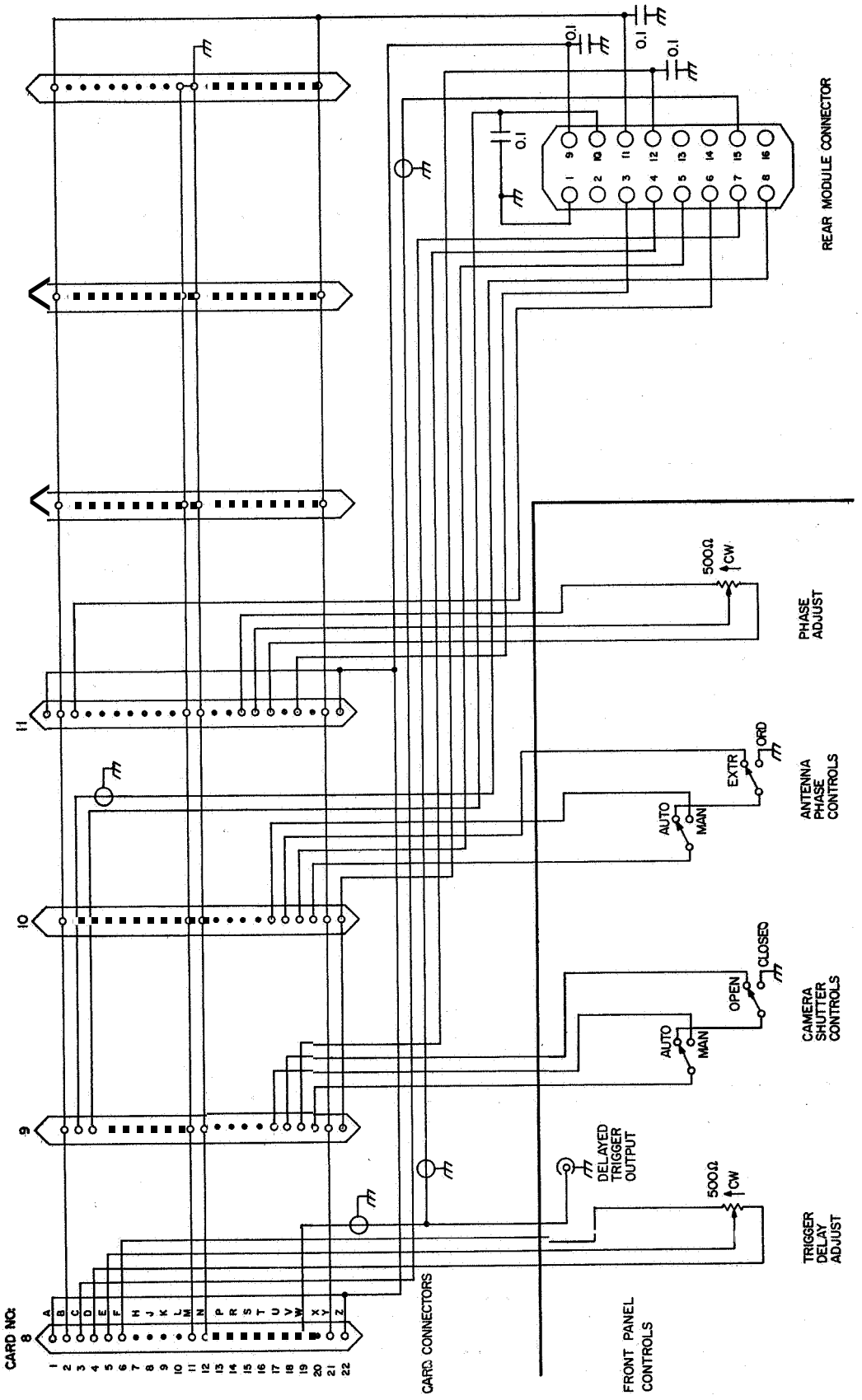

Figure 6.18 Modular TCS--module 2 wiring diagram.

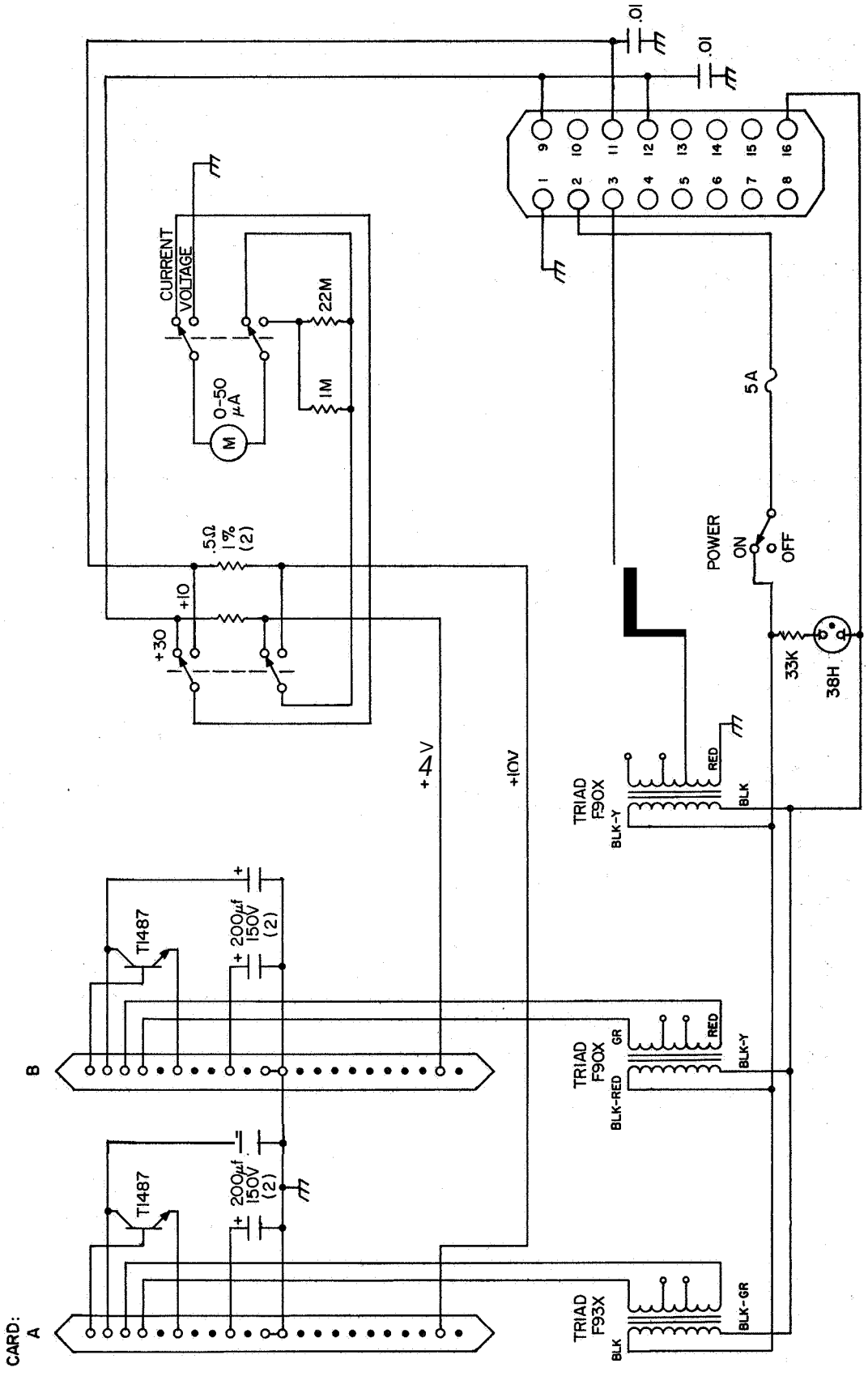

Figure 6.19 Modular TCS--module 3 wiring diagram.

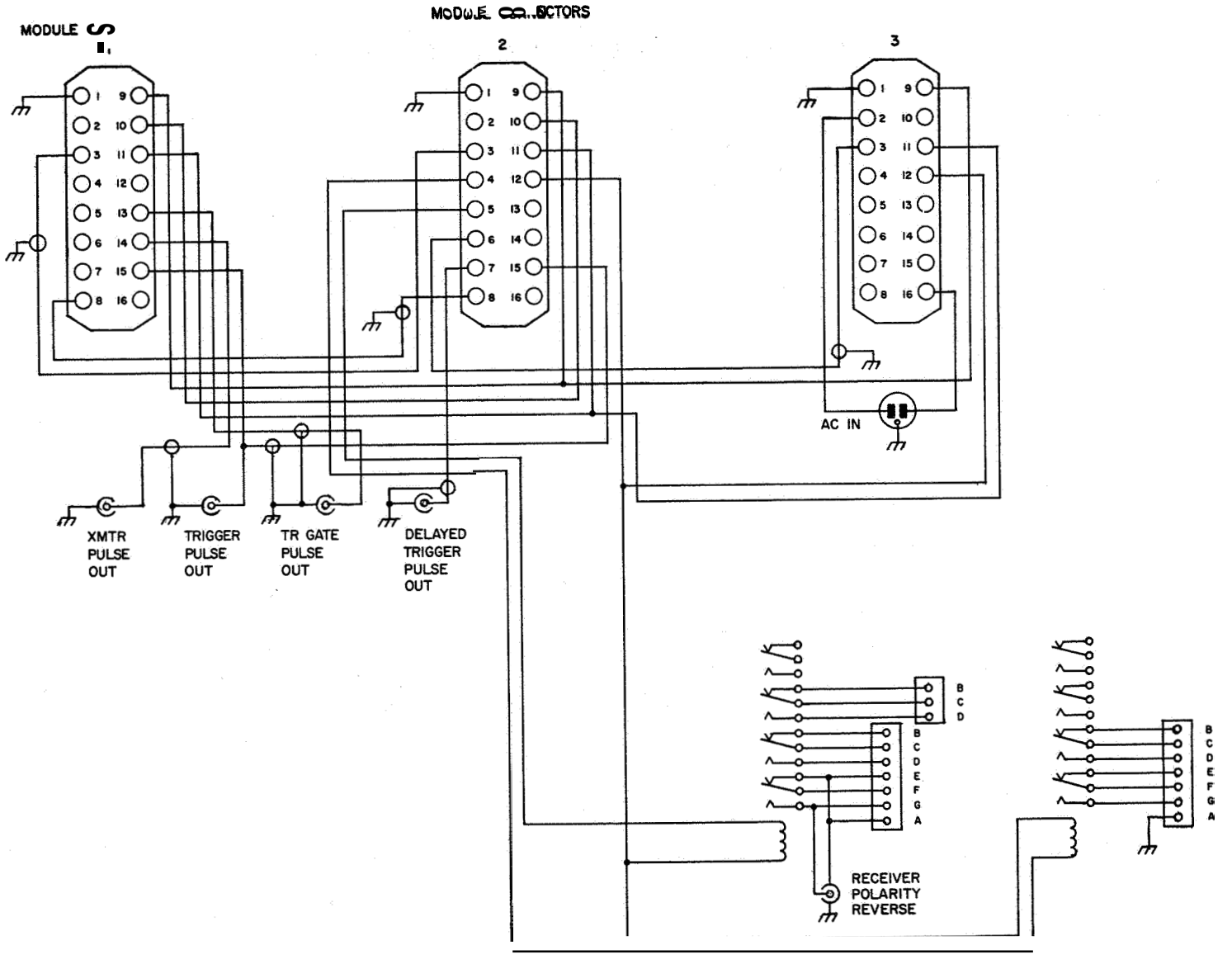

Figure 6.20 Modular TCS- manifold wiring diagram.

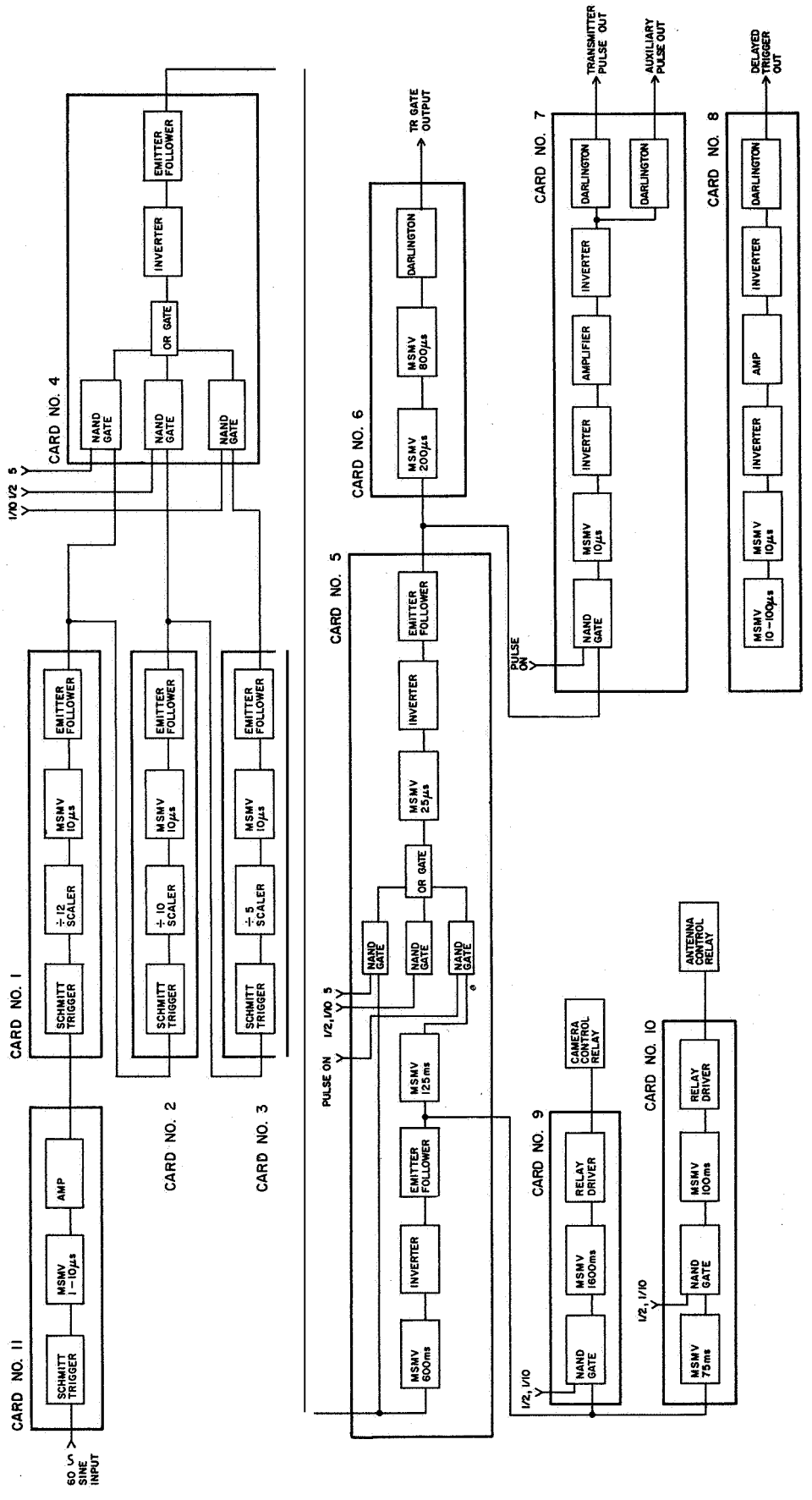

Figure 6.21 Modular TCS--logic block diagram.

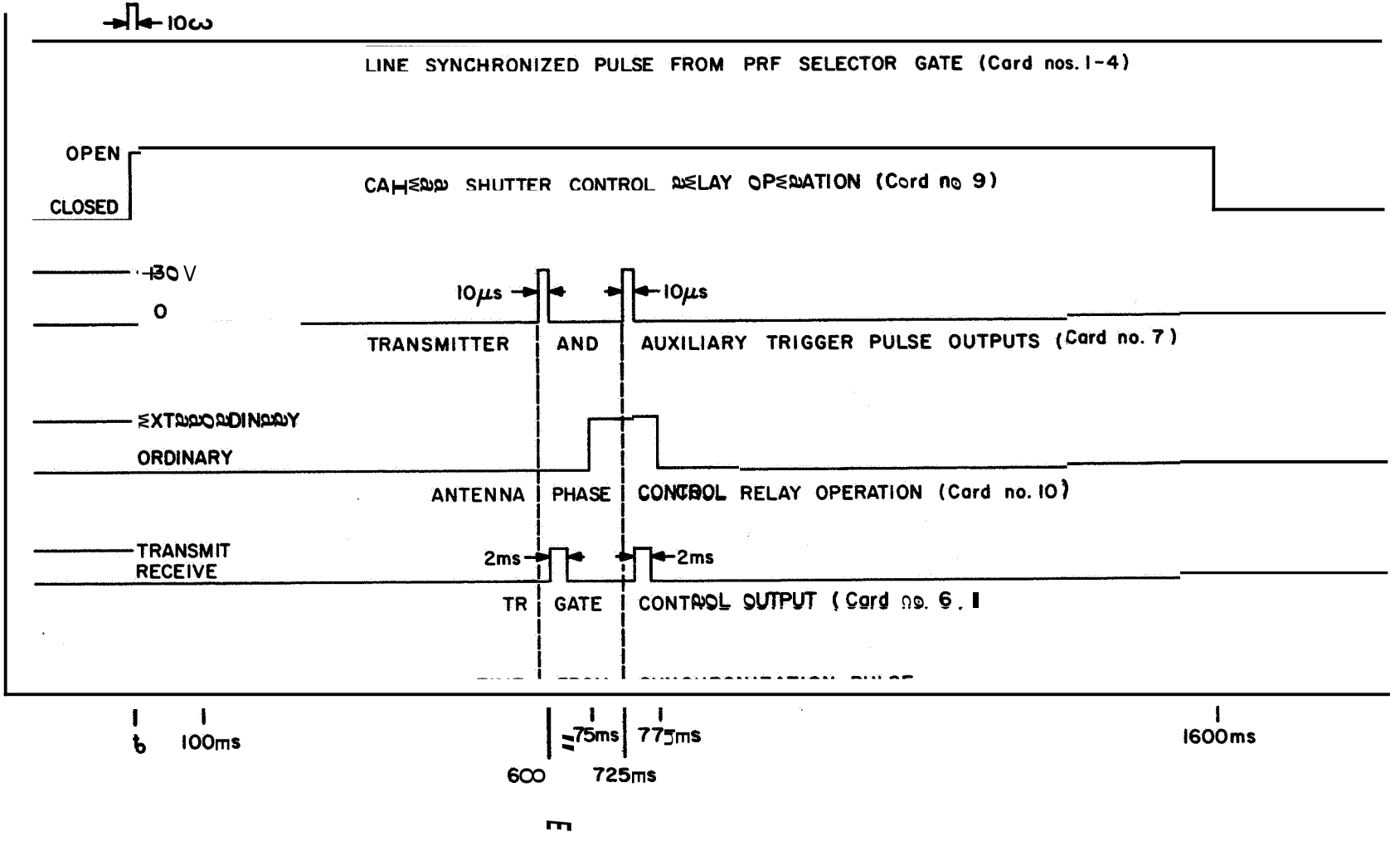

Figure 6 22 Modular TCS--typical sequence of operation

Figure 6.23 is the logic diagram of the high prf pulser and shows the stage-by-stage arrangement of the unit as well as the typical waveforms generated by it. Synchronization with the power line is achieved by driving a Schmitt trigger with either a 120 Hz or 60 Hz signal derived from a 12.6 VAC transformer. The 120 Hz signal is obtained by full-wave rectification of the transformer output. The unfiltered output is not sinusoidal, but it does retain the phase of the power line and is adequate for triggering the Schmitt circuit, A monostable multivibrator is triggered by the output of the Schmitt trigger and provdes means of adjusting the relative phase of the transmitter pulse to escape recurrent line-synchronized interference, The schematic diagram of the sync generator circuits and the power supply circuits is shown in Figure 6.24.

The schematic diagram of the timing circuitry of the unit is shown in Figure 6.25. The output of the phase-adjusting monostable multivibrator is squared in a Schmitt trigger and is used to activate the first bi-stable multivibrator in the timing chain, The output prf of this BSMV is also the frequency of the transmitter pulse rate, either 30 or 60 pps as chosen by the sync generator circuitry. In order that the three gate pulses will bracket the transmitter pulse, one of the BSMV outputs triggers the transmitter trigger pulse circuitry and the other output triggers the gate pulse generator circuitry, This system assures that the transmitter pulse will always fall in the center of each gate pulse.

The transmitter trigger pulse circuitry consists of a 10 μs monostable multivibrator and shaping and amplifier circuitry. A Darlington amplifier is used in the output circuit to achieve an output impedance of 100 ohms

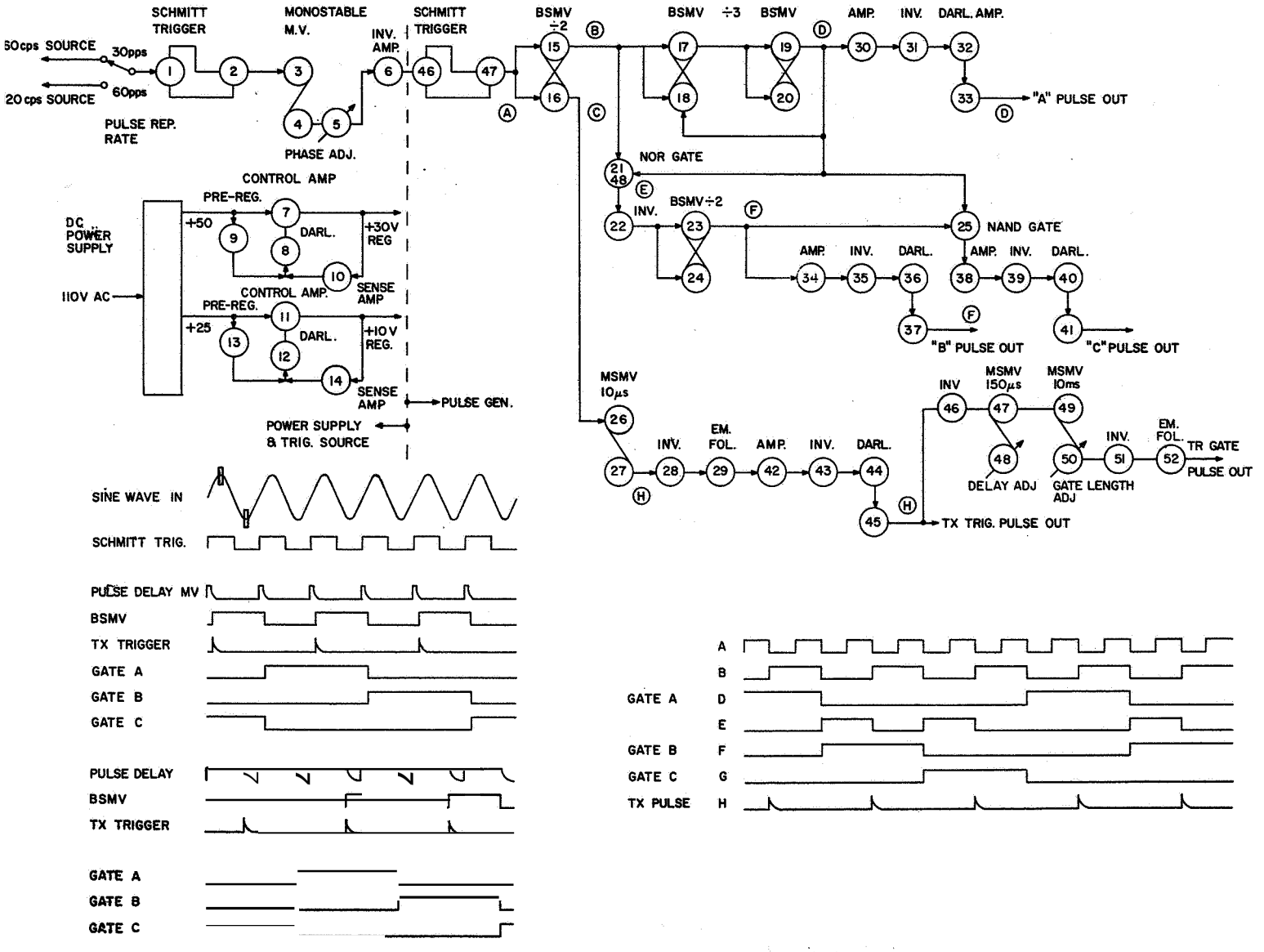

Figure 6 23 Block diagram of high pulse repetition rate timing and control system.

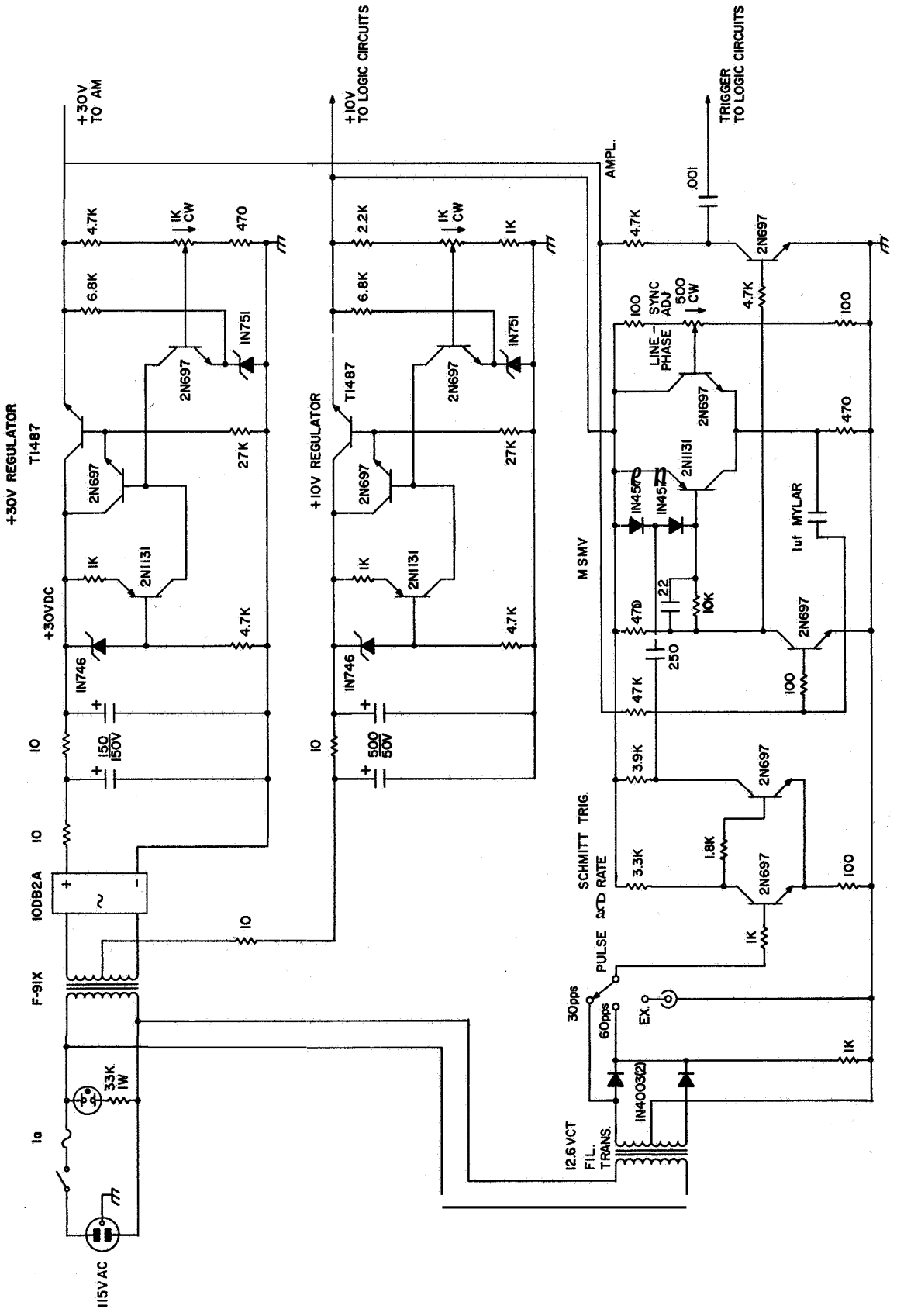

Figure 6.24 High pulse repetition rate system--trigger generator and power supply circuitry.

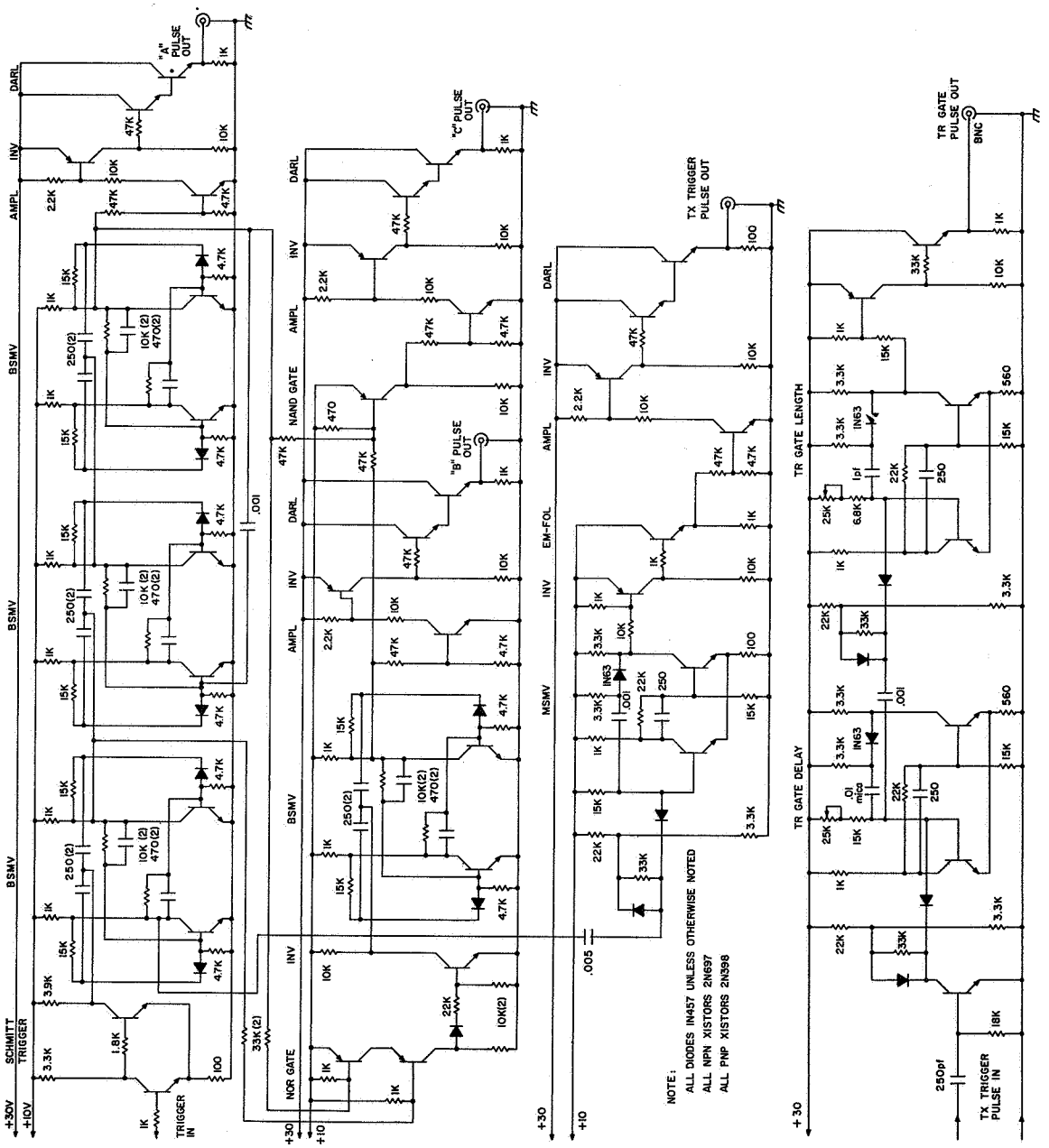

Figure 6.25 High pulse repetition rate system--logic and timing circuitry.

which prevents problems with RF retriggering of the timing circuits, Six type 2N697 and two type 2N398 transistors are used in the transmitter trigger pulse circuitry.

Two bistable multivibrators are used with a feedback system to divide the pulse repetition rate by three for generation of the three gate pulses. The output of this divide-by-three counter is gate pulse "A",, Gate pulse "B" is generated by mixing the input and output of the counter in a NOR circuit and dividing the resulting output by two in a bistable multivibrator circuit. Gate pulse "C" is generated by summing and inverting pulses "A") and "B" in the NAND gate. The waveforms associated with the generation of these gate pulses are also shown in Figure 6.25,

The TR gate enable pulse is generated by triggering a 200 μs delay monostable multivibrator circuit with each transmitter trigger pulse. This MSMV in turn triggers a 10 ms monostable multivibrator circuit generating the TR gate enable pulse. A two-transistor amplifier squares the waveshape of the pulse, amplifies it to a 30 volt level, and lowers the output impedance to 1000 ohms.,

Two regulated power supplies are used in the unit, a +30 volt and a +10 volt regulator. The +10 volt regulator supplies power to all timing and control circuitry but the TR gate circuit, and the +30 volt regulator supplies power to the TR gate circuit and to 30 volt amplifiers for each gate pulse and for the transmitter trigger pulse. The circuits of both regulators are similar in design to those used in the receiver power supply described in Chapter 3.

The entire timing and control system is constructed on standard circuit boards and housed in a shielded enclosure to prevent retriggering

by strong RF fields. Because of high ambient temperatures, it has been necessary to replace all of the germanium 2N398 transistors with silicon 2N1131 transistors. With this exception, the unit has proven to be highly reliable in the field. Future program planning indicates that it would be very desirable to incorporate the functions of this unit in the modular timing and control system described previously to avoid the necessity of switching cables from one unit to the other when changing the system from one type of measurement to another. Much of the circuitry of the two units is very similar and the high pulse repetition feature could be added to the modular unit without extensive modifications.

7. RECORDING SYSTEM, CALIBRATION TECHNIQUE, AM) PRELIMINARY DATA

Recording System:

As mentioned previously, the absorption and partial reflection data were recorded by filming an oscilloscope trace of the receiver output. The receiver output is connected to the vertical input of the oscilloscope and the transmitter trigger pulse from the timing and control system triggers the horizontal sweep circuits of the oscilloscope. Therefore the ionospheric reflections appear as pulses delayed in time by an amount proportional to the virtual height of the reflecting medium. By measuring the amplitude of these pulses as well as their displacement from the transmitter pulse, it is possible to calculate the amount of attenuation of the signal due to the ionosphere. Since the bandwidth of the receiver is 50 kHz, an oscilloscope with a vertical amplifier passband from DC to 500 kHz is sufficient to display the ionospheric reflections. The 500 kHz bandwidth is considerably greater than the minimum required, but assures that the oscilloscope circuitry itself does not distort the data recorded. The Tektronix type RM 504 oscilloscope was chosen for the data recording system.

The trace on the oscilloscope was photographed with a 35 mm camera, the shutter and film-advance mechanism of which were controlled by the timing and control system as outlined earlier. The Beattie-Colman KD-5HD camera and pulse-type magazine system were used in the shipboard experiment. This camera has an electrically operated shutter and a control system so that the 35 mm film is advanced one frame each time the shutter is closed. The camera is supplied by the manufacturer with a pushbutton type of shutter

control, intended to be used in much the same manner as a cable release is used in non-automatic cameras. The camera control relay in the timing and control system simply replaces this pushbutton switch. The camera control circuits have posed serious problems in that very strong RF interference is radiated from the camera during the film advancing and shutter opening and closing cycles. Extensive shielding of all camera control leads as well as adequate grounding of all portions of the camera body were necessary to prevent retriggering of the timing and control system by the camera noise. Furthermore, operation of the camera continuously over a period of several days has resulted in the failure of its internal shutter control power supply. The control system of the camera is evidently designed for applications in which exposures are spaced over relatively long periods of time since all circuit failures have been traced to overheating in the camera itself, The camera is optically ideal for this form of data recording since a wide range of focus and iris opening adjustment is provided.

The film used for data recording is Kodak type SP-417 Royal-X Panchromatic film expressly designed for oscilloscope photography. The film is designed for a spectral peak in the blue portion of the light spectrum so as to be particularly sensitive to the blue fluorescent trace from the P2 phosphor of the oscilloscope display tube. A disadvantage in the use of this special film is that it is not very sensitive to red light and therefore the graticule intensity must be quite strong to achieve a good exposure of both the oscilloscope trace and the graticule.

Filmed records of ionospheric reflections present the best of all means of preserving for future study all of the characteristics of each individual signal. However, the reduction of these films to produce an

absorption profile is a very tedious and laborious task. For this reason, an automatic recording system that electronically integrates a predetermined signal and records this average signal on a chart has been devised by R. Appel, This system is described in a separate report (Appel and Bowhill, 1965) and will not be discussed in detail in this report. The primary advantage of the automatic system is in the elimination of the film-reading operation in data reduction. The film recording system is still superior in applications requiring knowledge of rapid fading of the signal or when the splitting automatic system is not a present adaptable to measurement of partial reflections since it requires prior information as to what height range the system should search for ionospheric reflections. To date, partial reflections have not been observed with enough amplitude or regularity at a specific height for this system to be used. Possibly this integration technique can be applied to partial reflection recording by slowly sweeping the echo-selecting gate over the range of 50 to 80 km, with a plot of the average signal amplitude vs height printed every minute or so.

System Calibration Techniques:

The calibration of the system before recording data involves the following steps:

1. Calibrate the receiver gain controls as outlined in Chapter 3.
2. Align the antenna system as outlined in Chapter 5.
3. Align all tuned circuits of the transmitter for maximum output.
4. Measure the output of the transmitter.
5. Position the trace on the oscilloscope to obtain both a time and amplitude reference point.

6. Determine the system calibration constant each evening by observing the first and second E-layer reflections.

The output power of the transmitter was measured and recorded each day by measuring the amplitude of the pulse across the antenna with a 1000X high voltage scope probe and the RM33A test oscilloscope. The antenna impedance was checked periodically to assure that it did remain at 50 ohms resistive. Power output calculated from this voltage was always determined to be between 42 and 46 kW during the pulse. The RF output of the transmitter was continuously monitored to assure that it remained constant throughout a data run,

Time and amplitude reference points in the oscilloscope were set up with the oscilloscope graticule. The time zero reference was defined to be the beginning of the transmitter pulse and was positioned on the scope at the far left of the screen at the first major vertical graticule line. The zero-signal output of the receiver was used as the amplitude reference and its positioning on the screen was different for absorption and partial reflection records. For absorption records, the zero-signal reference was positioned one major horizontal graticule line up from the bottom of the screen since the lowest graticule line does not extend the full width of the oscilloscope screen. For partial reflection records, the zero-signal reference was set at the middle of the oscilloscope screen to allow room for display of both positive and negative deflections.

The calibrated sweep ranges of 0.5, 0.2, and 0.1 ms/cm of the oscilloscope were used as calibration of the time and therefore height scale of the records. The accuracy of the oscilloscope sweep circuit was checked periodically with a standard oscillator. The 0.1 ms/cm, or 15 km/cm, scale

was used exclusively for partial reflection recording. Recording of absorption was made with the time scales of 0.2 ms/cm (30 km/cm) and 0.5 ms/cm (75 km/cm). E-layer reflections were recorded on the 0.2 ms/cm scale exclusively. Early morning absorption recordings were usually made of F-layer reflections on the 0.5 ms/cm time scale since E-layer reflections were either non-existent or very weak in the hours near ground sunrise. The vertical amplifier of the oscilloscope was always maintained at a calibrated sensitivity of 1.0 volt/cm and was checked periodically with the oscilloscope calibrator.

The receiver gain controls were calibrated daily with the procedure previously outlined in Chapter 3 and the antenna polarization was also checked daily as discussed previously.

Calibration of the system sensitivity involves determining a system calibration constant by observation of the first and second reflections, as derived below:

The apparent reflection coefficient, P, can be defined as

$$P = E/E_o \qquad (7.1)$$

where

E = the amplitude of the signal reflected from the ionosphere.

E_o = the amplitude of the reflected signal if no ionospheric absorption were present.

Measurement of ionospheric absorption is usually expressed in terms of a loss in decibels, L, where

$$L = -20 \log (\rho). \qquad (7.2)$$

It can be further shown that

$$E_1 h_1 = \rho K \qquad \text{(Appel and Bowhill, 1965)} \qquad (7.3)$$

where

E_1 = The measured amplitude of the first ionospheric reflection.

h_1 = The virtual height of the first reflection.

K = System calibration constant equal to the amplitude-height product of a reflection without absorption.

Furthermore, the second order reflection may be expressed as

$$2E_2h_1 = \rho\rho_g E_1 h_1 = \rho^2 \rho_g K \tag{7.4}$$

where

E_2 = The measured amplitude of the second reflection.

ρ_g = The reflection coefficient of the ground, or, in the special case of the ship, the reflection coefficient of the sea.

With algebraic manipulation the following relationship between E_1 and E_2 can be derived:

$$\frac{E_1^2}{E_2} = \frac{2K}{\rho_g h_1} \tag{7.5}$$

which allows the system calibration coefficient to be calculated independent of the measurement of p. Also, since the measurements were conducted at sea, the reflection coefficient, ρ_g, can be assumed to be unity with reasonable accuracy. Therefore,

$$K = \frac{h_1 (E_1)^2}{2E_2} \tag{7.6}$$

Therefore p is calculated from the relationship

$$\rho = E_1 h_1 / K \tag{7.7}$$

The reader is referred to a report by Appel and Bowhill (1965) for a more complete derivation of these parameters.

The calibration constant, K, was determined for each day by measuring the average values of E_1 and E_2 over a ten minute period in the evening after ionospheric absorption dropped sufficiently to allow reliable observation of E_2. The calibration constants for each day that data was recorded were all within 10% of each other, providing verification that the system gain was indeed remaining constant.

Preliminary Data:

Recording of vertical incidence and partial reflection data on board the ship was initiated on April 21, 1966 and continued to the end of the cruise at Norfolk, Va. on May 2, 1965. A table of the ship position for each day as well as the times data were recorded is listed in Figure 7.1. Vertical incidence absorption data was recorded each day between the hours of 0900 EST and 1700 EST and from before sunrise to after sunset on three days to assure accurate system calibration. Partial reflection data was recorded only at the times when visual observation indicated that partial reflections might indeed be present, The normal operating schedule for data recording is outlined in Figure 7.2. This schedule provides for three ten-minute vertical incidence absorption data recording sessions, or runs, and three five-minute partial reflection recording sessions during each hour. This schedule was adhered to as rigidly as possible to assure a uniform sampling of the data.

A typical frame of data recorded for vertical incidence absorption measurement is shown in Figure 7.3. The horizontal scale of this trace has been converted directly to kilometers virtual height for greater clarity. By measuring the amplitude of the reflection from the film and knowing the

IONOSPHERIC SOUNDER POSITION DATA

DATE	TIME EST	TIME GMT	LATITUDE	LONGITUDE	HEADING	AV. SPEED	HOURS OF DATA
4-21	0800	1300	29°28' S	73°24' W	336°	15.88 N	1023 to
	1200	1700	28°24' S	75°56' W	340°		2020 EST
	2000	0100	26°24' S	74°42' W	343°		
4-22	0800	1300	23°55' S	75°35' W	343°	14.92 N	0901 to
	1200	1700	22°50' S	75°58' W	342°		2135 EST
	2000	0100	20°48' S	76°41' W	342°		
4 23	0800	1300	17°41' S	77°45' W	342°	16.08 N	0420 to
	1200	1700	16°39' S	78°09' W	342°		2323 EST
	2000	0100	14°33' S	78°49' W	342°		
⅂ 24	0800	1300	11°31' S	79°49' W	343°	16.33 N	0940 to
	1200	1700	10°25' S	80°11' W	343°		1920 EST
	2000	0100	08°24' S	80°49' W	343°		
4 25	0800	1300	05°20' S	81°34' W	343°	15.75 N	0415 to
	1200	1700	04°17' S	81°29' W	005°		1940 EST
	2000	0100	02°09' S	81°21' W	005°		
4-26	0800	1300	01°00' N	80°53' W	010°	16.25 N	1000 to
	1200	1700	02°09' N	80°42' W	010°		1730 EST
	2000	0100	04°16' N	80°17' W	010°		
4-27, 4-28	Passage through Panama Canal - No Data Recorded						
4-29	0800	1300	12°29' N	78°14' W	012°	14.55 N	081@ to
	1200	1700	13°14' N	77°49' W	012°		170@ EST
	2000	0100	15°05' N	76°49' W	015°		
4-30	0800	1300	17°40' N	75°19' W	022°	15.29 N	044@ to
	1200	1700	18°34' N	74°46' W	022°		193@ EST
	2000	0100	20°75' N	73°49' W	015°		
5 1	0800	1300	23°19' N	74°23' W	003°	15.29 N	073@ to
	1200	1700	24°17' N	76°16' W	351°		163@ EST
	2000	0100	26°20' N	74°28' W	353°		
5 2	Dismantle equipment and off-load at Norfolk, Va.						

Figure 7.1 Ionospheric sounder position data.

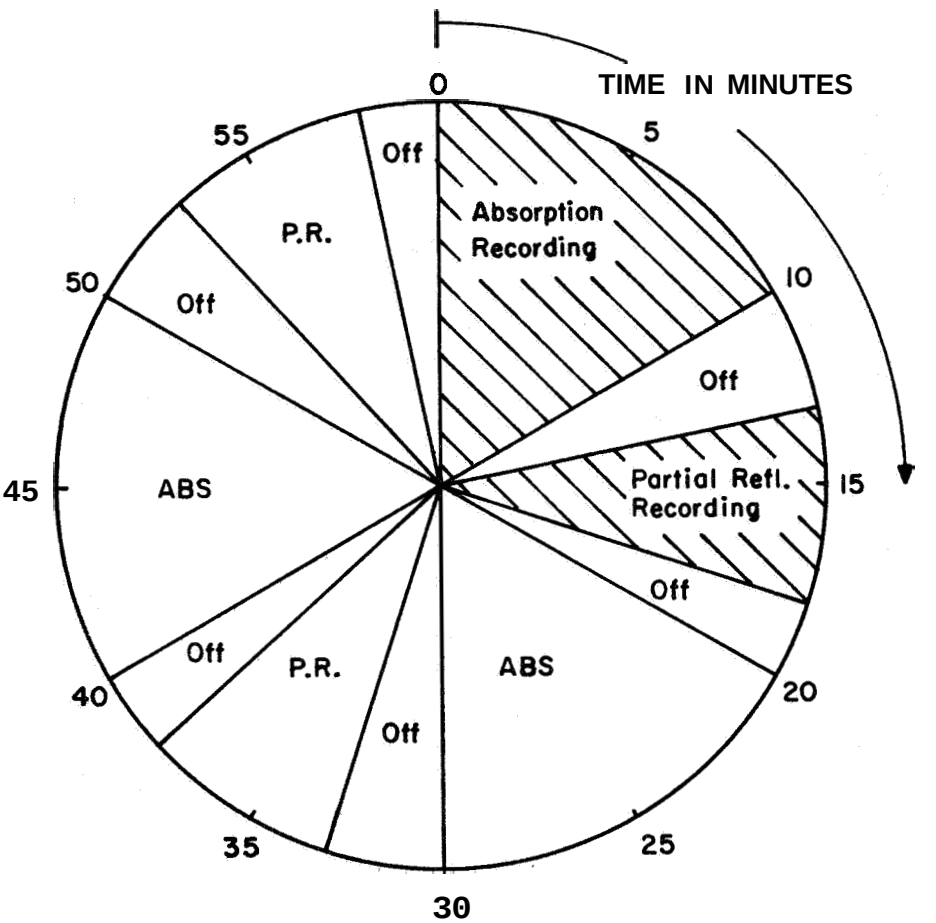

Figure 7.2 Normal operating schedule for data recording.

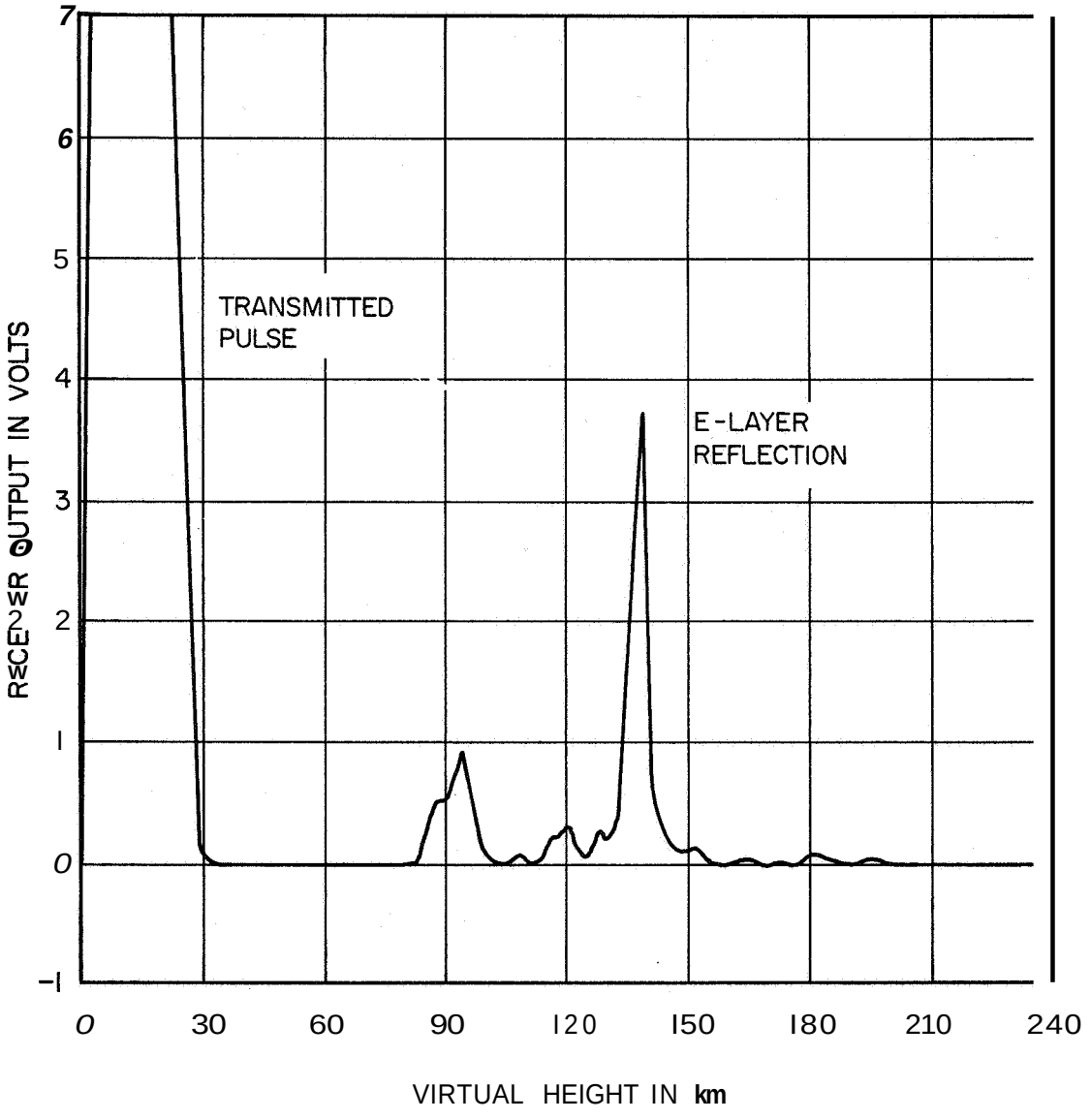

Figure 7.3 Typical frame of data recorded for absorption measurements.

receiver gain, it is possible to calculate the strength of the signal at the input to the receiver, The input voltage to the receiver is likewise calculated for each frame of interest during a ten-minute run of data and the median value for this ten-minute period is calculated. Median values are used for each period to remove rapid variations of the ionospheric signal from the data. A median of the virtual heights recorded in each frame is also computed for a ten-minute run. This median amplitude and height thus calculated are used in conjunction with the system calibration constant, K, in calculating the apparent reflection coefficient, ρ, with equation 7.7 previously derived. The median ionospheric attenuation during this ten-minute period is calculated by simply converting ρ into decibel units.

All filmed records of vertical incidence absorption were recorded at a pulse repetition rate of 1/2 pps. Therefore, 300 frames of data were recorded over a ten-minute period and approximately 900 frames were recorded each hour. Reading of the film to measure the amplitude and horizontal position of each pulse requires use of a standard microfilm reader and can be carried out at a maximum rate of 100 frames per hour; complete reduction of all 64,000 frames of absorption data would therefore require 640 man hours just to convert the film to two columns of figures. Because of this extensive time requirement, it was decided to reduce all of the data on a strict 10% sampling basis to determine the general trend of the data and to develop further insight into its interpretation and the means by which the remaining frames should be reduced. For a preliminary analysis, a 10% sampling of all the vertical incidence absorption data recorded on April 23, 1965 was reduced and plotted, The ionospheric absorption vs time of day is plotted in Figure 7.4.

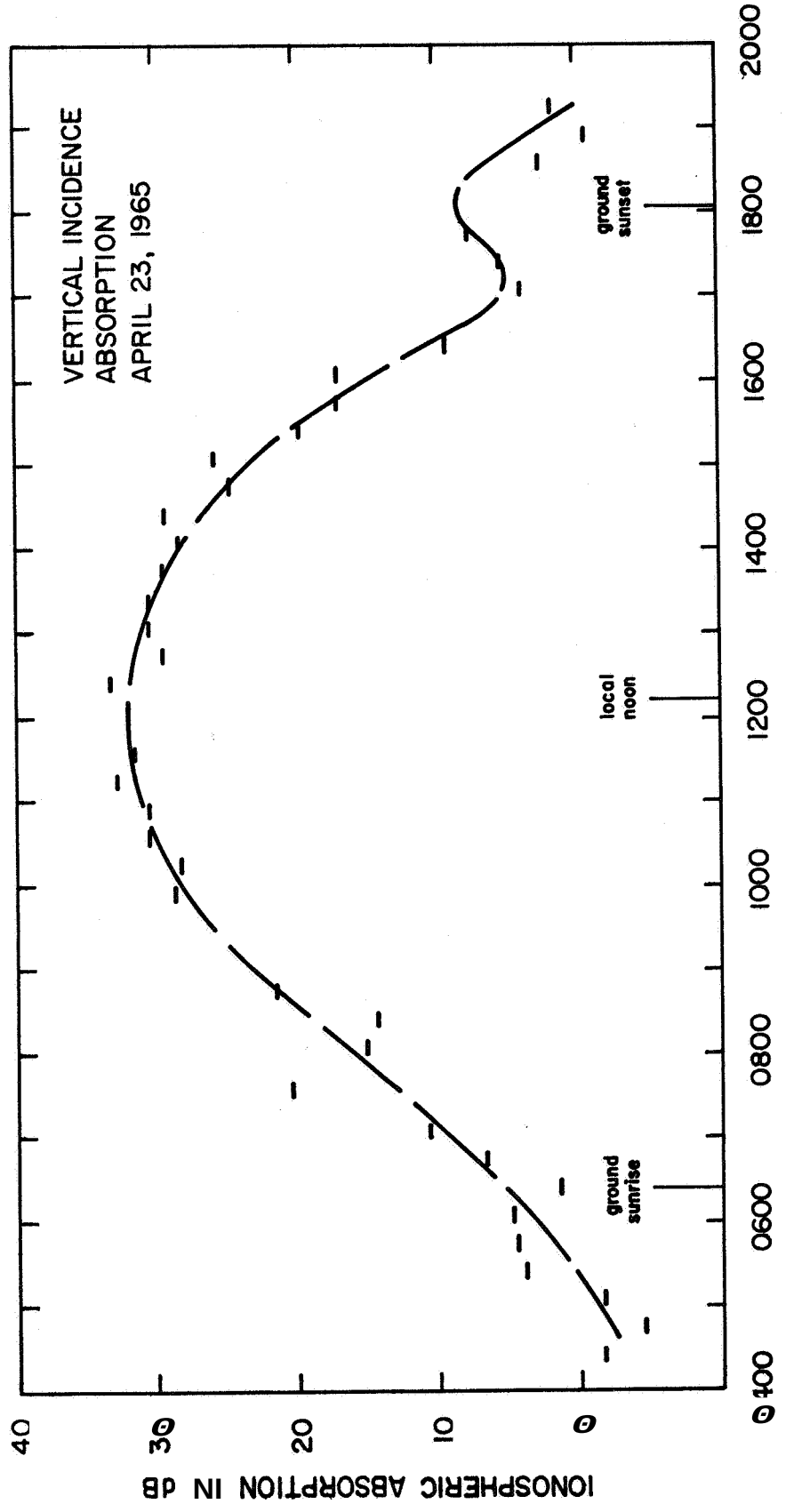

Figure 7.4 Ionospheric absorption vs. time of day for April 23, 1965.

This curve very clearly demonstrates the diurnal variation of ionospheric absorption due to solar radiation, The absorption data calculated for times between 0400 and 0800 (local time) was all determined by normalizing F-layer data since the E layer was not sufficiently well defined to produce observable reflection signals prior to ground sunrise. The balance of the data is that of the E layer. The horizontal lines on the graph represent the median attenuation values calculated for each data run. The curve represents a rough average of the median values, The variation of the median values from the average curve is probably due to long-term ionospheric fading of periods greater than 10 minutes. The presence of an E_s layer at approximately 1800 hours caused the apparent increase in ionospheric absorption at this time.

All nine days of data recordings are being reduced with the strict 10% sampling method as was applied to the data of April 23 in order to obtain an overall picture of the ionospheric conditions over this period as well as a preliminary indication of the latitudinal variation of the absorption, Dr. J. S. Shirke of the Electrical Engineering Department of the University of Illinois is presently interpreting these results and a more extensive discussion of them will be presented in a forthcoming paper (Shirke and Henry, 1966).

A typical frame of data recorded for partial reflection measurements is shown in Figure 7.5. The upper trace displays the received reflection of the ordinary polarized wave and the lower trace is that of the extraordinary wave. The analysis of this data, as outlined by Belrose and Burke (1961), requires comparison of the amplitudes of the two components of the signals reflected from ionospheric irregularities below 90 km. A major problem in the

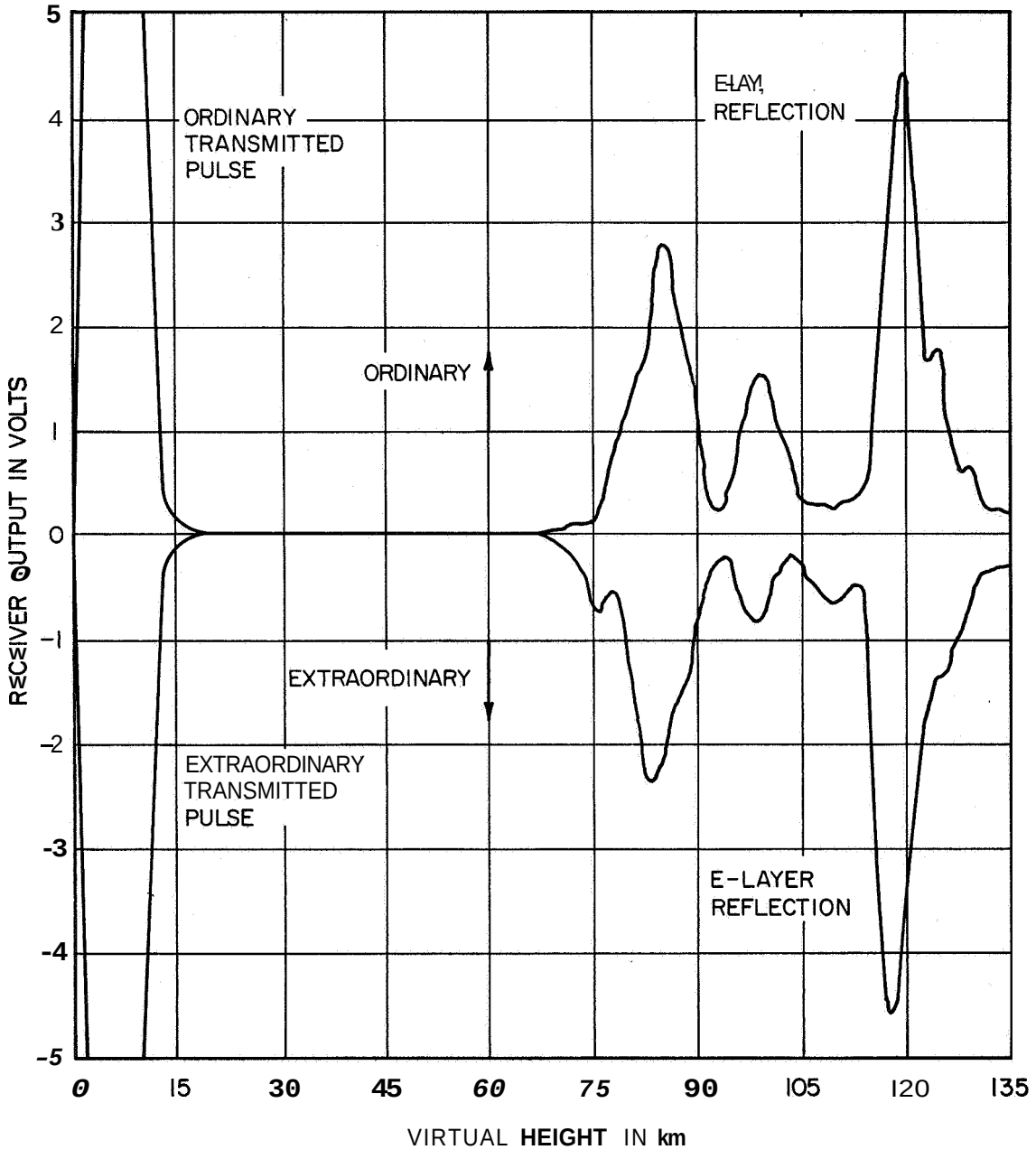

Figure 7.5 Typical frame of data recorded for partial reflection measurements.

reduction and interpretation of the very weak signals received is in differentiating between bonafide ionospheric reflections and noise pulses. A survey of the partial reflection data recorded indicates that the system signal-to-noise ratio is at best marginal and that reduction of this data will be quite difficult. It is hoped that further insight on the correct interpretation of this data will be gained from studying the vertical incidence absorption data. Furthermore, use of the partial reflection technique at the University of Illinois Aeronomy Field Station should provide even more information concerning correct data reduction techniques.

Conclusions:

The design and operation of the vertical incidence partial reflection sounder has provided considerable information concerning instrumentation design techniques and ionospheric properties of the middle latitudes. Since data was recorded for ship positions between 30° S and 26° N latitudes, the variation of ionospheric absorption with latitude can now be determined for the period of the cruise. Unfortunately, the ship was constantly moving and the latitudinal variation will be very difficult to separate from the normal diurnal variation. An ideal experiment for measurement of latitudinal variation of ionospheric absorption would be to use similar instrumentation on board a very slowly moving vessel. A cruise in which the ship would remain essentially motionless over the daylight hours and move one degree of latitude during the night would be optimum for this experiment. The closely spaced absorption profiles would then make it much easier to categorize individual variations and anomalies in ionospheric absorption as diurnal, latitudinal, or seasonal.

As mentioned in the introduction, instrumentation for measurement of ionospheric absorption and partial reflections is highly specialized and little information has been available concerning optimum system components or design techniques. The instrumentation designed and constructed for the cruise was a logical evolution in design from a similar system designed for and in use at Wallops Island, Va. Likewise, the shipboard system has been modified and, in some cases, redesigned in part for use at the Aeronomy Laboratory Field Station at the University of Illinois. Design information concerning the various components of all three systems has been included in this report to provide a logical background for the evolution of the present instrumentation and to provide sufficient information that a similar system could be constructed by other research groups. It is apparent from the discussions of each unit of the system that considerable redesign and modification has been made on each system, and probably many more modifications will be made in the future. It is highly desirable that any system intended for use in a research project be so designed that it is as flexible as possible to allow for future modifications and additions. In this way, the system can be employed in many applications and thus is utilized to its fullest extent. This concept of instrumentation flexibility provides the most economical use of equipment design and construction efforts and reduces the time required before data can be recorded and analyzed. Since the instrumentation in this type of research project is actually the tool and not the desired final product, it is highly desirable to minimize time delays generated by the design and construction of many similar systems.

Ideas for future modification and improvement of the basic system have been outlined in detail previously and need not be repeated at this point. It is sufficient to say that a functioning system of original and adequate design has been developed and that this system is readily adaptable for use in a wide variety of ionospheric research projects involving ground-based transmission and reception of high frequency radio waves. The use of a swept-frequency ionosonde in conjunction with this system provides a very powerful means of investigating D- and E-layer ionospheric phenomena.

REFERENCES

Appel, R. L. and S. A. Bowhill (1965), An automatic recording system for the determination of ionospheric absorption, Aeronomy Report No. 7 (University of Illinois, Urbana, Illinois).

ARRL Antenna Book, The (1960), (American Radio Relay League, Newington 11, Connecticut),

Belrose, J. S. and M. J. Burke (1961), Partial reflection of pulsed radio waves from the ionospheric D- and E-regions (presented to URSI/IRE meeting 4 May 1961, Washington, D. C.).

Belrose, J. S., L. R. Bode, L. W. Hewitt, and J. M. Griffin (1964), An experimental system for studying partial reflections from the lower ionosphere, Defense Research Telecommunications Establishment Report No. 1136 (Ottawa, Ontario).

Beneteau, P. J. (1961), The design of high-stability DC amplifiers, Application Data No. APP-23, Fairchild Semiconductor Corp, , Mountainview, California.

Chaffee, E. L. (1936), A simplified harmonic analysis, Review Sci. Inst. 7.

Knoebel, H., D. Skaperdas, J. Gooch, B. Kirkwood, and H. Krone (1965), High resolution measurements of Faraday rotation and differential absorption with rocket probes, Coordinated Science Laboratory Report R-273 (University of Illinois, Urbana, Illinois).

Landee, R. W., D. C. Davis, and A. P. Albrecht (1957), Electronic Designer's Handbook (McGraw-Hill Book Co., New York, New York).

Mayes, P. E, (1965), Electromagnetics for Engineers (Edwards Brothers, Inc., Ann Arbor, Michigan).

Mergner, F. L. (1966), Pin diode and FET's improve f-m reception, Electronics 39, No. 17.

Offutt, W. B., L. K. DeSize, and W. H. Yale (1961), Methods of obtaining circular polarization, Antenna Engineering Handbook, ed. H. Jasik (McGraw-Hill Book Co., New York, New York).

Papas, C. H. (1965), Theory of Electromagnetic Wave Propagation (McGraw-Hill Book Co,, New York, New York).

Ramsey, V. H., G. A. Deschamps, M. L. Kales, and J. L. Bohnert (1951), Techniques for handling elliptically polarized waves with special reference to antenna, Proc. IRE 39, No. 5.

REFERENCES (continued)

Reference Data for Radio Engineers (1956), ed. H. P. Westman (International Telephone and Telegraph Corp., New York, New York).

Schwartz, Mischa (1959), Information Transmission, Modulation, and Noise (McGraw-Hill Book Co., New York, New York).

Shirke, J. S. and G. W. Henry (1966), Equatorial and lower latitude anomaly in ionospheric absorption: results of observations on board the ship USNS Croatan (to be published).

Sevin, L. J. (1965), Field Effect Transistors (McGraw-Hill Book Co., New York, New York).

Texas Instruments, Inc. Engineering Staff (1963), Transistor Circuit Design, ed. J. A. Walston and J. R. Miller (McGraw-Hill Book Co., New York, New York).